ESTIMATION OF KINETIC PARAMETERS IN A CORN STARCH VISCOSITY MODEL AT DIFFERENT AMYLOSE CONTENTS

By

Rabiha Sulaiman

A DISSERTATION

Submitted to
Michigan State University
In partial fulfillment of the requirements
for the degree of

DOCTOR OF PHILOSOPHY

Biosystems Engineering
Food Science

2011

ABSTRACT

ESTIMATION OF KINETIC PARAMETERS IN A CORN STARCH VISCOSITY MODEL AT DIFFERENT AMYLOSE CONTENTS

By

Rabiha Sulaiman

Starch is a major source of energy in the human diet. Starch granules are mainly composed of glucose-based molecules: amylose (AM) and amylopectin (AP), and some minor components (protein, phosphorus and lipid). Besides being a major source of calories, starch is also one of the most multifunctional raw food ingredients in industry, being used as a product thickener; texture improvement agent, fat replacer, and mouth feel enhancer. The qualities that determine native starch functionality depend on their specific physicochemical properties. A model that could predict product viscosity during processing will benefit industry for quality control and process design purposes.

In this study, the kinetic parameters in a modified starch viscosity model were estimated for different amylose to amylopectin ratios. A total of 24 samples of corn starch blends were prepared from base corn starches (waxy, normal, and high amylose) at different different amylosecontents, by calculating the starch amylose content (adding high amylose corn starch to low amylose corn starch) and assuming the remainder was amylopectin. The actual amylose content of the starch samples was analyzed using Concanavalin A (Megazyme procedure). An empirical correlation of calculated and experimental amylose contents in the samples was presented in this study. The rheological properties of the corn starch blends were determined by collecting fundamental rheological data on 6% concentration (starch: water system) by applying

the mixer viscometry approach using a modified Brookfield viscometer equipped with a flag mixer impeller.

Pasting curve results showed that the starch rheological properties were a function of AM/AP. An empirical equation was proposed for peak viscosity, holding strength, and set back viscosity as function of AM/AP ratios. The peak viscosity, holding strength, and the setback viscosity increased as the starch amylose content decreased. Thermal properties of the corn starch blends were evaluated using a differential scanning calorimeter (DSC). Enthalpies of gelatinization were found to increase as the amylose content of the starch blends decreased.

Kinetic parameters of a starch viscosity model were estimated simultaneously, and sequentially, using mixer viscometer data. The estimated parameters contained narrow confidence intervals, and small relative standard errors under 12%. A comprehensive starch viscosity model for two common corn starches: waxy and normal corn starch was proposed and tested on an independent set of data collected from a different measuring system, the Rapid Visco Analyzer (RVA). The model with the estimated parameters predicted the observed data well for the overall pasting curve having a RMSE < 10% for the total testing period. Correlation between the rate constant and activation energy (kinetic parameters in the Arrhenius model) was found to be a strong function of the reference temperature. The gelatinization rate constant k_g and activation energy of gelatinization (E_g) increased as power-law functions with decreasing amylose levels.

To my parents, Hj. Sulaiman Abu Bakar and Hjh. Amina Mohamad Ghanie, for their true love, prayer, selfless sacrifice, patience, and continuous encouragement which allowed me to pursue my dreams, understanding and being my great companion. To the late grandma Allahyarhamah Mariam Bee who taught me true love and believing in me. To my sisters Anar Begum, Mumtaz Begum, Mastura, and my brother Nagur Ghanie for their true love and support. To my sister-in-law Ainun and brother-in-law Hanifa, Jehabar Sathique, Kamal Batcha for their care and support. To my nieces and nephews for their cheerfulness and love.

ACKNOWLEDGEMENTS

Syukur Alhamdulillah. I thank my God Allah S.W.T for His blessing, keeping me healthy and making me able to complete this work. I also thank Him for all the people He sends into my life that helped my life be blessed.

I am grateful to both my co-advisors Dr. Kirk Dolan and Dr. James Steffe, for their consistent guidance, knowledge, availability, continuous encouragement, and their expectations. I had asked God once when I did my pilgrimage to Mecca and in front of the *Kaabah* that if I am accepted to graduate school and do Ph.D., grant me with a great advisor. A year later, I went to MSU and work under these two great persons in my life. My wish was granted, instead of one, God gave me two.

I sincerely thank Dr. Perry Ng, Dr. Maurice Bennink, and Dr. Chris Saffron to be on my committee, for their time and helpful suggestions. I would especially thank Dr. Perry Ng for allowing me to work in his lab and use his equipments for amylose content determination and Dr. Bennink for contributions to changes in my initial research proposal.

I thank Mr. Phill Hill, Mr. Steve Marquie, Mr. Richard Wolthuis, Peter, and Charlie for their technical help in equipment set-up. My special thanks go to Dharmendra Mishra, Ibrahim Greiby, Kevser Kahraman, George Nyombaire, Shantanu Kelkar, and Wei Peng, for their technical help, scientific advice, and friendship.

I thank Dr. James Beck for being my first teacher in parameter estimation. I learned a slogan ‘Keep it Simple’ from him.

I thank Dr. Ferhan Ozadali for being a great mentor during first 9 months of internship at Nestle Gerber PTC Fremont Research Centre. I thank him for challenging me to apply the rheology knowledge that I had from school to the real world. I thank him and Gene Ford for permitting me to use the DSC. I thank my second mentor, Rolf Bachmann for giving me flexibility in time, and believing in me for rheology work on an ongoing project for seven months.

I thank the Department of Food Technology, University Putra Malaysia for the financial support.

I thank my roommate, Hayati Samsudin for friendship and moral support. I am grateful to Ibrahim's wife Samia and their kids for the love and care. I thank my old friend Ebtesam for her continuous love, friendship, prayer, and moral support.

I thank my labmates and friends in room 129 Food Science, Biosystems Engineering and Packaging for their friendship and good time.

I thank my close friends from the Malaysian student organization, at Gerber, and in Fremont for their help and moral support.

Thanks are extended to all staff in Department of Biosystems & Agricultural Engineering, Department of Food Science & Human Nutrition, and OISS for their resources.

TABLE OF CONTENTS

LIST OF TABLES xi

LIST OF FIGURES xii

CHAPTER 1 ....
INTRODUCTION
1.1 Overview of the Dissertation 2
1.2 Statement of the Problem 3
1.3 Significance of the Study 4
1.4 Objective of the Study 5

CHAPTER 2 ....
OVERVIEW OF LITERITURE REVIEW
2.1 Physicochemical Properties of Native Starches 7
2.2 Effect of Physicochemical Properties of Native Starch on Pasting Curves 7
 2.2.1 Effect of apparent amylose to amylopectin ratio 9
 2.2.2 Effect of Molecular Structure 11
  2.2.2.1 Amylopectin Branch Chain Length 11
  2.2.2.2 Molecular Weight Distribution 12
  2.2.2.3 Granule Size 13
 2.2.3 Effect of Minor Component: Lipid 14
 2.2.4 Summary of the Physicochemical Properties of Native Starch 15
2.3 Characterizing Rheological Behavior of Gelatinizing Starch Solutions 16
 2.3.1 Empirical Method: Pasting Curve using RVA and Others 16
 2.3.2 Fundamental Method: Mixer Viscometry Approach 18
2.4 Rheological Models for Gelatinizing Starch Solutions 19
 2.4.1 Starch Viscosity Model for Gelatinizing Starch Solution 19
 2.4.2 Modifications of Morgan's Model 21
2.5 Summary of Literature 23
References 25

CHAPTER 3 ....
OBJECTIVE ONE
Pasting Curve and Thermal Properties of Gelatinizing Corn Starch
Solutions at Different Amylose to Amylopectin (AM/AP) Ratios
3.1 Introduction 32
3.2 Materials and Methods 35
 3.2.1 Sample Preparation: Corn Starch Blends 36
 3.2.2 Starch Apparent AM/AP Ratio Determination 36
 3.2.3 Rheological Measurement 37
 3.2.4 Thermal Properties of Starches 39
3.3 Results and Discussion 40

3.3.1 Starch Amylose Content 40
3.3.2 Pasting Curves (Apparent Viscosity vs. time) at Different AM/AP Ratios 44
3.4 Differential Scanning Calorimetry Data 52
3.5 Conclusions 57
3.6 Acknowledgement 58
3.7 Nomenclature 59
Appendices A 60
References 82

CHAPTER 4 ....
OBJECTIVE TWO
Estimating Kinetic Parameters in a Starch Viscosity Model
using nonlinear Parameter Estimation Techniques
4.1 Introduction 87
4.2 Overview of Method 89
4.2.1 Mixer viscometer data collection 89
4.2.1.1 Sample Preparation 89
4.2.1.2 Equipment Set Up 90
4.2.2 Rapid Visco Analyzer (RVA) data collection 90
4.2.3 Mathematical Modeling 90
4.2.4 Arrhenius Reference Temperature 93
4.2.5 Parameter Estimation Techniques 94
4.2.5.1 Sensitivity Coefficient Plot 94
4.2.5.2 Ordinary Least Squares (OLS) Estimation Procedure 95
4.2.5.3 Sequential Estimation Procedure 96
4.3 Results and Discussion 97
4.3.1 Reference Temperature Plots 97
4.3.2 Scaled Sensitivity Coefficient Plot 101
4.3.3 Parameter Estimations (OLS) 103
4.3.4 Sequential Parameter Estimations 111
4.3.5 Recommended Corn Starch Viscosity Model 116
4.3.6 Application of the Starch Viscosity Model on RVA Data 118
4.4 Nomenclature 121
Appendices B 123
References 150

CHAPTER 5 ....
OBJECTIVE THREE
Kinetic Parameter Estimation for Starch Viscosity Model
as a Function of Amylose
5.1 Introduction 155
5.2 Overview of Method 156
5.2.1 Sample Preparation 156
5.2.2 Starch Apparent AM/AP Ratio Determination 157
5.2.3 Rheological Measurement: Mixer viscometer Data Collection 157
5.2.4 Starch Viscosity Model 159

5.2.5 Parameter Estimation: Sequential Estimation 161
5.3 Results and Discussion 162
5.3.1 Waxy Corn Starch: OLS and Sequential Estimation 162
5.3.2 Recommended Starch Viscosity Model for Waxy Corn Starch 171
5.3.3 Application of the starch viscosity model on RVA data 173
5.3.4 Parameter Estimation for Corn Starch Blends 176
5.4 Conclusions 184
5.5 Nomenclature 184
Appendices C 184
References 212

Chapter 6 216
Overall Conclusions and Recommendation
6.1 Summary and Conclusions 217
6.2 Recommendations for Future Research 220

LIST OF TABLES

Table 2.1 Some physicochemical and functional properties of common starches 8

Table 2.2 Amylose Contents of Starches…………………………………………………… 11

Table 2.3 Approximate size and shape of common food starch granules……………… 13

Table 3.1 Amylose content in corn starch blends 41

Table 3.2 DSC parameters for corn starch blends…………………………………… 54

Table 4.1 Estimates of parameters and standard deviation from OLS result................104

Table 4.2 Confidence interval of parameters for all three models from OLS result 104

Table 4.3 Percentage relative standard error of parameters for all three models........ 105

Table 4.4Correlation matrix table of parameters for model 1 108

Table 4.5 Correlation matrix table of parameters for model 2 108

Table 4.6 Correlation matrix table of parameters for model 3 109

Table 4.7 Model Comparison using Akaike's Information Criterion (AICc).................. 109

Table 4.8 List of activation energy value of gelatinization for starches........................ 112

Table 4.9 Comparison of the estimated parameters value 112

Table 5.1 Correlation matrix table of parameters for waxy corn starch 166

Table 5.2 Estimates of parameters and standard error for waxy corn starch………. 167

Table 5.3 Estimated parameters, gelatinization reference temperature, RMSE, and SS from OLS result for each corn 178

Table 5.4 Amylose content of starch blends determined experimentally and assumed 179

Table 5.5 Percentage relative standard error for parameters from OLS result for each corn starch blend.. 180

LIST OF FIGURES

Figure 2.1 Changes in starch granule during gelatinization.. 10

Figure 2.2 RVA viscosity profile 17

Figure 3.1 Schematic diagram of Brookfield equipment set up 38

Figure 3.2 Relationship between experimentally measured amylose content and assumed (calculated) amylose content in corn starch blends (all six systems). 44

Figure 3.3 Apparent viscosity profile of corn starch blends for System 1 (waxy and normal corn starch mixtures) 45

Figure 3.4 Apparent viscosity profile of corn starch blends for System 2 (waxy and Hylon V corn starch mixtures) 46

Figure 3.5 Apparent viscosity profile of corn starch blends for System 3 (waxy and Hylon & corn starch mixtures) 47

Figure 3.6 Apparent viscosity profile of corn starch blends for System 4 (normal and Hylon V corn starch mixtures) 47

Figure 3.7 Apparent viscosity profile of corn starch blends for System 5 (normal and Hylon VII corn starch mixtures) 48

FIigure 3.8 Apparent viscosity profile of corn starch blends for System 6 (Hylon V and Hylon VII corn starch mixtures) 48

Figure 3.9 Overall peak viscosity as function of amylose expression for corn starch blends.. 50

Figure 3.10 Overall holding strength viscosity as function of amylose expression for corn starch blends 51

Figure 3.11 Overall setback viscosity as function of amylose (assumed and experimental) expression for corn starch blends 52

Figure 4.1 Correlation behavior of parameters kg and Eg/R in the time-temperature history term as a function of the reference temperature (using heating and cooling data over the total experiment time of 22min) 99

Figure 4.2 Correlation behavior of parameters A^{α} and Ev/R in the temperature term as a function of the reference temperature (using heating data up to 12min) 100

Figure 4.3 Correlation behavior of parameters A^{α} and Ev/R in the temperature term as a function of the reference temperature (using heating and cooling data over the total experiment time of 22min) 100

Figure 4.4 Scaled sensitivity coefficient plots of 8 parameters 102

Figure 4.5 Plots of experimental torque and predicted torque versus time 106

Figure 4.6 Residual scatter plot of difference between observed and predicted torque from model 3 110

Figure 4.7 Plots of frequency versus difference between observed and predicted torque from model 3 110

Figure 4.8 Sequentially estimated parameter of kg 113

Figure 4.9 Sequentially estimated parameter of Eg/R 113

Figure 4.10 Sequentially estimated parameter of A^{α} 114

Figure 4.11 Sequentially estimated parameter of S 114

Figure 4.12 Sequentially estimated parameter of B 115

Figure 4.13 Sequentially estimated parameter of Ev/R 115

Figure 4.14 Inverse problem plots of observed apparent viscosity from experimental data and predicted apparent viscosity from suggested corn starch model (Eq.(15)) versus time using data from modified Brookfield viscometer for native normal corn starch 117

Figure 4.15 Plot of apparent viscosity versus shear rate showing a shear thickening behavior for corn starch 119

Figure 4.16 Plots of observed apparent viscosity from experimental data and predicted apparent viscosity from the corn starch model versus time using data from RVA for native normal corn starch at 6%w/w 120

Figure 5.1 Scaled Sensitivity Coefficient Plots of 5 parameters 163

Figure 5.2 Plot of experimental torque (yobs) and predicted torque (ypred) versus time 163

Figure 5.3 Residual histogram for OLS results in Fig.2 164

Figure 5.4 Residual scatter plot for OLS results in Fig.2 164

Figure 5.5 Correlation between parameters kg and Eg/R in the time-temperature history term as a function of the gelatinization reference temperature.................................. 166

Figure 5.6 Sequential estimation results for five parameters: 1) kg, 2) Eg/R, 3) A^{α}, 4) B, and 5) Ev/R) for waxy corn starch. 168

Figure 5.7 Inverse problem plots of observed apparent viscosity from experimental and predicted apparent viscosity from Eq. (5) versus time using data from modified Brookfield viscometer for native waxy corn starch at 6% w/w. 172

Figure 5.8 Plot of apparent viscosity versus shear rate showing a shear thickening behavior for waxy corn starch 174

Figure 5.9 Plots of observed apparent viscosity versus time for experimental and predicted apparent viscosity (Eq. 5 with S=89.13) from waxy corn starch model using data from RVA for native waxy corn starch at 6%w/w. 175

Figure 5.10 Parameter Eg/R as function of percentage starch amylose content....... 1820

Figure 5.11 Parameter Eg/R as function of percentage starch amylose content....... 1831

Figure 5.12 Gelatinization reference temperature as function of percentage starch amylose content 1831

CHAPTER 1

INTRODUCTION

1.1 Overview of the Dissertation

Starch is the most common carbohydrate polymer in foods. The most important qualities determining the starch functionality are amylose to amylopectin (AM/AP) ratios, viscosity development characteristics, and some other minor constituents of starch content. Different starches have different functional properties. For example, normal corn starch produces an opaque and short paste (not stringy), and gives a strong gel structure. On the other hand, waxy corn and potato starches produce clear and long pastes (sticky and stringy), with less tendency to set into gels. These differences are expected and may be due to the amylose content and the presence of phosphate derivates (Jane and Chen 1992).

Rheology is a term used to define the study of flow of matter. Rheological studies describe how a material behaves when exposed to certain stress and strain (Steffe 1996). There are two methods to measure rheological properties of aqueous starch solutions: fundamental and empirical. Rheological properties of starches determined using a fundamental approach are independent of the instrument used to acquire data, which means different instruments will yield the same results. According to Steffe (1996), common instruments capable of measuring fundamental rheological properties are divided into two major categories: rotational type (parallel plate, cone and plate, concentric cylinder, and mixer); and tube type (glass capillary, high pressure capillary, and pipe). Most rheological measurements of native starches are done using an empirical approach with instruments such as the Rapid Visco Analyzer (RVA), Brookfield and the Brabender Viscoamylograph, where the rheological data obtained are instrument dependent.

One can study the rheological behavior of gelatinizing starch solutions using the steady shear mixer viscometry approach. The results of these fundamental studies showed that the apparent viscosity of gelatinizing starch solutions is strongly influenced by time-temperature history and temperature (thermal effects); shear history and impeller speed (mechanical effects); and concentration (Dolan and Steffe 1990). A limitation of that work was that the effect of starch composition (mainly AM/AP ratios) and simultaneous parameter estimation were not taken into account in the mathematical model describing changes in apparent viscosity. Therefore, it is necessary to apply thorough parameter estimation techniques to estimate the parameters simultaneously in the existing model for well defined starch formulations.

1.2 Statement of the Problem

1. There are no fundamental rheological data or thermal properties data, and no generalized rheological model, for gelatinizing starch solutions with different amylose to amylopectin ratios for corn starch.

2. Sophisticated parameter estimation techniques have not been use to determine the best parameters in rheological models for gelatinizing starch solutions.

3. There are no published reports comparing or predicting results obtained from an empirical instrument (such as the RVA) and a fundamental instrument (such as a mixer viscometer) for gelatinizing corn starch solutions at different AM/AP ratios.

1.3 Significance of the Study

1. This work will provide an innovative experimental approach that includes the effect of apparent AM/AP ratios on apparent viscosity using a mixer viscometry approach. The data from steady shear testing will be used for developing a torque model based on composition (different apparent AM/AP ratio), and the parameters in the model will be estimated simultaneously, and then sequentially using advanced parameter estimation techniques.

2. The mathematical model will help process engineers in designing pumping systems for starch-based products, and will be useful for food and non-food product developers in their formulations by predicting apparent viscosity of native starch when exposed to certain processing conditions. Fundamental rheological data, thermal properties data, and the apparent viscosity predictions will help minimize trial and error work, will save money in formulation, and improve thermal process calculations and engineering process design.

1.4 Objective of the Study

The specific objectives of this study are:

1. To obtain pasting curves and thermal properties (gelatinization temperature and enthalpy) of gelatinizing corn starch solution at different amylose to amylopectin (AM/AP) ratios using a mixer viscometry approach and DSC, respectively;

2. To estimate parameters in the existing starch viscosity model and to show a comprehensive procedure to estimate the parameters simultaneously and sequentially using thorough parameter estimation techniques; and

3. To develop and validate a composition-based model for pasting curves of gelatinizing starch solutions as a function of AM/AP ratio.

This dissertation is composed of various sections. Chapter 2 contains the literature review. The remaining chapters of the dissertation consist primarily of three journal articles: Chapter 3, 4, and 5, based on each objective studied, respectively. The final section of this dissertation (Chapter 6) gives the overall conclusions and recommendations from the research.

CHAPTER 2

OVERVIEW OF LITERATURE REVIEW

2.1 Physicochemical Properties of Native Starches

The starch granule is composed of amylose and amylopectin that makes up to 98-99% of the starch dry weight. Amylose is a linear glucose unit joined by alpha (1-4) linkages. Amylopectin is a branched structure with glucose units joined by alpha (1-6) linkages at the branch points and alpha (1-4) linkages in the linear parts. The remainders are lipids, proteins, and phosphorus. The lipid content of native starches is related to the amylose content: the higher amylose content the more lipids are present in the native cereal starches. The starch granules usually have a moisture content of about 10% (Kearsley 1989; Copeland and others 2009). Table 2.1 gives a summary of physicochemical properties of some common starches. The remaining percentage in Table 2.1 is the amylopectin.

2.2 Effect of Physicochemical Properties of Native Starch on Pasting Curves

At the same ratio of starch to water, different starches give different pasting profiles. In general, the different characteristics of native starches in gelatinization temperature, viscosity, retrogradation, clarity after cooking and cooling, texture, and taste are due to the AM/AP ratio, molecular structure (size, shape, crystallinity, amylopectin branch chain length, and molecular weight) and minor constituents (lipid, protein, and phosphate). Many investigators have concluded that the viscosity profile and starch gelatinization temperature depend on the physico-chemical properties of the starches as well as the physical environment that starch is subjected to during gelatinize (Liu and others 2006; Noda and others 1998; Jane and others 1999; Tester and Morrison 1990; Sasaki and others 2000; Chang and Lin 2007). Starch paste

Table 2.1 Some physicochemical and functional properties of common starches

	CORN	WAXY CORN	WHEAT	POTATO	TAPIOCA
Amylose content (%)	28	0	28	21	17
Lipids content (%)	0.7-0.8	0.15-0.2	0.8-0.9	0.05-0.1	0.1
Protein content (%)	0.35	0.25	0.4	0.06	0.1
Phosphorus content (%)	0.02	0.01	0.06	0.08	0.01
Pasting Temperature, ^{o}C	75-80	65-70	80-85	60-65	65-70

Source: Yuryev, Tomasik and Ruck (2004)

has characteristic properties such as clarity, viscosity, texture, stability and taste. These properties depend on the degree of gelatinization. Therefore, the gelatinization profile of a starch is of major importance in comparing and controlling the behavior of different starches during industrial cooking (Kearsley 1989).

2.2.1 Effect of apparent amylose to amylopectin ratio

During gelatinization, the granular changes that occur can be reflected in viscosity profile (also known as pasting curve) as shown in Figure 2.1. At the initial heating stage, a rise in viscosity is due to granules starting to swell and amylose leaching out from the granules. The peak viscosity occurs when the majority of the granules are fully swollen. At the high- temperature hold stage, a drop in viscosity happens due to the granules breaking down within the shear field of the instrument. According to Lillford (1997), further shear not only solubilises but also shears the amylopectin molecules, which causes a large drop in molecular weight of amylopectin and leads to a subsequent viscosity drop. The cooling stage, referred as ‘set-back’, gives a second rise in viscosity because the amylose and amylopectin begin to reassociate (Thomas and Atwell 1999; Kearsley 1989). All these studies show that the AM/AP ratio present in the starch actually governs the overall pasting curve pattern. The amylose contents of some starches are shown in Table 2.2.

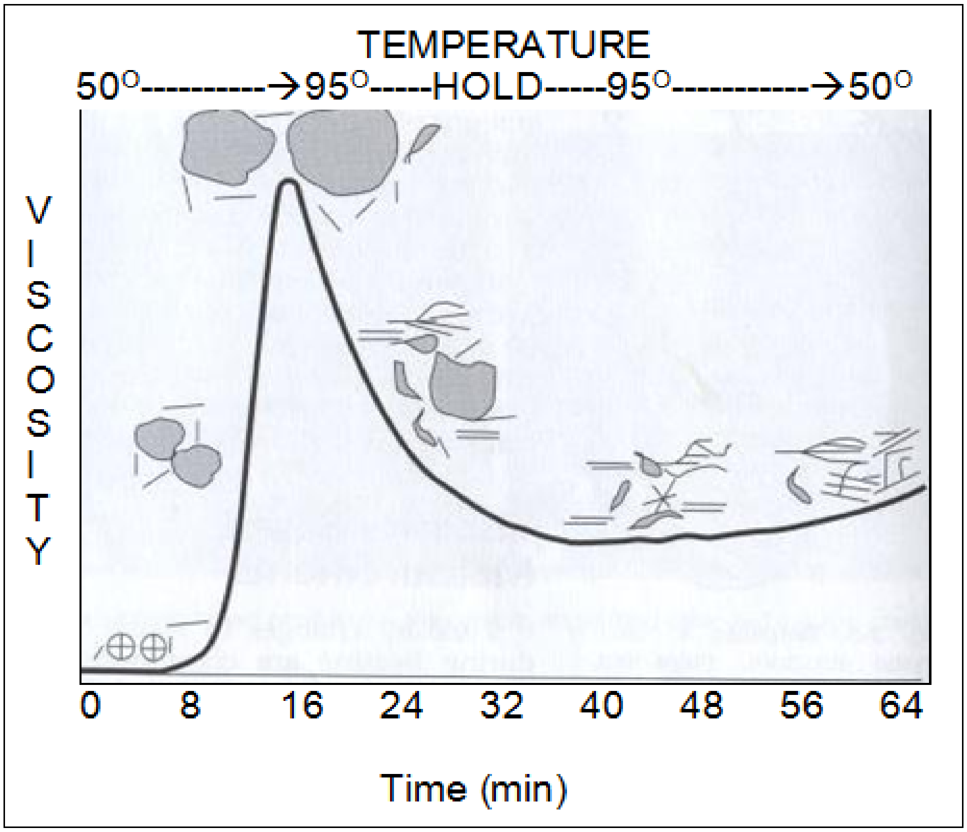

Figure 2.1 Changes in starch granule during gelatinization as reflected by the viscosity profile. Source: (Thomas and Atwell 1999)

Table 2.2 Amylose Contents of Starches
source: (Jane et al. 1999)

Source	Apparent amylose, %	Absolute amylose, %
A-type starch:		
Normal maize	29.4	22.5
Rice	25.0	20.5
Wheat	28.8	25.8
Barley	25.5	23.6
Cattail millet	19.8	15.3
Mung bean	37.9	30.7
Chinese Taro	13.8	13.8
Tapioca	23.5	17.8
B-type starch:		
Amylomaize V	52.0	27.3
Amylomaize VII	68.0	40.2
Potato	36.0	16.9
Green leaf canna	43.2	22.7
C-type starch:		
Water chestnut	29.0	16.0

2.2.2 Effect of Molecular Structure

2.2.2.1 Amylopectin Branch Chain Length

The amylopectins from five waxy cereal starches (rice, corn, wheat, barley, and sorghum) have been studied showed no difference in the average chain length (Chang and Lin 2007; Chung and others 2008). Similar results were observed for 51 samples of sweet potato roots and 27 kinds of buckwheat seeds differing in variety and/or cultivation conditions. These studies concluded that the differences in the amylopectin chain length were small within the same botanical origin (Noda et al. 1998). The branch chain length distributions of amylopectins having a shoulder of dp 18-21 (chain length of

6.3-7.4nm) were found in many starches, and generally had a lower gelatinization temperature (Song and Jane 2000; Jane et al. 1999).

2.2.2.2 Molecular Weight Distribution

High amylose content is always correlated to smaller molecular weights and has a broader molecular weight distribution (Noda et al. 1998; Jane et al. 1999; Hanashiro and others 1996; Song and Jane 2000; Park and others 2007). Waxy (~ pure amylopectin) starches show higher molecular weight than high amylose corn starch (Chen and others 2006). Average molecular weights of five waxy cereal amylopectins starches (corn, sorghum, barley, wheat, and rice) were reported to range from 204×10^6 to 344×10^6 g/mol (Chung et al. 2008). In studying the relationship of rice starch molecular size with amylose contents (1%-20%), (Park et al. 2007) found that higher weight-average molar masses (M_W) of rice starch correlated to lower amylose content ranging from 0.82 to 2.5×10^8 g/mol to 2.2 to 8.3×10^5 g/mol, respectively. The molecular weight measured by GPC provided by Penford (Lane Cove, NSW Australia) for maize starches with different amylose/amylopectin contents (waxy: 0/100; normal maize: 23/77; Gelose 50: 50/50; Gelose 80: 80/20) were 20,787,000; 13,000,000; 5,115,000; 673,000; respectively (Chen et al. 2006). Waxy starches have higher molecular weights than the high amylose cultivar maize. These studies showed that there is a correlation between molecular weight and the AM/AP ratios present in the starch.

2.2.2.3 Granule Size

The average granule size of maize starches with different apparent AM/AP ratios (waxy: 0/100; normal maize: 23/77; Gelose 50: 50/50; Gelose 80: 80/20) were 12.1, 10.9, 9.6, and 8.1μm, respectively (Chen et al. 2006). The size range and shapes of corn starch varieties (dent corn, waxy corn, and high amylose corn) are very similar (Thomas and Atwell 1999).

The size and shape of the granules depends on the source of the starch (Kearsley 1989). Approximate size and shape for some common food starch granules are shown in Table 2.3. The table shows that the range of diameter and shape for dent corn, waxy corn, and high amylose corn are similar. Amylopectin starches tend to be more regular in shape compare to high amylose starches (Yuryev 2002; Jayakody and Hoover 2008).

Table 2.3 Approximate Size and Shape of Common Food Starch Granules (Source: Alexander, 1995)

Starch	Property		
	Diameter(μm)	Shape	Source
Dent corn	5-30	Polygonal, round	Cereal
Waxy corn	5-30	Polygonal, round	Cereal
High amylose	5-30	Polygonal, round, irregular	Cereal
Wheat	1-45	Round, lenticular	Cereal
Rice	1-3	Polygonal, spherical	Cereal
Potato	5-100	Oval, spherical	Tuber
Tapioca	4-35	Oval, truncated, “kettle drum”	Root

According to Andreev (2002), the granule sizes and amylose content are the factors that most influence thermodynamic and rheology features of native starch dispersions in water. In general, starch granule size varies from less than 1μm to more than 100μm. The granule size refers to the average diameter of the starch granules. Although there is no precise categorization of granule size, Lindeboom and others (2004) used the following guidelines: large (>25μm), medium (10-25μm), small (5-10μm) and very small (<5μm) granules. The approximate trend in granule size of starch granules may be described as: rice<corn<barley<pea<wheat<rye<potato (Yuryev 2002; Alexander 1995).

2.2.3 Effect of Minor Component: Lipid

Other physico-chemical properties of starch are reported to be correlated with amylose content as well. For example the lipid content of native starches is related to the amylose content such that the higher the amylose content, the more lipids are present in the native starch (Copeland et al. 2009). Similar observations were made by Yoshimoto and others (2000): high-amylose cultivars of barley had a higher proportion of amylose-lipid complex than did normal barley starch. The formation of amylose-lipid complexes happens only when starch dispersions are heated (Yuryev 2002).

Andreev and others (1999) summarized that amylose macromolecules interact with lipid, fatty acids and other hydrophobic components present. Lipids present at the starch surface could shift inside the starch granule to form more amylose-lipid complexes.

Lindeboom and others (2004) found that the dissociation enthalpy of the amylose-lipid complexes of small granules is higher than large granules and could be based on the higher lipid content present in B-type wheat granules. The small granules contain more amylose and lipids (Vasanthan and Bhatty 1996). The B-granules had more lipid than the A-granules, suggesting that lipid content was responsible for the differences in swelling factor (Tester and Morrison 1990). These studies show that there is a relationship between starch amylose content and the lipid content present in the starch.

2.2.4 Summary of the Physicochemical Properties of Native Starch

Based on most studies reported, it appears that the amylose content has an influence on the molecular structure and minor component composition. Opposite to starch molecular structure and minor components, the apparent amylose to amylopectin content of starch has a significant effect on the pasting curve. High amylopectin contents result in a high peak viscosity, and amylose content is associated with ‘set back’ viscosity. If one assumes the composition of starch has an effect on the pasting curve of starch, then studies based on amylose and amylopectin content of the starches would be essential in representing the composition effect on starch pasting curves

2.3 Characterizing Rheological Behavior of Gelatinizing Starch Solutions

Lagarrigue and Alvarez (2001) reviewed experimental devices and methods used to obtain rheological data for starch dispersions. The comprehensive review concludes that many researchers have studied starch dispersions during gelatinization below 95^{o}C in two ways. All measurements were made using empirical instruments (equipment dependent measurements) such as Brabender Visco/Amylograph, RVA, and the Ottawa starch viscometer, or using mixer viscometry (equipment independent approach) where the average shear rate could be calculated. The review also states that the rest of the studies on rheological measurements are carried out using rotational rheometers with different geometries such as concentric cylinder, cone and plate or parallel plates, where some were capable of running at high temperatures and high shear rates using pressurized rotational rheometers; and mostly done on 'gelatinized' starch (cold water soluble) dispersions because 'ungelatinized' starch (cold water insoluble) will have sedimentation and water evaporation problems.

2.3.1 Empirical Method: Pasting Curve using RVA and Others

There are many common instruments used to measure starch slurry viscosities: Viscoamylograph (C.W. Brabender, Inc., South Hackensack, NJ), the Ottawa Starch Viscometer, and the Rapid Visco Analyser (RVA) (Newport Scientific Pty. Ltd, Warriewood, NSW, Australia). These instruments generate highly reproducible results using controlled mixing, heating, and cooling programs. Brabender and RVA viscometers use arbitrary units of measurement such as the Brabender Unit (Burhin and others 2003) and the Rapid Visco Unit (RVU), respectively. Many possible cooking conditions also can be achieve by different heating and cooling programs to gelatinize starch, which yields a wide variety of viscoamylograms (Thomas and Atwell 1999).

Haase and others (1995) studied the viscosity measurement of potato starch paste with the RVA. Standard profile 1 of RVA (13 min including heating, stable hot paste, and cooling) is shown in Figure 2.2. The viscosity profile is very helpful in determining starch behavior under various processing conditions. It can illustrate relative differences between starches when the procedure is kept constant over time.

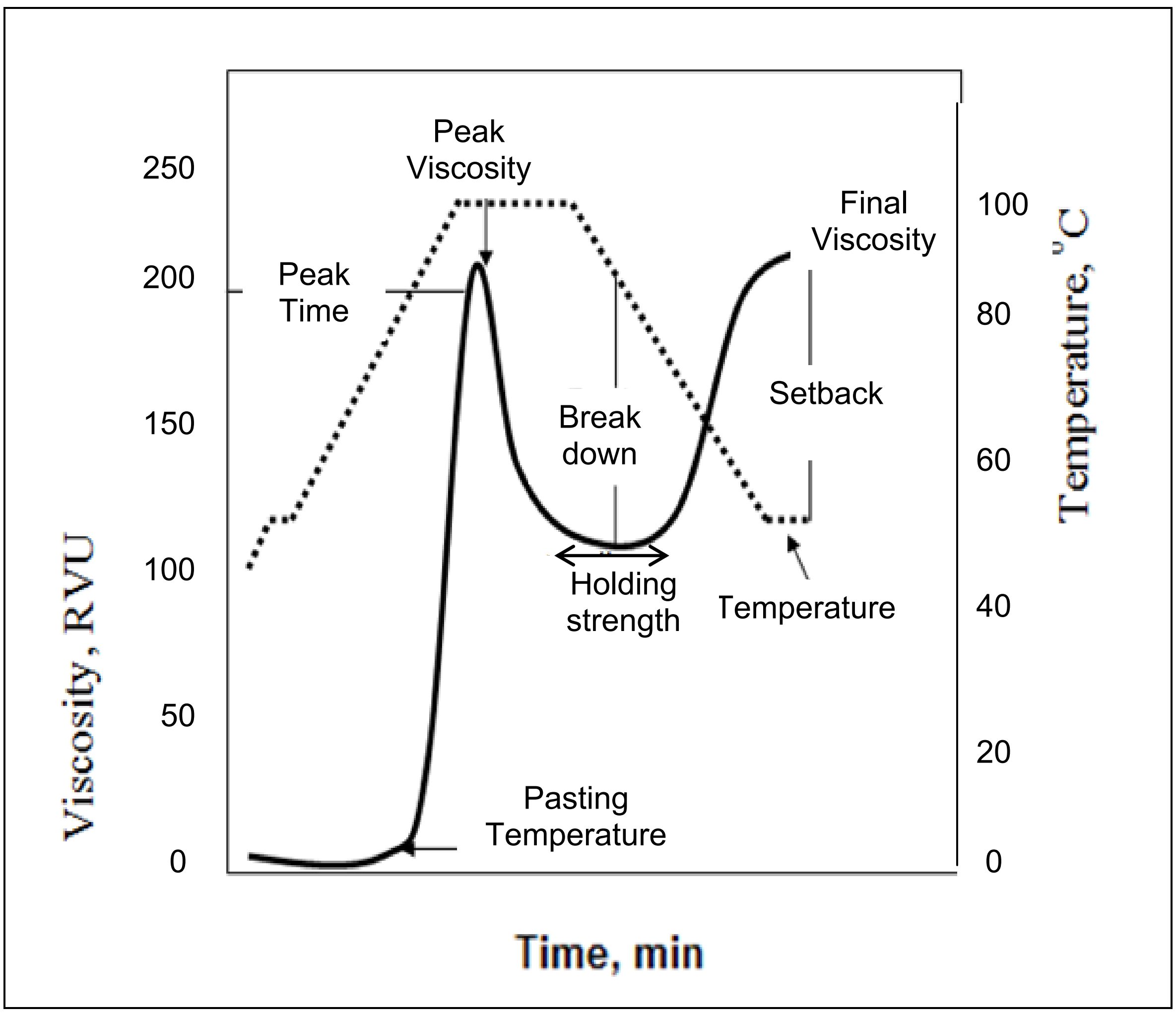

Figure 2.2. RVA viscosity profile. Source: (Haase et al. 1995)

Initially, the RVA was developed to evaluate pasting behavior as a quick test for sprout damage in the Australian wheat industry (Walker and others 1988). The RVA is now used widely to study starch gelatinization behavior. Lack of instrument–to-instrument reproducibility, non uniform sample temperature (Hazelton and Walker 1996), and unknown shear rates indicated a need for an improvement. The average shear rates in the RVA mixing system were determined using the mixer viscometry method (Lai and others 2000). Although, there have been many improvements in the RVA instruments, the temperature measurement is still taken in one place and the sample size is large. A comprehensive fundamental approach using mixer viscometry techniques could enhance technological advancement in empirical instruments currently in use.

2.3.2 Fundamental Method: Mixer Viscometry Approach

Starch rheology, using mixer viscometry which provides a more fundamental rheological testing approach, was first developed by Steffe and others (1989) as a response to a need expressed by the wet corn milling industry for new instrumentation to evaluate the rheological behavior of gelatinizing normal corn starch slurries. They developed a mixer system using the Brookfield RVTD viscometer with a modified Brookfield small adapter, equipped with a flag impeller and thermocouple, to evaluate the flow behavior of 6% d.b. normal corn starch slurries during gelatinization.

According to Steffe and Daubert (2006), laborious and time consuming work has been done to characterize the mixer constants for different laboratory-scale mixer impellers. The mixer viscometry approach is needed when studying rheological fluids with large particles, or for fluids having settling problems, or phase separation issues. The apparent viscosity is proportional to torque; and average shear rate is proportional to the impeller speed. Many studies have been done on rheological properties of starch-based products using mixer viscometry techniques (Ford and Steffe 1986; Castellperez and others 1988; Mackey and others 1987; Castellperez and Steffe 1990; Dolan and Steffe 1990; Castellperez and others 1991; Omura and Steffe 2003).

Currently, empirical instruments are widely used to determine pasting curves of gelatinizing starch solutions. The rheological data collected from these instruments vary from instrument to instrument and give empirical results that are only suitable for quality control purposes. Results from empirical instruments have no value in pipeline design calculations. The mixer viscometry provides a valuable method to document the 'true' apparent viscosity profile (pasting curves) of gelatinizing starch solutions.

2.4 Rheological Models for Gelatinizing Starch Solutions

2.4.1 Starch Viscosity Model for Gelatinizing Starch Solution

Dolan and Steffe (1990) assumed a first-order kinetic reaction for starch gelatinization. Five independent variables (temperature-time history, strain history, temperature, concentration and impeller speed) were identified as the most important independent variables influencing rheological properties of gelatinizing starch solutions. Each of the five independent variables was varied individually with all others held constant, to estimate the model parameters. The estimated parameters were used to predict pasting curves in the mixer viscometer. The model was based from the work of

Morgan et al. (1989) for extrusion of protein doughs as shown in Eq. (1):

$$\eta = T * MC * SR * tTH * SH$$

where

$$T = e^{\frac{\Delta E_v}{R}\left(T^{-1} - T_r{}^{-1}\right)}$$

$$MC = e^{b(MC - MC_r)}$$

$$SR = \left[\left(\frac{\tau_r}{\dot{\gamma}}\right)^n + \mu_r^n\right]^{\frac{1}{n}}$$

$$tTH = \left[1 + \beta_r \left[A_3 \left(MC\right)^{\varepsilon} C_p\right]^{\alpha(\dot{\gamma})} \left(1 - e^{-k_a \psi}\right)^{\alpha(\dot{\gamma})}\right]$$

$$SH = \left[1 - \beta_o \left(1 - e^{-d\phi}\right)\right]$$

The increase of apparent viscosity in protein is due to protein denaturation, while for starch it is due to starch gelatinization. Dolan and Steffe (1990), showed the feasibility of using Morgan et al. (1989), model with some modification, to study the apparent viscosity of gelatinizing starch solutions.

2.4.2 Modifications of Morgan's Model

Several of assumptions were made in Dolan and Steffe (1990) model to modify the Morgan et al. (1989) model.

- The dry basis starch concentration, C_p was set to 1. Assumption: No composition effect since only starch and moisture content present in corn starch.
- In an excess-water system, the molecular weight of gelatinized starch independent of moisture. This makes ε=0. Shear rate is varied, but the dependence of α on shear rate was not investigated. Therefore, β and A_3 were combined as one constant, A. Assumption: No dependence upon maximum shear rate.
- Assuming no elastic effects, in the dilute starch solution, the Heinz-Casson model is replaced by power law model: $\eta = K\left(\dot{\gamma}\right)^{n-1}$.

The shear rate term is replaced with power law equation instead of Heinz-Casson model. Torque (M) can replace η on the left side by using the two basic assumptions of mixer viscometry: shear stress is directly proportional to torque, and shear rate is directly proportional to impeller speed. Substituting N for $\dot{\gamma}$ yields Eq. (2):

$$M = SR * T * MC * tTH * SH$$

Where

$$SR = K_r N^n$$

$$T = \left[e^{\frac{E_v}{R}\left(T^{-1}\right)} \right]$$

$$MC = e^{b(MC - MC_r)}$$

$$tTH = \left[1 + A^{\alpha} \left(1 - e^{-k\psi} \right)^{\alpha} \right]$$

$$SH = \left[1 - \beta_o \left(1 - e^{-d\phi} \right) \right]$$

where

$$\psi = \int_0^{t_f} T(t)\, e^{\frac{-E_g}{R}\left(\frac{1}{T(t)}\right)} dt$$

$$\phi = \int_0^{t_f} N dt = Nt$$

Dolan and Steffe (1990) evaluated the model given using 6.4% native normal corn starch solutions. The model was further tested using a 6%d.b. bean starch solution.

2.5 Summary of Literature

Corn starch contains much a broader composition variation compared to other cereal starches. Waxy, normal, and high amylomaize starches are composed of different apparent AM/AP ratios. The United States ranks as the world's largest grower of corn. The native corn starches are utilized by the food industry in condiments, desserts, baby food, syrup, soups, fruit fillings, and gum; and by the non-food industry in papermaking, building materials, pastes. Many of these applications require the knowledge of starch viscosity (Corn Refiners Associations 2006). Therefore, documenting the rheological and thermal properties of these corn starches and predicting the pasting model using absolute measurements (equipment independent data) can be very useful in commercial applications.

This leads to the overall summary of the literature that been discussed in this chapter:

1. Apparent amylose to amylopectin ratios could represent the overall starch compostion effect on the starch pasting curve; and measurements of the apparent amylose content of starch will take into account the role of molecular structure.

2. The mixer viscometry approach, using a modified Brookfield viscometer, could be useful to determine fundamental rheological data of the starch pasting curve compared to most instruments that only give empirical results.

3. A composition-based model (including apparent AM/AP ratios of corn starches) obtained through simultaneous, and sequential parameter estimation, will give a generic predictive model for cereal starch pasting curves.

REFERENCES

References

Alexander RJ. 1995. Potato Starch - New Prospects for an Old Product. Cereal Foods World 40(10):763-764.

Andreev NR. 2002. Chapter 12: Classification of Native Starches and Starch Content Raw Materials. In Book Dietary Starches and Sugars in Man: A Comparison In book Starch and Starch containing origins: Structure, Properties and New Technologies by Yuryev V.P, Cesaro A., and Bergthaller W.J. (2002).165-175.

Andreev NR, Kalistratova EN, Wasserman LA & Yuryev VP. 1999. The influence of heating rate and annealing on the melting thermodynamic parameters of some cereal starches in excess water. Starch-Starke 51(11-12):422-429.

Ballman RL & Simon R. 1964. Cited in Collins and Bauer (1965). J.Polymer Sci.A2:3557.

Bird RB, Stewart WE & Lightfoot EN. 1960. Transport Phenomena. John Wiley & Sons, New York.

Burhin HG, Rodger ER & Kiener P. 2003. Compound visco-elastic measurements and neural network software modelling - Proactive extrusion control through die swell prediction. Kautschuk Gummi Kunststoffe 56(9):444-449.

Casson N. 1959. A flow equation for pigment-oil suspensions of the printing ink type. Ch.5, In Rheology of Disperse Systems, (C.C. Mill, ed.) Pergamon Press.

Castellperez ME & Steffe JF. 190. Evaluating Shear Rates for Power Law Fluids in Mixer Viscometry. Journal of Texture Studies 21(4):439-453.

Castellperez ME, Steffe JF & Moreira RG. 1991. Simple Determination of Power Law Flow Curves Using a Paddle Type Mixer Viscometer. Journal of Texture Studies 22(3):303-316.

Castellperez ME, Steffe JF & Morgan RG. 1988. Adaptation of a Brookfield (Hbtd) Viscometer for Mixer Viscometry Studies. Journal of Texture Studies 18(4):359-365.

Cervone NW & Harper JM. 1978. Viscosity of an intermediate moisture dough. J.Food Proc. Eng. 2:83-95.

Chang YH & Lin JH. 2007. Effects of molecular size and structure of amylopectin on the retrogradation thermal properties of waxy rice and waxy cornstarches. Food Hydrocolloids 21(4):645-653.

Chen P, Yu L, Chen L & Li XX. 2006. Morphology and microstructure of maize starches with different amylose/amylopectin content. Starch-Starke 58(12):611-615.

Chung JH, Han JA, Yoo B, Seib PA & Lim ST. 2008. Effects of molecular size and chain profile of waxy cereal amylopectins on paste rheology during retrogradation. Carbohydrate Polymers 71(3):365-371.

Collins EA & Bauer WH. 1965. Analysis of flow properties in relation to molecular parameters for polymer melts. Tran. Soc.Rheol. 9(2):1-16.

Copeland L, Blazek J, Salman H & Tang MCM. 2009. Form and functionality of starch. Food Hydrocolloids 23(6):1527-1534.

Corn Refiners Associations. 2006. Corn Starch. 11th Edition Corn Refiners Association, Pennsylvania Avenue, Washington, D.C.(www.corn.org).

Darby R. 1976. Viscoelastic Fluids, an introduction to their properties and behavior. Marcel Dekker New York.

Dolan KD. 1989. Modeling the rheological behavior of gelatinizing starch solutions. Ph.D. Dissertation, Agricultural Engineering, Michigan State University.

Dolan KD & Steffe JF. 1990. Modeling Rheological Behavior of Gelatinizing Starch Solutions using Mixer Viscometry Data. Journal of Texture Studies 21(3):265-294.

Eyring H & Stearn AE. 1939. The application of the theory of absolute reaction rates to proteins. Chemical Reviews, 24:253-270.

Ferry JD. 1970. Viscoelastic Properties of Polymers. 2nd ed. John Wiley & Sons, New York.

Ford EW & Steffe JF. 1986. Quantifying Thixotropy in Starch-Thickened, Strained Apricots Using Mixer Viscometry Techniques. Journal of Texture Studies 17(1):71-85.

Glasstone S, Laidler KJ & Eyring H. 1941. Theory of rate processes. McGraw-Hill, New York.

Haase NU, Mintus T & Weipert D. 1995. Viscosity Measurements of Potato Starch Paste with the Rapid-Visco-Analyzer. Starch-Starke 47(4):123-126.

Hanashiro I, Abe J & Hizukuri S. 1996. A periodic distribution of the chain length of amylopectin as revealed by high-performance anion-exchange chromatography. Carbohydrate Research 283:151-159.

Harper JM. 1981. Extrusion of foods. Vol.1, CRC Press, Boca Raton,FL.

Harper JM, Rhodes TP & Wanninger J. 1971. Viscosity model for cooked cereal doughs. Amer. Inst. Chem. Engl. Symp. Serv. No.108.

Hazelton JL & Walker CE. 1996. Temperature of liquid contents in RVA cans during operation. Cereal Chemistry 73(2):284-289.

Heinz W. 1959. Quoted in Fincke, A. 1961. Beitrage zur Losung rheologischer Probleme in der Schokoladentechnologie. Dissertation, TH Karlsruhe.

Huang B. 1983. Protein reactions in texturizing extruders. Ph.D. dissertation,Univ. of Massachusetts. Univ. Microfilm International, Ann Arbor,MI.

Jane J, Chen YY, Lee LF, McPherson AE, Wong KS, Radosavljevic M & Kasemsuwan T. 1999. Effects of amylopectin branch chain length and amylose content on the gelatinization and pasting properties of starch. Cereal Chemistry 76(5):629-637.

Jane JL & Chen JF. 1992. Effect of Amylose Molecular-Size and Amylopectin Branch Chain-Length on Paste Properties of Starch. Cereal Chemistry 69(1):60-65.

Jayakody L & Hoover R. 2008. Effect of annealing on the molecular structure and physicochemical properties of starches from different botanical origins - A review. Carbohydrate Polymers 74(3):691-703.

Kearsley MWaS, P.J. 1989. Chapter 1: The Chemistry of Starches and Sugars Present in Food. In Book Dietary Starches and Sugars in Man: A Comparison Edited by John Dobbing(Springer-Verlag, ILSI Human Nutrition Reviews):1-7.

Lagarrigue S & Alvarez G. 2001. The rheology of starch dispersions at high temperatures and high shear rates: a review. Journal of Food Engineering 50(4):189-202.

Lai KP, Steffe JF & Ng PKW. 2000. Average shear rates in the rapid visco analyser (RVA) mixing system. Cereal Chemistry 77(6):714-716.

Lillford PJaM, A. 1997. Structure/Function Relationship of Starches in Food. in Book Starch: Structure and Functionality edited by P.J. Frazier, A.M. Donald and P.Richmond(The Royal Society of Chemistry. Thomas Graham House, Science Park, Milton Road, Cambridge, UK.):1-8.

Lindeboom N, Chang PR & Tyler RT. 2004. Analytical, biochemical and physicochemical aspects of starch granule size, with emphasis on small granule starches: A review. Starch-Starke 56(3-4):89-99.

Liu HS, Yu L, Xie FW & Chen L. 2006. Gelatinization of cornstarch with different amylose/amylopectin content. Carbohydrate Polymers 65(3):357-363.

Luxenburg LA, Baird DG & Joseph EG. 1985. Background studies in the modeling of extrusion cooking processes for soy flour doughs. Biotechnology Progress 1(1):33-38.

Mackey KL, Morgan RG & Steffe JF. 1987. Effects of Shear-Thinning Behavior on Mixer Viscometry Techniques. Journal of Texture Studies 18(3):231-240.

Metzner AB. 1959. Flow behavior of thermoplastics. In processing of thermoplastic materials. E.C. Bernhardt, ed Van Nostrand Reinhold Co., New York.

Morgan RG. 1979. Modeling the effects of temperature-time history, temperature, shear rate and moisture on viscosity of defatted soy flour dough. . Ph.D. dissertation. Agricultural Engineering. Texas A&M University.:1-114.

Morgan RG, Steffe JF & Ofoli RY. 1989. A generalized viscosity model for extrusion of protein doughs. J. Food Process Engr. 11:55-78.

Noda T, Takahata Y, Sato T, Suda I, Morishita T, Ishiguro K & Yamakawa O. 1998. Relationships between chain length distribution of amylopectin and gelatinization properties within the same botanical origin for sweet potato and buckwheat. Carbohydrate Polymers 37(2):153-158.

Omura AP & Steffe JF. 2003. Mixer viscometry to characterize fluid foods with large particulates. Journal of Food Process Engineering 26(5):435-445.

Park IM, Ibanez AM & Shoemaker CF. 2007. Rice starch molecular size and its relationship with amylose content. Starch-Starke 59(2):69-77.

Sasaki T, Yasui Ta & Matsuki J. 2000. Effect of amylose content on gelatinization, retrogradation, and pasting properties of starches from waxy and nonwaxy wheat and their F1 seeds. Cereal Chemistry 77(1):58-63.

Song Y & Jane J. 2000. Characterization of barley starches of waxy, normal, and high amylose varieties. Carbohydrate Polymers 41(4):365-377.

Steffe JF. 1996. Rheological Methods in Food Process Engineering. Second Edition Freeman Press(East Lansing, MI):2.

Steffe JF, Castellperez ME, Rose KJ & Zabik ME. 1989. Rapid Testing Method for Characterizing the Rheological Behavior of Gelatinizing Corn Starch Slurries. Cereal Chemistry 66(1):65-68.

Steffe JF & Daubert CR. 2006. Bioprocessing Pipelines: Rheology and Analysis. Freeman Press, East Lansing, MI, USA:1-32.

Tester RF & Morrison WR. 1990. Swelling and Gelatinization of Cereal Starches .1. Effects of Amylopectin, Amylose, and Lipids. Cereal Chemistry 67(6):551-557.

Thomas DJ, & Atwell WA. 1999. Starches: Practical Guides For The Food Industry. Eagan Press Handbook Series Eagan Press. St. Paul, Minnesota, USA.

Vasanthan T & Bhatty RS. 1996. Physicochemical properties of small- and large-granule starches of waxy, regular, and high-amylose barleys. Cereal Chemistry 73(2):199-207.

Walker CE, Ross AS, Wrigley CW & Mcmaster GJ. 1988. Accelerated Starch-Paste Characterization with the Rapid Visco-Analyzer. Cereal Foods World 33(6):491-494.

Williams DJ. 1971. Polymer Science in Engineering. Prentice-Hall Englewood Cliffs, New Jersey.

Yoshimoto Y, Tashiro J, Takenouchi T & Takeda Y. 2000. Molecular structure and some physicochemical properties of high-amylose barley starches. Cereal Chemistry 77(3):279-285.

Yuryev VPW, Luybov A.; Andreev,Nicolai R. ; and Tolstoguzov,Vladimir B. . 2002. Chapter 2:Structural and Thermodynamic Features of Low- and High Amylose Starches. A Review. in Book Starch and Starch Containing Origins: Structure, Properties and New Technologies:47-48.

CHAPTER 3

OBJECTIVE ONE

Pasting Curve and Thermal Properties of Gelatinizing Corn Starch Solutions at Different Amylose to Amylopectin Ratios

Abstract

The pasting curve and thermal properties of 24 native corn starch mixtures (6%w/w concentration) with different amylose to amylopectin (AM/AP) ratios prepared from the four base native corn starches (waxy, normal, Hylon V and Hylon VII) were studied using the modified Brookfield viscometer by applying a mixer viscometry approach and differential scanning calorimetry, respectively. The AM/AP ratio of the starches was initially determined by using the Concanavalin A (Megazyme procedure). A data acquisition system with Labview was used to record continuous torques readings with time. The data were used to characterize the viscosity profile of the starches. Empirical relationships of the pasting curve points (peak viscosity, holding strength, and the setback viscosity) were obtained as a function of the AM/AP ratio. Overall, the pasting curve points decreased with the AM/AP ratio. DSC parameters were obtained at temperatures below 110^{o}C for 30% AM/AP ratios on all the corn starch mixtures studied. The enthalpy value of corn starch mixtures increased with increased in amylopectin.

Keywords: Corn Starch; Rheology; Gelatinization; Differential Scanning Calorimetry; Amylose/Amylopectin; Mixer viscometry ; Brookfield Viscometer

3.1 Introduction

Starch is the main storage carbohydrate of plants and its unique chemical and physical characteristics set starch apart from all other carbohydrates. It is utilized by industry for food and non-food application (Thomas and Atwell 1999). Starches are mainly composed of glucose: two different polymers of D-glucose: amylose and amylopectin. Naturally occurring starch contains relatively constant amylose contents of about 23± 3% amylose in most cereal starches. However, mutants that have changed AM/AP ratios are found in corn (also known as maize starch), sorghum, barley, and rice cereals. Mutants containing almost 100% AP are called *waxy* starches, and mutants containing high levels of AM are known as *amylotypes*. Certain corn starches have been reported to contain 70% AM (Carl Hoseney 1998).

Pasting curves are powerful tools to investigate starch functional properties. Rheological changes while heating starch in water has been studied by many researchers because the starch pasting curves have been very useful to the food industry in food formulation and in designing processing systems (Thomas and Atwell 1999). Lagarrigue and Alvarez (2001) have reviewed experimental devices and methods used to obtain rheological data for starch dispersions. Rheological properties of fluid foods can be studied using two different types of measurements. The first type of rheological instrument measures absolute properties that are independent of the instrument, which means different instruments, will yield the same results. The second type of instrument yields empirical measurements which depend on the instrument used to collect the data, so different instruments give different results (Steffe 1996).

Corn starch rheology using mixer viscometry techniques, which falls in the first type of measurements, provides a more fundamental rheological testing approach than empirical instruments. Mixer viscometry has been employed by Steffe and others (1989). A modified Brookfield RVTD small adapter equipped with a flag impeller and thermocouple was used to evaluate the rheological behavior of gelatinizing normal corn starch slurries. The mixer viscometry approach provides a known average shear rate in the system, a uniform temperature distribution due to the small sample volume, and is reliable, low cost, and flexible.

Many researchers have reported the pasting curves as functions of AM/AP ratios of starch (Sasaki et al. 2000; Kurakake and others 2009; Juhasz and Salgo 2008) but no attempts have been made to study pasting curves using the mixer viscometry approach. Previous studies using empirical instruments show that the pasting curve is a strong function of AM/AP ratios present in the starch. Although starch pasting curves are greatly affected by the AM/AP ratios present in the starch, the amylose content reported in the literature are mostly apparent amyloses.

There are many ways to determine amylose content in starch: the enzymatic method, near-infrared, spectroscopy techniques, HPSEC techniques, blue value method, and thermogravimetric analysis (Ahromrit and others). The blue value method takes advantage of differences in the creation of iodine complexes. The blue method is the most commonly used even though it is a very time consuming (Stawski 2008). When amylose content in starch is quantified by the iodine titration method or blue method, the amylopectin with long chain lengths interacts with iodine giving a higher iodine affinity resulting in an overestimation of the amylose content. Some estimate the amylose content in starch using Concanavalin A (Con A) using Megazyme procedure (Park et al. 2007) .

The differential scanning calorimetry (DSC) is among the most widely used analytical instruments and many researchers have used it to collect thermal data of starch samples (Russell 1987; Wang and Sastry 1997; Rolee and LeMeste 1997; Zaidul and others 2008; Kohyama and others 2004; Xue and others 2008; Liu and others

2009; Ratnayake and Jackson 2007). Proper techniques of DSC measurement have been reported such as baseline application, sample preparation, pan selection, methods of adding water, effect of sample mass, effect of heating rate, and effect of moisture equilibration time (Yu and Christie 2001; Kousksou and others 2011); calibration temperature and heat flow rate of DSCs (Hemminger and Sarge 1994); and sample weight measurement in hermetically sealed DSC pans (Shalaev and Steponkus 2000). Starch gelatinization temperatures have been determined by DSC (Nuessli and others). At temperature above 60^{o}C most starches begin to gelatinize (Liu et al. 2006; Noda et al. 1998; Jane et al. 1999; Tester and Morrison 1990; Sasaki et al. 2000; Chang and Lin 2007). The loss of birefringence (the “maltese cross” found on all native starches) is closely associated with the phenomena known as “gelatinization” (Thomas and Atwell 1999).

Since understanding starch pasting curves and thermal behavior with variable composition (apparent AM/AP ratios) is useful for the food industry in product formulation**,** the specific objective of this study was to obtain pasting curves and thermal properties (gelatinization temperature and enthalpy) of gelatinizing corn starch solutions at different amylose to amylopectin (AM/AP) ratios using a mixer viscometry approach and DSC, respectively.

3.2 Materials and Methods

Four commercially available corn starch samples containing different AM/AP ratios (waxy:0/100; normal: 27:73; high-amylose Hylon V: 50/50; high-amylose Hylon VII: 70/30) were obtained from National Starch (New Jersey, USA).

3.2.1 Sample Preparation: Corn Starch Blends

The four corn starches: waxy, normal, Hylon V, and Hylon VII were used as a base to prepare six starch systems with different AM/AP ratios. The AM/AP ratio of starch was increased by adding higher AM/AP ratio content starch to lower AM/AP ratio content starch. The six systems containing corn starch mixtures at different AM/AP ratios were prepared as follow: System I contained waxy and normal corn starch mixtures (0, 10, and 27% AM); System II contained waxy and high amylose Hylon V mixtures (10, 20, 30, 40, 50%AM); System III contained waxy and high amylose Hylon VII mixtures (10, 20, 30, 40, 50, and 60%); System IV contained normal and high amylose Hylon V mixtures (20, 30, 40%); System V contained normal and high amylose Hylon VII mixtures (20, 30, 40, 50, and 60%); and System VI contained high amylose Hylon V and high amylose Hylon VII mixtures (60, and 70%).

There were a total of 24 samples. Each sample, weighing 5g, was placed in a small glass vial and mixed well by vigorous manual shaking and a vortex mixer. The apparent AM/AP ratio, pasting curves, and DSC parameters were experimentally measured for all samples.

3.2.2 Starch Apparent AM/AP Ratio Determination

The amylose content of the samples was determined experimentally by the Con A method using the Megazyme AM/AP content assay kit (Megazyme 2006). Samples were centrifuged using the bench centrifuge at 4000xg for 10min instead of 2000xg for 5min to obtain a clear supernatant. The measurements were done at least in duplicates.

The amylose content present in the sample was determined based on Con A supernatant and total starch aliquot absorbance readings at 510 nm as follows:

$$\text{Amylose experimental, (\%w/w)} = \frac{\text{Absorbance (Con A Supernatant)}}{\text{Absorbance (Total Starch Aliquot)}} \times 66.8$$

3.2.3 Rheological Measurement

This study used the mixer viscometry to evaluate the rheological profile of ungelatinized corn starch mixtures at a concentration of 6% (w/w) with different AM/AP ratios. A detailed explanation on the mixer viscometry procedure was presented in (Steffe and Daubert 2006a).

Experimental equipment was set up as shown in the schematic diagram in Fig. 3.1. The modified Brookfield instrument consisting of the Brookfield RVDV viscometer with a flag type impeller sensor was connected to three glycol-water mixture baths held at constant temperatures (95^{o}C, 5^{o}C, and 60^{o}C), and switched for flow through the sample cup using six solenoid valves. The output torque reading of the Brookfield instrument, sample temperature from RTD output signal, and time were collected with a data acquisition (DAQ) system using LabView 8.5 software for continuous data collection. The measurements of the output readings of the instrument were determined from calibration curves of voltage to torque, and voltage to temperature, and time was recorded using LabView 8.5 program organized with a block diagram.

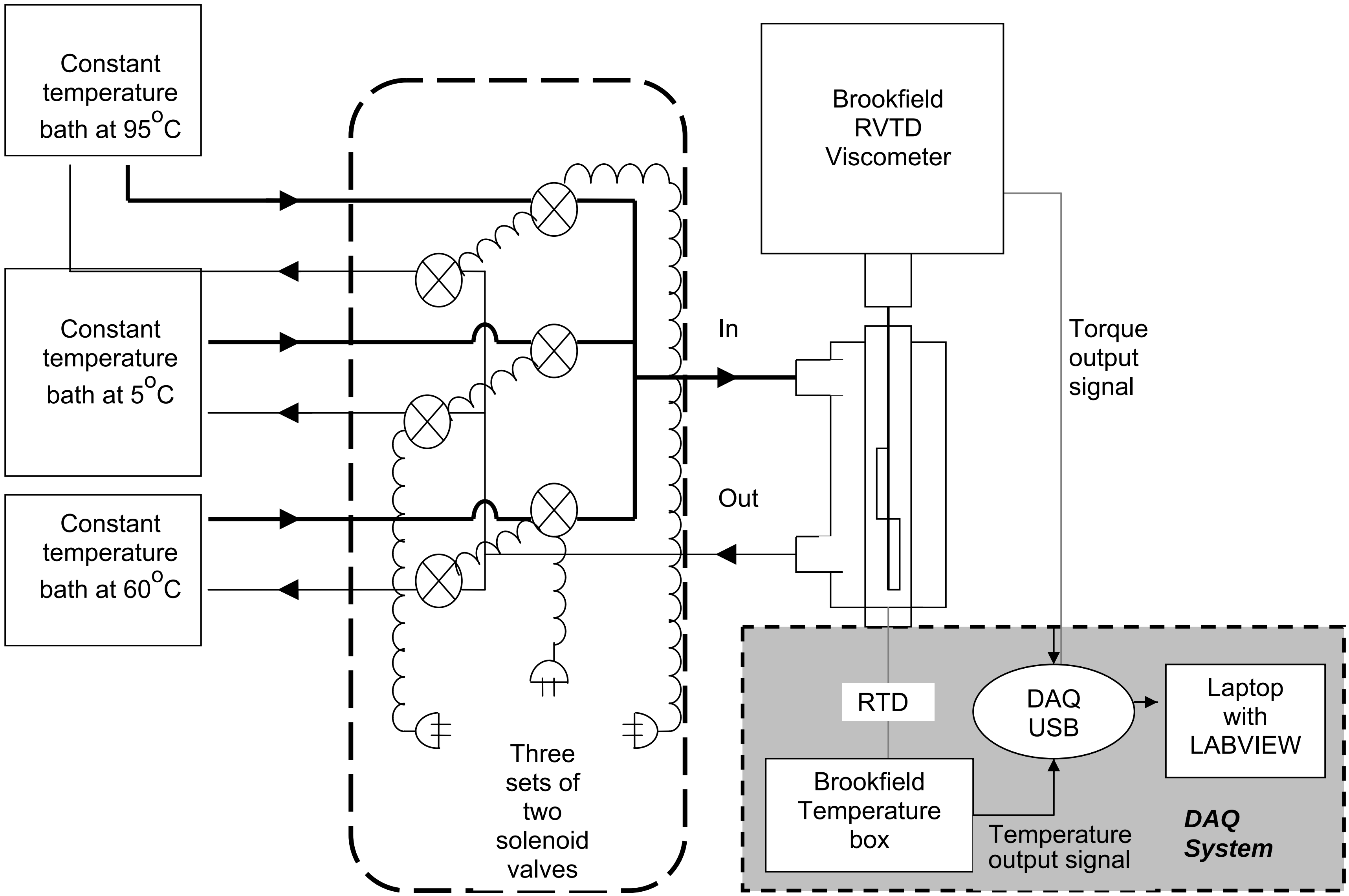

Figure 3.1. Schematic diagram of equipment set up (modification of Dolan and Steffe 1990).

Corn starch samples were heated from 60°C to 95°C for 12min, and then cooled to 60°C in 13sec, and held at 60°C for 10min. A total time of 22min and 13sec at a constant impeller speed of 100rpm was used for each experiment. Continuous torque, time, and temperatures data were collected using LabView. The apparent viscosity and average shear rates were calculated based on known mixer constants (k″ and k' values) for the Brookfield flag impeller in a 13cc cup based on research (Briggs and Steffe 1996). The apparent viscosity and shear rate were calculated using equations presented in (Steffe and Daubert 2006), respectively:

$$\eta = \frac{k''M}{\Omega} \tag{3}$$

$$\dot{\gamma}_a = k'\Omega \tag{4}$$

3.2.4 Thermal Properties of Starches

The thermal properties of starches were studied by using DSC (Q2000, TA Instruments, USA). A starch sample of approximately 4mg was loaded into a Tzero aluminium pan (T100826/Lot 603097/901683.901, Switzerland), and 18µl distilled water were added directly into pan using a micro pipette. The starch and water inside the pan was shaken gently using the twister to make sure the sample covered all pan surfaces. Samples were hermetically sealed using Tzero Hermetic Lid (T100826/Lot 603097/901684.901, Switzerland) and allowed to stand for 6hr at room temperature before heating in the DSC. The pans were sealed by flipping the lids up side down to give enough space for the gelatinization to occur inside the pan and minimize the pressure build up. A sealed Tzero aluminum pan containing 18µl of water was used as a reference. Sample pans were heated at a rate of 10°C/min from 20°C to 140°C. The DSC analyzer was calibrated using baseline and sapphire before sample measurement. The DSC parameters - T_S (start temperature), T_O (onset temperature), T_P (peak of gelatinization temperature), T_C (conclusion temperature), and ΔH (enthalpy of gelatinization) - were determined from the DSC data and heat flow curve was obtained using the integrated peak linear option of TA Universal Analysis.

3.3 Results and Discussion

3.3.1 Starch Amylose Content

The percentage of amylose present in the six systems of the corn starch blends determined using the Con A method are tabulated in Table 3.1. Results indicate that the experimental value showed a lower value compare to the calculated (assumed) amylose content except for the waxy corn starch (WN-0). The mean value of the amylose contents of the corn starch blends, standard deviations and the correlation of variation (CV) values are presented in the Table 3.1, as well. The relationship between analytically measured amylose content and calculated amylose content was plotted in Figure 3.2. Results indicate that it is possible to predict the value of the amylose content present in the corn starch blends for all the six systems using the following expression: Experimental amylose % = 0.86(calculated amylose %) + 0.07 with R^2= 0.87.

Table 3.1 Amylose content in corn starch blends

Code	Sample No.	weight, mg	Total Starch (A)	Samples (A)	**%AM exp.**	mean	std.deviation	%CV	**%AM assumed**
Starch blend (System 1): Waxy and normal corn starches									
waxy	1	25.8	0.511	0.028	3.66	3.56	0.12	3.277	0
		23.1	0.331	0.017	3.43				0
		24.5	0.429	0.023	3.58				0
WN-10	2	24.8	0.361	0.031	5.74	6.15	0.59	0.096	10
		23.9	0.356	0.035	6.57				10
normal	3	25	0.728	0.148	13.58	13.63	0.11	0.782	27
		24.8	0.743	0.153	13.76				27
		24.4	0.527	0.107	13.56				27
Starch blend (System 2): Waxy and high-amylose Hylon V corn starches									
WHV-10	4	24.4	0.582	0.05	5.74	5.81	0.10	1.676	10
		24	0.557	0.049	5.88				10
WHV-20	5	24.2	0.727	0.155	14.24	13.98	0.37	2.652	20
		24.6	0.784	0.161	13.72				20
WHV-30	6	25	0.772	0.25	21.63	21.28	0.49	2.321	30
		23.3	0.785	0.246	20.93				30
WHV-40	7	24.8	0.742	0.385	34.66	34.03	0.89	2.619	40
		23.9	0.762	0.381	33.40				40
Hylon V	8	24.7	0.666	0.474	47.54	46.99	0.95	2.019	50
		23.7	0.674	0.46	45.59				50
		21.3	0.685	0.484	47.20				50
		23.6	0.679	0.484	47.62				50

Table 3.1 (cont'd)

Code	Sample No.	weight,mg	Total Starch (A)	Samples (A)	**%AM exp.**	mean	Std.deviation	%CV	**%AM assumed**
Starch blend (System 3): Waxy and high-amylose Hylon VII corn starches									
WHVII-10	9	24.1	0.597	0.079	8.84	9.27	0.61	0.065	10
		24.7	0.558	0.081	9.70				10
WHVII-20	10	26.1	0.407	0.063	10.34	10.46	0.17	1.619	27
		23.4	0.764	0.121	10.58				27
WHVII-30	11	24.1	0.707	0.198	18.71				30
		24.9	0.706	0.21	19.87	19.00	0.77	4.051	30
		26.2	0.711	0.196	18.41				30
WHVII-40	12	25.7	0.32	0.169	35.28	34.85	0.61	1.759	40
		23.2	0.33	0.17	34.41				40
WHVII-60	13	26.8	0.749	0.481	42.90	43.09	0.27	0.635	60
		24	0.767	0.497	43.29				60
Hylon VII	14	23.6	0.629	0.575	61.07	61.46	0.56	0.905	70
		22.2	0.594	0.55	61.85				70
Starch blend (System 4): Normal and high-amylose Hylon V corn starches									
NHV-20	15	23.9	0.687	0.303	29.46	28.62	0.73	2.560	20
		24.70	0.76	0.32	28.16				20
		23.9	0.781	0.33	28.23				20
NHV-30	16	25.2	0.656	0.313	31.87	32.39	0.74	2.278	30
		24.3	0.69	0.34	32.92				30
NHV-40	17	24.4	0.783	0.424	36.17	35.95	0.31	0.858	40
		23.5	0.729	0.39	35.74				40

Table 3.1 (cont'd)

Code	Samples	weight mg)	Total Starch (A)	Samples (A)	**%AM exp.**	mean	Std.deviation	%CV	**%AM assumed**
Starch blend (System 5): Normal and high-amylose Hylon VII corn starches									
NHVII-20	18	25.7	0.696	0.287	27.55	28.23	0.96	0.034	27
		24.6	0.684	0.296	28.91				27
NHVII-30	19	24	0.741	0.357	32.18	32.77	0.83	2.526	30
		23.7	0.717	0.358	33.35				30
NHVII-40	20	24	0.833	0.482	38.65	38.29	0.51	1.344	40
		23.2	0.812	0.461	37.92				40
NHVII-50	21	23.1	0.72	0.516	47.87	48.39	0.73	1.518	50
		24.8	0.717	0.525	48.91				50
NHVII-60	22	23.60	0.83	0.67	53.99				60
		25.50	0.87	0.69	52.80	53.31	0.61	1.146	60
		24.5	0.842	0.67	53.15				60
Starch blend (System 6): High-amylose Hylon V and high-amylose Hylon VII corn starches									
HVHVII-50	23	24.5	0.678	0.481	47.39	47.66	0.38	0.805	50
		24.1	0.655	0.47	47.93				50
HVHVII-60	24	24.3	0.727	0.626	57.52	57.82	0.43	0.743	60
		23.7	0.724	0.63	58.13				60

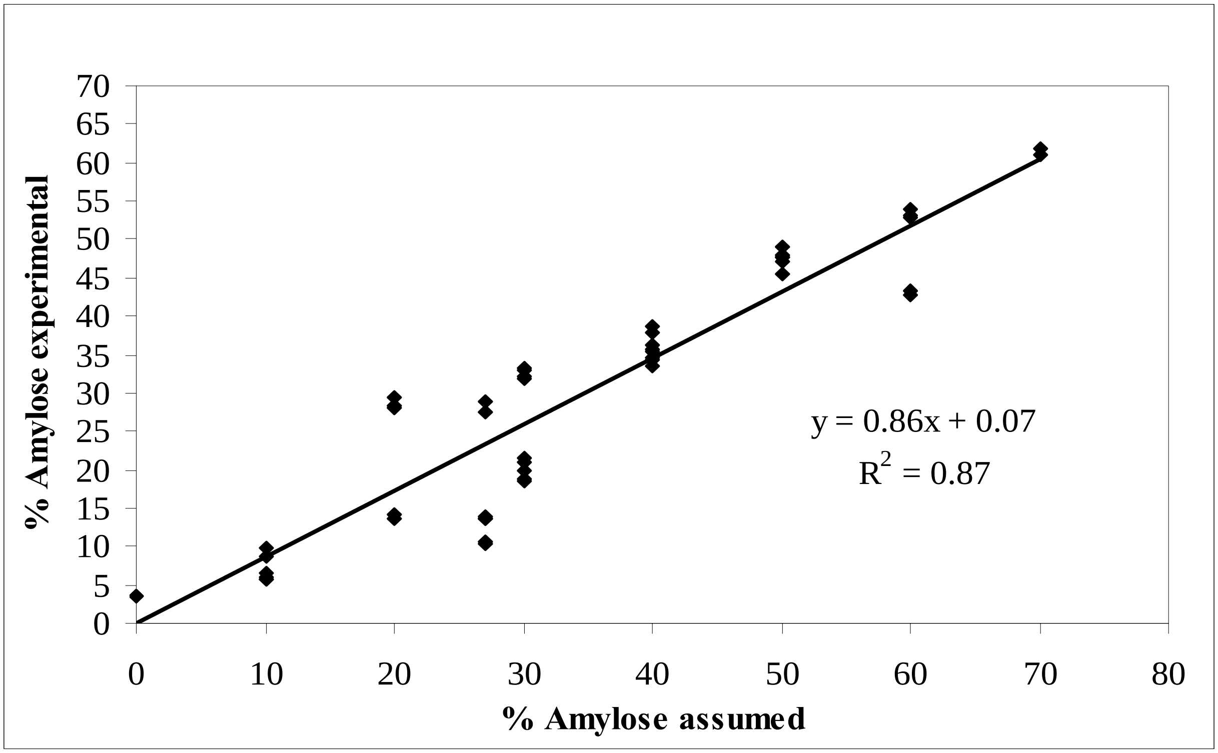

Figure 3.2. Relationship between experimentally measured amylose content and assumed amylose content in corn starch blends (all six systems).

3.3.2 Pasting Curves (Apparent Viscosity vs. time) at Different AM/AP Ratio

Fig. 3.3, 3.4, 3.5, 3.6, 3.7, and 3.8 show a decreasing trend in apparent viscosity as the percentage of amylose content in corn starches increases. Pasting temperature and peak time showed an increasing trend as amylose content increased. The peak viscosity, holding strength and setback viscosity decreased with an increase in percentage of amylose content in corn starches. A slight Weissenberg effect was noted for the lowest amylose content (waxy) corn starch during the experimentation. For higher percentage amylose content, gelatinization did not take place at 95^{O}C (Fig. 3.4-

3.8). No reports of studies on pasting properties of corn starch blends using mixer viscometry have been found in published literature.

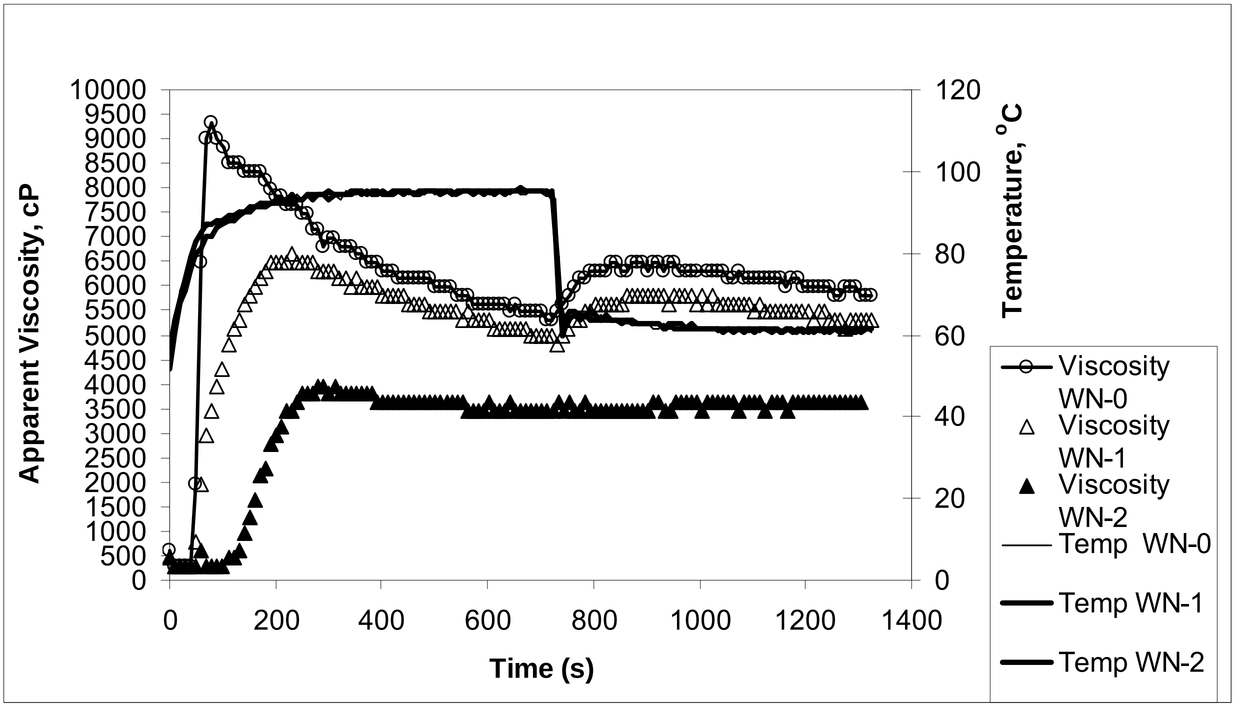

Figure 3.3. Apparent viscosity profile of corn starch blends for System 1 (waxy and normal corn starch mixtures).

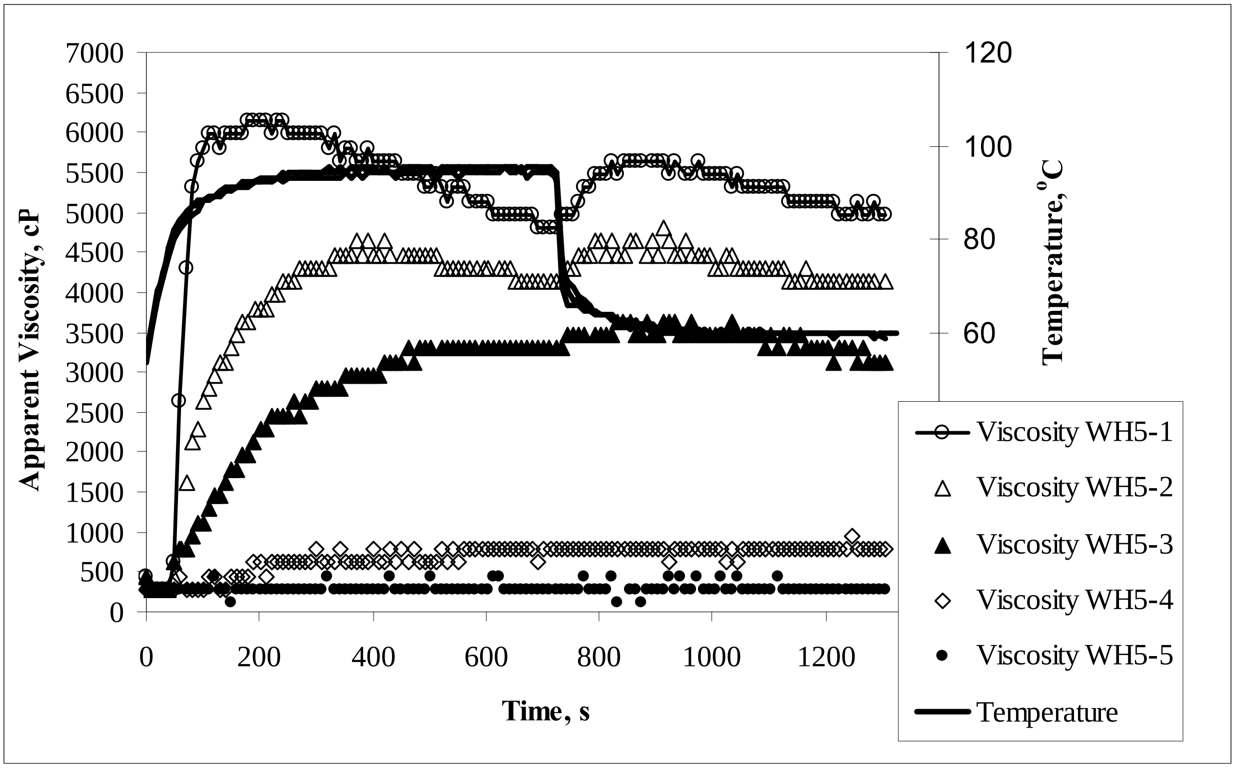

Figure 3.4. Apparent viscosity profile of corn starch blends for System 2 (waxy and Hylon V corn starch mixtures).

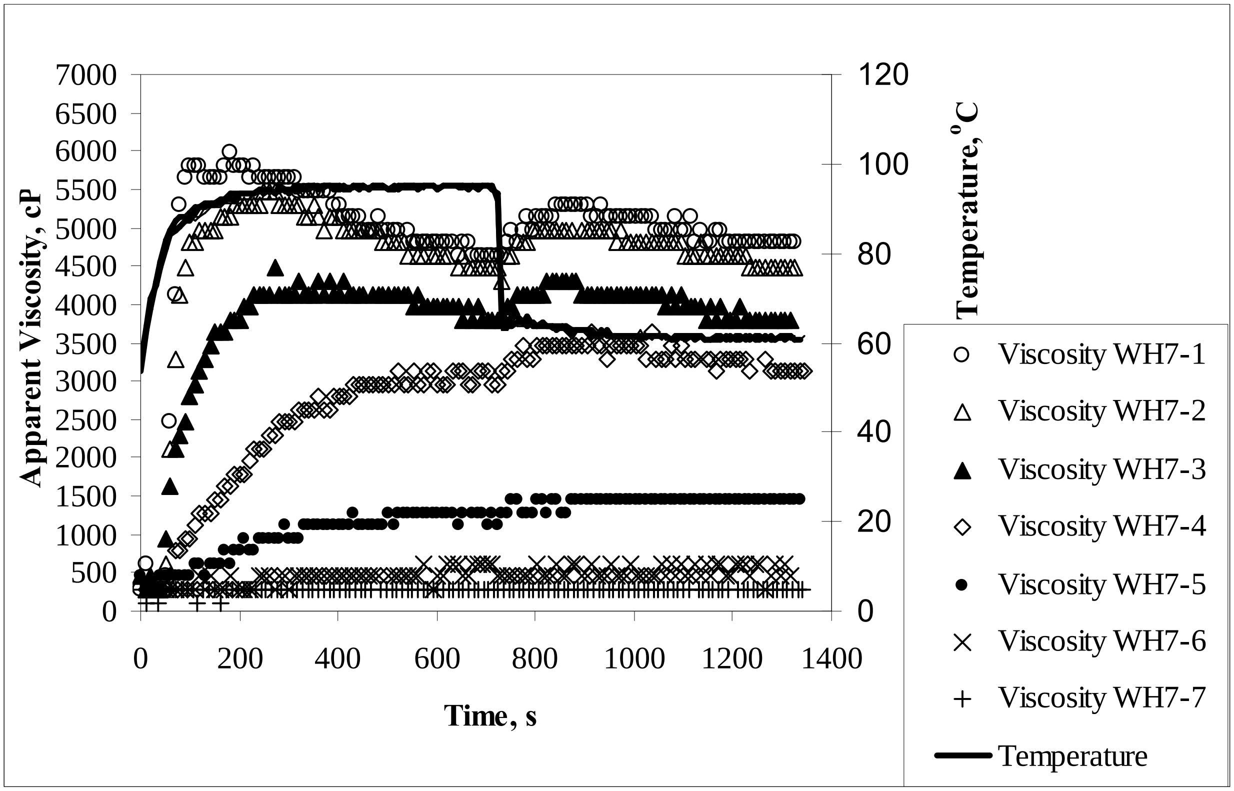

Figure 3.5. Apparent viscosity profile of corn starch blends for System 3 (waxy and Hylon & corn starch mixtures).

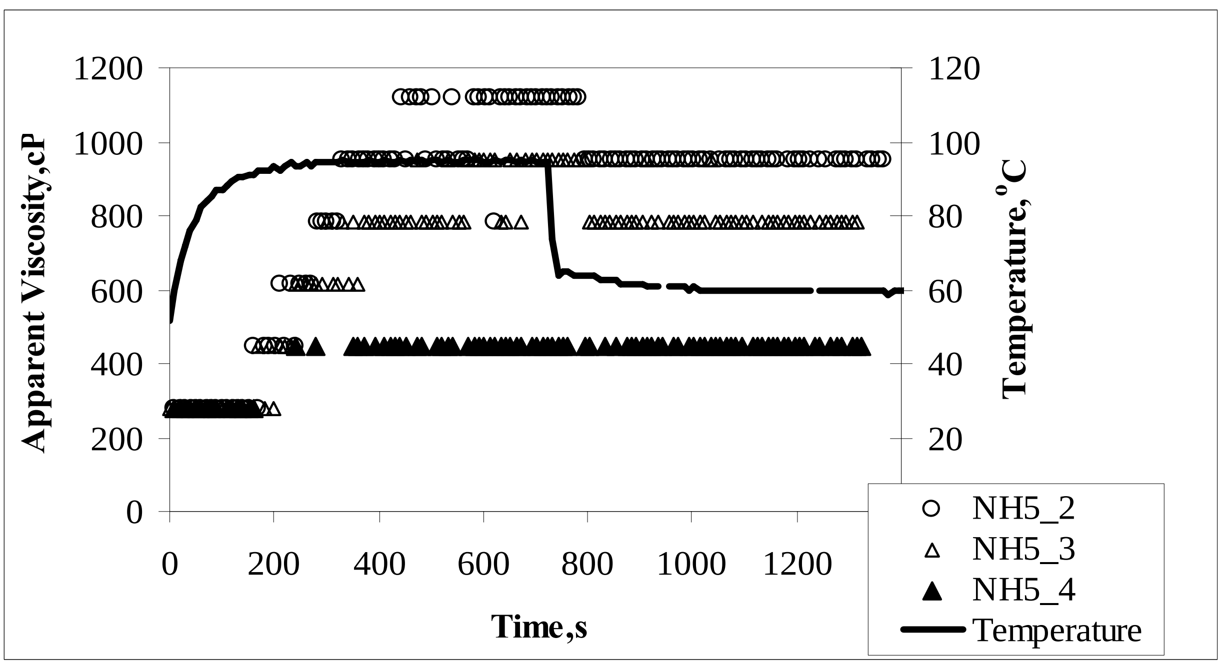

Figure 3.6. Apparent viscosity profile of corn starch blends for System 4 (normal and Hylon V corn starch mixtures).

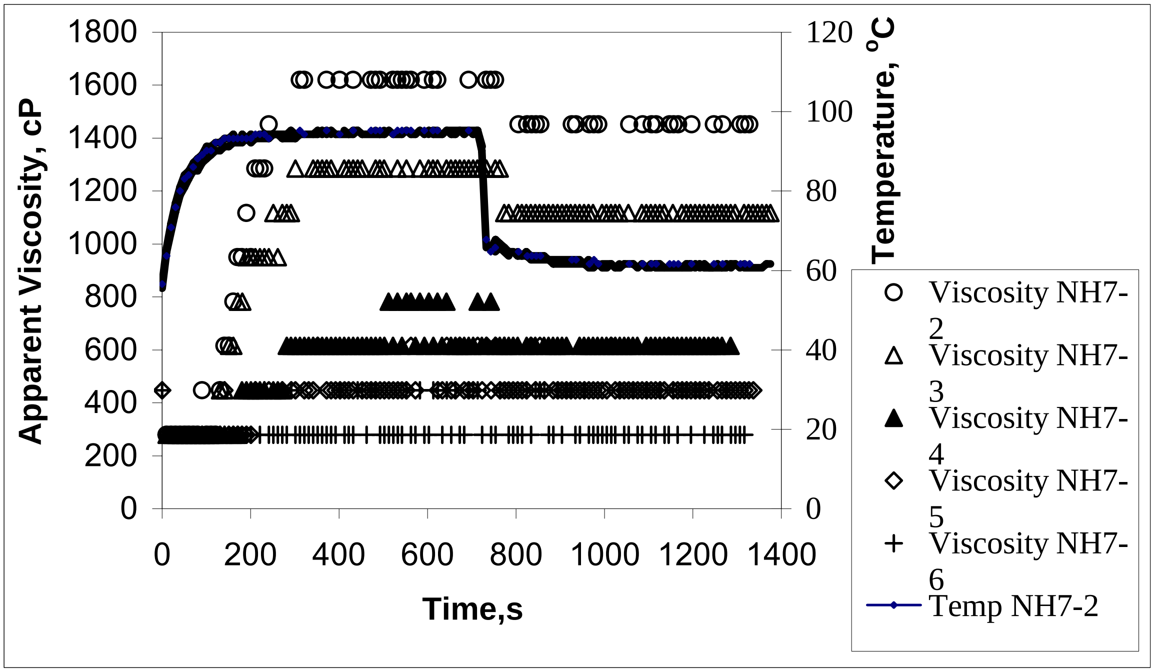

Figure 3.7. Apparent viscosity profile of corn starch blends for System 5 (normal and Hylon VII corn starch mixtures).

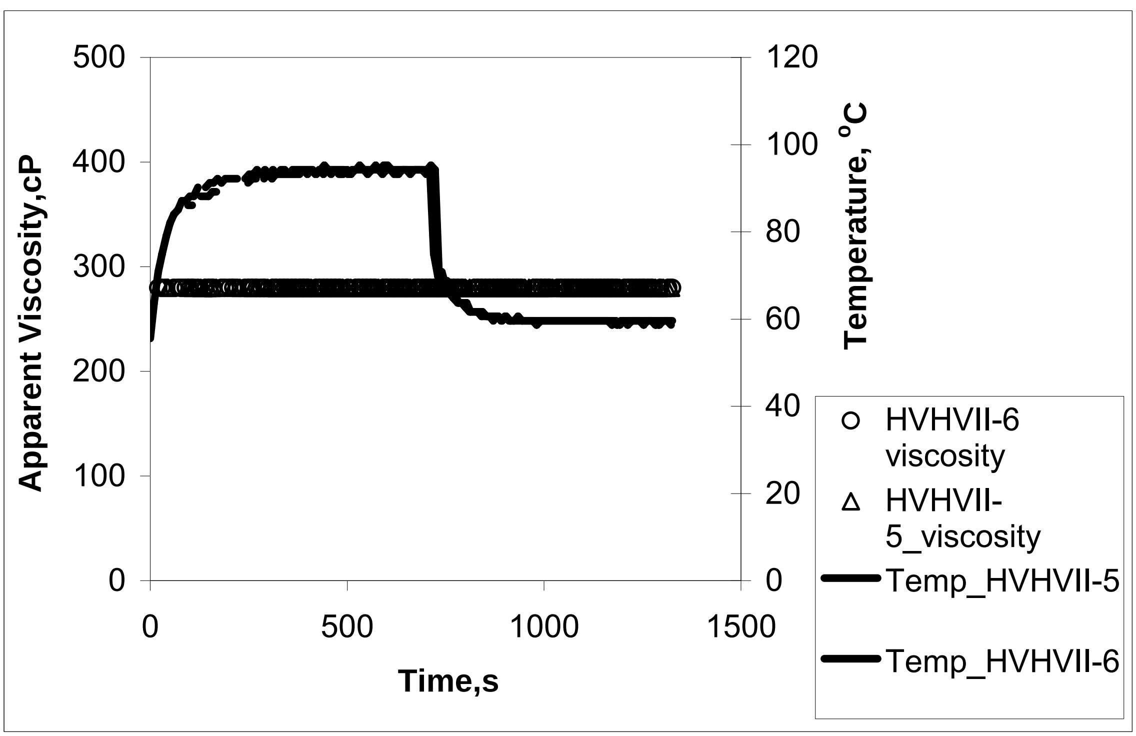

Figure 3.8. Apparent viscosity profile of corn starch blends for System 6 (Hylon V and Hylon VII corn starch mixtures).

A sharp curve and the highest peak viscosity for corn starch blends occurred in System1 for waxy corn starch (WN-0), giving ~9500 cP (Fig. 3.3). Flat viscosity profiles were observed for higher amylose content starches with viscosity values of approximately 280cP (Fig. 3.8). A similar viscosity profile with 'peak viscosity negatively correlated with amylose content (confirming that amylopectin is mainly responsible for water uptake) was reported by (Juhasz and Salgo 2008).

The results obtained from this study yielded empirical expressions for the estimation of the peak viscosity, holding strength and setback viscosity as a function of amylose content in corn starch blends (Fig. 3.9 to Fig. 3.11). The mathematical expressions specific for each system are given in Appendix A.

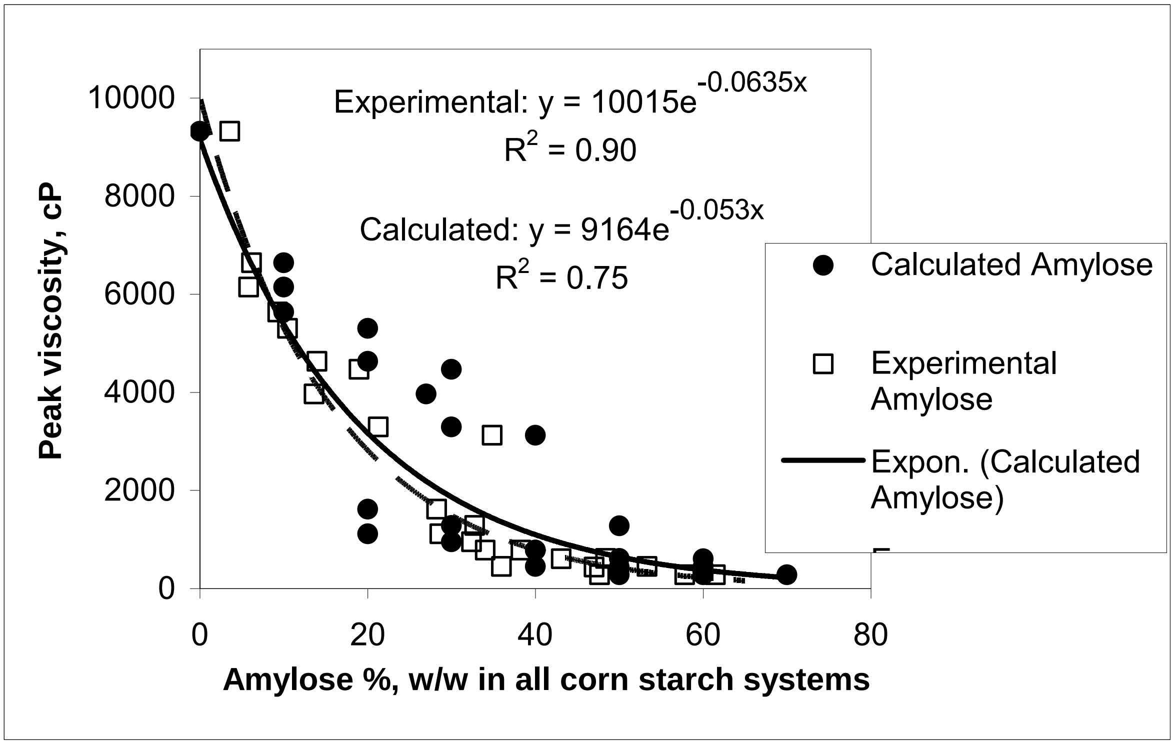

Figure 3.9. Overall peak viscosity as function of amylose expression for corn starch blends.

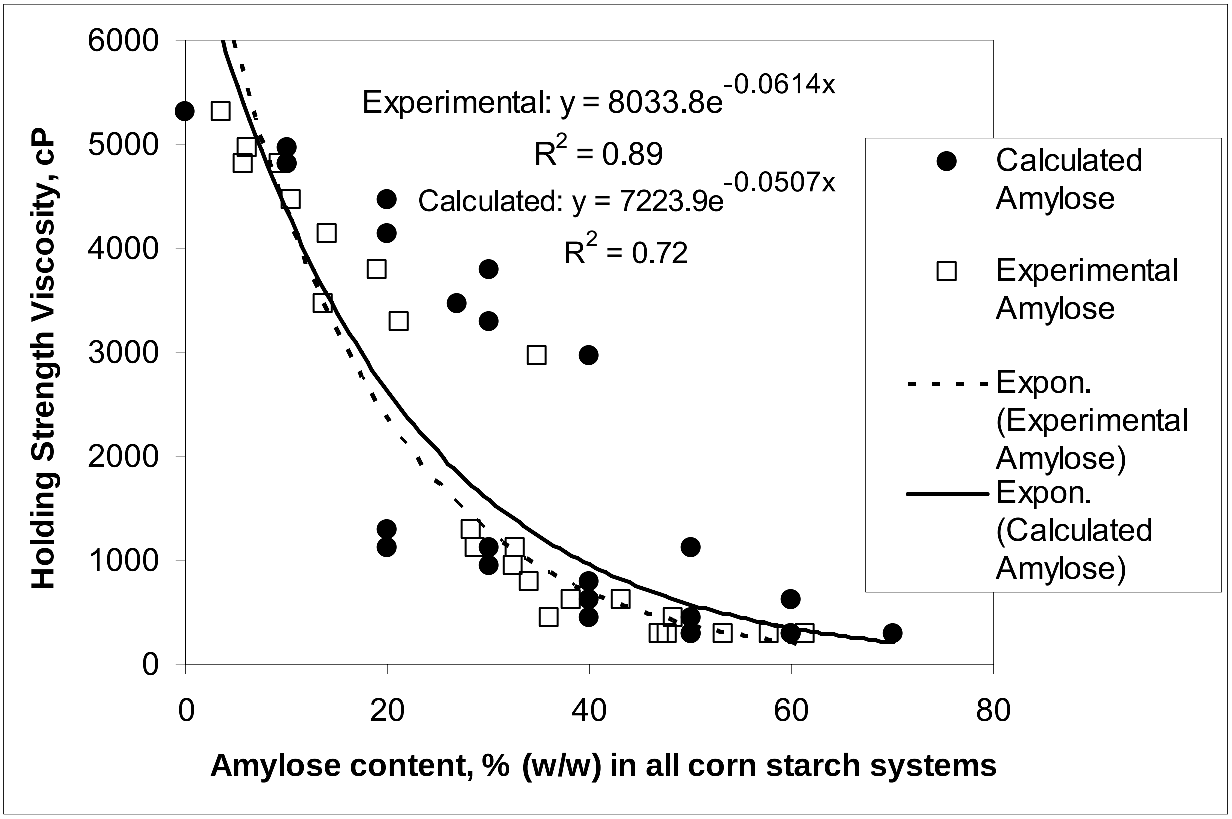

Figure 3.10. Overall holding strength viscosity as function of amylose expression for corn starch blends.

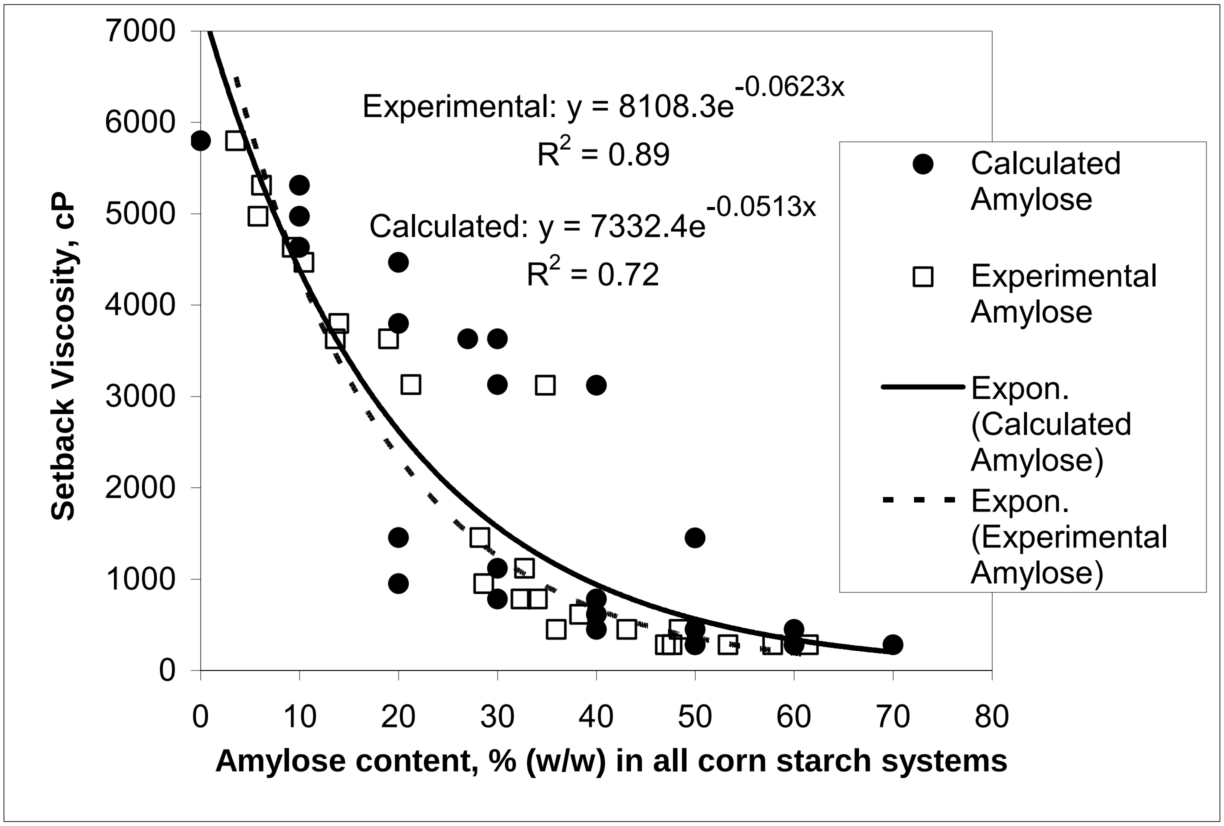

Figure 3.11. Overall setback viscosity as function of amylose (assumed and experimental) expression for corn starch blends.

This study also confirmed that the mixer viscometry approach, using a modified Brookfield viscometer, is a good rheological tool for studying viscosity of gelatinizing starch solutions. This rheological tool, and methodology presented, can provide accurate fundamental data at low cost.

3.4 Differential Scanning Calorimetry Data

The intention of this study was to provide gelatinization data using DSC for corn starch blends. The start (T_S), onset (T_O), peak (T_P), conclusion (T_C) and enthalpy (ΔH) of gelatinization for native corn starches with different AM/AP ratios were measured using

DSC. The endotherm enthalpies were measured with reference to a straight baseline joining T_o and T_c. These were done by using the TA Universal Analysis software. The mean values from triplicates of T_s, T_o, T_p, ΔH, and T_c at different AM/AP ratio for the 24 corn starch samples determined from this study are listed in Table 3.2.

The following analyses are based on Table 3.2, and the letters listed in the superscripts for each column separately. The Tukey HSD test at a 95% confidence interval shows that there is no significant difference in Ts for all samples tested (Table 3.2, column 4). A significantly lower To was observed for normal corn starch and its mixtures with high amylose starches, compared to waxy and its mixtures with high amylose starches (Table 3.2, column 5). Normal corn starch and its mixture with high amylose corn starches tend to have significantly higher enthalpy values as the amylose content increases (Table 3.2, column 6). The peak temperatures, Tp is significantly lower for normal corn starch and its mixture with high amylose corn starches compared to other corn starches blends (Table 3.2, column 7). The Tc values go up with increase in amylose content for normal corn starch and its mixture with high amylose corn starches (Table 3.2, column 8). Those differences on the DSC parameters on different corn starch blends might due to the difference in amylose-lipid interaction and amylopectin branch chain length (Eliasson 1994; Jane et al. 1999).

Table 3.2 DSC parameters for corn starch blends

Amylose experimental	Amylose assumed	Starch Mixtures	DSC parameters				
			Ts	To	delta H (J/g)	Tp	Tc
SYSTEM 1							
3.56	0	(waxy)	$63.34^{c,d}$	67.09^{f}	$14.7^{a,b,c}$	$72.59^{b,c}$	$82.96^{c,d}$
6.15	10	WN10	$64.74^{a,b,c,d}$	67.44^{f}	$12.32^{a,b,c,d,e}$	$72.17^{b,c}$	81.19^{d}
13.63	27	(normal)	$63.82^{b,c,d}$	$67.66^{e,f}$	$10.75^{b,c,d,e,f}$	71.42^{c}	$82.96^{c,d}$
SYSTEM 2							
5.81	10	WHV_10	$64.04^{a,b,c,d}$	67.18^{f}	$10.15^{b,c,d,e,f,g}$	$72.51^{b,c}$	80.27^{d}
13.98	20	WHV_20	$64.84^{a,b,c,d}$	$67.57^{e,f}$	$7.65^{d,e,f,g}$	$72.48^{b,c}$	78.72^{d}
21.28	30	WHV_30	$65.06^{a,b,c,d}$	$67.8^{d,e,f}$	$5.57^{e,f,g}$	$72.57^{b,c}$	79.31^{d}
34.03	40	WHV_40	$65.7^{a,b,c}$	$68.81^{a,b,c}$	16.29^{a}	73.89^{a}	$108.61^{a,b}$
34.03	50	HV (Hylon V)	$65.35^{a,b,c}$	$69.58^{a,b,c}$	18.38^{a}	77.81^{a}	$113.43^{a,b}$
SYSTEM 3							
9.27	10	WHVII_10	62.64^{d}	$67.95^{d,e,f}$	$13.0^{a,b,c,d}$	$73.01^{b,c}$	$87.32^{c,d}$
10.46	20	WHVII_20	$63.67^{b,c,d}$	$67.55^{e,f}$	$10.1^{b,c,d,e,f,g}$	$72.45^{b,c}$	$82.72^{c,d}$
19	30	WHVII_30	$63.1^{c,d}$	$67.55^{e,f}$	$8.77^{c,d,e,f,g}$	$72.65^{b,c}$	$83.53^{c,d}$
34.85	40	WHVII_40	$64.69^{a,b,c,d}$	$68.11^{d,e,f}$	$5.87^{e,f,g}$	$72.68^{b,c}$	80.8^{d}
46.2	50	WHVII_50	$65.54^{a,b,c}$	$68.81^{b,c,d}$	3.483^{g}	$72.53^{b,c}$	78.61^{d}
57.82	60	WHVII_60	65.76^{a}	$69.5^{a,b}$	$3.27^{b,c,d,e,f}$	$72.78^{b,c}$	$80.84^{b,c}$
SYSTEM 4							

Table 3.2 (Cont'd)

28.62	20	NHV_20	65.01[a,b,c,d]	67.8[d,e,f]	4.583[f,g]	71.22[c]	78.87[d]
32.39	30	NHV_30	65.49[a,b,c]	68.01[d,e,f]	4.58[f,g]	71.44[c]	78.02[d]
35.95	40	NHV_40	65.38[a,b,c,d]	67.78[d,e,f]	16.06[a,b]	72.27[b,c]	108.18[a,b]
SYSTEM 5							
28.23	20	NH7_20	65.43[a,b,c]	67.66[e,f]	5.7[e,f,g]	71.38[c]	77.1[d]
32.77	30	NH7_30	65.7[a,b,c]	67.98[d,e,f]	5.08[f,g]	71.46[c]	76.89[d]
38.29	40	NH7_40	66.24[a,b]	68.03[d,e,f]	3.86[g]	71.4[c]	76.03[d]
48.39	50	NH7_50	65.59[a,b,c]	68.14[c,d,e,f]	3.88[g]	71.78[b,c]	77.37[d]
53.31	60	NHVII_60	66.73[a]	68.57[c,d,e]	15.17[a,b,c]	72.62[b,c]	112.27[a,b]
SYSTEM 6							
57.82	60	HVHVII_60	67.37[a]	69.83[a,b]	17.5[b,c,d,e,f]	73.52[b,c]	116.57[b,c]
61.46	70	HVII (Hylon VII)	66.35[a,b]	70.0[a]	15.18[a,b,c]	73.63[a,b]	115.06[a]

- refers to amylose-lipid endotherm
- starch mixtures with 'code N' are normal, 'code W' is waxy, and 'code HV and HVII' are high amylose.
- within one column, any means sharing the same letter are not significantly different.

It is interesting to note that the difference due to variation in AM/AP ratios in corn starch blends did not affect the gelatinization temperature. The peak temperature (T_p) for corn starch blends studied occurred between 71^{O}C to 78^{O}C (Table 3.2), which is in agreement with (Russell 1987).

This study showed that the gelatinization enthalpies of amylopectin rich corn starch blends are higher than that of amylose rich starch. The enthalpy (ΔH) of gelatinization increased with increasing amylopectin. This increase might be due to the high amount of double helical structure in high amylopectin starches compared to high amylose starches. "The enthalpy (ΔH) of a transition was interpreted as corresponding to the amount of crystal order (or double-helical structure) in the starch suspensions that disrupted at heating scans" (Liu et al. 2006). The decrease in the enthalpy is correlated to the decrease in the degree of crystallinity (DC). Low amylose starches (waxy and normal starches) contain A-type crystalline packing, while high amylose starches (at least 50% amylose) contain B-type and V-type crystalline packing. C-type crystalline packing is a mixture of A and B-type crystalline packing (Matveev and others 2001). 'A change of the A-type crystallinity is observed for waxy and normal maize starch to C-type and B-type crystallinity for maize starches with intermediate and high amylose contents (>40% w/w)' (Cheetham and Tao 1998).

There is no gelatinization peak observed for high amylose content but the high amylose corn starches exhibited a broad endotherm between T_O=65.3^{O}C and T_C=116.5^{O}C. Out of the 24 corn starch samples, broad endotherms were observed for Hylon V, Hylon VII, normal and Hylon V corn starch blends with 40% assumed amylose, normal and Hylon VII corn starch blends with 60% assumed amylose, and Hylon V and Hylon VII with 60% assumed amylose. The reason for a broad endotherm might be due to starch molecular size, chain length, and amylose-lipid complex. According to Cheetham and Tao (1997), corn starches with the highest amylose content have the lowest amylose molecular size and the longest amylopectin chains. They concluded that long chains of amylopectin in high amylose starches contributed significantly to apparent amylose content. Broad endotherms were only observed on high amylose content corn starches and this might due to the amylose-lipid endotherm (Matveev et al. 2001). These results confirm the need for a better understanding of the influence of starch molecular chemistry on starch thermal properties.

From all the corn starch mixtures studied under the conditions tested, in general lower amylose content starches tends to have larger enthalpy . The results from this study are in agreement with (Russell 1987). The range of enthalpy of corn starch mixtures obtained from this study was from 3.27 to 18.38 J/g (Table 3.2).

3.5 Conclusions

An empirical mathematical expression was presented for experimental amylose and assumed amylose contents in the corn starch blends. The mixer viscometry approaches which absolute measurements (equipment-independent), and was used to document the apparent viscosity profile (pasting curves) of gelatinizing starch solutions. This study shows that the starch pasting curves and thermal properties were influenced by amylose to amylopectin ratios. The peak viscosity, setback viscosity, and holding strength increased with decreasing amylose content for corn starch blends. The DSC data showed that the enthalpies of gelatinization increased as the amylose content of corn starch blends decreases.

3.6 Acknowledgement

We thank National Starch Co. for their donation of corn starches, and the fabrication shop of Department Biosystems and Agricultural Engineering, Michigan State University for constructing the solenoid valve switching unit for the Brookfield viscometer. We thank Professor Perry Ng for use of equipment in the cereal science laboratory to conduct the amylose content measurement and his technical advice. We thank Dr.Ozadali and Gene Ford from Nestle Gerber for use of the DSC.

3.7 Nomenclature

A	absorbance at wavelength 510nm
AM	amylose
AP	amylopectin
DAQ	data acquisition system
DSC	differential scanning calorimeter
M	torque, Nm
RTD	resistance temperature detector
RVA	rapid visco analyzer
Ω	angular velocity, rad/s
k'	mixer viscometer constant, rad^{-1}
k''	mixer coefficient, rad m^{-3}
η	apparent viscosity, Pa.s
$\dot{\gamma}_a$	average shear rate, s^{-1}

APPENDICES

Appendix A1

Equipment Set up

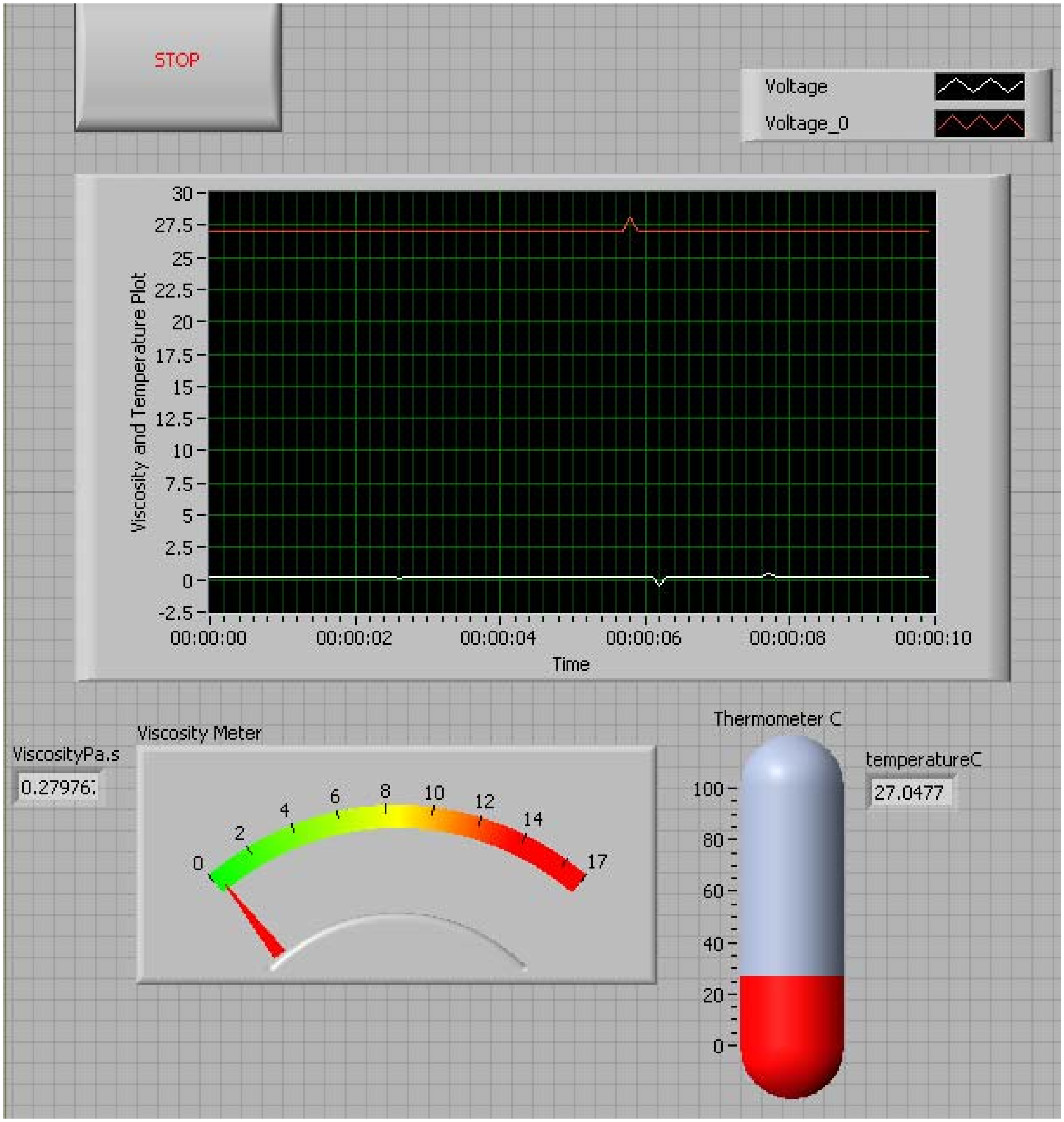

Figure A.1.1. Front panel created on Labview to measure the calculated viscosity (from torque) and temperature. **"For interpretation of the references to color in this and all other figures, the reader is referred to the electronic version of this dissertation"**

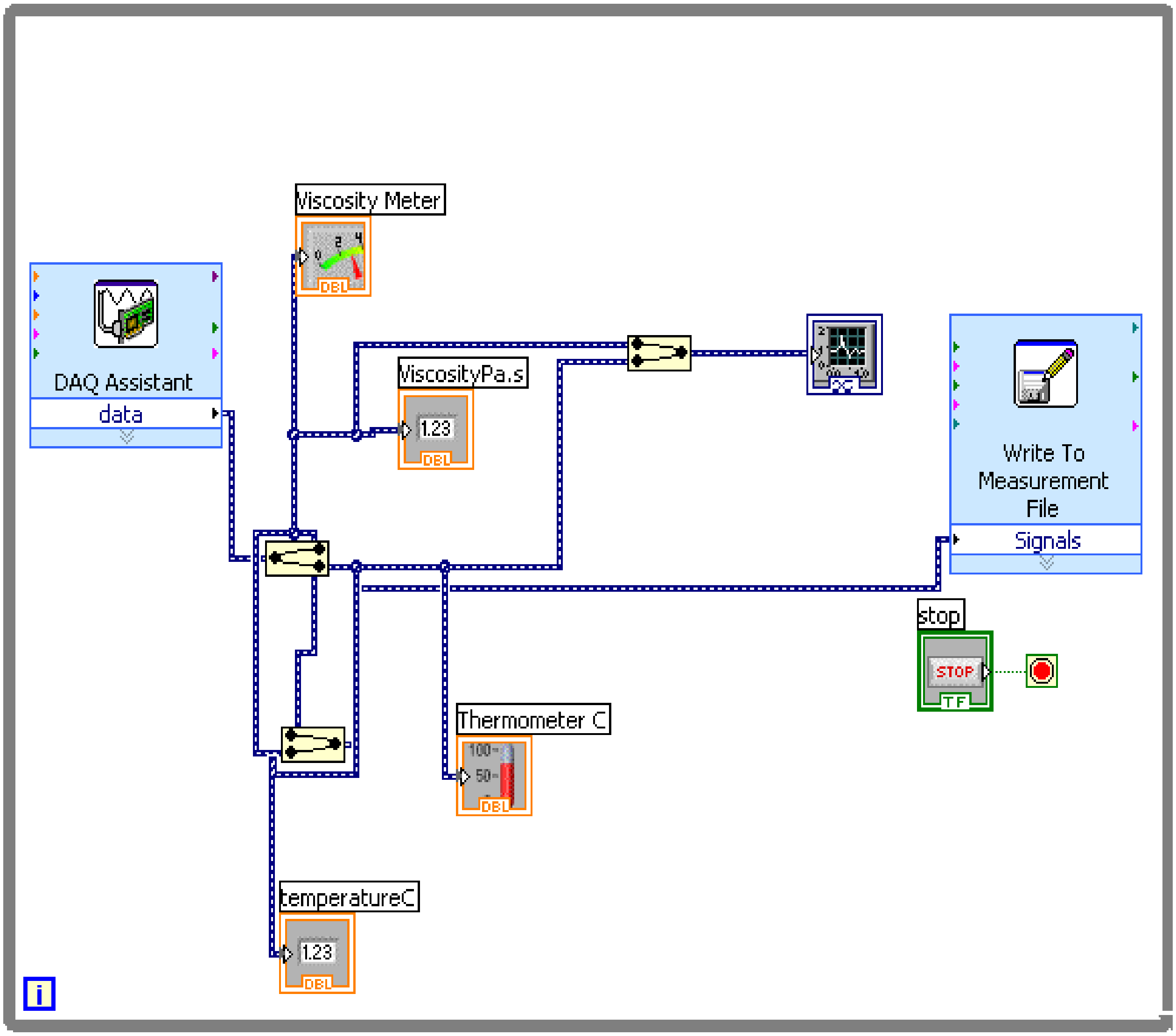

Figure A.1.2. Block diagram created on Labview to measure the calculated viscosity (from torque) and temperature, and save the files to Excel.

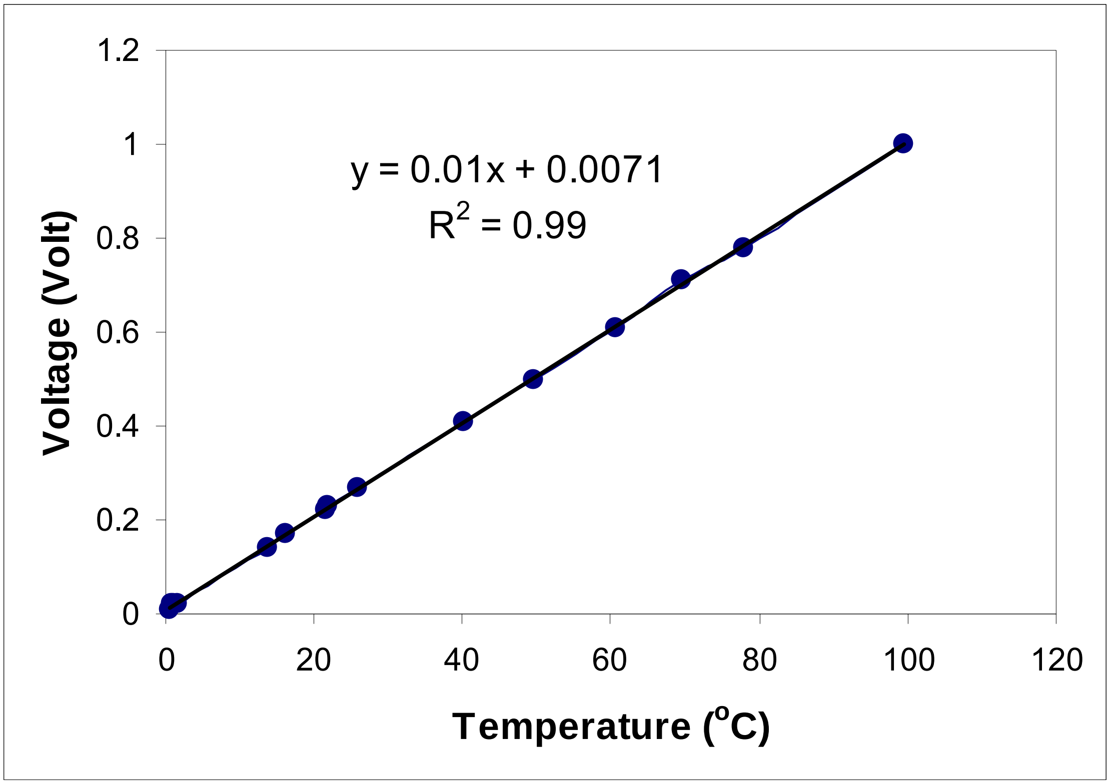

Figure A.1.3. Calibration curve for temperature and voltage reading from Brookfield viscometer.

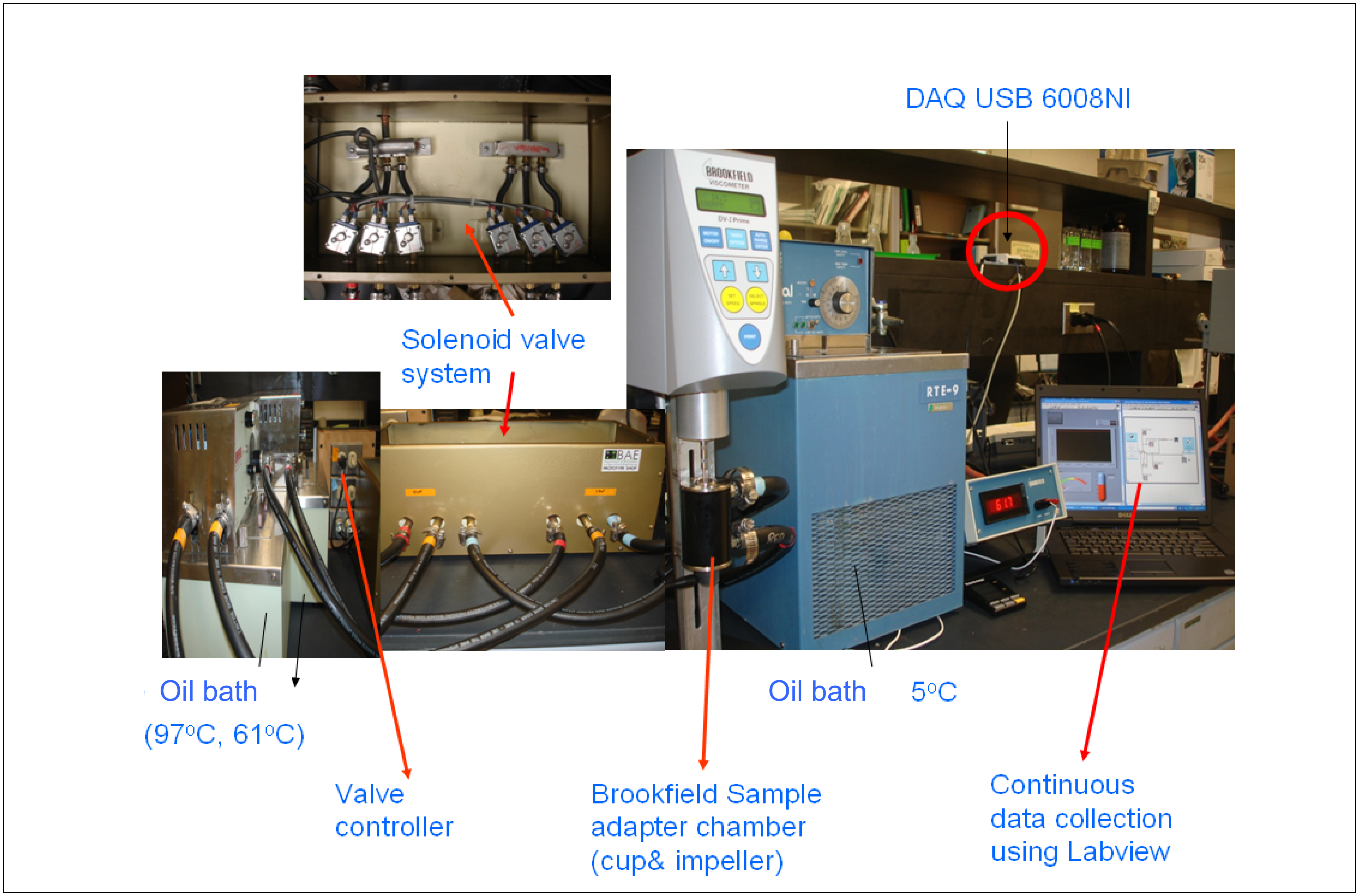

Figure A.1.4. Equipment set up for modified Brookfield viscometer.

Analog output for torque reading which connects to USB6008

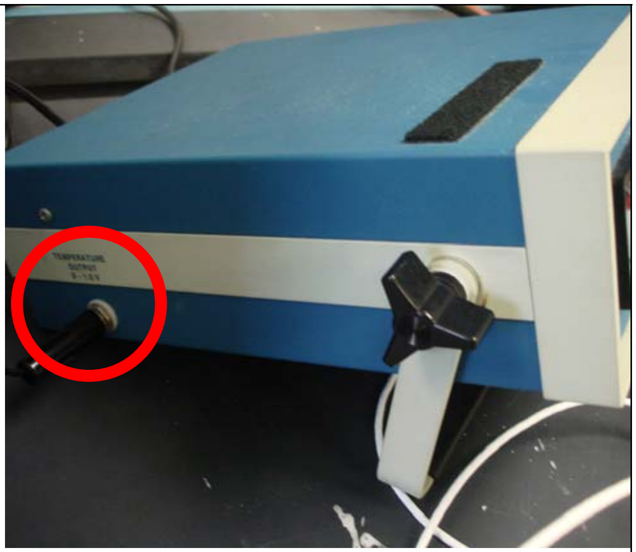

Analog output for temperature reading which connects to USB6008

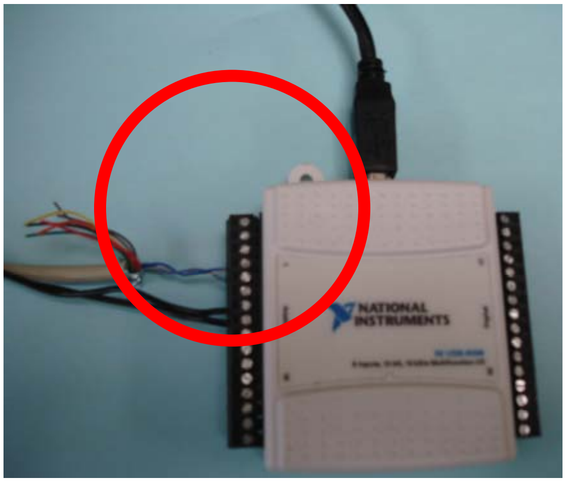

USB6008

Brookfield flag impeller and cup with RTD connector

Figure A.1.5. DAQ set up for modified Brookfield viscometer.

Appendix A2

Amylose Content Determination

Table A.2.1 Prepare total of 5g (Assumed Amylose)

SYSTEM 1 (WAXY+NORMAL) = WN SYSTEM

%AMYLOSE	waxy (g)	normal (g)	code
0	5	0	WN-0
10	3.148	1.852	WN-1
27	0	5	WN-2

SYSTEM 2 (WAXY+HYLON 7) = WH7 SYSTEM

%AMYLOSE	waxy (g)	Hylon VII (g)	code
0	5	0	WH7-0
10	4.285	0.714	WH7-1
20	3.571	1.428	WH7-2
30	2.857	2.142	WH7-3
40	2.143	2.857	WH7-4
50	1.428	3.571	WH7-5
60	0.714	4.285	WH7-6
70	0	5	WH7-7

SYSTEM 3 (NORMAL+HYLON 7) = NH7 SYSTEM

%AMYLOSE	normal (g)	Hylon VII (g)	code
27	3.071	1.928	NH7-2
30	2.857	2.143	NH7-3
40	2.143	2.857	NH7-4
50	1.428	3.571	NH7-5
60	0.714	4.285	NH7-6
70	0	5	NH7-7

SYSTEM 4 (Hylon V+ Hylon VII) = HVHVII SYSTEM

%AMYLOSE	Hylon V (g)	Hylon VII (g)	code
50	1.428	3.571	HVHVII-5
60	0.714	4.285	HVHVII-6
70	0	5	HVHVII-7

SYSTEM 5 (WAXY+HYLON 5) = WH5 SYSTEM

%AMYLOSE	waxy (g)	Hylon V (g)	code
0	5	0	WH5-0

Table A.2.1 (cont'd)

10	4	1	WH5-1
20	3	2	WH5-2
30	2	3	WH5-3
40	1	4	WH5-4
50	0	5	WH5-5

SYSTEM 6 (NORMAL+HYLON 5) = NH5 SYSTEM

%AMYLOSE	normal (g)	Hylon V (g)	code
27	2.3	2.7	NH5-2
30	2	3	NH5-3
40	1	4	NH5-4
50	0	5	NH5-5

Table A.2.2 Prepare total of 0.025g (Assumed Amylose)

SYSTEM 1 (WAXY+NORMAL) = WN SYSTEM

%AMYLOSE	waxy (g)	normal (g)	code
0	0.025	0	WN-0
10	0.015	0.0092	WN-1
27	0	0.025	WN-2

SYSTEM 2 (WAXY+HYLON 7) = WH7 SYSTEM

%AMYLOSE	waxy (g)	Hylon VII (g)	code
0	0.025	0	WH7-0
10	0.0214	0.0035	WH7-1
20	0.0178	0.0071	WH7-2
30	0.0143	0.0107	WH7-3
40	0.0107	0.0143	WH7-4
50	0.0071	0.0179	WH7-5
60	0.0035	0.0214	WH7-6
70	0	0.025	WH7-7

SYSTEM 3 (NORMAL+HYLON 7) = NH7 SYSTEM

%AMYLOSE	normal (g)	Hylon VII (g)	code
27	0.0153	0.0096	NH7-2
30	0.0143	0.0107	NH7-3
40	0.0107	0.0143	NH7-4
50	0.0071	0.0179	NH7-5
60	0.0036	0.0214	NH7-6
70	0	0.025	NH7-7

Table A.2.2 (cont'd)

SYSTEM 4 (Hylon V+ Hylon VII) = HVHVII SYSTEM

%AMYLOSE	Hylon V (g)	Hylon VII (g)	code
50	0.0071	0.0179	HVHVII-5
60	0.0035	0.0214	HVHVII-6
70	0	0.025	HVHVII-7

SYSTEM 5 (WAXY+HYLON 5) = WH5 SYSTEM

%AMYLOSE	waxy (g)	Hylon V (g)	code
0	0.025	0	WH5-0
10	0.02	0.005	WH5-1
20	0.015	0.01	WH5-2
30	0.01	0.015	WH5-3
40	0.005	0.02	WH5-4
50	0	0.025	WH5-5

SYSTEM 6 (NORMAL+HYLON 5) = NH5 SYSTEM

%AMYLOSE	normal (g)	Hylon V (g)	code
27	0.0115	0.0135	NH5-2
30	0.01	0.015	NH5-3
40	0.005	0.02	NH5-4
50	0	0.025	NH5-5

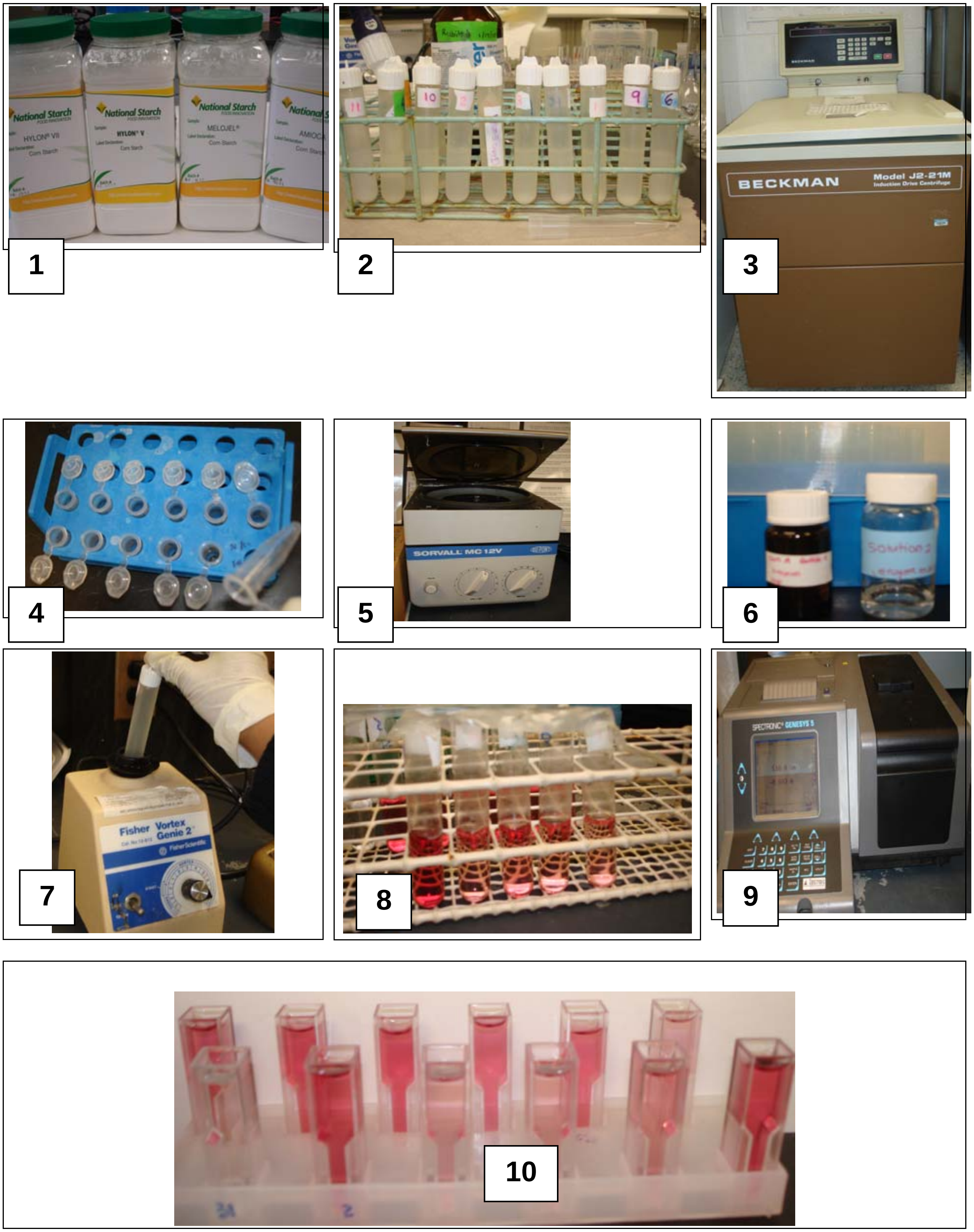

Figure A.2.1. Amylose contents measurement using CON A(Megazyme).

Appendix A3

Thermal Properties Determination (DSC)

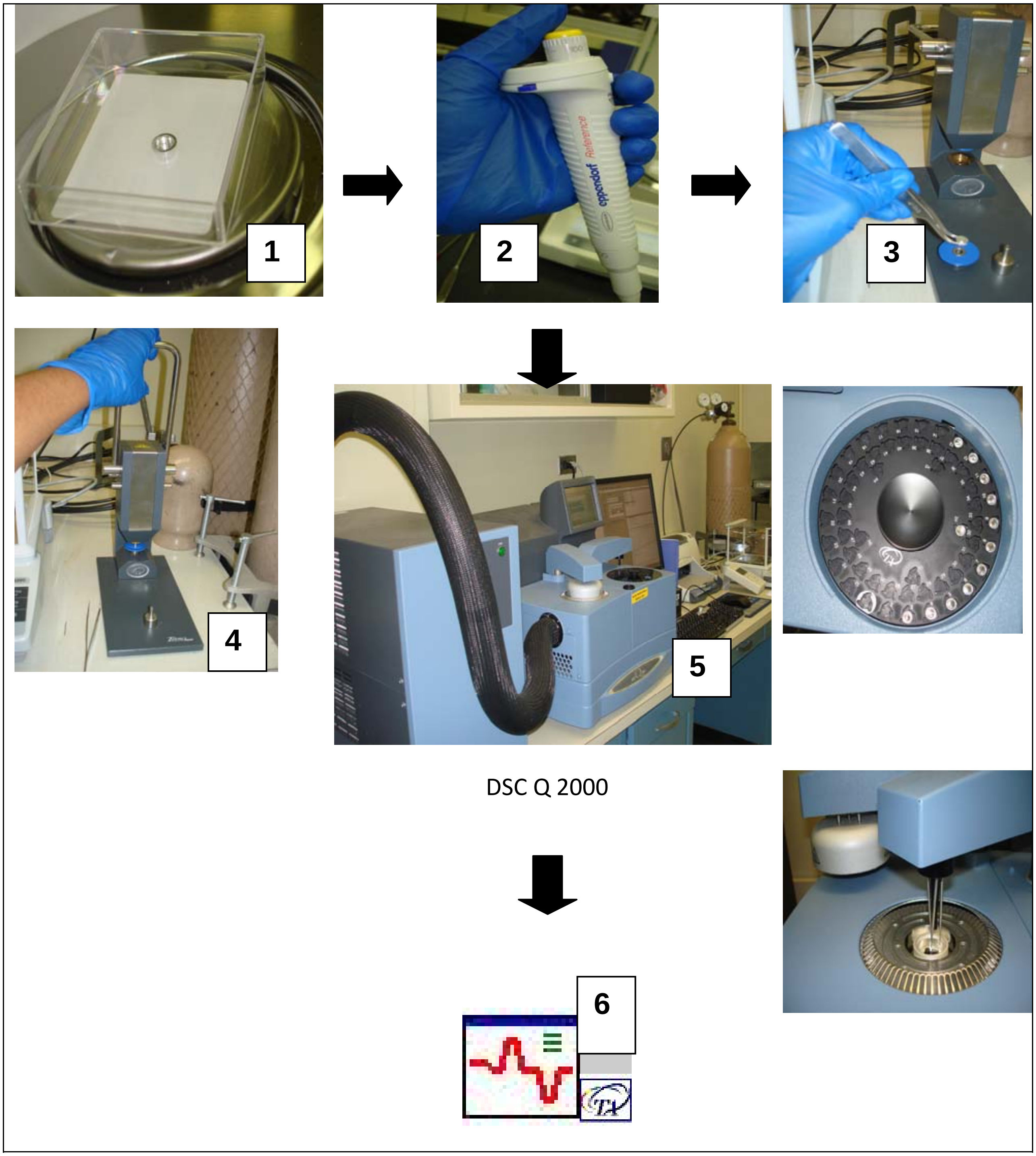

Figure A.3.1. Starch thermal properties measurement using DSC.

Table A.3.1Thermal properties data for corn starch blends

Amylose experimental	Amylose assumed	Starch Mixtures	DSC parameters				
			T_s	T_o	delta H (J/g)	T_p	T_c
SYSTEM 1							
3.56	0	waxy_R1	64.14	67.2	15.05	72.66	80.6
3.56	0	waxy_R2	62.21	66.7	14.22	72.38	84.47
3.56	0	waxy_R3	63.66	67.3	14.82	72.74	83.82
6.15	10	WN10_R1	65.27	67.4	12.67	72.08	81.4
6.15	10	WN10_R2	64.63	67.6	11.75	72.27	81.57
6.15	10	WN10_R3	64.31	67.3	12.54	72.16	80.6
13.63	27	normal_R1	64.14	67.5	10.43	71.31	80.76
13.63	27	normal_R2	64.14	67.8	9.765	71.6	82.05
13.63	27	normal_R3	63.18	67.6	12.06	71.36	86.08
SYSTEM 2							
5.81	10	WHV_10R1	63.66	67.2	10.95	72.57	81.08
5.81	10	WHV_10R2	64.63	67.3	10.02	72.52	79.63
5.81	10	WHV_10R3	63.82	67	9.495	72.43	80.11
13.98	20	WHV_20R1	63.82	67.6	7.541	72.49	78.82
13.98	20	WHV_20R2	65.11	67.5	8.348	72.62	79.31
13.98	20	WHV_20R3	65.6	67.6	7.053	72.33	78.02
21.28	30	WHV_30R1	65.27	67.6	5.734	72.52	78.5
21.28	30	WHV_30R2	65.11	68.1	5.252	72.64	79.31
21.28	30	WHV_30R3	64.79	67.7	5.74	72.54	80.11
34.03	40	WHV_40R1	64.95	69	17.29	74.36	105.8
34.03	40	WHV_40R2	66.4	68.8	15.48	73.78	108.7
34.03	40	WHV_40R3	65.76	68.6	16.11	73.53	111.4
34.03	50	HV_R2	65.27	69.6	18.45	78.06	115.3
34.03	50	HV_R3	65.43	69.6	18.31	77.56	111.6
SYSTEM 3							
9.27	10	WHVII_10R1	63.34	69.4	13.03	73.5	86.08
9.27	10	WHVII_10R2	62.21	67.3	14.01	72.81	91.24
9.27	10	WHVII_10R3	62.37	67.2	11.97	72.73	84.63
10.46	20	WHVII_20R1	64.49	68	10.16	72.13	81.8
10.46	20	WHVII_20R2	62.85	67.5	9.93	72.59	82.37
10.46	20	WHVII_20R3	63.66	67.2	10.22	72.63	83.99
19	30	WHVII_30R1	62.93	67.8	9.12	72.95	82.7
19	30	WHVII_30R2	63.52	67.2	8.557	72.18	83.28
19	30	WHVII_30R3	62.85	67.7	8.621	72.83	84.63
34.85	40	WHVII_40R1	64.79	68.1	6.066	72.58	79.79

Table A.3.1 (cont'd)							
34.85	40	WHVII_40R2	64.49	68.1	5.87	72.68	80.73
34.85	40	WHVII_40R3	64.79	68.2	5.662	72.79	81.89
46.2	50	WHVII_50R1	65.43	68.7	3.43	72.54	78.66
46.2	50	WHVII_50R2	65.6	68.9	3.748	72.59	78.34
46.2	50	WHVII_50R3	65.6	68.8	3.271	72.46	78.82
57.82	60	WHVII_60R2	65.92	69.6	3.336	72.78	81.08
57.82	60	WHVII_60R3	65.6	69.4	3.204	72.78	80.6
SYSTEM 4							
28.62	20	NHV_20R1	65.92	68	4.75	71.6	77.37
28.62	20	NHV_20R2	64.63	67.6	4.525	71.1	77.21
28.62	20	NHV_20R3	64.47	67.8	4.474	70.96	82.05
32.39	30	NHV_30R1	65.11	68	4.632	71.48	79.63
32.39	30	NHV_30R2	65.92	67.8	4.53	71.29	77.05
32.39	30	NHV_30R3	65.43	68.2	4.584	71.54	77.37
35.95	40	NHV_40R1	66.24		16.92	72.17	106.4
35.95	40	NHV_40R2	66.08	67.7	16.78	72.17	106.4
35.95	40	NHV_40R3	63.82	67.9	14.48	72.47	111.7
SYSTEM 5							
28.23	20	NHVII_20R1	65.27	67.4	5.55	71.2	76.73
28.23	20	NHVII_20R2	65.27	67.7	6.016	71.31	77.05
28.23	20	NHVII_20R3	65.76	67.9	5.53	71.64	77.53
32.77	30	NHVII_30R1	64.95	67.8	5.466	71.22	76.57
32.77	30	NHVII_30R2	66.08	68	5.272	71.6	77.86
32.77	30	NHVII_30R3	66.08	68.2	4.5	71.56	76.24
38.29	40	NHVII_40R1	65.92	68.1	3.649	71.48	77.05
38.29	40	NHVII_40R2	66.73	68.1	3.589	71.33	76.08
38.29	40	NHVII_40R3	66.08	67.9	4.349	71.39	74.95
48.39	50	NHVII_50R1	65.11	68	4.051	71.69	77.37
48.39	50	NHVII_50R2	65.27	68.2	3.833	71.85	77.69
48.39	50	NHVII_50R3	66.4	68.3	3.751	71.81	77.05
53.31	60	NHVII_60R1	66.56	68.5	15.14	72.62	111.9
53.31	60	NHVII_60R2	66.73	68.5	14.5	72.57	110.9
53.31	60	NHVII_60R3	66.89	68.8	15.86	72.68	114
SYSTEM 6							
57.82	60	HVHVII_60R1	67.53	69.8	17.15	73.58	116.6
57.82	60	HVHVII_60R2	67.21	69.8	17.92	73.46	116.6
61.46	70	HVII_R1	63.02	69.7	15.51	73.17	115.3
61.46	70	HVII_R2	68.5	70.5	15.39	74.04	112.9
61.46	70	HVII_R3	67.53	69.8	14.64	73.69	117.1

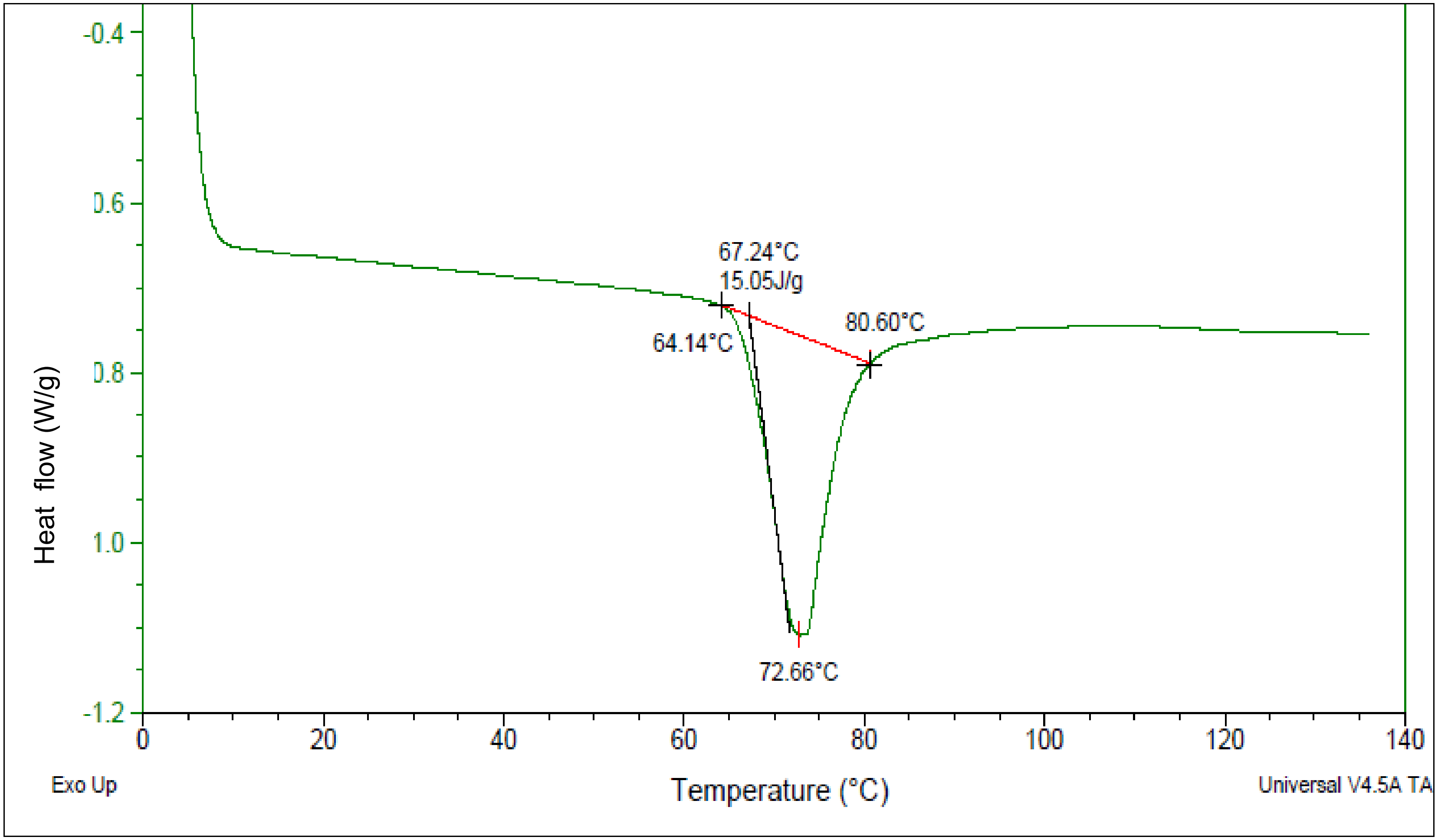

Figure A.3.4 Example of DSC results for waxy corn starch

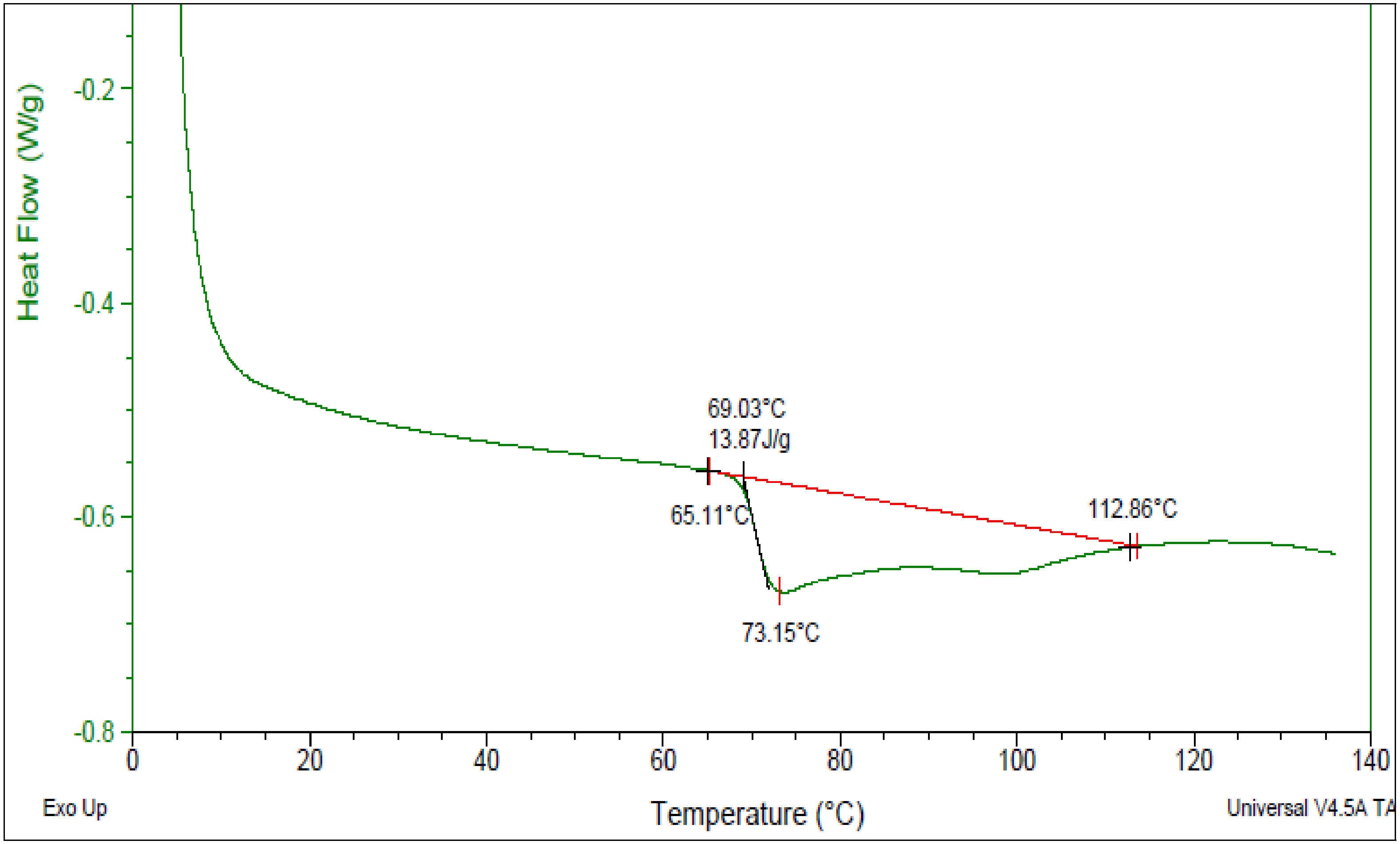

Figure A.3.5 DSC results for NH7_6 (normal and HylonVII corn starch blends at 60%AM)

Appendix A4

Empirical equations from pasting curves

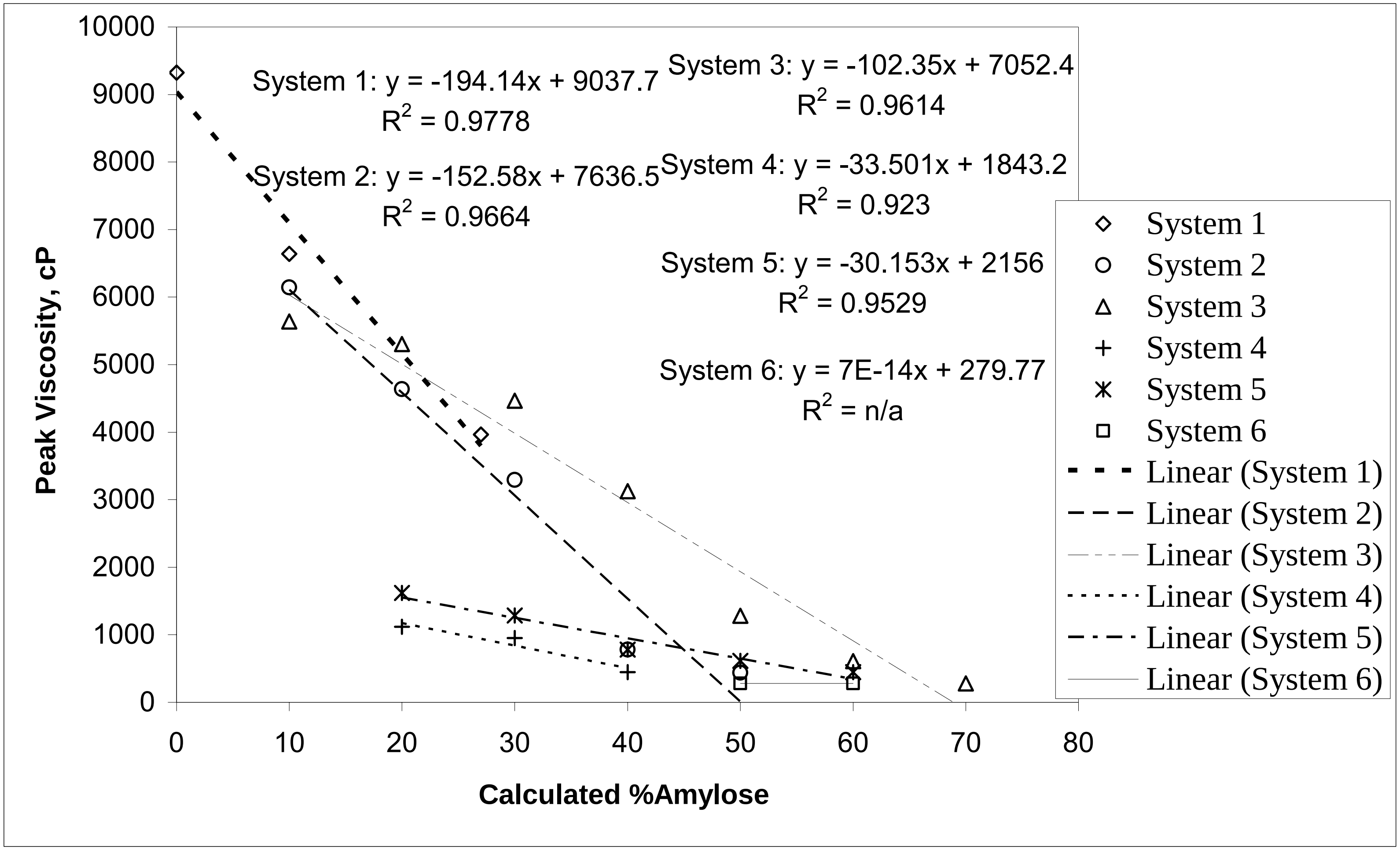

Figure A.4.1. Peak Viscosity as function of amylose (assumed) for corn starch blends in all six systems studied.

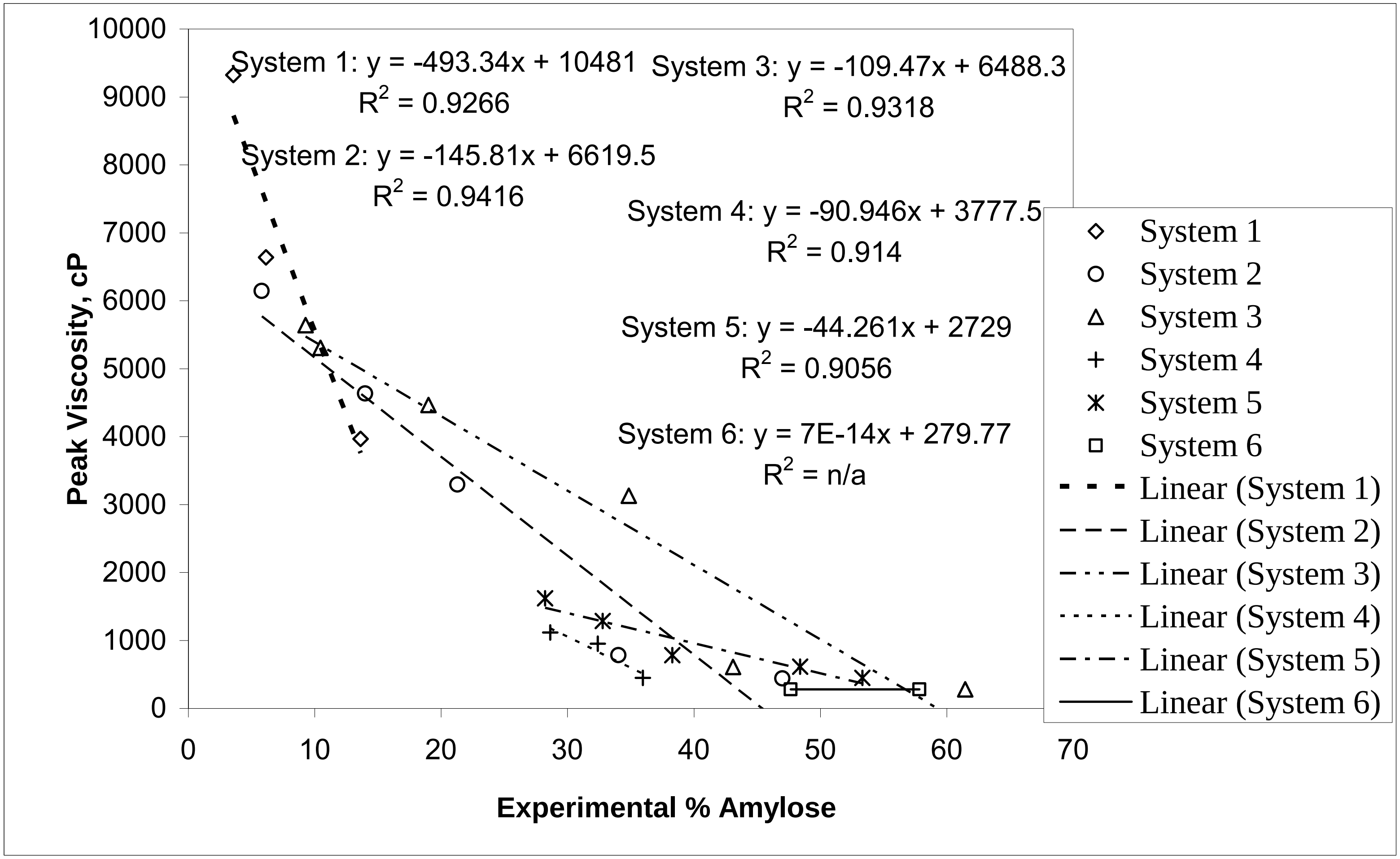

Figure A.4.2. Peak Viscosity as function of amylose (analytically) for corn starch blends in all six systems studied.

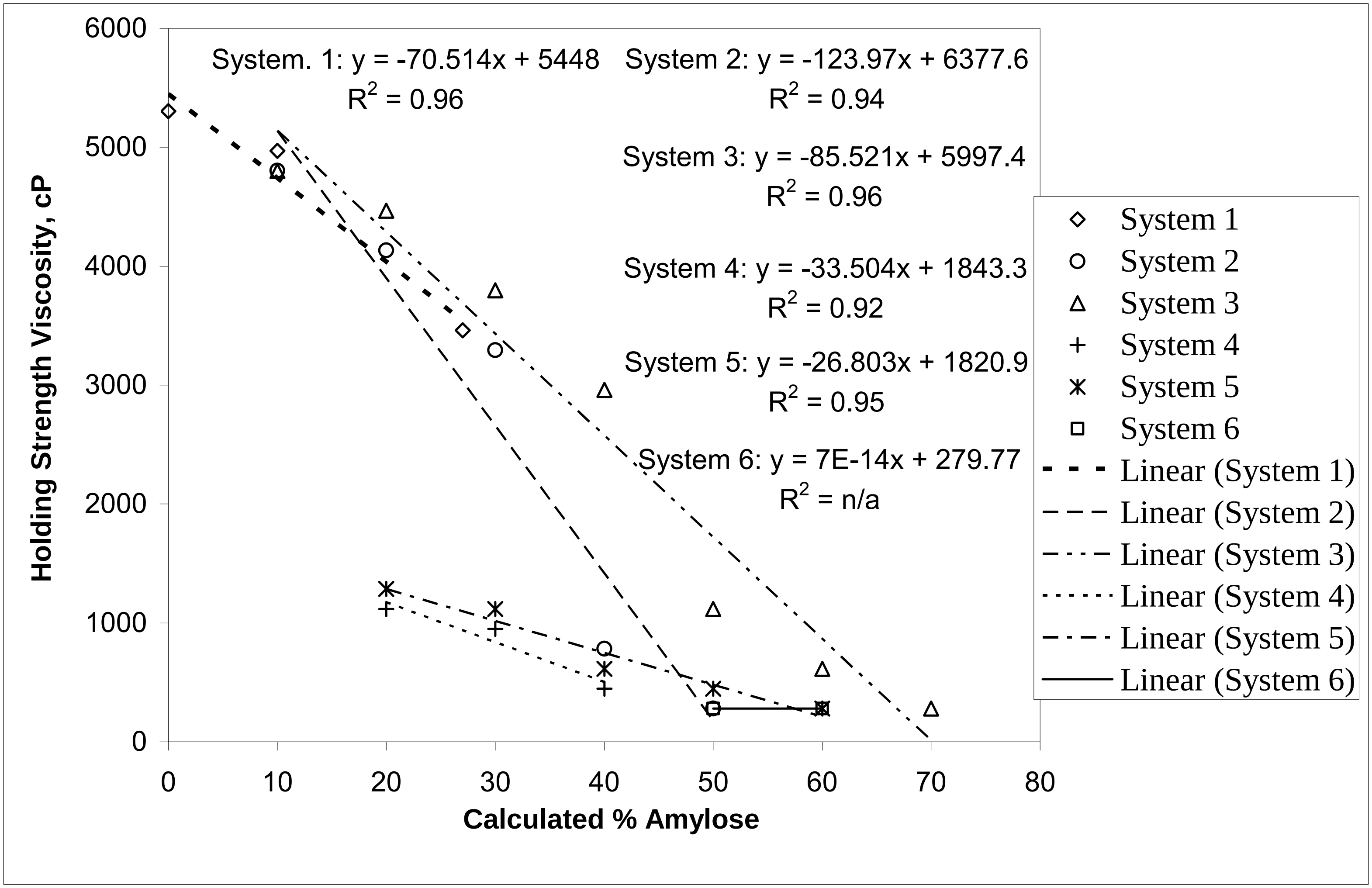

Figure A.4.3. Holding strength viscosity as function of amylose (assumed) for corn starch blends in all six systems studied.

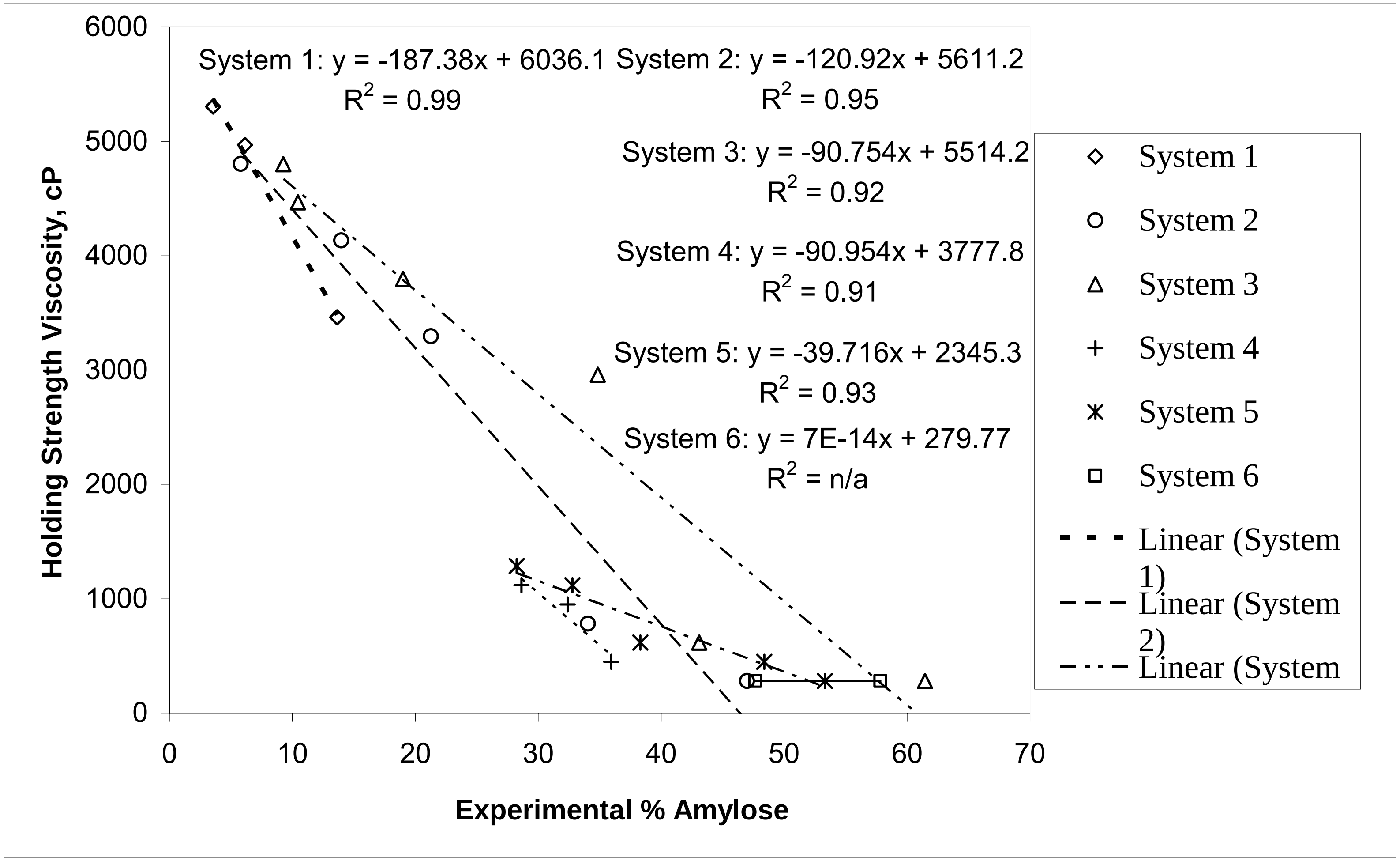

Figure A.4.4. Holding strength viscosity as function of amylose (analytically) for corn starch blends in all six systems studied.

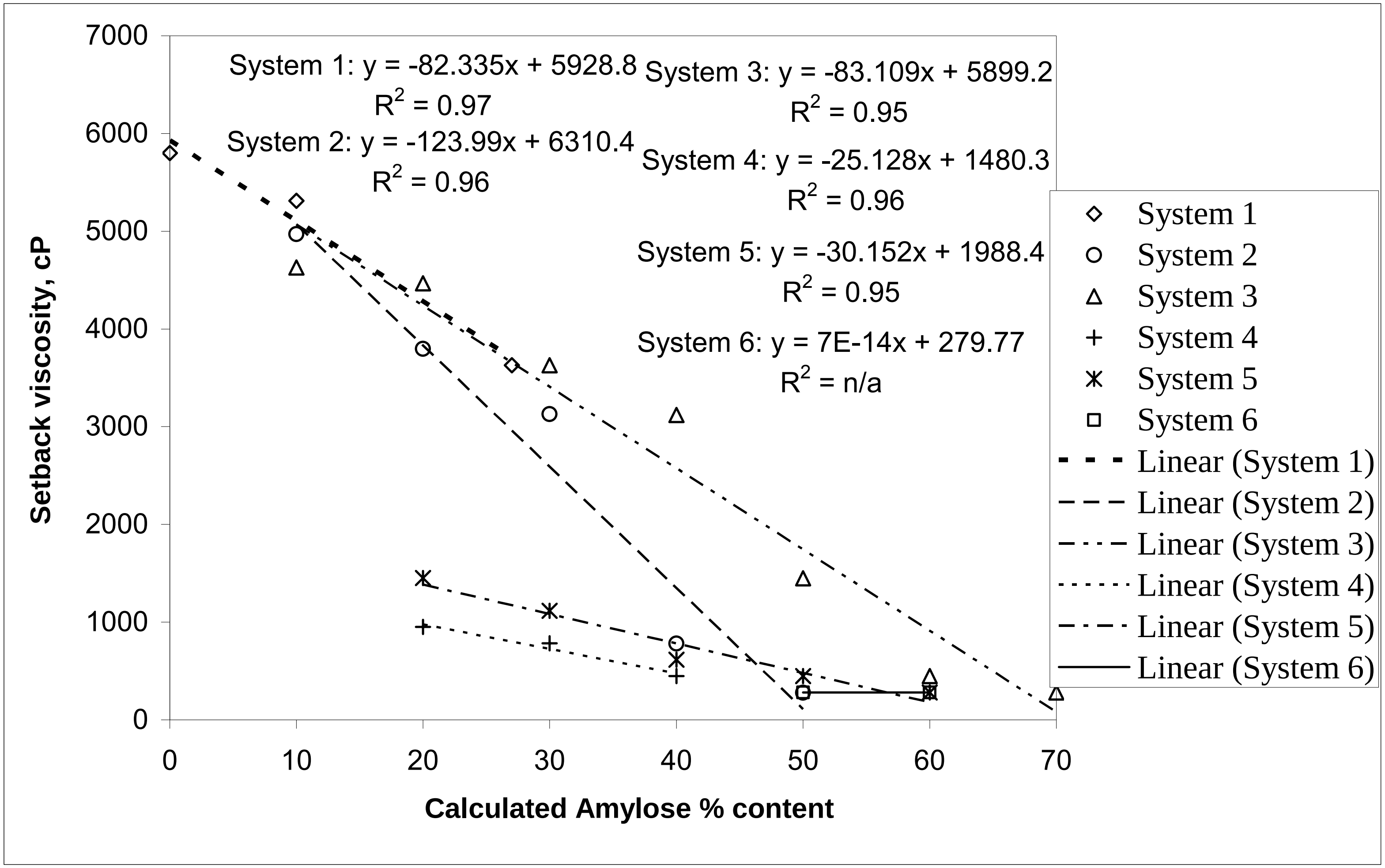

Figure A.4.5. Setback viscosity as function of amylose (assumed) for corn starch blends in all six systems studied.

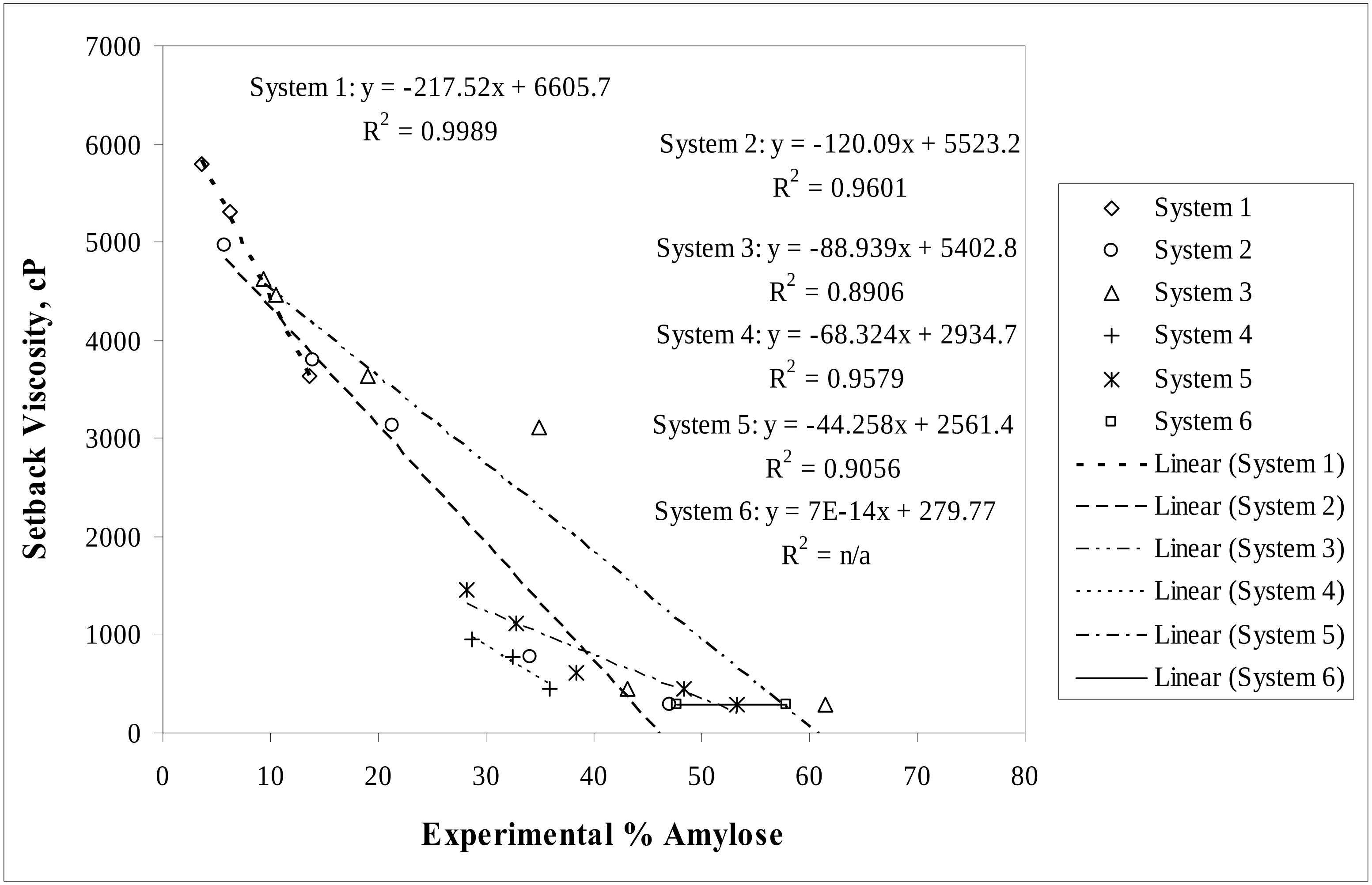

Figure A.4.6. Setback viscosity as function of amylose (analytically) for corn starch blends in all six systems studied.

REFERENCES

References

Ahromrit A, Ledward DA & Niranjan K. 2006. High pressure induced water uptake characteristics of Thai glutinous rice. Journal of Food Engineering 72(3):225-233.

Briggs JL & Steffe JF. 1996. Mixer viscometer constant (k') for the Brookfield small sample adapter and flag impeller. Journal of Texture Studies 27(6):671-677.

Carl Hoseney R. 1998. Principles of Cereal: Science And Technology American Association of Cereal Chemists, Inc. St. Paul, Minnesota, USA Second edition:13-57.

Chang YH & Lin JH. 2007. Effects of molecular size and structure of amylopectin on the retrogradation thermal properties of waxy rice and waxy cornstarches. Food Hydrocolloids 21(4):645-653.

Cheetham NWH & Tao LP. 1997. The effects of amylose content on the molecular size of amylose, and on the distribution of amylopectin chain length in maize starches. Carbohydrate Polymers 33(4):251-261.

Cheetham NWH & Tao LP. 1998. Variation in crystalline type with amylose content in maize starch granules: an X-ray powder diffraction study. Carbohydrate Polymers 36(4):277-284.

Hemminger W & Sarge SM. 1994. Calibration as an Aspect of Quality Assurance in Differential Scanning Calorimetry (DSC) Measurements.Thermochimica Acta 245:181-187.

Jane J, Chen YY, Lee LF, McPherson AE, Wong KS, Radosavljevic M & Kasemsuwan T. 1999. Effects of amylopectin branch chain length and amylose content on the gelatinization and pasting properties of starch. Cereal Chemistry 76(5):629-637.

Juhasz R & Salgo A. 2008. Pasting behavior of amylose amylopectin and, their mixtures as determined by RVA curves and first derivatives. Starch-Starke 60(2):70-78.

Kohyama K, Matsuki J, Yasui T & Sasaki T. 2004. A differential thermal analysis of the gelatinization and retrogradation of wheat starches with different amylopectin chain lengths. Carbohydrate Polymers 58(1):71-77.

Kousksou T, Jamil A, El Omari K, Zeraouli Y & Le Guer Y. 2011. Effect of heating rate and sample geometry on the apparent specific heat capacity: DSC applications. Thermochimica Acta 519(1-2):59-64.

Kurakake M, Akiyama Y, Hagiwara H & Komaki T. 2009. Effects of cross-linking and low molecular amylose on pasting characteristics of waxy corn starch. Food Chemistry 116(1):66-70.

Lagarrigue S & Alvarez G. 2001. The rheology of starch dispersions at high temperatures and high shear rates: a review. Journal of Food Engineering 50(4):189-202.

Liu HS, Yu L, Xie FW & Chen L. 2006. Gelatinization of cornstarch with different amylose/amylopectin content. Carbohydrate Polymers 65(3):357-363.

Liu P, Yu L, Liu HS, Chen L & Li L. 2009. Glass transition temperature of starch studied by a high-speed DSC. Carbohydrate Polymers 77(2):250-253.

Matveev YI, van Soest JJG, Nieman C, Wasserman LA, Protserov V, Ezernitskaja M & Yuryev VP. 2001. The relationship between thermodynamic and structural properties of low and high amylose maize starches. Carbohydrate Polymers 44(2):151-160.

Megazyme. 2006. Amylose/Amylopectin assay procedure K-AMYL 04/06 : for the measurement of the amylose and amylopectin contents of starch. Megazyme International Ireland Ltd, Bray Business Park, Bray, Co.Wicklow, Ireland.

Noda T, Takahata Y, Sato T, Suda I, Morishita T, Ishiguro K & Yamakawa O. 1998. Relationships between chain length distribution of amylopectin and gelatinization properties within the same botanical origin for sweet potato and buckwheat. Carbohydrate Polymers 37(2):153-158.

Nuessli J, Handschin S, Conde-Petit B & Escher F. 2000. Rheology and structure of amylopectin potato starch dispersions without and with emulsifier addition. Starch-Starke 52(1):22-27.

Park IM, Ibanez AM & Shoemaker CF. 2007. Rice starch molecular size and its relationship with amylose content. Starch-Starke 59(2):69-77.

Ratnayake WS & Jackson DS. 2007. A new insight into the gelatinization process of native starches. Carbohydrate Polymers 67(4):511-529.

Rolee A & LeMeste M. 1997. Thermomechanical behavior of concentrated starch-water preparations. Cereal Chemistry 74(5):581-588.

Russell PL. 1987. Gelatinization of Starches of Different Amylose Amylopectin Content - a Study by Differential Scanning Calorimetry. Journal of Cereal Science 6(2):133-145.

Sasaki T, Yasui Ta & Matsuki J. 2000. Effect of amylose content on gelatinization, retrogradation, and pasting properties of starches from waxy and nonwaxy wheat and their F1 seeds. Cereal Chemistry 77(1):58-63.

Shalaev EY & Steponkus PL. 2000. Correction of the sample weight in hermetically sealed DSC pans. Thermochimica Acta 345(2):141-143.

Stawski D. 2008. New determination method of amylose content in potato starch. Food Chemistry 110(3):777-781.

Steffe JF. 1996. Rheological Methods in Food Process Engineering. Second Edition Freeman Press(East Lansing, MI):2.

Steffe JF, Castellperez ME, Rose KJ & Zabik ME. 1989. Rapid Testing Method for Characterizing the Rheological Behavior of Gelatinizing Corn Starch Slurries. Cereal Chemistry 66(1):65-68.

Steffe JF & Daubert CR. 2006. Bioprocessing Pipelines: Rheology and Analysis. Freeman Press, East Lansing, MI, USA.

Tester RF & Morrison WR. 1990. Swelling and Gelatinization of Cereal Starches .1. Effects of Amylopectin, Amylose, and Lipids. Cereal Chemistry 67(6):551-557.

Thomas DJ & Atwell WA. 1999. Starches. American Association of Cereal Chemists. Eagan Press Handbook Series, St. Paul, Minnesota, USA.

Thomas DJA, W.A. 1999. Starches: Practical Guides For The Food Industry. Eagan Press Handbook Series Eagan Press. St. Paul, Minnesota, USA.

Wang WC & Sastry SK. 1997. Starch gelatinization in ohmic heating. Journal of Food Engineering 34(3):225-242.

Xue T, Yu L, Xie FW, Chen L & Li L. 2008. Rheological properties and phase transition of starch under shear stress. Food Hydrocolloids 22(6):973-978.

Yu L & Christie G. 2001. Measurement of starch thermal transitions using differential scanning calorimetry. Carbohydrate Polymers 46(2):179-184.

Zaidul ISM, Absar N, Kim SJ, Suzuki T, Karim AA, Yamauchi H & Noda T. 2008. DSC study of mixtures of wheat flour and potato, sweet potato, cassava, and yam starches. Journal of Food Engineering 86(1):68-73.

CHAPTER 4

OBJECTIVE TWO

Estimating Kinetic Parameters in a Starch Viscosity Model using Nonlinear Parameter Estimation Techniques

Abstract

A modified Brookfield viscometer equipped with a data acquisition system using LabView was used to study the gelatinizing behavior of native corn starch in water solutions at 6% (w/w) concentration. Data for the dependent variable (continuous torque), and independent variables were collected. The independent variables were time-temperature history, shear history, and temperature, corresponding to the three main regions in a pasting curve. The variables were then entered into the MATLAB program and the kinetic parameters of the starch viscosity model were estimated. Parameters were determined simultaneously using both ordinary least squares, and the sequential method. The model fit very well as shown by RMSE of approximately 2% of full scale, and relative standard error of all parameters estimated was less than 11%. These parameters were then used to predict pasting curves for the same starch in the RVA system. The estimation of the rheological activation energy of gelatinization E_g= 964±39 kJ/mol, was much larger than all other studies. Scaled sensitivity coefficients showed that the most important parameters were time-temperature history, followed by shear history, and the temperature parameter was the least important. The predicted rise of the RVA viscosity lagged the observed rise by approximately 1min; and the observed RVA peak was underestimated by approximately 10%. The overall trend of the RVA data was predicted accurately. This work is the first to show that starch-pasting curve parameters can be estimated simultaneously and sequentially, and can be used to predict pasting curves in other systems reasonably well.

Keywords: Gelatinization; Corn Starch; Viscosity Model; Nonlinear Parameter Estimation; Pasting Curve; Mixer Viscometry; LabView; Brookfield Viscometer; Non-isothermal; Inverse Problem; Rheology; Rapid Visco Analyzer (RVA); Non-Newtonian

4.1 Introduction

Most rheological studies of starch dispersions have been conducted on *gelatinized* starches. Apparent viscosity models for gelatinized starch dispersions are reported to show power law, Herschel Bulkley, Bingham plastic, and Casson model behavior. The consistency coefficient (K) and the flow behavior index (n) of those models are reported to depend on the kind of starch, starch concentration, and temperature (Lagarrigue and Alvarez 2001). However, process design also requires the knowledge of rheological properties for gelatinizing starch during heating, cooling, and the mechanical effect with time.

Very few studies have modeled the kinetics of *gelatinizing* starch solutions using a complete mathematical development. This situation may be due to lack of fundamental theory for data collected from empirical testing systems or some limitation in the rheometer. (Dolan and Steffe 1990) developed a complete starch model for rheological behavior of gelatinizing starch solutions using mixer viscometer data for 5.5-7.3% db native corn starch solutions, and 6% bean starch solution based on the viscosity model of protein doughs proposed by Morgan and others (1989). The model equation is derived mainly from the power law model for the shear rate term, Eyring's kinetic theory for the temperature term, and polymer chemistry for the temperature-time history term (Morgan 1979). Dolan and Steffe (1990) used a mixer viscometry approach to collect the starch gelatinization data and then demonstrated the feasibility of the model with some modifications (Morgan et al. 1989) to account for starch dispersions in excess water.

The kinetic model for gelatinizing starch solutions proposed by Dolan and Steffe (1990), which predicts torque during starch gelatinization based on five independent variables with ten parameters, shows good agreement between the simulated and the experimental results for native corn starch (5.5 -7.3%) and a 6% bean starch solution. Although the Dolan and Steffe (1990) model provides valuable information for kinetic modeling of starch gelatinization, there were two major limitations:

1. Each parameter in the model was identified separately by varying only one independent variable in each experiment, but the fact is that interaction among variables is strong so it is more accurate to estimate the parameters simultaneously. No simultaneous parameter estimation techniques were applied to estimate the parameters in the model.
2. The effect of reference temperature on the estimated parameters was not investigated, leading to an inability to estimate the reaction rate accurately.

Better parameter estimation techniques could be applied as a modeling approach when estimating the parameters in the model. Parameter estimation techniques discussed in (Beck and Arnold 1977), such as sensitivity coefficient, residual plots, sequential estimation, correlation coefficient matrix, and confidence interval were used in this study to provide an approach to estimate parameters present in the starch viscosity model proposed by Dolan and Steffe (1990). Estimating parameters in nonlinear models is complex compared to linear models (Dolan 2003). However, parameter estimation techniques provide several ways to accurately estimate constants in non-linear equations if input and the output data are known. A better estimate of a parameter is obtained with prior information of the parameters. In addition, sequential MAP estimation can be used for estimating the parameters in the model simultaneously and sequentially (Beck and Arnold 1977). When this approach is used successfully, the resulting model will enhance theoretical investigations to develop a generic starch viscosity model. Therefore the objectives of this study were:

(1) To estimate the parameters in the starch viscosity model by applying sequential parameter estimation techniques, and taking into consideration the reference temperature;

(2) To propose and test a generic starch viscosity model to predict pasting curves of gelatinizing native corn starch in a different mechanical system (RVA);

4.2 Overview of Method

4.2.1 Mixer Viscometer Data Collection

4.2.1.1 Sample Preparation

Native corn starch (Melojel, National Starch, NJ) at 6%w/w concentration in a starch: water system was prepared. A small sample size of 0.829g in 13mL water was used. The sample was mixed vortex for 30sec in a test tube before measurements. The sample, at room temperature, was poured into the heated cup while the impeller was agitated to avoid sample settling problems. The temperature profile involved heating the sample rapidly from 60^{o}C to 95^{o}C in 5min, holding at 95^{o}C for 7min, cooling to 60^{o}C in 13sec, and then holding constant at 60^{o}C for 10min.

4.2.1.2 Equipment Set Up

A Brookfield viscometer equipped with three water baths (temperatures set at 96^{o}C, 60^{o}C, and 5^{o}C) and a solenoid valve system was constructed. A brookfield flag impeller and small cup adapter with RTD on bottom of the sample cup was used. Calibration of instrument voltage and torque were done by using a few standard samples of silicon oil. Calibration of voltage and temperature were done by using ice, boiling water, and also by heating the water at fixed water bath temperatures. A data acquisition system (USB 6008), and a block diagram using Lab View, was created to collect the continuous time, temperature, and torque data.

4.2.2 Rapid Visco Analyzer (RVA) data collection

Standard profile 1 of the RVA was used for the time-temperature profile. Native corn starch (Melojel, National Starch, NJ) at 6%w/w concentration in a starch: water system was prepared. The total sample volume was 25mL. Time, temperature, and apparent viscosity of the samples during the 13min test were recorded.

4.2.3 Mathematical Modeling

Eq. (5) shows the modification of starch model proposed by Dolan and Steffe (1990). The dependent variable is torque (M), five independent variables are (N, T, C,Ψ,ϕ), and the model consisted of ten parameters in total (K_r, n, E_v, b, A^{α} ,α, k, E_g, B, and d). The model Eq. (5) from left to right includes terms for shear rate, temperature, concentration, time-temperature, and shear history, respectively. In this study, Dolan's model was modified. The modification includes :(1) include the reference temperature in the time-temperature history (T_{rg}) and temperature terms (T_{rt}) on Arrhenius equation, and find the parameters at optimum reference temperature where the correlation between the parameters are minimum; (2) emphasized on scaled sensitivity coefficient to minimize number of parameters to be estimated.

$$M(t) = K_r N^n * e^{\frac{E_v}{R}\left(\frac{1}{T(t)} - \frac{1}{T_{rt}}\right)} * e^{b(C-C_r)} * \left[1 + A^{\alpha}\left(1 - e^{-k_g \psi}\right)^{\alpha}\right] * \left[1 - B\left(1 - e^{-d\phi}\right)\right]$$

(5)

Where $\psi = \int_0^{t_f} \frac{T(t)}{300} e^{\frac{-E_g}{R}\left(\frac{1}{T(t)} - \frac{1}{T_{rg}}\right)} dt$ and

$$\phi = \int_0^{t_f} N\,dt = N\,t$$

(6)

For estimation purposes, ψ was divided by 300 to stabilize the sensitivity matrix (Jacobian). The torque model allows starch apparent viscosity prediction by applying the mixer viscometry equation as shown in Equation (7) (Steffe and Daubert, 2006).

$$\eta = \frac{k''M}{\Omega} \tag{7}$$

Since the torque model in Eq. (5) is very important in determining the apparent viscosity of gelatinizing starch solutions using Eq.(7), the influence of each term appearing in the torque model was investigated in this study. In any one experiment, the impeller speed and the starch sample concentration are held constant. Thus, the shear rate term and concentration term in Eq. (5) can be combined and treated as a constant (parameter S). This way we could reduce the number of parameters to be estimated from 10 parameters to 8. In addition, it allowed better focus on investigating the importance of the time-temperature history, the shear history, and the temperature in the torque model. To compare the relative effect of the terms, the model was formulated having only the time-temperature history term (model 1), or the time-temperature history and shear history terms (model 2), and finally the time-temperature history, shear history and temperature terms (model 3).

Model 1:

$$M(t) = S * \left[1 + A^{\alpha}\left(1 - e^{-k_g \psi}\right)^{\alpha}\right] \tag{8}$$

Model 2:

$$M(t) = S * \left[1 + A^{\alpha}\left(1 - e^{-k_g \psi}\right)^{\alpha}\right] * \left[1 - B\left(1 - e^{-d\phi}\right)\right] \tag{9}$$

Model 3:

$$M(t) = S * \left[1 + A^{\alpha}\left(1 - e^{-k_g \psi}\right)^{\alpha}\right] * \left[1 - B\left(1 - e^{-d\phi}\right)\right] * e^{\frac{E_v}{R}\left(\frac{1}{T(t)} - \frac{1}{T_{rt}}\right)}$$

(10)

The corrected Akaike's Information Criterion (AIC_C) (Motulsky and Christopoulos 2004) was used to compare models:

$$AIC_c = N * \ln\left(\frac{SS}{N}\right) + 2K + \frac{2K(K+1)}{N-K-1} \qquad (11)$$

Where the N is the number of data points, K is the number of parameters fit by the regression plus one, and SS is the sum of the squares of the vertical distance of the points from the curve. A lower AIC_C score indicates the best accuracy with fewest parameters.

4.2.4 Arrhenius Reference Temperature

The gelatinization reference temperature T_{rg} is a "nuisance parameter," because it cannot be estimated by minimizing error sum of squares (SS). Changing T_{rg} will result in exactly the same SS for the Arrhenius model. The importance of the reference temperature T_{rg} is that it controls the correlation coefficient between the rate constant (k_g) and activation energy (E_g). As the correlation coefficient is minimized, the confidence interval for k_g is also minimized, allowing estimation of both parameters simultaneously. The optimum T_{rg} was found iteratively by holding T_{rg} at different fixed values, estimating the parameters for Model 1, plotting the correlation coefficient and choosing the T_{rg} where the correlation was nearly zero (Schwaab and Pinto 2007).

A similar approach was used to find the reference temperature T_{rt} for temperature in Model 3. The T_{rt} controls the correlation coefficient between the A^{α} and activation energy (E_v). The optimum T_{rt} was found iteratively by holding T_{rt} at different fixed values, estimating the parameters for Model 3, plotting the correlation coefficient and choosing the T_{rg} where the correlation was nearly zero.

4.2.5 Parameter Estimation Techniques

4.2.5.1 Sensitivity Coefficient Plot

The sensitivity coefficient (x_{ij}) is formed by taking the first derivative of a dependent variable with respect to a specific parameter. The parameters in the model can be estimated most accurately when its x_{ij} is maximized (Beck and Arnold 1977). Estimation of kinetic parameters for nonisothermal food processes using nonlinear parameter estimation has been discussed by (Dolan 2003). To place the x_{ij} on the same scale, we used a scaled sensitivity coefficient (X'_{ij}). The scaled sensitivity coefficient plots are helpful in determining which parameters can be estimated most accurately, and which parameters are most important in the model. Here, we determined the sensitivity coefficient (x_{ij}) of parameter (β) using the finite difference method of forward difference approximation (Beck and Arnold 1977) for each parameter as presented in Eq. (12). The δb_j is some relatively small quantity and given as Eq. (13). The scaled sensitivity coefficients shown in Eq. (14) were computed using MATLAB programming. To have a sensitivity coefficient plot, we have to have independent variables and approximate value of parameters.

$$\frac{\partial M(i)}{\partial \beta_j} = x_{ij} = \frac{M(b_1,...,b_j + \delta b_j,...b_p) - M(b_1,...,b_j,...,b_p)}{\delta b_j} \tag{12}$$

$$\delta b_j = 0.0001 b_j \tag{13}$$

$$X'_{ij} = \beta_j \frac{\partial M(i)}{\partial \beta_j} = \frac{M(b_1,...,b_j + \delta b_j,...b_p) - M(b_1,...,b_j,...,b_p)}{0.0001} \tag{14}$$

4.2.5.2 Ordinary Least Squares (OLS) Estimation Procedure

The command “nlinfit” in MATLAB program was use to estimate the parameters in the model by minimizing the sum of squares (SS) given in Eq.(15). The MATLAB command to solve nlinfit is [beta,r,J]=nlinfit(X,y,@fun,beta0),where beta is the estimated parameters, r is the residuals and J is the Jacobian (Mishra and others 2009). The MATLAB command for determing the confidence interval (ci) of the parameters is ci=nlparci(beta,resids,J) and the procedure to determine the correlation coefficent matrix of parameters is given in detail in (Mishra and others 2008; Dolan and others 2007). Estimated parameters are significant when the ci does not contain zero.

$$SS = \sum_i \left[\left(Y_{obs} \right)_i - \left(\hat{Y}_{pred} \right)_i \right]^2 \qquad (15)$$

4.2.5.3 Sequential Estimation Procedure

Non-linear Maximum A Posteriori (MAP) sequential estimation procedure given in (Beck and Arnold 1977 p. 277) was used in this study. The MAP equation is shown in Eq. (16).

$$\mathbf{b_{MAP}} = \boldsymbol{\mu_\beta} + \mathbf{P_{MAP}} \mathbf{X}^{\mathbf{T}} \boldsymbol{\psi}^{\mathbf{-1}} \left(\mathbf{Y} - \mathbf{X} \boldsymbol{\mu_\beta} \right) \qquad (16)$$

Where $\mathbf{P_{MAP}} = \left(\mathbf{X}^{\mathbf{T}} \boldsymbol{\psi}^{\mathbf{-1}} \mathbf{X} + \mathbf{V_\beta}^{\mathbf{-1}} \right)^{\mathbf{-1}}$ (17)

Eq. (16) expressions are in a vector matrix. Where b_{MAP} is in matrix (px1) vector parameter to be estimated, μ_β is matrix (px1) vector with prior information on parameter, P_{MAP} is covariance vector matrix of parameter (pxp) which gives information about variance (on diagonal matrix) and covariance (correlation between parameter) on off diagonal matrix, X is the sensitivity coefficient matrix (nxp), ψ^{-1} is covariance matrix (nxn) of error, and Y is the measurement (nx1) vector.

Sequential parameter estimation gives more insight into the estimation process and improvement in the estimation can be noticed when estimating the parameters at each time steps (Mohamed 2009). Under sequential estimation we expect the parameters to approach true values as the number of observations increases. MATLAB programming was used to manage the complexity of the sequential iteration.

4.3 Results and Discussion

4.3.1 Reference Temperature Plots

There are two reference temperatures in the models studied: T_{rg} (in time-temperature term) and T_{rt} (in temperature term). The correlations of parameters with reference temperature T_{rg} are illustrated in Fig.4.1. This was done with a numerical procedure in MATLAB. An initial guess of parameters, model equations, and experimental data collected on time and temperature of the sample were entered into the program. Nonlinear regressions, using the nlinfit function in MATLAB, were used to estimate the parameters. Finding the optimum reference temperature which lead to uncorrelated model parameters involved a number of steps: after an initial parameter estimates with initial guess of reference temperature, the reference temperatures was allowed to vary and then the new covariance matrix of the parameter estimates was recalculated for each new reference temperature in Model 1. A T_{rg} value of 91.6^oC was found to be the temperature where the parameter correlation between k_g and E_g/R was nearly zero. This was then fixed as the optimum T_{rg} value for subsequent modeling.

Similar approach was used to find the optimum T_{rt} value by fixing T_{rg} in Model 3. The parameter correlation between A^{α} and E_g/R are nearly zero at T_{rt} equal to 87.5^oC when using the heating data (first 12min of total experiment time) as shown in Fig.4.2. However, the optimum T_{rt} value in Model 3 was not obtained when cooling data are included. The reason for this is unknown but one speculation would be that the pasting curve phenomenon is complicated by the heating and cooling profile. The mechanism become complex because of temperature (dependency with time or without) remains as a major contributor for the viscosity changes. Only a trend of parameter correlation, going down with increasing temperature, was noticed as shown in Fig. 4.3. Therefore, to keep the study manageable, the value of T_{rt} was fixed as T_{rg} since during heating and cooling all data points are used to estimate the parameters in the models. Results from Fig. 4.1, Fig. 4.2 and Fig. 4.3 show that the parameter correlation is dependent on the reference temperature for the Arrhenius equation. The same observation of parameter correlation dependence on the reference temperature was also reported in studies conducted by (Schwaab and Pinto 2007).

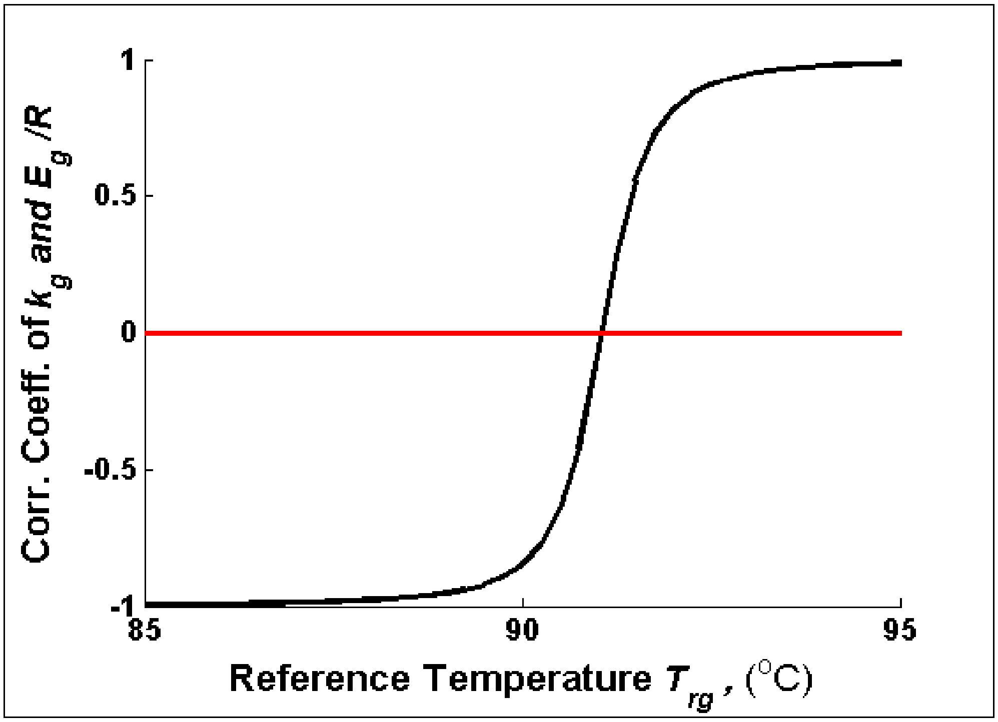

Figure 4.1. Correlation behavior of parameters k_g and E_g/R in the time-temperature history term as a function of the reference temperature (using heating and cooling data over the total experiment time of 22min).

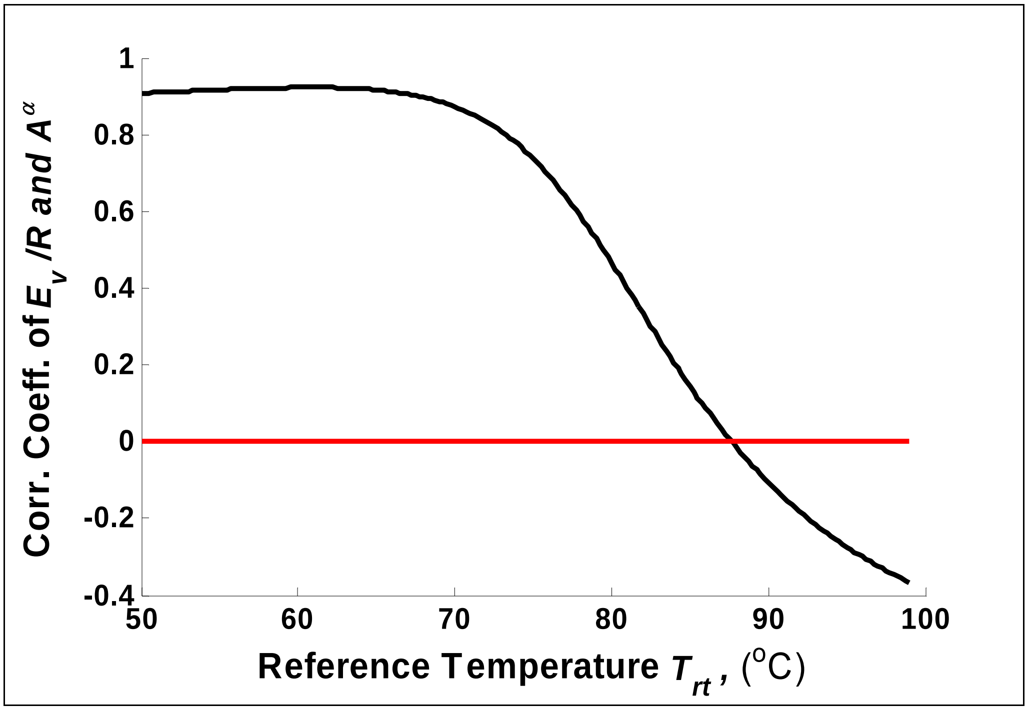

Figure 4.2. Correlation behavior of parameters A^{α} and Ev/R in the temperature term as a function of the reference temperature (using heating data up to 12min).

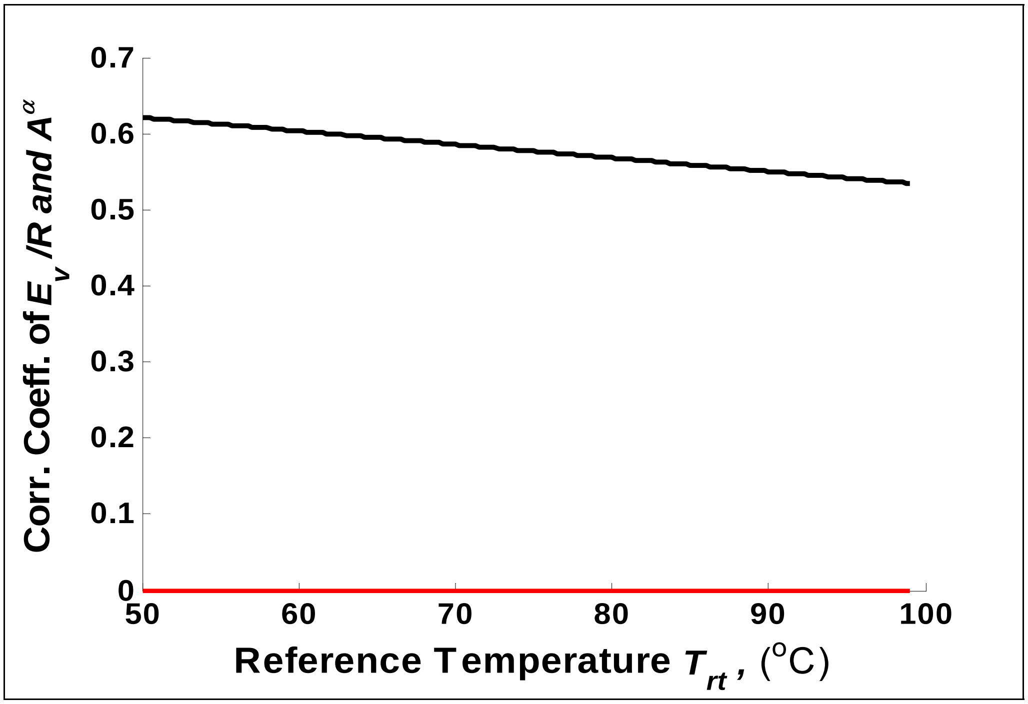

Figure 4.3. Correlation behavior of parameters A^{α} and E_V/R in the temperature term as a function of the reference temperature (using heating and cooling data over the total experiment time of 22min).

4.3.2 Scaled Sensitivity Coefficient Plot

The maximum number of parameters found in the simplified models was 8 and they can be identify as: A^{α}, k_g, E_g/R, α, B, d, E_v/R, and S. Fig. 4.4 shows the result of the scaled sensitivity coefficient plot. Sensitivity coefficient analysis is very important to know whether or not the parameters are linearly dependent or independent of each other. Based on the absolute value of the scaled sensitivity coefficient plots in Fig.4.4, the parameters in the model that can be estimated are, in the order from easiest to most difficulty: S, A^{α},α, k_g, E_g/R, B, E_v/R, and d. The most easily estimated parameters are also the parameters that contribute the most to the model (the most sensitive) and linearly independent.

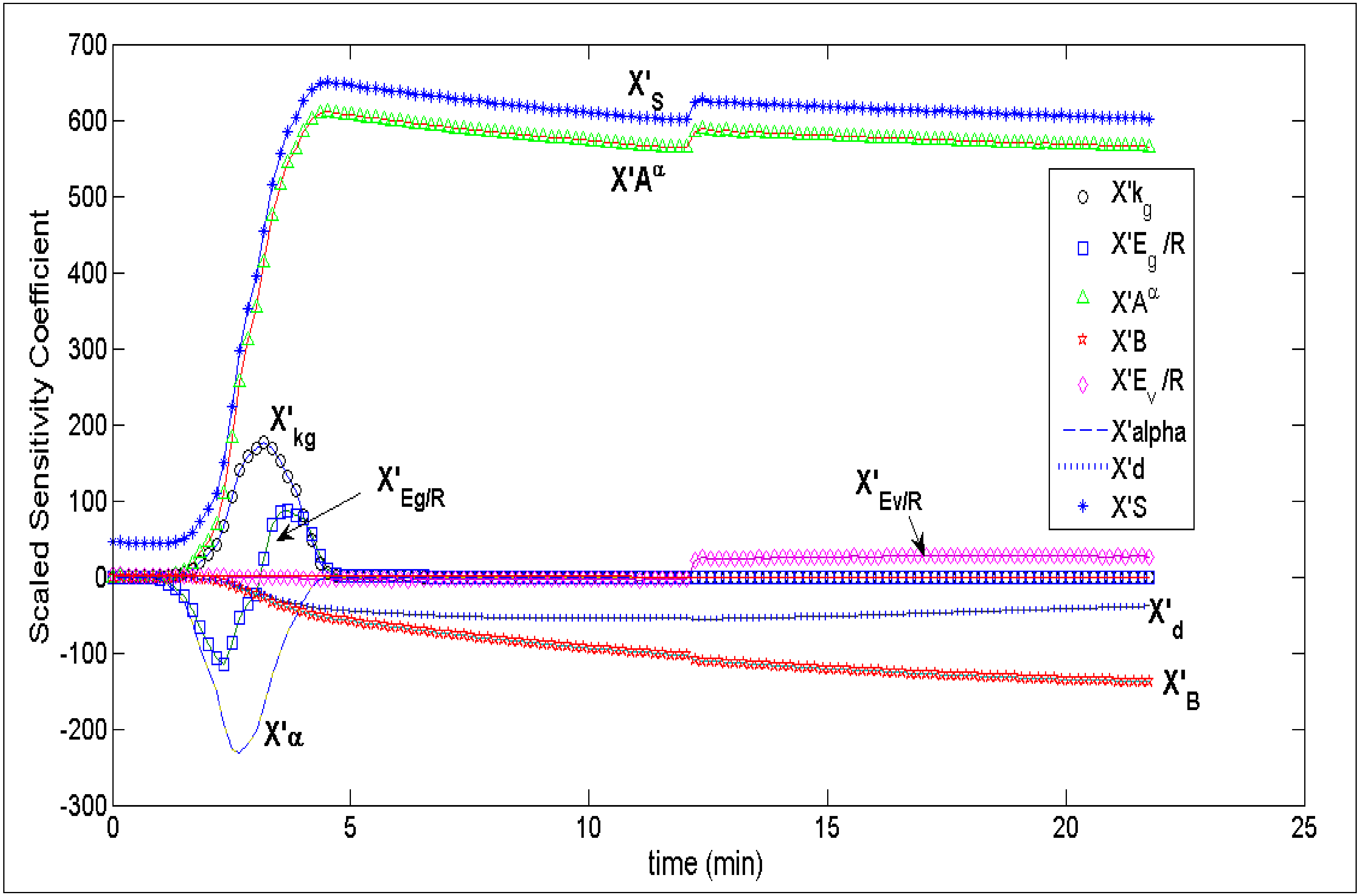

Figure 4.4. Scaled sensitivity coefficient plots of 8 parameters.

4.3.3 Parameter Estimations (Nlinfit)

Estimated parameters in model 1, model 2, and model 3 are shown in Table 4.1. They were found using the nlinfit function in MATLAB. Initially, there were five parameters in the model 1 (Eq.(8)) that was estimated. However, the estimation with five parameters was not realistic because some of parameters contain zero in the confidence interval making them very broad. Only the value of α equal to 0.62 was well estimated, and contained a narrow confidence interval, because X'_{α} was highly correlated to X'_{kg} and X'_{Eg}. Since we are most interested in the Arrhenius parameters, the α value was fixed, and T_{rg} was established where the correlation coefficient between k_g and E_g is nearly zero, and then k_g and E_g parameters were estimated again.

Similar approaches applied to model 2 and model 3. The seven parameters in the Eq. (9) and Eq. (10) were then reduced to five and six parameters, respectively, by fixing the α value at 0.62 and d value at 0.0057. The value of d was fixed because X'_d was too small to allow simultaneous estimation. The results of the estimated parameters with the standard deviation for all three models studied are presented in Table 4.1. The confidence interval, and the percentage relative error of the estimated parameters, are given in Table 4.2 and Table 4.3, respectively. In general, the standard deviation (σ), the confidence interval, and the percentage relative standard error become smaller from model 1 to model 3. The RMSE value reduced from 20.3 to 13.9.

Table 4.1 Estimates of parameters and standard deviation from Nlinfit result for all three models

Parameters/unit	**Initial Values**	**Final Estimate (OLS)**			σ		
		Model 1	*Model 2*	*Model 3*	*Model 1*	*Model 2*	*Model 3*
$k_{g,}$ (K^{-1} min^{-1})	0.3	0.6302	0.3814	0.3556	0.0374	0.0191	0.0186
E_g/R, (K)	$6x10^4$	$14.5x10^4$	$11.8x10^4$	$11.6x10^4$	$1.3x10^4$	$0.52x10^4$	$0.47x10^4$
A^{α}, (dimensionless)	14.7	10.3	22.84	25.83	1.3	2.44	2.79
S, (mNmm min^n)	43	54.8	64.65	64.58	6.1	5.53	5.39
B, (dimensionless)	0.1	n/a	0.6048	0.6519	n/a	0.0234	0.0225
E_v/R, (K)	2077	n/a	n/a	64.82	n/a	n/a	20.59

Table 4.2 Confidence interval of parameters for all three models from Nlinfit result

Parameters	**Confidence Interval**					
	Model 1		*Model 2*		*Model 3*	
$k_{g,}$(K^{-1} min^{-1})	0.5562	0.7042	0.3436	0.4191	0.3193	0.3917
E_g/R, (K)	$11.8x10^4$	$17.1x10^4$	$10.7x10^4$	$12.85x10^4$	$10.6\ x10^4$	$12.5x10^4$
A^{α}(dimensionless)	7.8	12.8	18.02	27.67	20.3	31.36
S, (mNmm min^n)	42.8	66.8	53.7	75.6	53.9	75.26
B, (dimensionless)	n/a		0.55	0.65	0.6074	0.6964
E_v/R, (K)	n/a		n/a		24.06	105.59
RMSE (mNmm)	20.3		14.39		13.91	

Table 4.3 Percentage relative standard error of parameters for all three models

Parameters	**%Relative Standard Error**		
	Model 1	*Model 2*	*Model 3*
$k_{g,}$(K^{-1} min^{-1})	5.9	5	5.1
E_g/R, (K)	9.3	4.48	4.1
A^{α}.(dimensionless)	12.2	10.7	10.8
S, (mNmm min^n)	11.1	8.56	8.36
B, (dimensionless)	n/a	3.87	3.45
E_V/R, (K)	n/a	n/a	31.7

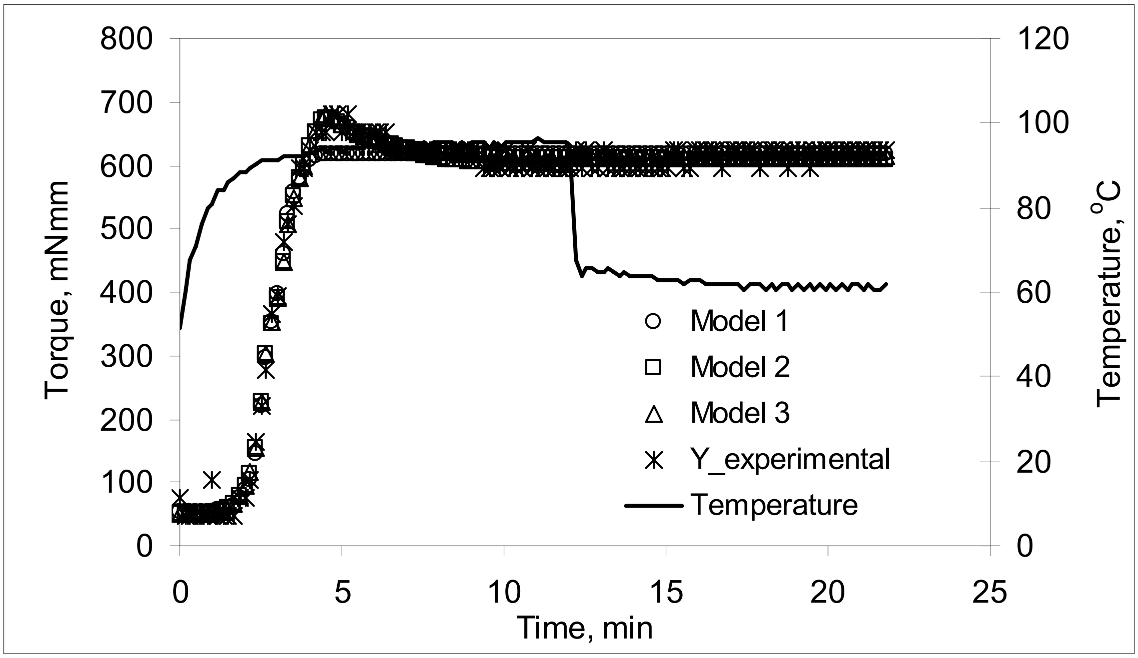

Figure 4.5. Plots of experimental torque and predicted torque versus time.

Fig. 4.5 shows the experimental torque data and the predicted torque based on the three models. The predicted torque from all the three models shows a close prediction with the experimental torque data. Since all the predicted torque models contain the time-temperature history term, this confirms that time-temperature history is the main factor contributing to the torque values during starch gelatinizing (1 to 5min) compare to the shear history and temperature terms.

In the first stage of pasting curve, the starch gelatinization process is overwhelmed by the time-temperature history term until the starch granules fully swell and reach the peak viscosity. The second stage of the pasting curve, which also is sometimes called 'breakdown stage' that happens after reaching peak viscosity, could be overwhelmed by shear history term. According to Lillford (1997), further shear after starch granules reach peak viscosity causes a drop in the torque value (correspond to drop in viscosity) because amylopectin molecules present are damaged by shearing causing a large drop in amylopectin molecular weight. In the third stage of pasting curve, the cooling stage ($95^{o}C$ to $60^{o}C$), the temperature term is most important. The torque value of gelatinized starch (free of time-dependency) at cooling stage is mostly dependent on the temperature term. Amylose molecules in starch granules reassociate and cause in increase of viscosity. This is sometimes referred to as 'set back viscosity' stage (Thomas and Atwell 1999).

To further investigate the best model that can predict the gelatinization behavior of normal corn starch, the correlation matrix of parameters and AIC_c results were computed. The correlation matrix of parameters for each model is presented in Tables 4 to 6. A drastic parameter correlation change was observed between model 1 and model 3. Lowest correlation between parameters is expected so the parameters will be more independent and can be estimated better. Most of the lowest correlations are observed in model 3. The highest correlation is found between parameter kg and B with a value of 0.84, followed by correlation between parameter A^{α} and S with a value of 0.8. The parameter E_v for the temperature term only appears in model 3 and has lowest correlation with most parameters (S, E_g, A^{α}, k_g) and slightly higher correlation with parameter B. Results from AIC_c with lowest score in Table 4.7 shows that model 3 is the best equation to explain starch gelatinization behavior. The scatter plot, and histogram plot, of residuals for model 3 are presented in Fig.4.6 and Fig.4.7, respectively. The most scatter is observed during the starch gelatinizing period (heating time) and during the cooling stage. Some correlation is observed immediately after peak viscosity (6 to 10min). There is less scatter toward the end of testing. The mean residuals are 0.0029.

Table 4.4 Correlation matrix table of parameters for model 1

	k_g	E_g/R	A^α	S
k_g	1			
E_g/R	-0.2721	1	SYMMETRIC	
A^α	0.3865	-0.4605	1	
S	-0.3915	0.4586	-0.9996	1

Table 4.5 Correlation matrix table of parameters for model 2

	k_g	E_g/R	A^α	S	B
k_g	1				
E_g/R	0.0394	1	SYMMETRIC		
A^α	-0.2664	-0.4771	1		
S	-0.2347	0.3691	-0.8231	1	
B	-0.8109	-0.2926	0.5467	0.0249	1

Table 4.6 Correlation matrix table of parameters for model 3

	k_g	E_g/R	A^α	S	B	E_v/R
k_g	1					
E_g/R	0.0641	1		SYMMETRIC		
A^α	-0.3526	-0.4629	1			
S	-0.1896	0.3636	-0.8040	1		
B	-0.8432	-0.2808	0.5943	-0.0005	1	
E_v/R	-0.3972	-0.0792	0.3293	-0.0061	0.5717	1

Table 4.7 Model Comparison using Akaike's Information Criterion (AICc)

Model	Parameters	N	K	SS	AIC_c
1	A^α , k_g , E_g , S		5	52235	794.9
2	A^α, k_g, E_g, B , S	131	6	26078	706.1
3	A^α, k_g, E_g, B, E_v , S		7	24182	698.5

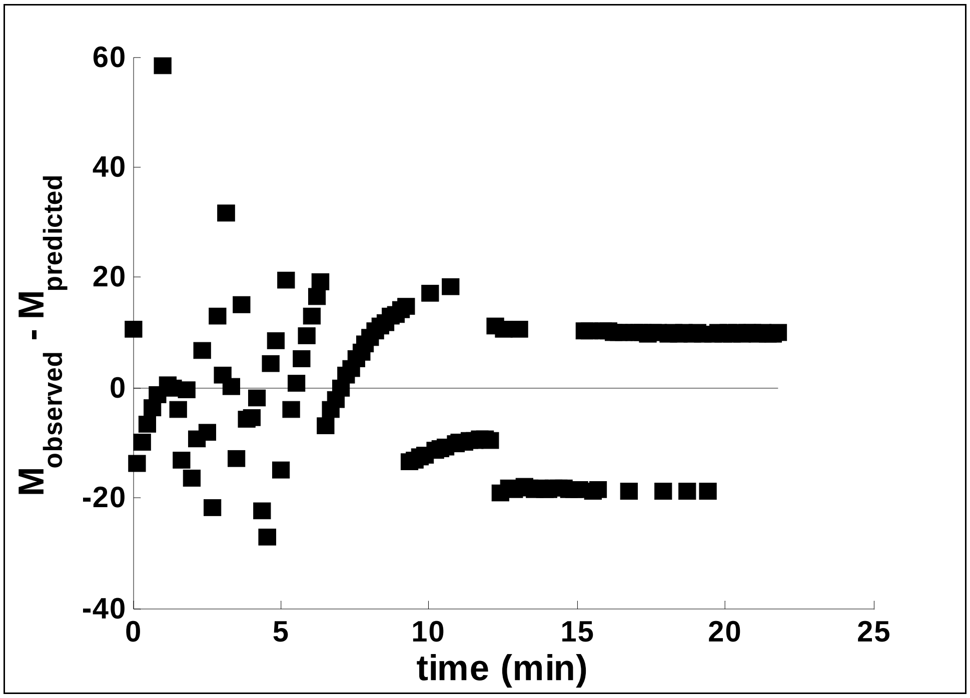

Figure 4.6. Residual scatter plot of difference between observed and predicted torque from model 3.

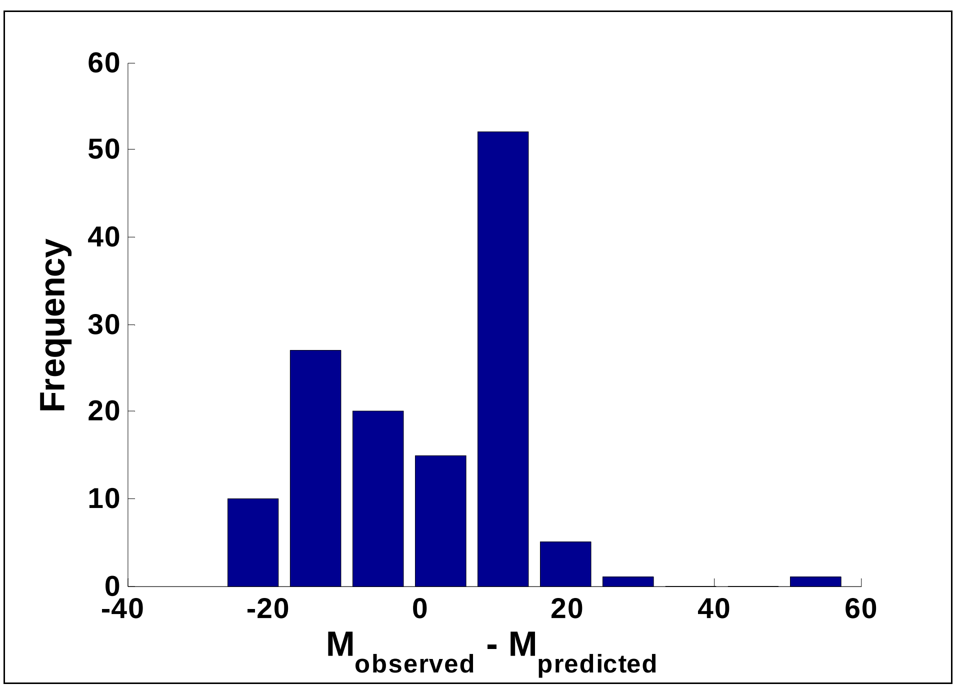

Figure 4.7. Plots of frequency versus difference between observed and predicted torque from model 3.

4.3.4 Sequential Parameter Estimations

Another method to estimate model parameters beside the nlinfit method, is the sequential method. Algorithms used in MATLAB to find parameters in model 3 using sequential MAP estimation are given in Beck & Arnold pg 277. Parameter values are updated in sequential estimation as experimental data of time and temperature are added. The benefit of the sequential method is that it shows the changes in the values of parameter being estimated until they reach a steady value, which is a limitation in nlinfit method.

The sequentially estimated parameter values of k_g, E_g/R, A^{α}, S, B, and E_v/R were 0.35, 115980, 25.87, 64.54, 0.652, and 64.88 obtained after about 4min, 21min, 5min, 13min, 7min, and 21min, respectively (Fig. 4.8 to Fig.4.13). The final values of the sequentially estimated parameters are very similar to the nlinfit results given in Table 1 for model 3. The sequential results are the best possible estimates for the model studied, and parameter values approach a constant value as the experimental data are added.

The parameter values obtained in this study may be compared with the values reported in literature. Table 4.8 shows a list for activation energies of gelatinization for starch. Table 4.9 shows the comparison of the parameters estimated in this study with parameter values from a previous study by Dolan and Steffe (1990). In this study, all the parameters were estimated simultaneously and sequentially. While in previous study by Dolan and Steffe (1990) the parameters were estimated one by one, and held constant when estimating another parameter. Estimating all parameters simultaneously is a superior method because it reflects the real phenomena of the starch gelatinization where all the parameters in the model are involved at the same time and have an influence throughout the starch gelatinization process. The value of parameter S for Dolan and Steffe (1990) is very different because it was calculated based on the parameters K_r= 0.11 Nm min^n and n=0.204 in the shear rate term and parameter b=-0.511 in concentration term that they have reported in their study.

Table 4.8 List of activation energy value of gelatinization for starches

SAMPLE	Starch: Water Ratios (w/w)	Temperature, °C	Activation Energy, (kJ/mol)	References
Basmati rice starch	25%	< 74.4	32.3-42.2	(Ahmed and others 2008)
Rice starch	10%	>82.8	67-124	(Spigno and De Faveri 2004)
Cowpea starch	33%	67-86	233.6	(Okechukwu and Rao 1996)
Corn starch	5.5-7.3%	<95	740	(Dolan and Steffe 1990)
Corn starch	-	-	197	(Liu and others 2010)
Corn Starch	6%	<95	964	THIS STUDY

Table 4.9 Comparison of the estimated parameters value with Dolan & Steffe (1990)

Parameters	(Dolan and Steffe 1990)	THIS STUDY
k_g	2.36 (scaled to Ψ)	0.35 $(Kmin)^{-1}$
E_g	740 kJ/mol	964 kJ/mol
A^α	5.3 (dimensionless)	25.86 (dimensionless)
S	282020.3 mNmm min^n	64.54 mNmm min^n
B	0.39 (dimensionless)	0.652 (dimensionless)
E_v	11.5 kJ/mol	0.539 kJ/mol
α	0.310 (dimensionless)	0.62 (dimensionless)
d	0.00639 (dimensionless)	0.0057 (dimensionless)

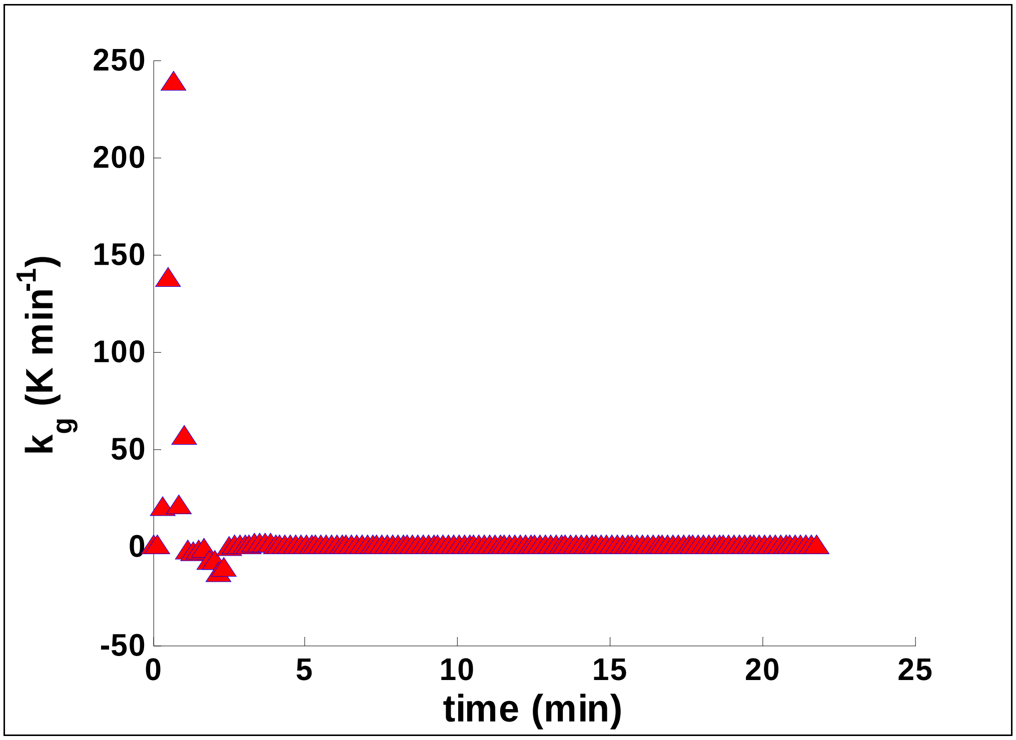

Figure 4.8. Sequentially estimated parameter of k_g.

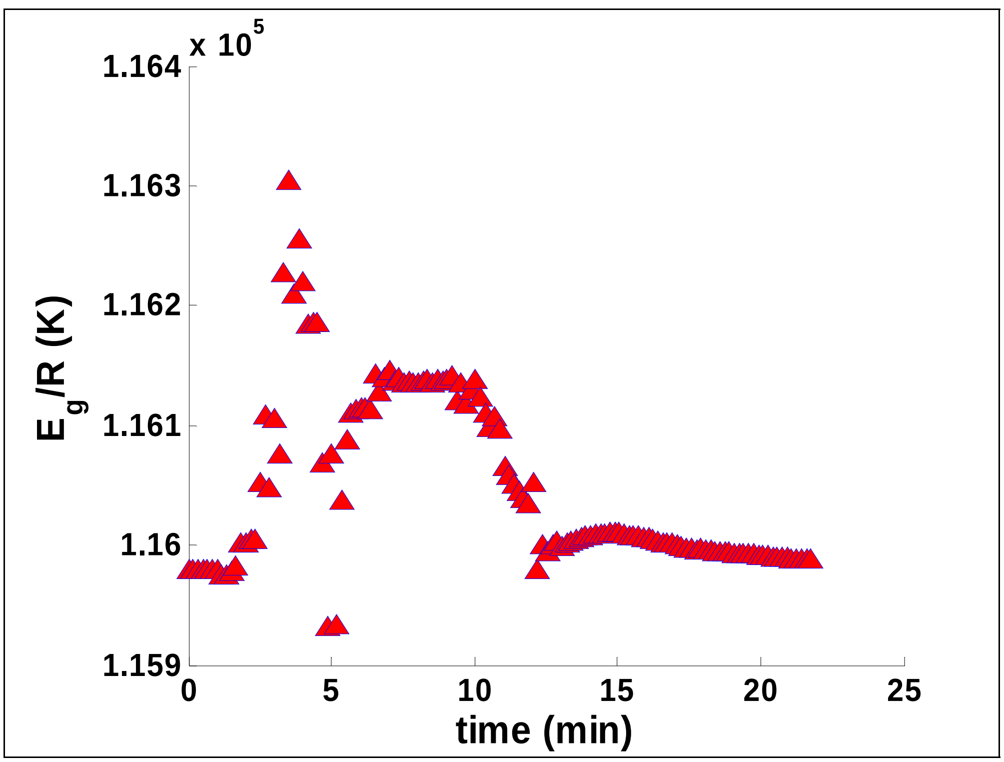

Figure 4.9. Sequentially estimated parameter of E_g/R

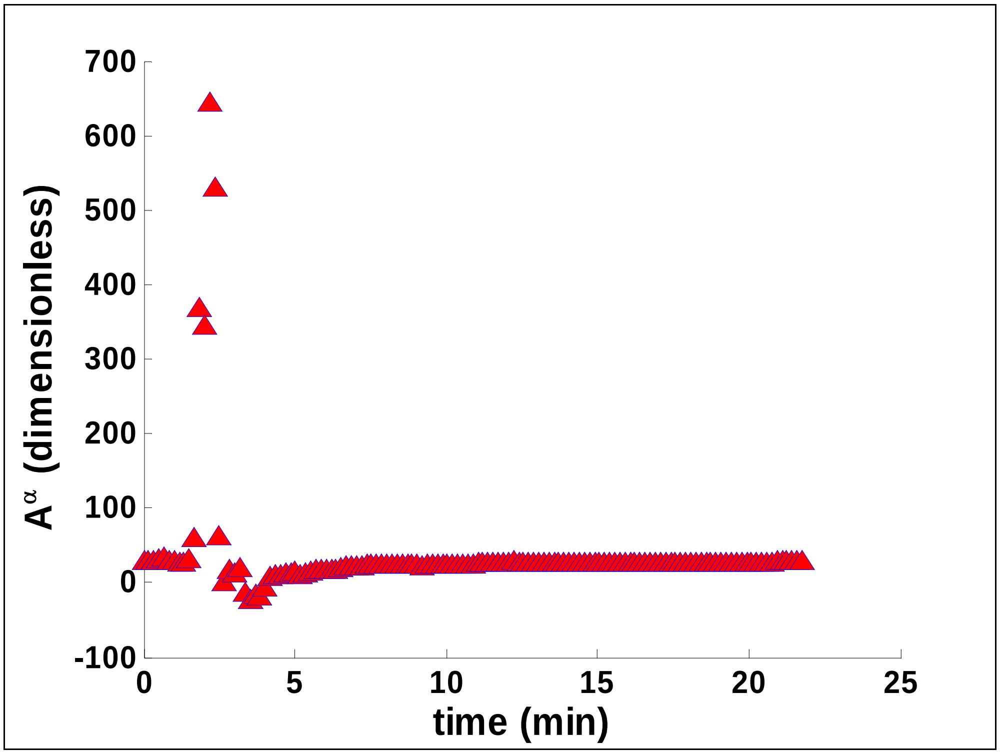

Figure 4.10. Sequentially estimated parameter of A^{α}.

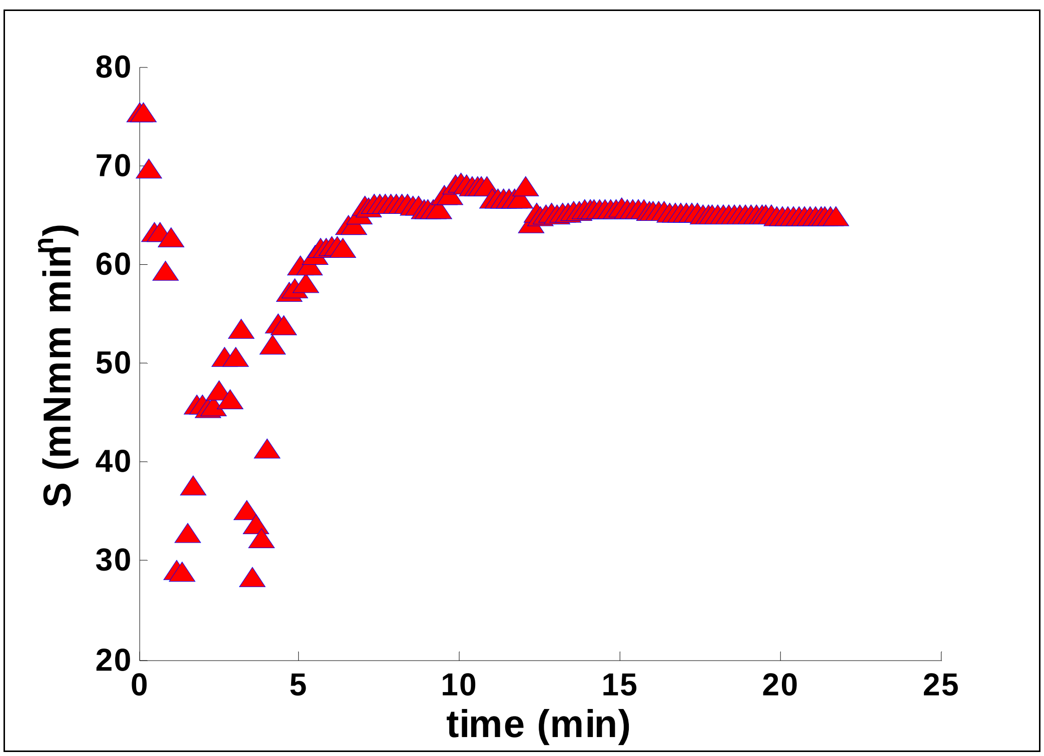

Figure 4.11. Sequentially estimated parameter of S.

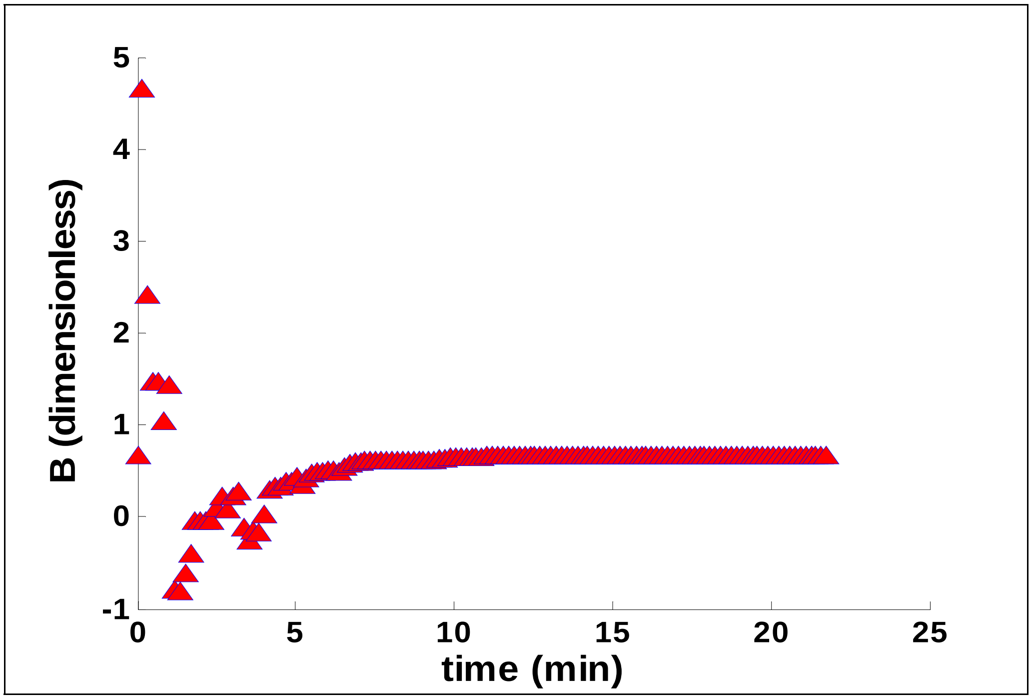

Figure 4.12. Sequentially estimated parameter of B.

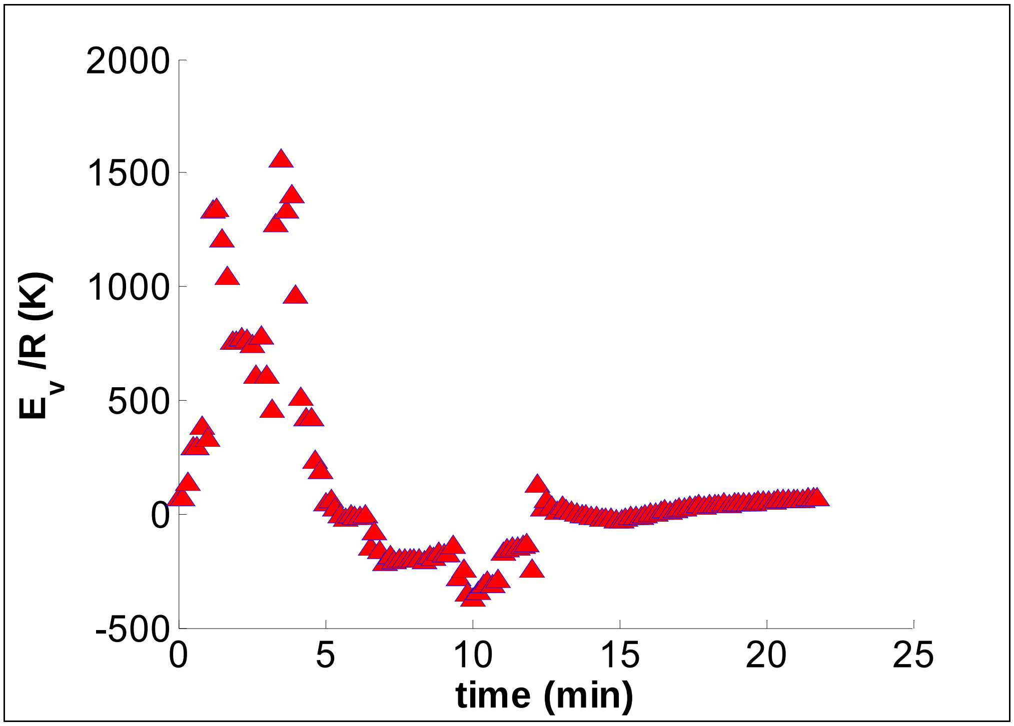

Figure 4.13. Sequentially estimated parameter of E_v/R.

4.3.5 Recommended Corn Starch Viscosity Model

The complete torque model from Eq.(10), with the estimated parameters found in this study is presented as below:

$$M(t)=64.5*\left[1+25.9\left(1-e^{-0.35\psi}\right)^{0.62}\right]*\left[1-0.65\left(1-e^{-0.0057\phi}\right)\right]*e^{64.9\left(\frac{1}{T(t)}-\frac{1}{T_{rt}}\right)} \quad (18)$$

Where

$$\psi=\int_0^{t_f}\frac{T(t)}{300}e^{-115980\left(\frac{1}{T(t)}-\frac{1}{T_{rg}}\right)}dt \quad \text{and} \quad (19)$$

$$\phi=\int_0^{t_f}N\,dt=Nt \quad (20)$$

The unit of the torque here is in mNmm. By having the ability to predict the torque value from the generic torque model for corn starch suggested in Eq.(18), the apparent viscosity of starch gelatinization also can be predicted using Eq. (7) where k" is the mixer coefficient constant and Ω is the angular velocity (Steffe and Daubert 2006b). The value of k" for Brookfield flag impeller is 61220 rad m^{-3} (Briggs and Steffe 1996) and Ω is 10.47 rad/s used for this study. Fig. 4.14 presents the observed apparent viscosity values from experimental data and the predicted apparent viscosity values from Eq.(18).

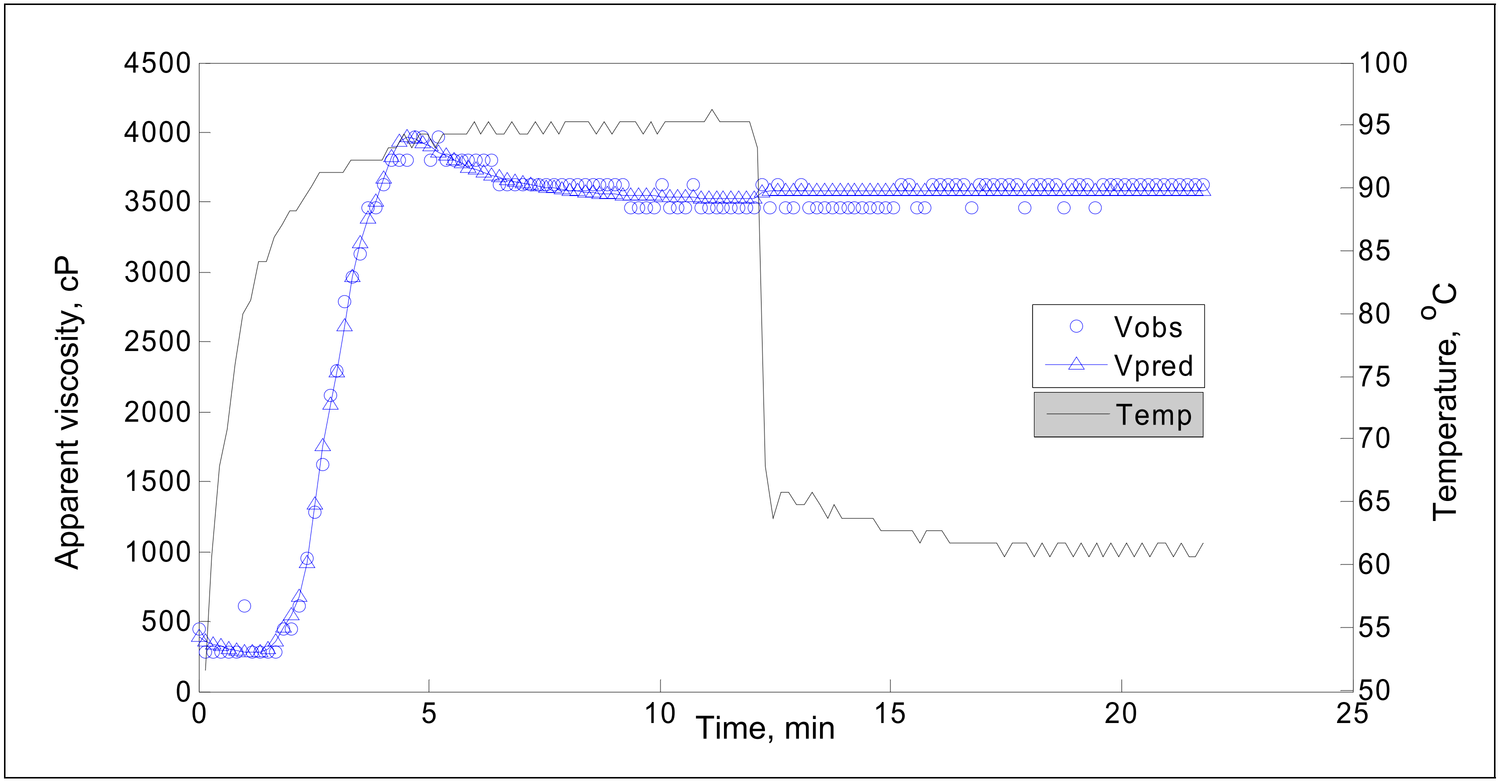

Figure 4.14. Inverse problem plots of observed apparent viscosity from experimental data and predicted apparent viscosity from suggested corn starch model (Eq.(15)) versus time using data from modified Brookfield viscometer for native normal corn starch.

4.3.6 Application of the Starch Viscosity Model on RVA Data

The generic torque model for native corn starch can also be applied to another set of data collected from different device (RVA) for the same starch at same concentration. A forward problem to predict RVA pasting curve is done by using Eq. (18). The only parameter value that needs to be changed is the parameter S because different shear rates are involved. Since after the initial rapid impeller speed, the standard profile RVA uses an impeller speed of 160 rpm for the rest of the experiment. A new parameter S (for 160 rpm) was calculated based on the known parameter S value (of 100rpm) from the inverse problem results obtained earlier in this study using the following relationship:

$$S_{RVA} = S_{BF} * \left(\frac{N_{RVA}}{N_{BF}} \right)^{n} \qquad (21)$$

The n value was obtained from experiments conducted at different impeller speeds after the corn starch sample was fully gelatinized. Fig. 4.15 shows the plot of apparent viscosity versus shear rate for the gelatinized corn starch sample. The n value of 1.27 was obtained by fitting the line to the power law model (Steffe 1996). Dail and Steffe (1990b) also observed shear thickening behavior for corn starch solutions. The value of parameter S for RVA then becomes 91.89 mNmm.

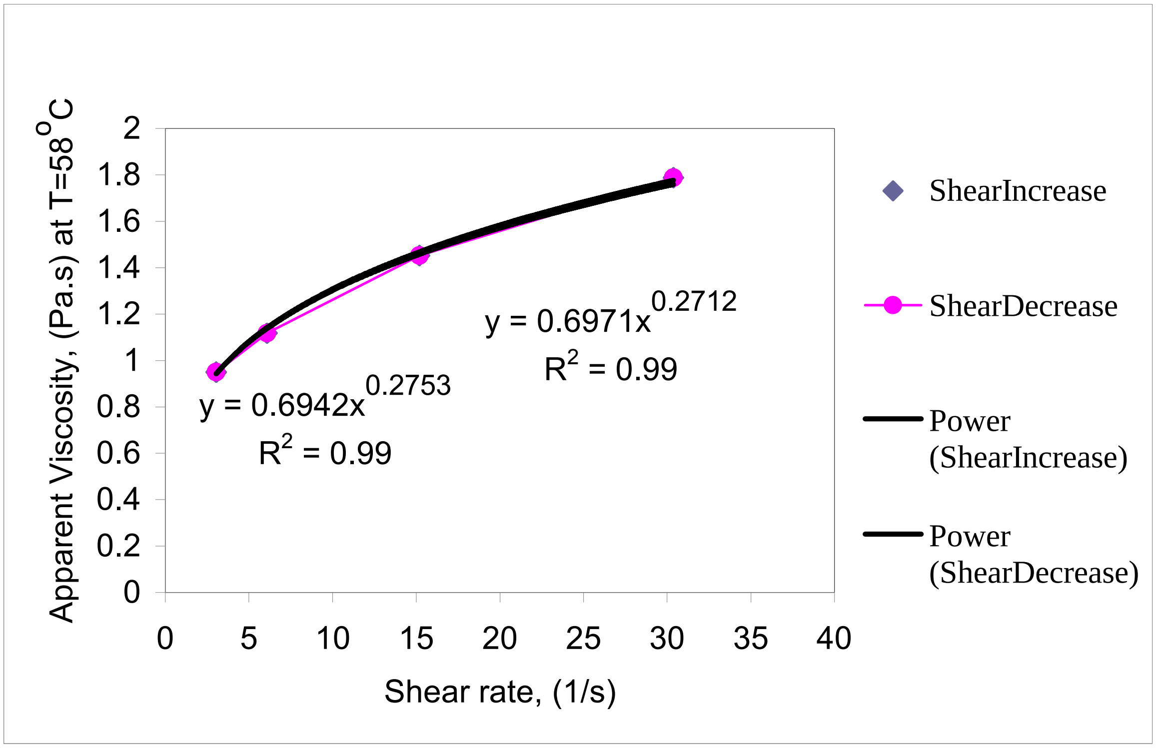

Figure 4.15. Plot of apparent viscosity versus shear rate showing a shear thickening behavior for corn starch.

With the above results, Eq. (7) was used to predict the apparent viscosity. The value of k" for RVA used is 12570 rad m^{-3} (Lai et al. 2000) and Ω is 16.75 rad/s. Fig. 4.16 presents the observed apparent viscosity values from experimental data and the predicted values from the RVA study. A good prediction was observed. A perfect match was not expected due to the difference in actual sample temperature recorded by RVA, the larger sample size (Hazelton and Walker 1996), and the insensitivity of initial torque measurement for the RVA.

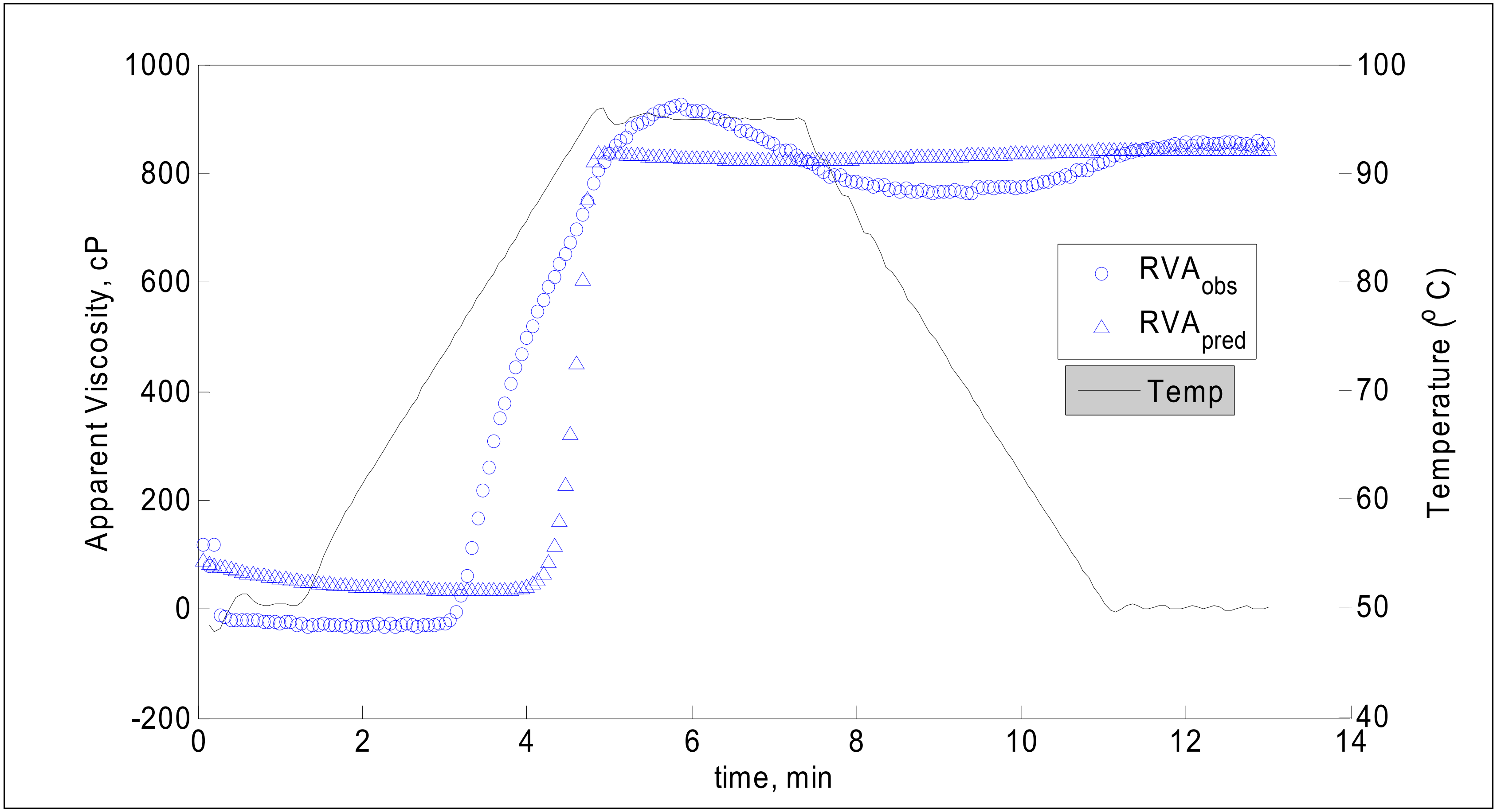

Figure 4.16. Forward problem plots of observed apparent viscosity from experimental data and predicted apparent viscosity from the corn starch model versus time using data from RVA for native normal corn starch at 6%w/w.

4.4 Conclusions

This study shows a better method of parameter estimation techniques to determine the parameters for starch viscosity model. The predicted apparent viscosity data show a very close prediction with experimental data. A generic model for native normal corn starch viscosity proposed in this study will be helpful for food engineers to design the processing systems, and food product developers in their formulations when corn starch is used as a product thickener.

4.5 Nomenclature

A^{α}	relative increase in apparent viscosity, dimensionless
AM	amylose
AP	amylopectin
B	relative decrease in apparent viscosity, dimensionless
BF	Brookfield viscometer
CON A	concanavalin A
E_v	viscous activation energy, kJ/mol
E_g	gelatinization activation energy, kJ/mol
d	shear-decay rate parameter
k_g	gelatinization rate constant, $(Kmin)^{-1}$
K_r	pseudo consistency coefficient, Nm min^n
M	torque, mNmm

N	speed, rpm
RMSE	root mean square error
RTD	resistance temperature detector
RVA	rapid visco analyzer
S	parameter combine shear rate and concentration term, mNmm min^n
SS	sum square of error
t	time, min
t_f	time when the experiment ends, min
T	temperature, Kelvin
T_{rg}	gelatinization reference temperature on Arrhenius equation, Kelvin
T_{rt}	reference temperature on Arrhenius equation for temperature term, Kelvin
α	dimensionless parameter
ψ	time-temperature history, (Kmin)
ϕ	shear history, rpm min

APPENDICES

Appendix B1

Pasting Curve Mixer Viscometer Data

Table B.1.1 Melojel (normal) corn starch data

Time (s)	T (^oC)	η ,(Pa.s) calculated	Torque (Nm)
0	51.485406	0.447285	7.672E-05
10.047	60.649543	0.279767	4.798E-05
20.093	67.777205	0.279767	4.798E-05
30.125	70.831918	0.279767	4.798E-05
40.171	75.923105	0.279767	4.798E-05
50.218	79.996055	0.279767	4.798E-05
60.265	81.014292	0.614803	0.0001054
70.312	84.069005	0.279767	4.798E-05
80.359	84.069005	0.279767	4.798E-05
90.39	86.10548	0.279767	4.798E-05
100.44	87.123717	0.279767	4.798E-05
110.483	88.141955	0.447285	7.672E-05
120.53	88.141955	0.447285	7.672E-05
130.58	89.160192	0.614803	0.0001054
140.62	90.17843	0.949839	0.0001629
150.67	91.196667	1.284875	0.0002204
160.7	91.196667	1.61991	0.0002778
170.75	91.196667	2.122464	0.000364
180.8	91.196667	2.289982	0.0003928
190.84	92.214905	2.792536	0.000479
200.89	92.214905	2.960054	0.0005077
210.94	92.214905	3.127572	0.0005364
220.97	92.214905	3.462608	0.0005939
231.01	92.214905	3.462608	0.0005939
241.06	93.233142	3.630126	0.0006226
251.11	93.233142	3.797643	0.0006513
261.15	94.251379	3.797643	0.0006513
271.19	93.233142	3.797643	0.0006513
281.232	94.251379	3.965161	0.0006801
291.28	94.251379	3.965161	0.0006801
301.33	93.233142	3.797643	0.0006513
311.36	94.251379	3.965161	0.0006801
321.4	94.251379	3.797643	0.0006513

Table B.1.1 (cont'd)

331.45	94.251379	3.797643	0.0006513
341.48	94.251379	3.797643	0.0006513
351.53	95.269617	3.797643	0.0006513
361.58	94.251379	3.797643	0.0006513
371.62	95.269617	3.797643	0.0006513
381.65	94.251379	3.797643	0.0006513
391.7	94.251379	3.630126	0.0006226
401.75	95.269617	3.630126	0.0006226
411.79	94.251379	3.630126	0.0006226
421.83	94.251379	3.630126	0.0006226
431.87	95.269617	3.630126	0.0006226
441.92	94.251379	3.630126	0.0006226
451.97	95.269617	3.630126	0.0006226
462	94.251379	3.630126	0.0006226
472.04	95.269617	3.630126	0.0006226
482.09	95.269617	3.630126	0.0006226
492.12	95.269617	3.630126	0.0006226
502.17	95.269617	3.630126	0.0006226
512.22	94.251379	3.630126	0.0006226
522.25	95.269617	3.630126	0.0006226
532.29	94.251379	3.630126	0.0006226
542.34	95.269617	3.630126	0.0006226
552.37	95.269617	3.630126	0.0006226
562.42	95.269617	3.462608	0.0005939
572.46	94.251379	3.462608	0.0005939
582.5	95.269617	3.462608	0.0005939
592.54	94.251379	3.462608	0.0005939
602.59	95.269617	3.630126	0.0006226
612.62	95.269617	3.462608	0.0005939
622.67	95.269617	3.462608	0.0005939
632.7	95.269617	3.462608	0.0005939
642.75	95.269617	3.630126	0.0006226
652.79	95.269617	3.462608	0.0005939
662.82	96.287854	3.462608	0.0005939
672.87	95.269617	3.462608	0.0005939
682.92	95.269617	3.462608	0.0005939
692.95	95.269617	3.462608	0.0005939
703	95.269617	3.462608	0.0005939
713.042	95.269617	3.462608	0.0005939
723.073	93.233142	3.462608	0.0005939

Table B.1.1 (cont'd)

733.12	67.777205	3.630126	0.0006226
743.17	63.704255	3.462608	0.0005939
753.2	65.74073	3.630126	0.0006226
763.24	65.74073	3.462608	0.0005939
773.29	64.722493	3.462608	0.0005939
783.34	64.722493	3.630126	0.0006226
793.37	65.74073	3.462608	0.0005939
803.42	64.722493	3.462608	0.0005939
813.46	63.704255	3.462608	0.0005939
823.51	64.722493	3.462608	0.0005939
833.54	63.704255	3.462608	0.0005939
843.59	63.704255	3.462608	0.0005939
853.63	63.704255	3.462608	0.0005939
863.68	63.704255	3.462608	0.0005939
873.73	63.704255	3.462608	0.0005939
883.76	62.686018	3.462608	0.0005939
893.81	62.686018	3.462608	0.0005939
903.85	62.686018	3.462608	0.0005939
913.9	62.686018	3.630126	0.0006226
923.93	62.686018	3.630126	0.0006226
933.98	61.66778	3.462608	0.0005939
944.03	62.686018	3.462608	0.0005939
954.07	62.686018	3.630126	0.0006226
964.1	62.686018	3.630126	0.0006226
974.15	61.66778	3.630126	0.0006226
984.2	61.66778	3.630126	0.0006226
994.24	61.66778	3.630126	0.0006226
1004.3	61.66778	3.462608	0.0005939
1014.3	61.66778	3.630126	0.0006226
1024.4	61.66778	3.630126	0.0006226
1034.4	61.66778	3.630126	0.0006226
1044.4	60.649543	3.630126	0.0006226
1054.5	61.66778	3.630126	0.0006226
1064.5	61.66778	3.630126	0.0006226
1074.6	61.66778	3.462608	0.0005939
1084.6	60.649543	3.630126	0.0006226
1094.7	61.66778	3.630126	0.0006226
1104.7	60.649543	3.630126	0.0006226
1114.8	61.66778	3.630126	0.0006226
1124.8	61.66778	3.462608	0.0005939

Table B.1.1 (cont'd)

1134.9	60.649543	3.630126	0.0006226
1144.9	61.66778	3.630126	0.0006226
1154.9	60.649543	3.630126	0.0006226
1165	61.66778	3.462608	0.0005939
1175	60.649543	3.630126	0.0006226
1185.1	61.66778	3.630126	0.0006226
1195.1	60.649543	3.630126	0.0006226
1205.1	61.66778	3.630126	0.0006226
1215.2	60.649543	3.630126	0.0006226
1225.2	61.66778	3.630126	0.0006226
1235.3	60.649543	3.630126	0.0006226
1245.3	61.66778	3.630126	0.0006226
1255.4	61.66778	3.630126	0.0006226
1265.4	60.649543	3.630126	0.0006226
1275.5	61.66778	3.630126	0.0006226
1285.5	60.649543	3.630126	0.0006226
1295.53	60.649543	3.630126	0.0006226
1305.6	61.66778	3.630126	0.0006226

Table B.1.2 RVA melojel corn starch data

Normal_rep1				Normal_rep2			
Time(s)	Visc (cp)	T(C)	N (rpm)	Time(s)	Visc (cp)	T(C)	N(rpm)
4	133	48.75	960	4	131	48.1	960
8	95	47.95	960	8	94	47.35	960
12	177	48.15	160	12	175	47.9	160
16	28	49.05	160	16	32	49.1	160
20	30	50.1	160	20	31	50.1	160
24	28	50.75	160	24	31	50.8	160
28	28	51.15	160	28	31	51.15	160
32	29	50.95	160	32	30	50.95	160
36	26	50.6	160	36	31	50.55	160
40	25	50.25	160	40	30	50.2	160
44	26	50.2	160	44	31	50.2	160
48	20	50.25	160	48	33	50.2	160
52	26	50.35	160	52	28	50.35	160
56	20	50.35	160	56	28	50.35	160
60	22	50.4	160	60	28	50.2	160
64	19	50.3	160	64	22	50.05	160
68	15	50.3	160	68	30	50.05	160
72	17	50.7	160	72	26	50.4	160
76	22	51.35	160	76	25	51.3	160
80	22	52.35	160	80	26	52.4	160
84	18	53.55	160	84	23	53.6	160
88	22	54.6	160	88	20	54.75	160
92	17	55.85	160	92	22	55.95	160
96	17	56.9	160	96	25	56.9	160
100	20	57.85	160	100	21	57.95	160
104	19	58.75	160	104	17	58.85	160
108	19	59.65	160	108	20	59.7	160
112	17	60.45	160	112	21	60.5	160
116	22	61.3	160	116	20	61.35	160
120	14	62.05	160	120	22	62.15	160
124	17	62.85	160	124	23	62.95	160
128	17	63.7	160	128	15	63.75	160
132	15	64.5	160	132	20	64.5	160
136	15	65.3	160	136	18	65.3	160
140	18	66.1	160	140	20	66.2	160
144	15	67	160	144	22	66.9	160
148	20	67.75	160	148	23	67.7	160
152	18	68.6	160	152	19	68.55	160
156	10	69.4	160	156	19	69.35	160
160	17	70.25	160	160	18	70.25	160

Table B.1.2 (cont'd)

164	12	71.05	160	164	20	71.05	160
168	17	71.9	160	168	17	71.85	160
172	19	72.7	160	172	18	72.7	160
176	12	73.45	160	176	20	73.5	160
180	15	74.3	160	180	27	74.35	160
184	22	75.15	160	184	32	75.15	160
188	31	75.9	160	188	49	75.95	160
192	51	76.7	160	192	84	76.75	160
196	85	77.6	160	196	141	77.55	160
200	140	78.4	160	200	244	78.35	160
204	249	79.25	160	204	379	79.15	160
208	382	80.05	160	208	524	80	160
212	514	80.8	160	212	672	80.8	160
216	662	81.55	160	216	818	81.65	160
220	801	82.4	160	220	965	82.4	160
224	939	83.15	160	224	1110	83.15	160
228	1077	84.05	160	228	1247	84	160
232	1210	84.8	160	232	1382	84.7	160
236	1341	85.6	160	236	1514	85.5	160
240	1469	86.35	160	240	1647	86.4	160
244	1586	87.15	160	244	1778	87.2	160
248	1714	88.05	160	248	1913	88.1	160
252	1834	88.9	160	252	2049	88.8	160
256	1962	89.65	160	256	2185	89.7	160
260	2088	90.5	160	260	2318	90.5	160
264	2219	91.25	160	264	2445	91.25	160
268	2360	92.05	160	268	2564	92	160
272	2494	92.85	160	272	2673	92.85	160
276	2623	93.6	160	276	2774	93.6	160
280	2739	94.45	160	280	2872	94.5	160
284	2845	95.25	160	284	2953	95.25	160
288	2916	95.8	160	288	3027	95.8	160
292	2991	95.95	160	292	3085	95.85	160
296	3069	95.2	160	296	3148	95.15	160
300	3124	94.6	160	300	3218	94.8	160
304	3194	94.6	160	304	3266	94.8	160
308	3257	94.7	160	308	3295	95	160
312	3304	95.05	160	312	3305	95.15	160
316	3340	95.2	160	316	3301	95.2	160
320	3353	95.4	160	320	3289	95.3	160
324	3362	95.45	160	324	3267	95.3	160
328	3355	95.4	160	328	3238	95.2	160
332	3346	95.3	160	332	3215	95.2	160

Table B.1.2 (cont'd)

336	3328	95.15	160	336	3175	95.1	160
340	3306	95.05	160	340	3135	95.05	160
344	3280	95.05	160	344	3095	95.1	160
348	3259	95	160	348	3053	95	160
352	3232	95	160	352	3019	95	160
356	3196	94.95	160	356	2982	95	160
360	3156	95	160	360	2950	95	160
364	3119	95	160	364	2919	95	160
368	3087	95	160	368	2887	95	160
372	3051	95.1	160	372	2848	95.1	160
376	3018	95.05	160	376	2815	95.05	160
380	2986	95.05	160	380	2782	95.1	160
384	2952	95.05	160	384	2752	95.05	160
388	2924	95.05	160	388	2721	95	160
392	2886	95	160	392	2694	95	160
396	2858	95.05	160	396	2662	95	160
400	2829	95.05	160	400	2625	95	160
404	2800	95.05	160	404	2599	95	160
408	2764	95	160	408	2570	95	160
412	2736	95	160	412	2541	95	160
416	2705	95	160	416	2509	95.05	160
420	2683	95	160	420	2486	95	160
424	2652	95	160	424	2461	95	160
428	2627	95	160	428	2433	95	160
432	2596	95.1	160	432	2415	95.05	160
436	2573	95.05	160	436	2396	95.05	160
440	2541	94.7	160	440	2373	94.8	160
444	2515	93.25	160	444	2361	93.35	160
448	2504	91.95	160	448	2357	91.85	160
452	2494	91.4	160	452	2354	91.35	160
456	2483	91.25	160	456	2351	91.25	160
460	2478	90.1	160	460	2350	90.05	160
464	2467	88.65	160	464	2356	88.65	160
468	2465	87.9	160	468	2362	88.05	160
472	2467	87.8	160	472	2372	87.95	160
476	2469	87	160	476	2372	86.95	160
480	2478	85.5	160	480	2377	85.45	160
484	2480	84.6	160	484	2395	84.5	160
488	2492	84.35	160	488	2406	84.3	160
492	2501	83.9	160	492	2408	83.75	160
496	2505	82.55	160	496	2417	82.5	160
500	2521	81.25	160	500	2426	81.4	160
504	2528	80.6	160	504	2438	81	160

Table B.1.2 (cont'd)

508	2541	80.45	160	508	2446	80.35	160
512	2552	79.8	160	512	2456	79.25	160
516	2562	78.55	160	516	2462	78.25	160
520	2573	77.45	160	520	2479	77.85	160
524	2580	76.85	160	524	2486	77.4	160
528	2593	76.4	160	528	2499	76.25	160
532	2601	75.45	160	532	2509	75.15	160
536	2616	74.4	160	536	2519	74.35	160
540	2626	73.7	160	540	2534	73.9	160
544	2635	73.1	160	544	2545	73.15	160
548	2647	72.35	160	548	2553	72.2	160
552	2652	71.45	160	552	2565	71.3	160
556	2657	70.55	160	556	2578	70.5	160
560	2669	69.75	160	560	2586	69.8	160
564	2678	69.05	160	564	2602	69.2	160
568	2684	68.2	160	568	2615	68.25	160
572	2693	67.5	160	572	2626	67.45	160
576	2703	66.8	160	576	2644	66.8	160
580	2710	65.9	160	580	2656	66	160
584	2725	65.2	160	584	2679	65.2	160
588	2739	64.4	160	588	2692	64.45	160
592	2750	63.6	160	592	2713	63.6	160
596	2759	62.85	160	596	2735	62.85	160
600	2772	62.1	160	600	2755	62.05	160
604	2793	61.3	160	604	2779	61.3	160
608	2814	60.45	160	608	2803	60.5	160
612	2840	59.7	160	612	2831	59.7	160
616	2854	58.9	160	616	2860	58.95	160
620	2874	58.15	160	620	2890	58.1	160
624	2895	57.35	160	624	2922	57.3	160
628	2919	56.6	160	628	2959	56.55	160
632	2943	55.8	160	632	2994	55.8	160
636	2972	55.05	160	636	3029	55.05	160
640	3004	54.3	160	640	3070	54.3	160
644	3035	53.5	160	644	3113	53.45	160
648	3072	52.8	160	648	3156	52.75	160
652	3110	51.95	160	652	3198	51.9	160
656	3143	51.1	160	656	3243	51.2	160
660	3184	50.35	160	660	3291	50.45	160
664	3230	49.75	160	664	3337	49.8	160
668	3267	49.7	160	668	3383	49.75	160
672	3305	49.85	160	672	3422	49.8	160
676	3342	50.15	160	676	3462	50.15	160

Table B.1.2 (cont'd)

680	3377	50.35	160	680	3495	50.35	160
684	3407	50.15	160	684	3529	50.35	160
688	3436	50	160	688	3565	50.15	160
692	3473	50.05	160	692	3597	49.9	160
696	3504	50	160	696	3639	49.85	160
700	3534	50.1	160	700	3668	50	160
704	3565	50.2	160	704	3701	50.15	160
708	3589	50.15	160	708	3732	50.2	160
712	3610	49.95	160	712	3755	50.1	160
716	3637	49.95	160	716	3777	49.85	160
720	3658	50.1	160	720	3795	49.85	160
724	3680	50.05	160	724	3819	49.9	160
728	3695	49.95	160	728	3841	49.95	160
732	3716	49.9	160	732	3856	50.2	160
736	3735	49.95	160	736	3878	50.2	160
740	3756	50.1	160	740	3898	49.9	160
744	3774	50.1	160	744	3916	49.9	160
748	3795	50	160	748	3932	49.95	160
752	3811	49.95	160	752	3949	50	160
756	3832	50	160	756	3966	50.15	160
760	3846	50.05	160	760	3980	50.15	160
764	3861	50	160	764	3998	50	160
768	3874	50.05	160	768	4010	49.85	160
772	3887	50	160	772	4021	49.9	160
776	3903	50	160	776	4035	50.1	160
780	3919	49.9	160	780	4046	50.1	160

Appendix B2

Pasting Curve RVA

Figure B.2.1. RVA equipment and RVA impeller

Appendix B3

Example of Matlab syntax

Example of Syntax (for Objective Two)

Section 1: MATLAB files for Sensitivity Coefficient Plot
First functions syntax: file name:- torque

```
function y = torque(beta,x)
data=xlsread('MelojelData.xls');
t=x(:,1);T=x(:,2);
Tr=91.06+273.15; %reference temperature for Trg
N=100;
intgrnd = (T).*exp(-(beta(2))*(1./T-1/Tr));
psi=cumtrapz(t,intgrnd);

y=(beta(8)*(1+beta(3)*(1-exp(-beta(1)*(psi))).^beta(6))).*(1-beta(4)*(1-exp(-
beta(7)*N*t))).*(exp(beta(5)*(1./T-1/(90.6+273.15))));%I fix the Trt to 90.6C
end
```

Second functions syntax: file name:- SSC

```
function Xp=SSC(beta,x,yfunc)
%Computes scaled sensitivity coefficients =Xp, nxp matrix
%n is the number of data
%p is the number of parameters
%Xp1 = dY/dbeta1~[y(beta1(1+d), beta2,...betap) - y(beta1,
%beta2,...betap)]/d...
%d is the arbitrary delta;to compute finite difference method
%beta is the p x 1 parameter vector
%yhat is nx1 vector, the y values when only one parameter has been successively
perturbed by d
%ypred is nx1 vector,  the y values when parameters are set to beta
%betain is px1 vector, the parameter values with only one parameter perturbed by d
%x are the independent variables (can be one or more independent variables)
%yfunc is a function (m file or an anonymous) defined by the user outside
%of this file
p=length(beta);

%ypred=yfunc(beta,x)';
ypred=yfunc(beta,x);
d=0.001;
for i = 1:p
   betain = beta;
   betain(i) = beta(i)*(1+d);%perturb one parameter at a time
   %yhat{i} = yfunc(betain, x)';
   yhat{i} = yfunc(betain, x);
```

```
   X1{i} = (yhat{i}-ypred)/d;%each scaled sens coeff is stored
end
%Xp=[X1{:,1}];
   Xp=[X1{1}];
for i=2:p
%     Xp = [Xp X1{:,i}];
   Xp =[Xp X1{i}];
end
```

Microsoft Word File : Paste this command on MATLAB window file when both the previous file are been open.

```
data=xlsread('MelojelData.xls');
tfact=60;
t=data(:,1)/tfact;
T=data(:,2)+273.15;
x(:,1)=t;
x(:,2)=T;
beta=[0.00176 121740.8 15.4259 0.210668 184.9417 0.6235 0.001 43.1];
Xp=SSC(beta,x,@torque);
plot(x(:,1),Xp)
hold on

h(1)=plot(t*tfact/60,Xp(:,1),'ok');
h(2)=plot(t*tfact/60,Xp(:,2),'sb');
h(3)=plot(t*tfact/60,Xp(:,3),'^g');
h(4)=plot(t*tfact/60,Xp(:,4),'pr');
h(5)=plot(t*tfact/60,Xp(:,5),'dm');
h(6)=plot(t*tfact/60,Xp(:,6),'--');
h(7)=plot(t*tfact/60,Xp(:,7), ':');
h(8)=plot(t*tfact/60,Xp(:,8),'*');
legend(h,'X''k_g','X''E_g/R','X''A^{\alpha}','X''B','X''E_v/R','X''alpha','X''d','X''C')

set(gca, 'fontsize',14,'fontweight','bold');
plot([0,max(t)],[0,0], 'R')
xlabel('time (min)','fontsize',16,'fontweight','bold')
ylabel('Scaled Sensitivity Coefficient','fontsize',16,'fontweight','bold')
```

Section 2: MATLAB files for Reference Temperature Plot

A) Reference temperature for gelatinization (T_{rg}) only involves time-temperature history term.

Consist of 3 files (folder name: Tr_g files), first open all files and then run the starch_Tr file.

I) Function file name: st_torqueTr

```
function M = st_torqueTr( b,X )
%computes psi(t) given time-temperature history
```

```
%  t is a nx1 vector of time (Hemminger and Sarge)
%X independent variables column 1 is time, column2 T (K)
% T is nx1 vector of temperature (C)
%Tr is a scalar (C)
R=8.314;
t=X(:,1);
T=X(:,2);
Tr=X(1,3)+273.15;
intgrnd = (T).*exp(-(b(2))*(1./T-1/Tr));
psi=cumtrapz(t,intgrnd);

  M=43.1*(1+b(3)*(1-exp(-b(1)*psi)).^0.6235);
end
```

II) Function file name: starch_test_Tr

```
function corrkE=starch_test_Tr(Tr)

%beta0(1)=.6346*exp(-131000*(1/Tr-1/(91.06+273.15)));%k
beta0(1)=(.6346*exp(-131000*(1/Tr-1/(91.06+273.15))))/300;
beta0(2)=6.01e4;%Eg/R
beta0(3)=14.7; %A^alpha
beta0=beta0';
alpha = 1;

data=xlsread('MelojelData.xls');
tfact=60;
t=data(:,1)/tfact;
T=data(:,2)+273.15;
yobs=data(:,4)*1e6;%torque in mN-mm
tT=t;
tT(:,2)=T;
tT(:,3)=Tr;%Tr is only one value

%inverse problem
[beta,resids,J,COVB,mse] = nlinfit(tT, yobs,'st_torqueTr', beta0);

%R is the correlation matrix for the parameters, sigma is the standard error vector
[R,sigma]=corrcov(COVB);
corrkE=R(2,1
end
```

III) File name: Call_Starch_diff_V_Tr

```
clc
clear
```

```
%%%%%%%%%%%%%%%%%%%%%%%%%%%%%%%%%%%%%%%%%%%%%%%%%%%%%%%%%%%%%%%%%%%%%%%%
% PLOT OF Tr VS CORR
%%%%%%%%%%%%%%%%%%%%%%%%%%%%%%%%%%%%%%%%%%%%%%%%%%%%%%%%%%%%%%%%%%%%%%%%%%%
TrV=85:0.25:95
for i = 1:length(TrV)
   Tr = TrV(i);
%     corr(i) = get_ypar4_3(Tr);
%     corr(i) = get_ypar4_4(Tr);
%      corr(i) = get_ypar4_Wb_2(Tr);
%     corr(i) = Wb_diff_V(Tr);
     corr(i) = starch_test_Tr(Tr);
end

figure
hold on
set(gca, 'fontsize',14,'fontweight','bold');
h = plot(TrV,corr,'-k', 'linewidth',2.5);
% xlabel('Reference Temperature \it{T_r}, (^oC_','FontSize',16,'fontweight','bold');
xlabel('Reference Temperature \it{T_r_g} , \rm(^oC)','FontSize',16,'fontweight','bold');
% ylabel('Correlation Coefficient of \itd_r and \itz','FontSize',16,'fontweight','bold');
% ylabel('Correlation Coefficient of \it{AsymD_r} and
\itz','FontSize',16,'fontweight','bold');
ylabel('Corr. Coeff. of \it{k_g} and \itE_g /R','FontSize',16,'fontweight','bold');
plot([min(TrV),max(TrV)],[0,0], 'R','linewidth',2.5)
```

***B)** Reference temperature for temperature term (T_{rt}) involves time-temperature history, shear history and temperature terms. Trg was fixed in here.*
Consist of 3 files (folder name: Trtemp files), first open all files and then run the starch_Tr file. Note: Trt plot using heating data only without cooling data of the experiment (Rabiha_tT excel file data) are different than when use the Melojel excel file data which includes the cooling data.
I)Function file name: st_torqueTr

```
function M = st_torqueTr( b,X )

N=100;
t=X(:,1);
T=X(:,2);
Tr=X(1,3)+273.15;

intgrnd = (T).*exp(-(b(2))*(1./T-1/(90.6+273.15)));%I fix the Trg at 90.6C based on Trg
file

psi=cumtrapz(t,intgrnd);
M=(43.1*(1+b(3)*(1-exp(-b(1)*(psi))).^0.6235)).*(1-b(4)*(1-exp(-
0.0057*N*t))).*(exp(b(5)*(1./T-1/Tr)));%this is Trt
```

```
end
```

II) Function file name: starch_test_Tr

```
function corrEvAalpha=starch_test_Tr(Tr)%***********
% clear all

% beta0(1)=0.3;%k
beta0(1)=0.3/300;%k
% beta0(2)=6.01e4;%E/R
beta0(2)=60100;%Eg/R
beta0(3)=14.7; %A^alpha
beta0(4)=0.1; %B ~150mNmm*****estimate from exp data
beta0(5)=2077;%Ev/R from AACC poster data

beta0=beta0';
alpha = 1;
% Tr=91.06+273.15;%for 3 parameters of time-temp history term only
% Tr=92.19+273.15;%for 4 parameters of time-temp history term only
data=xlsread('Rabiha_tT.xls');
tfact=60;
t=data(:,1)/tfact;
T=data(:,2)+273.15;
yobs=data(:,4)*1e6;%torque in mN-mm
tT=t;
tT(:,2)=T;
tT(:,3)=Tr;%Tr is only one value
% beta=beta0;

%inverse problem
[beta,resids,J,COVB,mse] = nlinfit(tT, yobs,'st_torqueTr', beta0);

%R is the correlation matrix for the parameters, sigma is the standard error vector
[R,sigma]=corrcov(COVB);
%corrkE=R(2,1);%NEW STATEMENT for correlation coefficient for k and E/R
corrEvAalpha=R(5,3);%NEW STATEMENT for correlation coefficient for A^alpha and
Ev/R
end
```

III) File name: Call_Starch_Tr

```
clc
clear
%%%%%%%%%%%%%%%%%%%%%%%%%%%%%%%%%%
% PLOT OF Trt VS CORR
%%%%%%%%%%%%%%%%%%%%%%%%%%%%%%%%%%%

TrV=50:0.25:99;
```

```
for i = 1:length(TrV)
    Tr = TrV(i);
    corr(i) = starch_test_Tr(Tr);
end

figure
hold on
set(gca, 'fontsize',14,'fontweight','bold');
h = plot(TrV,corr,'-k', 'linewidth',2.5);

xlabel('Reference Temperature \it{T_r_t} , \rm(^oC)','FontSize',16,'fontweight','bold');

ylabel('Corr. Coeff. of \it{E_v /R} and \itA^a^l^p^h^a','FontSize',16,'fontweight','bold');
plot([min(TrV),max(TrV)],[0,0], 'R','linewidth',2.5)
```

Section: Matlab syntax for 3 terms (Model 3)

I) Function file name: st_torque_3new

```
function M = st_torque_3new( b,X )% M is the dependent value, b is the parameter, and
the X is the independent variable.
%global Tr ind
global Tr
%%computes psi(t) given time-temperature history
%  t is a nx1 vector of time (min)
%X independent variables column 1 is time, column2 T (K)
% T is nx1 vector of temperature (C)
%Tr is a scalar (C)
R=8.314;
t=X(:,1);
T=X(:,2);
N=100;
intgrnd = (T).*exp(-(b(2))*(1./T-1/Tr));
psi=cumtrapz(t,intgrnd);

%ind is the index of tSH% %tSH is time where shear history begins
% n=length(t);
%  tSH=t(ind);
%
% SH=ones(n,1);
%
% SH(ind:n)= 1-b(5)*(1-exp(-0.0057*(t(ind:n)-tSH)*N));

%Torque Model
```

```
%M=(b(4)*(1+b(3)*(1-exp(-b(1)*(psi/300))).^0.6235)).*SH.*(exp(b(6)*(1./T-
1/(90.6+273.15))));


 M=(b(4)*(1+b(3)*(1-exp(-b(1)*(psi/300))).^0.6235)).*(1-b(5)*(1-exp(-
0.0057*N*t))).*(exp(b(6)*(1./T-1/(90.6+273.15))));

end
```

II) Mother file name: starch_test_3new

```
%%Initial estimate
clear all
%global Tr ind
global Tr
tfact=60;% in min,
beta0(1)=(tfact*(.005));%kg% so b(0)=0.3 is k at Tr in second^-1
beta0(2)=60100;%Eg/R
beta0(3)=14.7; %A^alpha
beta0(4)=43;% s%constant which include shear rate and concentration terms
beta0(5)=0.1;%B
beta0(6)=2077;%Ev/R

beta0=beta0';

Tr=91.06+273.15;

data=xlsread('MelojelData.xls');

t=data(:,1)/tfact;
T=data(:,2)+273.15;
yobs=data(:,4)*1e6;%torque in mN-mm

%******
% index=find(yobs>3*yobs(1));%find y when it starts to gelatinize, to use in SH term
later
% ind=index(1);%the first point Y where starch about to gelatinize
%******

tT=t;
tT(:,2)=T;

%%inverse problem
[beta,resids,J,COVB,mse] = nlinfit(tT, yobs,'st_torque_3new', beta0);
rmse=sqrt(mse); %mean square error = SS/(n-p)
SS=resids'*resids;
```

```
%%R is the correlation matrix for the parameters, sigma is the standard error vector
[R,sigma]=corrcov(COVB);
relsterr=sigma./beta;
%confidence intervals for parameters
ci=nlparci(beta,resids,J);

%%forward problem
ypred=st_torque_3new(beta,tT);
% figure
%  set(gca, 'fontsize',14,'fontweight','bold');
% plot(t*tfact/60,ypred,'--',t*tfact/60,yobs,'or')
% legend('ypred','yobs')
% xlabel('time (min)','fontsize',14);ylabel('M (mNmm)','fontsize',14)

%Torque plot begin here
x = t*tfact/60;
V1 =yobs;
V2 = ypred;
T1  =data(:,2);
% T2  =data(:,2);

color1 = 'k';
color2 = 'k';

% Make the first set of plots on the first axes
ht1 = line(x,V1,'Marker','o','Linestyle','none');

hold on;

ht2 = line(x,V2,'Marker','^', 'LineStyle', '-');
%legend('Mobs','Mpred')

ax1 = gca;

set(ax1,'XColor',color1,'YColor',color1)
xlabel('time, min')
ylabel('Torque(M), mNmm')

% Second set of plots on the second axes
ax2 = axes('Position',get(ax1,'Position'),...
        'XAxisLocation','top',...
        'YAxisLocation','right',...
        'Color','none',...
        'YColor',color2, ...
        'XTick',[ ]);
```

```
ylabel('Temperature (^o Celcius)')

hv1 = line(x,T1,'Color',color2,'Parent',ax2);

% hold on;
% hv2 = line(x,T2,'Color',color2, 'LineStyle', '--', 'Parent',ax2);
%legend('temp')
 legend(ax1,'Mobs','Mpred')
 legend(ax2,'Temp')

%Torque plot ends here

%%scaled sensitivity coefficients

Xp(:,1)=beta(1)*J(:,1);%Xp mean Xprime which mean scaled sensitivity coeff. J is the
jacobian or known as the sensitivity coefficient
Xp(:,2)=beta(2)*J(:,2);
Xp(:,3)=beta(3)*J(:,3);
Xp(:,4)=beta(4)*J(:,4);
Xp(:,5)=beta(5)*J(:,5);
Xp(:,6)=beta(6)*J(:,6);
figure
hold on
h(1)=plot(t*tfact/60,Xp(:,1),'ok');
h(2)=plot(t*tfact/60,Xp(:,2),'sb');
h(3)=plot(t*tfact/60,Xp(:,3),'^g');
h(4)=plot(t*tfact/60,Xp(:,4),'pr');
h(5)=plot(t*tfact/60,Xp(:,5),'m');
h(6)=plot(t*tfact/60,Xp(:,6),'*');
legend(h,'X''k_g','X''E_g /R','X''A^{\alpha}','X''C','X''B','X''E_v /R')
% legend(h,'X''k','X''E','X''A^{\alpha}','X''\alpha')
xlabel('time (min)','fontsize',14); ylabel('scaled sens coeffs','fontsize',14)
set(gca, 'fontsize',14,'fontweight','bold');% increases font size of the plot axes

%%residuals histogram
[n1, xout] = hist(resids,10);
 figure
 hold on
 set(gca, 'fontsize',14,'fontweight','bold');
 bar(xout, n1) % plots the histogram
 xlabel('M_{observed} - M_{predicted}','fontsize',16,'fontweight','bold')
 ylabel('Frequency','fontsize',16,'fontweight','bold')

 %%residuals scatter
 figure
 hold on
```

```
 set(gca, 'fontsize',14,'fontweight','bold');
 plot(t*tfact/60, resids, 'square', 'Markerfacecolor', 'k', 'markeredgecolor','k',
'markersize',10)
 plot([0,max(t)*tfact/60],[0,0], 'k')
 ylabel('M_{observed} - M_{predicted}','fontsize',16,'fontweight','bold')
 xlabel('time (min)','fontsize',16,'fontweight','bold')
```

III) Sequential file name: Sequential_starch_3new

```
%------------------------------------
clc
%-------------------------------------
set(0,'defaultaxesfontsize',16);

tol=1e-4;
xvals=tT;

yvals=yobs;

%%Initial estimate
 beta=[(tfact*(.005));100100;14.7;43;0.1; 2077];
%---------------------------------------------------------------
Y = yvals;
sX = [length(yvals) length(beta)];

sig = .1*ones(sX(1),1);

Ratio1 = 1; Ratio2 = 1; Ratio3= 1; Ratio4= 1; Ratio5= 1; Ratio6= 1;%need one Ratio per
parameter , %*************
plots=0;
clear betain X1 A delta K BBbP b SeqBeta
b_old =beta ;

figure
hold on
while Ratio1 > tol || Ratio2 > tol || Ratio3 > tol || Ratio4 > tol || Ratio5 > tol || Ratio6 > tol
   P = 100^1*eye(sX(2));
   b0 = b_old;
   beta = b0;

     ypred = st_torque_3new(beta,tT);%***

   e = yvals-ypred;
         %-------------------------------------
      d=0.0001;
      for i = 1:length(beta)
```

```
        betain = beta;
        betain(i) = beta(i)+beta(i)*d;
%
          yhat{i}=st_torque_3new(betain,tT);%***********
%
        X{i} = (yhat{i}-ypred)/(beta(i)*d); %sensitivity coeff cell array
      end
   for k = 1:sX(1)
      if k == 1
         b = b0;
      end
      clear A delta
         X1 = [X{:,1} X{:,2} X{:,3} X{:,4} X{:,5} X{:,6}];%pull out sens coeff from cell array
%*******
         A(:,k) = P*X1(k,:)';
         delta(k) = sig(k)^2+X1(k,:)*A(:,k);
         K(:,k) = A(:,k)/delta(k);
         b = b + K(:,k)*(e(k)-X1(k,:)*(b-b0));
         P = P - K(:,k)*A(:,k)';
         BBbP{k} = [b P];
%
   end


h2(1)=plot(plots,b_old(1),'s','MarkerEdgeColor','k','MarkerFaceColor','r','MarkerSize',5);

h2(2)=plot(plots,b_old(2)/5e4,'s','MarkerEdgeColor','k','MarkerFaceColor','g','MarkerSize
',5);

h2(3)=plot(plots,b_old(3),'s','MarkerEdgeColor','k','MarkerFaceColor','b','MarkerSize',5);

h2(4)=plot(plots,b_old(4),'s','MarkerEdgeColor','k','MarkerFaceColor','c','MarkerSize',5);
%***********

h2(5)=plot(plots,b_old(5),'s','MarkerEdgeColor','k','MarkerFaceColor','c','MarkerSize',5);
%***********

h2(6)=plot(plots,b_old(6),'s','MarkerEdgeColor','k','MarkerFaceColor','c','MarkerSize',5);
xlabel('Iteration','FontSize',15,'fontweight','bold');
    ylabel('Sequentially Estimated Parameters','FontSize',15,'fontweight','bold');
    b_new = BBbP{end};
    plots = plots+1;
    Ratioall = abs((b_new(:,1)-b_old)./b_old);
    Ratio1 = Ratioall(1);
    Ratio2 = Ratioall(2);
    Ratio3 = Ratioall(3);
```

```
    Ratio4 = Ratioall(4);
    Ratio5 = Ratioall(5);
    Ratio6 = Ratioall(6);
    b_old = b_new(:,1);

end

legend(h2,'k_g','E_g /R','A^\alpha','C','B','E_v /R')
covmat = P;
corrcoef = covmat(2,1)/(sqrt(covmat(1,1))*sqrt(covmat(2,2)));

Result = BBbP{end};

hold off

for i = 1:length(BBbP)
   BB = BBbP{i};
   SeqBeta(:,i) = BB(:,1);
end

set(gca, 'fontsize',14,'fontweight','bold');
figure
hold on

h3(1) =
plot(xvals(:,1),SeqBeta(1,:),'^','MarkerEdgeColor','b','MarkerFaceColor','r','MarkerSize',1
0);

xlabel('time (min)','FontSize',16,'fontweight','bold');
ylabel('k_g (K min^{-1})','FontSize',16,'fontweight','bold');

set(gca, 'fontsize',14,'fontweight','bold');
figure
hold on

h4(1) =
plot(xvals(:,1),SeqBeta(2,:),'^','MarkerEdgeColor','b','MarkerFaceColor','r','MarkerSize',1
0);

xlabel('time (min)','FontSize',16,'fontweight','bold');
ylabel('E_g/R (K)','FontSize',16,'fontweight','bold');

set(gca, 'fontsize',14,'fontweight','bold');
figure
hold on
```

```
h5(1) =
plot(xvals(:,1),SeqBeta(3,:),'^','MarkerEdgeColor','b','MarkerFaceColor','r','MarkerSize',1
0);

xlabel('time (min)','FontSize',16,'fontweight','bold');
ylabel('A^\alpha (dimensionless)','FontSize',16,'fontweight','bold');


set(gca, 'fontsize',14,'fontweight','bold');
figure
hold on
h6(1) =
plot(xvals(:,1),SeqBeta(4,:),'^','MarkerEdgeColor','b','MarkerFaceColor','r','MarkerSize',1
0);%*****
xlabel('time (min)','FontSize',16,'fontweight','bold');
ylabel('S (mNmm min^n)','FontSize',16,'fontweight','bold');


set(gca, 'fontsize',14,'fontweight','bold');
figure
hold on
h7(1) =
plot(xvals(:,1),SeqBeta(5,:),'^','MarkerEdgeColor','b','MarkerFaceColor','r','MarkerSize',1
0);%*****
xlabel('time (min)','FontSize',16,'fontweight','bold');
ylabel('B (dimensionless)','FontSize',16,'fontweight','bold');

set(gca, 'fontsize',14,'fontweight','bold');
figure
hold on
h8(1) =
plot(xvals(:,1),SeqBeta(6,:),'^','MarkerEdgeColor','b','MarkerFaceColor','r','MarkerSize',1
0);%*****
xlabel('time (min)','FontSize',16,'fontweight','bold');
ylabel('E_v /R (K)','FontSize',16,'fontweight','bold');
```

SECTION: MATLAB syntax for RVA curve prediction (forward problem)

I) Function file name: st_torque_RVA

```
function M = st_torque_RVA( b,X )% M is the dependent value, b is the paarameter, and
the X is the independent variable.
%global Tr ind
global Tr
%%computes psi(t) given time-temperature history
%  t is a nx1 vector of time (min)
```

```
%X independent variables column 1 is time, column2 T (K)
% T is nx1 vector of temperature (C)
%Tr is a scalar (C)

t=X(:,1);
T=X(:,2);
N=160;%rpm*
intgrnd = (T).*exp(-(b(2))*(1./T-1/Tr));
psi=cumtrapz(t,intgrnd);

%ind is the index of tSH% %tSH is time where shear history begins
% n=length(t);
%  tSH=t(ind);
%
% SH=ones(n,1);
%
% SH(ind:n)= 1-b(5)*(1-exp(-0.0057*(t(ind:n)-tSH)*N));

%M=(b(4)*(1+b(3)*(1-exp(-b(1)*(psi/300))).^0.6235)).*SH.*(exp(b(6)*(1./T-
1/(90.6+273.15))));

% M=(b(4)*(1+b(3)*(1-exp(-b(1)*(psi/300))).^0.6235)).*(1-b(5)*(1-exp(-0.005
% 7*N*t))).*(exp(b(6)*(1./T-1/(90.6+273.15))));
M=(b(4)*(1+b(3)*(1-exp(-b(1)*(psi/300))).^0.6235)).*(1-b(5)*(1-exp(-
0.0057*N*t))).*(exp(b(6)*(1./T-1/(90.6+273.15))));
end
```

II) Mother file name: starch_test_RVA

```
%%Initial estimate
clear all
%global Tr ind
global Tr
tfact=60;% in min,
%Use the final estimate from sequential result of Model3 (all terms)
b(1)=0.3401;%kg at Tr in second^-1
b(2)=121450;%Eg/R

b(3)=15.7036;

b(4)=50.6659*(1.6^1.27);
b(5)=0.2872;%B
b(6)=64.9361;

b=b';
```

```
Tr=91.06+273.15;


data=xlsread('RVA_Melojel.xls');

t=data(:,1)/tfact;
T=data(:,2)+273.15;
yobs=data(:,7)*1e6;%torque in mN-mm


% ind=index(1);%the first point Y where starch about to gelatinize
% check=0;i=1;
% while check<4%30%15%4
%     if yobs(i+1)>yobs(i)
%         check=check+1;
%     else
%         check=0;
%     end
%     i=i+1;
% end
% ind=i-1;

tT=t;
tT(:,2)=T;


%forward problem
 ypred=st_torque_RVA(b,tT);

figure
hold on
%Torque plot begin here
x = t*tfact/60;
V1 =yobs;
V2 = ypred;%scaling 2times than observed
T1  =data(:,2);
% T2  =data(:,2);

color1 = 'b';
color2 = 'b';

% Make the first set of plots on the first axes
ht1 = line(x,V1,'Marker','o','Linestyle','none');

hold on;
```

```
ht2 = line(x,V2,'Marker','^', 'LineStyle', 'none');
%legend('Mobs','Mpred')

ax1 = gca;

set(ax1,'XColor',color1,'YColor',color1)
xlabel('time, min')
ylabel('Torque(M), mNmm')

% Second set of plots on the second axes
ax2 = axes('Position',get(ax1,'Position'),...
        'XAxisLocation','top',...
        'YAxisLocation','right',...
        'Color','none',...
        'YColor',color2, ...
        'XTick',[ ]);
ylabel('Temperature (^o Celcius)')

hv1 = line(x,T1,'Color',color2,'Parent',ax2);

% hold on;
% hv2 = line(x,T2,'Color',color2, 'LineStyle', '--', 'Parent',ax2);
%legend('temp')
 legend(ax1,'RVA_o_b_s','RVA_p_r_e_d')
 legend(ax2,'Temp')

%Torque plot ends here
```

REFERENCES

References

Ahmed J, Ramaswamy HS, Ayad A & Alli I. 2008. Thermal and dynamic rheology of insoluble starch from basmati rice. Food Hydrocolloids 22(2):278-287.

Beck JV & Arnold KJ. 1977. Parameter Estimation in Engineering and Science. John Wiley & Sons, New York.

Briggs JL & Steffe JF. 1996. Mixer viscometer constant (k') for the Brookfield small sample adapter and flag impeller. Journal of Texture Studies 27(6):671-677.

Dail RV & Steffe JF. 1990. Rheological Characterization of Cross-Linked Waxy Maize Starch Solutions under Low Acid Aseptic Processing Conditions Using Tube Viscometry Techniques. Journal of Food Science 55(6):1660-1665.

Dolan KD. 2003. Estimation of kinetic parameters for nonisothermal food processes. Journal of Food Science 68(3):728-741.

Dolan KD & Steffe JF. 1990. Modeling Rheological Behavior of Gelatinizing Starch Solutions Using Mixer Viscometry Data. Journal of Texture Studies 21(3):265-294.

Dolan KD, Yang L & Trampel CP. 2007. Nonlinear regression technique to estimate kinetic parameters and confidence intervals in unsteady-state conduction-heated foods. Journal of Food Engineering 80(2):581-593.

Hazelton JL & Walker CE. 1996. Temperature of liquid contents in RVA cans during operation. Cereal Chemistry 73(2):284-289.

Lagarrigue S & Alvarez G. 2001. The rheology of starch dispersions at high temperatures and high shear rates: a review. Journal of Food Engineering 50(4):189-202.

Lai KP, Steffe JF & Ng PKW. 2000. Average shear rates in the rapid visco analyser (RVA) mixing system. Cereal Chemistry 77(6):714-716.

Lillford PJaM, A. 1997. Structure/Function Relationship of Starches in Food. in Book Starch: Structure and Functionality edited by P.J. Frazier, A.M. Donald and P.Richmond(The Royal Society of Chemistry. Thomas Graham House, Science Park, Milton Road, Cambridge, UK.):1-8.

Liu XX, Yu L, Xie FW, Li M, Chen L & Li XX. 2010. Kinetics and mechanism of thermal decomposition of cornstarches with different amylose/amylopectin ratios. Starch-Starke 62(3-4):139-146.

Mishra DK, Dolan KD & Yang L. 2008. Confidence intervals for modeling anthocyanin retention in grape pomace during nonisothermal heating. Journal of Food Science 73(1):E9-E15.

Mishra DK, Dolan KD & Yang L. 2009. Bootstrap confidence intervals for the kinetic parameters of degradation of anthocyanins in grape pomace. Journal of Food Process Engineering 34(4):1220-1233.

Mohamed IO. 2009. Simultaneous estimation of thermal conductivity and volumetric heat capacity for solid foods using sequential parameter estimation technique. Food Res Int 42(2):231-236.

Morgan RG. 1979. Modeling the effects of temperature-time history, temperature, shear rate and moisture on viscosity of defatted soy flour dough. Ph.D. dissertation. Agricultural Engineering. Texas A&M University :1-114.

Morgan RG, Steffe JF & Ofoli RY. 1989. A Generalized Rheological Model for Extrusion Modeling of Protein Doughs. J. Food Process Engr. 11:55-78.

Motulsky H, Christopoulos A. 2004. Fitting models to biological data using linear and nonlinear regression: A practical guide to curve fitting. Oxford University Press, New York: 143-147.

Okechukwu PE & Rao MA. 1996. Kinetics of cowpea starch gelatinization based on granule swelling. Starch-Starke 48(2):43-47.

Schwaab M & Pinto JC. 2007. Optimum reference temperature for reparameterization of the Arrhenius equation. Part 1: Problems involving one kinetic constant. Chemical Engineering Science 62(10):2750-2764.

Spigno G & De Faveri DM. 2004. Gelatinization kinetics of rice starch studied by non-isothermal calorimetric technique: influence of extraction method, water concentration and heating rate. Journal of Food Engineering 62(4):337-344.

Steffe JF. 1996. Rheological Methods in Food Process Engineering. Second Edition Freeman Press(East Lansing, MI):2.

Steffe JF & Daubert CR. 2006. Bioprocessing Pipelines: Rheology and Analysis. Freeman Press, East Lansing, MI, USA:1-32.

Thomas DJ & Atwell WA. 1999. Starches. American Association of Cereal Chemists. Eagan Press Handbook Series, St. Paul, Minnesota, USA.

CHAPTER 5
OBJECTIVE THREE

Kinetic Parameter Estimation for Starch Viscosity Model as a Function of Amylose

Abstract

The apparent viscosity profile of starches during gelatinization varies with different amylose to amylopectin ratios. This study focused on the influence of amylose to amylopectin ratios on the kinetic parameters of the starch viscosity model for corn starches. Five parameters were considered: gelatinization rate constant (k_g), gelatinization activation energy (E_g), relative increase in apparent viscosity (A^{α}), relative decrease in apparent viscosity (B), and viscous activation energy (E_v). They were estimated at different ratios of amylose to amylopectin (AM/AP) using nonlinear regression and the sequential method written in MATLAB program. The mixer viscometry approach was used to model viscosity as a function of five independent variables for different amylose to amylopectin ratios. The first part of this paper presents parameter estimation results for waxy corn starch. The parameters were used to predict viscosity for a different measuring system, i.e., the RVA. The second part of this paper presents the estimated parameters for corn starch blends at different amylose to amylopectin ratios. The following parameters were significantly affected by amylose content: k_g and E_g decreased with amylose content by a power-law relationship. Activation energy of gelatinization ranged from 121 to 1169 kJ/mol. The other parameters A^{α}, B, and E_v were not significantly influenced by amylose content. In summary, the gelatinization parameters k_g and E_g dramatically decrease as amylose increases from 3% to 35% in waxy corn starch blends.

Keywords: Gelatinization; Corn Starch; Viscosity Model; Amylose; Amylopectin; nonlinear Kinetic Parameter Estimation; Pasting Curve; Mixer Viscometry; LabView; Brookfield Viscometer; Non isothermal; Inverse Problem; Rheology, Rapid Visco Analyzer (RVA)

5.1 Introduction

Starch is one of the major components in the diet of the world population. Starch plays a very important role in food functionality and nutritional quality enhancement, and this leads to increasing interest in starch research (Yuryev and others 2002). Starch is mainly composed two types of glucose molecules: amylose and amylopectin. The amylose to amylopectin ratio present in starch depends on the botanical source (Jane et al. 1999; Yuryev et al. 2002). Corn starch is a notable example of cereal starch that has varying amylose to amylopectin ratios due to three varieties available commercially: waxy, normal, and high amylose starches. Some research has been done on the behavior of corn starch regarding gelatinization, solubility, thermal properties, rheological properties, and molecular structure (Jane et al. 1999; Juhasz and Salgo 2008; Liu et al. 2006; Liu et al. 2010; Matveev et al. 2001; Dail and Steffe 1990a; Dolan and Steffe 1990; Ratnayake and Jackson 2006; Xie and others 2009; Cheetham and Tao 1997; Cheetham and Tao 1998; Uzman and Sahbaz 2000; Villwock and others 1999; Wu and others 2006).

Waxy starch contains the highest amylopectin, and when heated in water produces the most dramatic increase in peak viscosity among other varity of starches (Juhasz and Salgo 2008). Waxy starch is used to address certain common problems in the food industry for example, (1) to avoid the texture of pourable dressing being too thin, waxy starch content in the formulation is increased; (2) to avoid having a gummy texture of dressings, waxy starch content is in the formulation is decreased; (3) to have a uniform cell structure, desired moistness and high volume of final product in bakery products, waxy starch is added in the formulation ; (4) to have a crispness in extruded products, amylose content is increased if high-shear conditions are used or amylopectin content is increased if low-shear conditions are used (Thomas and Atwell 1999).

Viscosity profiles (pasting curves) are powerful tools to represent starch functional properties. Each starch produces a different viscosity profile even under the same processing conditions. This paper is focused on the influence of starch amylose and amylopectin ratios on gelatinization kinetic parameters using parameter estimation techniques on the viscosity model presented by Dolan and Steffe (1990) for gelatinizing starch solutions. To the best of our knowledge, no such study has been reported. The results of this study will be useful for (1) food engineers when calculating the velocity profile of products since viscosity plays a major role in the flow characteristics; and (2) product developers when formulating a product especially when corn starch is used as the product thickener.

5.2 Overview of Method

5.2.1 Sample Preparation

Commercial native waxy, Melojel, and high amylose corn starches (Hylon V and Hylon VII) were obtained from a starch company (National Starch, NJ). Corn starch blends with different AM/AP ratios of starch were prepared by adding higher AM/AP ratio content starches to lower AM/AP ratio content starches. Samples at different AM/AP ratios were prepared as follows: System I contained waxy and normal corn starch mixtures (0, 10, and 27% AM); System II contained waxy and high amylose Hylon V mixtures (10, 20, 30%AM); System III contained waxy and high amylose Hylon VII mixtures (10, 20, 30, 40, 50%). There was a total of 11 samples. Each sample, weighing 5g, was placed in a small glass vial and mixed well by vigorous manual shaking and a vortex mixer. The samples were then used to measure the apparent AM/AP ratios experimentally, and to produce the pasting curves.

5.2.2 Starch Apparent AM/AP Ratio Determination

The apparent AM/AP content of the samples was determined experimentally by the Con A method using the Megazyme AM/AP content assay kit (Megazyme 2006). The Con A method is commonly used to measure the amylose content in starch and flours (Gibson and others 1997). In this study, the exact method given by Megazyme was used with slight modifications. Samples were centrifuged using the bench centrifuge at 4000xg for 10min instead of 2000xg for 5min. The measurements were done at least in duplicates. The amylose content present in the sample was determined based on Con A supernatant and total starch aliquot absorbance readings at 510 nm as follows:

$$\text{Amylose experimental, \%(w/w)} = \frac{\text{Absorbance (Con A Supernatant)}}{\text{Absorbance (Total Starch Aliquot)}} \times 66.8$$

5.2.3 Rheological measurement

5.2.3.1 Mixer Viscometer Data Collection

Equipment set up consisted of a RVDV Brookfield viscometer equipped with three ethylene glycol baths (temperatures set at 96^{O}C, 60^{O}C, and 5^{O}C) and a solenoid valve system to switch between baths. The Brookfield flag impeller and the 13cc small cup adapter with RTD on the bottom of the sample cup, was used to hold the sample during agitation. Calibrations of instrument voltage and torque were done using standard fluids of silicon oil. Calibration of voltage and temperature were done by using ice, boiling water, and also by heating the water at fixed water bath temperatures. A data acquisition system (USB 6008), and a block diagram using Lab View, were used to collect the continuous raw data of time, temperature, and torque.

A starch solution at 6%w/w concentration in starch: water system was prepared. A small sample size of 0.829g in 13mL water was used. The sample was mixed with a vortex for 30sec in a test tube before the sample was ready for measurement. The sample, at room temperature, was poured into the heated cup while the impeller was being rotated to avoid sample settling. A fixed temperature profile was maintained: from 60^{O}C to 95^{O}C in 12min, cool to 60^{O}C in 13sec, and then hold constant at 60^{O}C for 10min.

5.2.3.2 Rapid Visco Analyzer (RVA) Data Collection

Standard profile 1 of RVA was used for the time-temperature profile. Native waxy corn starch (National Starch, NJ) at 6%w/w concentration in starch: water system was prepared. Total sample volume was 25mL. Time, temperature, and viscosity of the samples during the 13min test were obtained from the RVA data.

5.2.4 Starch Viscosity Model

In this study, the starch viscosity model proposed by Dolan and Steffe (1990) was used with some modification by including the reference temperature in Arrhenius equation: in the time-temperature history term (T_{rg}) and in the temperature term (T_{rt}) as shown in Eq. (22). The dependent variable was torque (M). The five independent variables were N, T, C,ψ, and ϕ; and the model consisted of ten parameters in total (K_r, n, E_v, b, A^{α},α, k, E_g, B, and d). The model Eq. (22) from left to right includes the shear rate term, temperature term, concentration term, time-temperature term, and shear history term, respectively.

$$M(t) = K_r N^n * e^{\frac{E_v}{R}\left(\frac{1}{T(t)} - \frac{1}{T_{rt}}\right)} * e^{b(C-C_r)} * \left[1 + A^{\alpha}\left(1 - e^{-k_g \psi}\right)^{\alpha}\right] * \left[1 - B\left(1 - e^{-d\phi}\right)\right] \quad (22)$$

where $\psi = \int_0^{t_f} T(t) e^{\frac{-\Delta E_g}{R}\left(\frac{1}{T(t)} - \frac{1}{T_{rg}}\right)} dt$ and (23)

$$\phi = \int_0^{t_f} N dt = Nt \quad (24)$$

The torque model allows starch apparent viscosity prediction by applying the mixer viscometry equation as shown in Equation (4) (Steffe and Daubert 2006).

$$\eta = \frac{k"M}{\Omega} \tag{25}$$

k'' was a known value for the Brookfield and a different known value for the RVA. Ω was held constant at 100rpm for Brookfield, and 160rpm for RVA. Since the torque model in Eq. (22) is very important in determining the apparent viscosity of gelatinizing starch solution using Eq.(25), the influence of starch amylose to amylopectin ratios on gelatinization kinetic parameters appearing in the torque model was investigated in this study. In any one experiment conducted, the impeller speed and the starch sample concentration are held constant when studying the starch pasting curve. Thus, the shear rate term and concentration term in Eq. (22) can be combined and treated as a constant (parameter S). In this way, we can reduce the number from 10 parameters to 8 parameters to be estimated, potentially making the parameter estimation easier. Eq. (26) shows the torque model of Eq. (22) consisting of the time-temperature history, shear history, and temperature terms.

$$M(t) = S * \left[1 + A^{\alpha}\left(1 - e^{-k_g \psi}\right)^{\alpha}\right] * \left[1 - B\left(1 - e^{-d\phi}\right)\right] * e^{\frac{E_v}{R}\left(\frac{1}{T(t)} - \frac{1}{T_{rt}}\right)} \tag{26}$$

5.2.5 Parameter Estimation

To estimate the parameters occuring in the torque model accurately, the following parameter estimation techniques were applied.

5.2.5.1 Sensitivity analysis

The sensitivity coefficient plots are helpful in explaining the dependency criteria between the parameters in the model (Beck and Arnold 1977). The scaled sensitivity coefficients were computed using MATLAB programming with a forward finite difference method. The larger and the more uncorrelated the scaled sensitivity coefficients are, the more easily those parameters can be estimated.

5.2.5.2 Ordinary Least Squares Estimation (OLS)

The command “nlinfit” in MATLAB was use to estimate the parameters in the model by minimizing the sum of squares (Mishra and others 2009). The MATLAB command for determing the asymptotic confidence interval (ci) of the parameters is ci=nlparci(beta,resids,J) and the procedure to determine the correlation coefficent matric of parameters is given in detail by (Mishra et al. 2008; Dolan et al. 2007).

5.2.5.3 Sequential Estimation

Sequential estimation allows updating the parameter values as new observations are added. Non-linear Maximum A Posteriori (MAP) sequential estimation procedure given in (Beck and Arnold 1977 p. 277) was used in this study.

5.3 Results and Discussion

5.3.1 Waxy Corn Starch

5.3.1.1 OLS and Sequential Estimation

The AM/AP ratio found experimentally for waxy corn starch in this study was 3% amylose, and assuming the rest is the amylopectin, the ratio becomes 3:97. The results of parameter estimation to determine the gelatinization kinetic parameters for waxy corn starch data obtained from the mixer viscometer are presented in this section. Based on the absolute value of the scaled sensitivity coefficient plots (Fig. 5.1), the parameters in the model that can be estimated for waxy corn starch are, in order from easiest to most difficult, A^{α}, B, k, E_g/R, and E_v/R. The 8 parameters in Eq. (26) were reduced to 5 parameters by fixing α, d, and S. At α=0.62 and d=0.0057, the estimation was good and had narrow confidence intervals. The parameter S was estimated alone and fixed at 44.6 because $X'S$ was highly correlated to $X'A^{\alpha}$.

Fig. 5.2 shows the predicted torque obtained from nlinfit result from MATLAB. The histogram plot and scatter plot of residuals for waxy corn starch are presented in Fig. 5.3 and Fig. 5.4, respectively. The mean residual obtained by using dfittool on MATLAB gives a normal distribution and a mean residual value of -0.33.

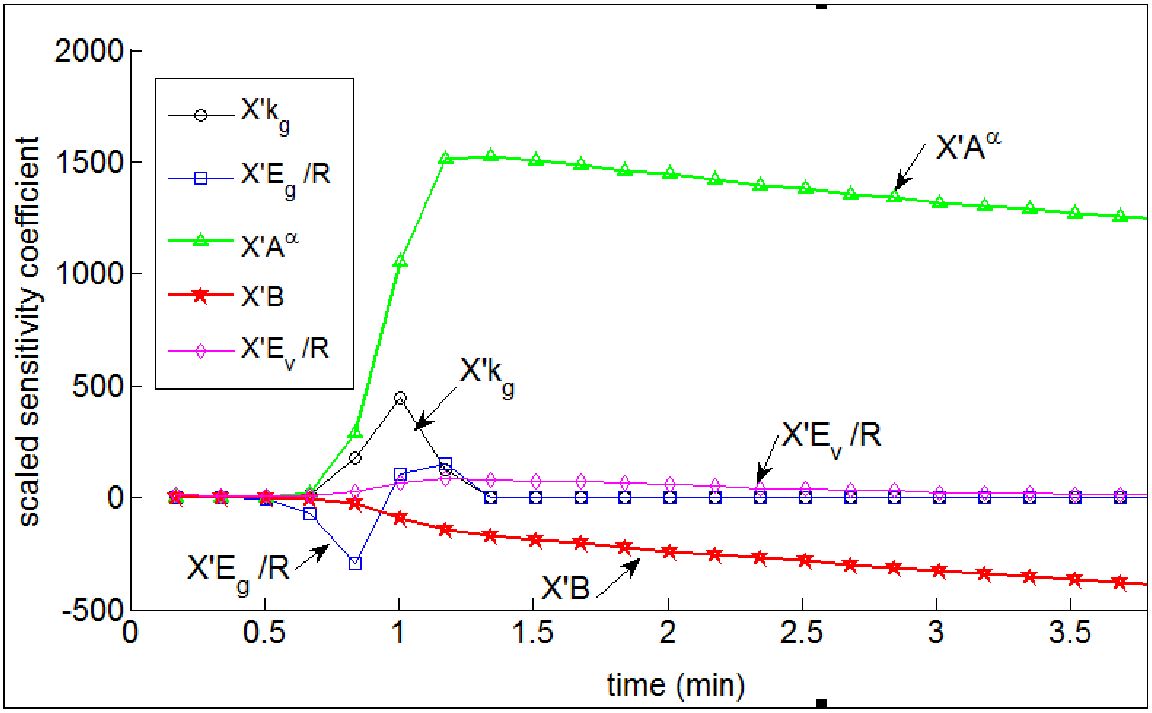

Figure 5.1. Zoom-in of scaled sensitivity coefficient plots of 5 parameters.

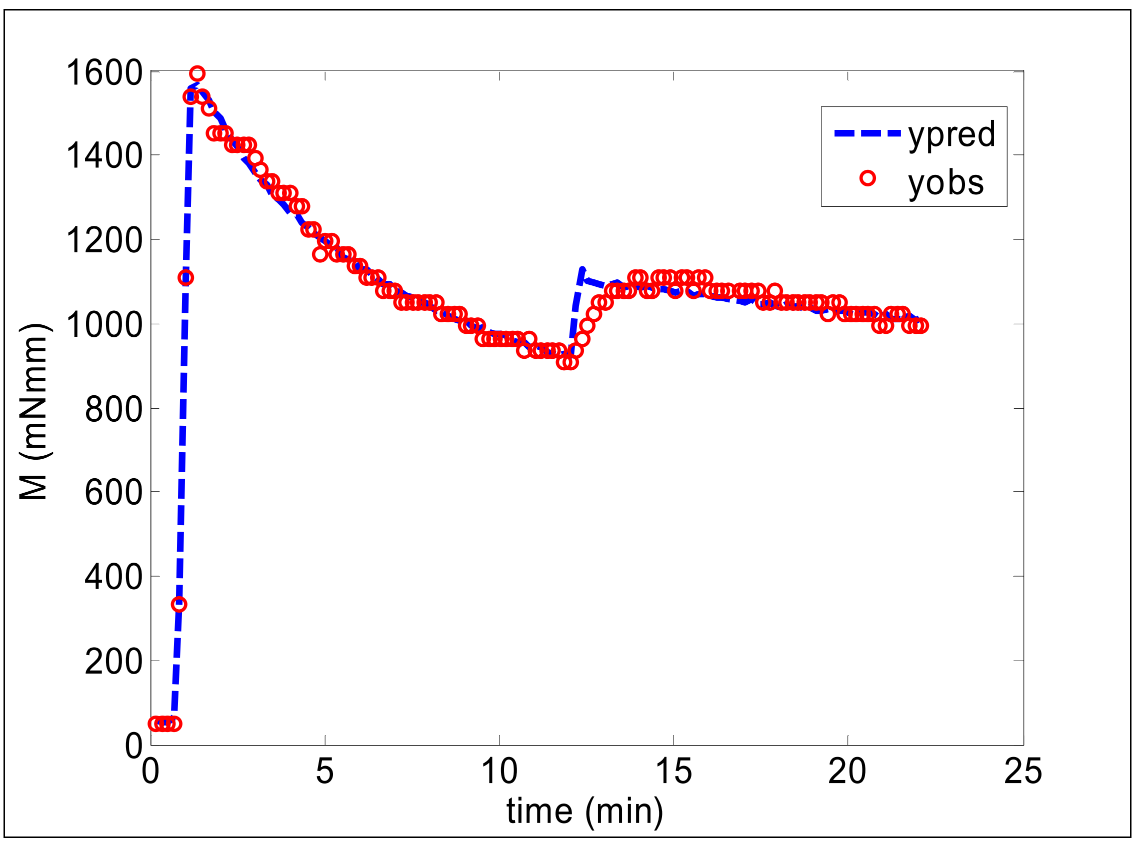

Figure 5.2. Plot of experimental torque (yobs) and predicted torque (ypred) versus time.

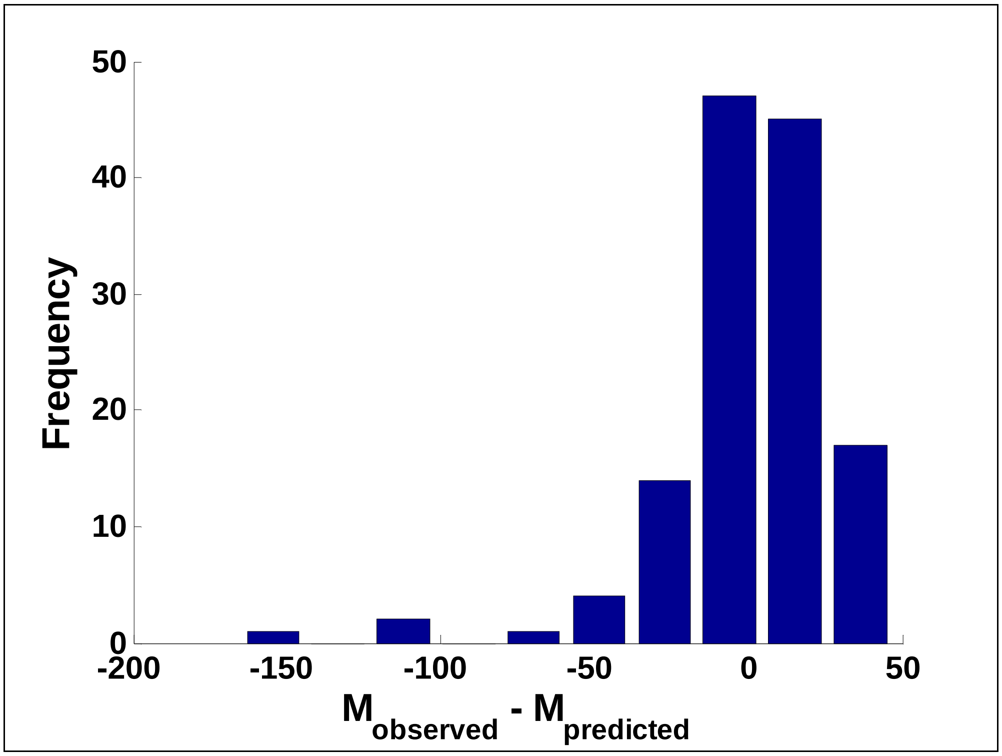

Figure 5.3. Residual histogram for OLS results in Fig.2.

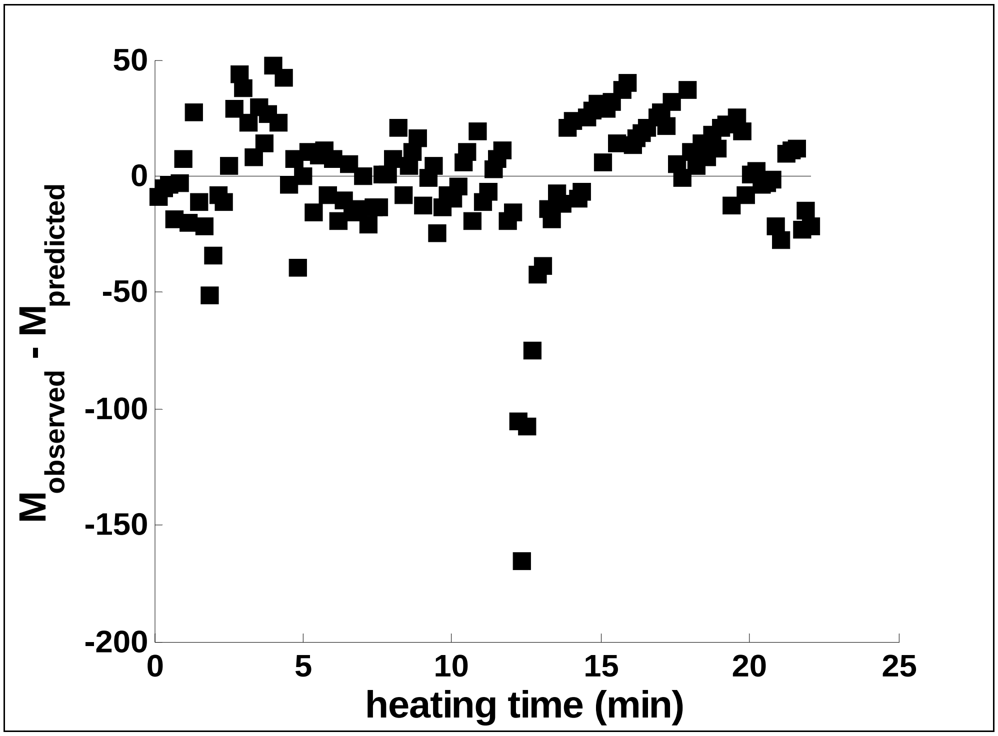

Figure 5.4. Residual scatter plot for OLS results in Fig.2.

The correlation matrix of parameters for waxy corn starch is presented in Table 5.1. Lowest correlation between parameters is expected when the parameters are more independent from each other and can be estimated better. The lowest correlation is found between k_g and E_g/R with value of 0.04 at T_{rg} of 84.5^{o}C, and then followed by E_g/R and E_v/R with value of approximately 0.07. Parameter correlation is dependent on the reference temperature for the Arrhenius equation. Fig. 5.5 shows the parameter correlation between k_g and E_g/R with T_{rg}. The optimum value, where the parameter correlation between k_g and E_g/R nearly zero, is found at T_{rg}= 84.5^{o}C. Among all the parameters, the highest correlation is found between A^{α} and B with value of 0.83, followed by B and E_v/R with value of 0.79.

The estimated values of parameters obtained from the nlinfit result for waxy corn starch data, and the relative standard error for each parameter estimated, is given in Table 5.2. Note that, as expected, lowest relative standard error was for A^{α}, and B, which had the largest scaled sensitivity coefficients. All the parameters have a relative standard error below 8%. The RMSE and sum square of error values was found to be 28.9 mNmm (~28.9/1600% of the torque span, an excellent low result) and 105026, respectively, for waxy corn starch parameter estimation.

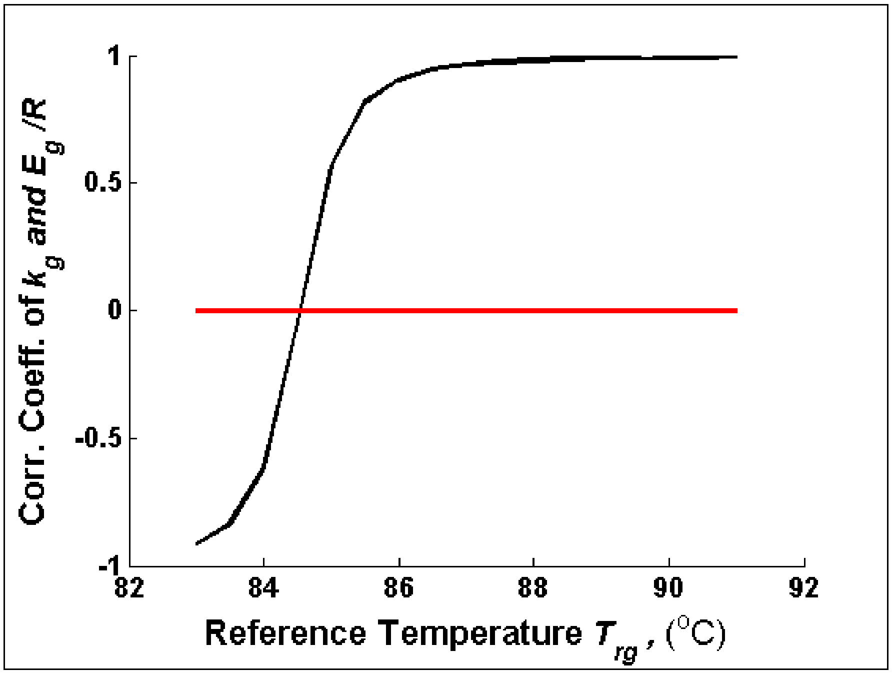

Figure 5.5. Correlation between parameters k_g and E_g/R in the time-temperature history term as a function of the gelatinization reference temperature.

Table 5.1 Correlation matrix table of parameters for waxy corn starch

	k_g	E_g/R	A^{α}	B	E_v/R
k_g	1				
E_g/R	-0.0426	1		SYMMETRIC	
A^{α}	-0.2860	-0.1206	1		
B	-0.2724	-0.1084	0.8356	1	
E_v/R	-0.1911	-0.0691	0.4260	0.7910	1

Table 5.2 Estimates of parameters and % relative standard error for waxy corn starch

Parameters	Waxy Corn Starch			
	OLS	% Relative Std. Error	Confidence Interval	
k_g, $(Kmin)^{-1}$	3.2±0.2	6.3	2.8	3.6
E_g (kJ/mol)	1169±95	8.1	117.9	163.3
A^{α}	34.5±0.2	0.6	34.1	34.9
B	0.53±0.01	1.9	0.5	0.5
E_v (kJ/mol)	7±0.25	3.6	758.6	879.5

OLS estimation of kinetic parameters for nonisothermal food processes using nonlinear parameter estimation has also been discussed (Dolan 2003; Mishra et al. 2008; Dolan et al. 2007). Sequential estimation allows updating the parameter values as new observations are added. Under sequential estimation, one expects the parameters to approach a constant as the number of observations is increased (Mohamed 2009). The sequentially estimated parameter values of k_g, E_g/R, A, B, and E_v/R were 3.2 $(Kmin)^{-1}$, 13.8×10^4K, 34.5, 0.5, and 819 K obtained after about 2.5min, 21min, 2.5min, 10min, and 18min, respectively, of the total experimental time are shown in Fig.5.6 (a to e).

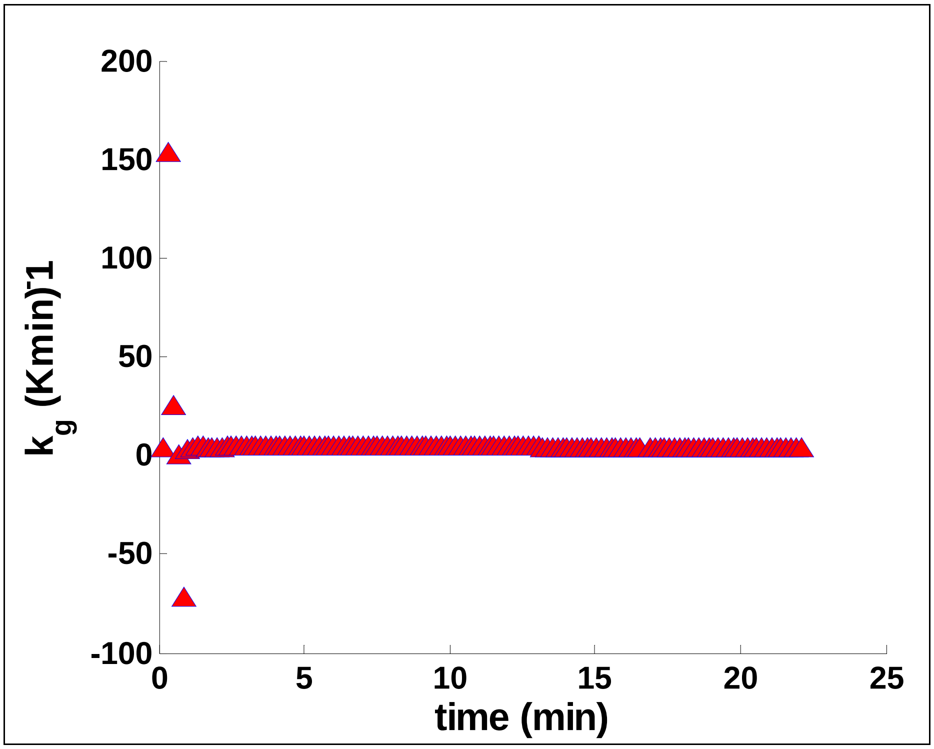

Figure 5.6a.Sequential estimation results of kg for waxy corn starch.

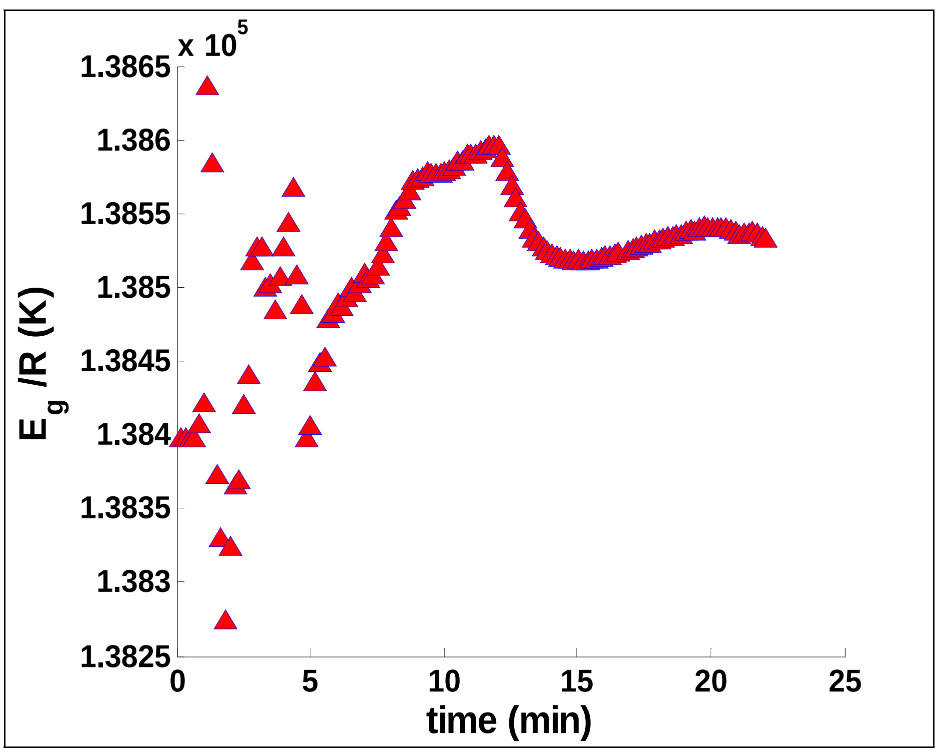

Figure 5.6b.Sequential estimation results of Eg/R for waxy corn starch.

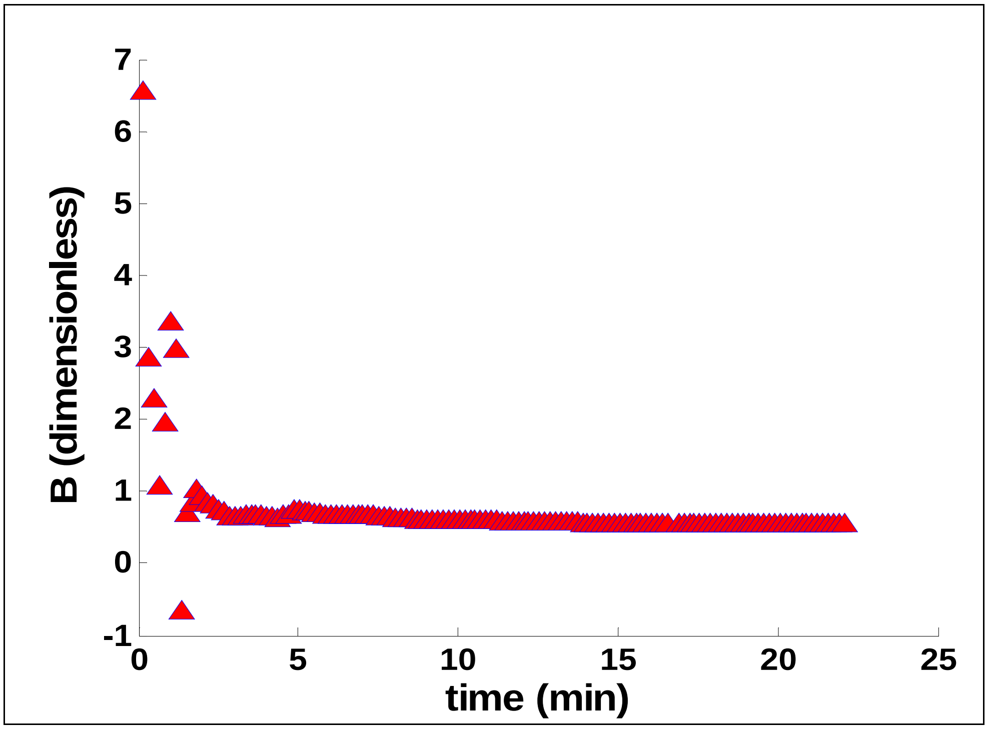

Figure 5.6c.Sequential estimation results of B for waxy corn starch.

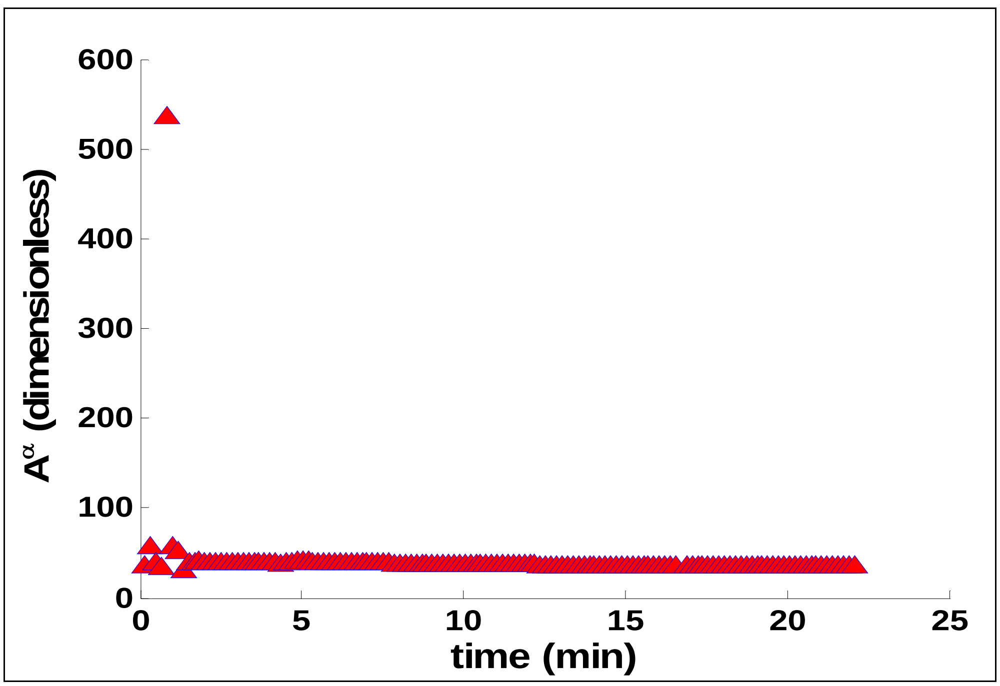

Figure 5.6d.Sequential estimation results of A^{α} for waxy corn starch.

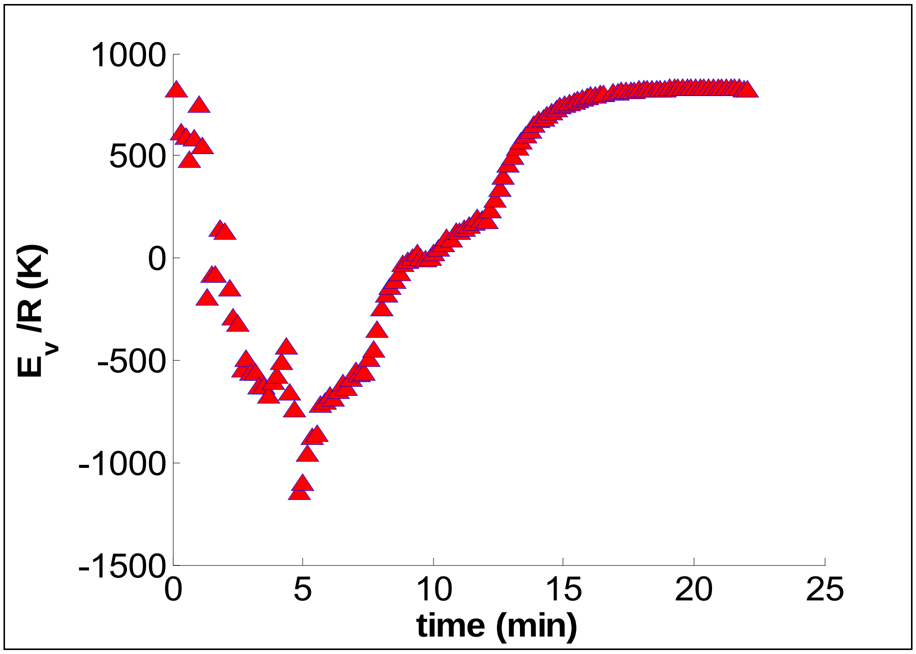

Figure 5.6e.Sequential estimation results of E_V for waxy corn starch.

5.3.2 Recommended Starch Viscosity Model for Waxy Corn Starch

A complete torque model from Eq. (22) with the estimated parameters for waxy corn starch from this study is presented below:

$$M(t) = 46.6 * \left[1 + 34.5\left(1 - e^{-3.2\psi}\right)^{0.62}\right] * \left[1 - 0.5\left(1 - e^{-0.0057\phi}\right)\right]$$

$$* e^{819\left(\frac{1}{T(t)} - \frac{1}{368.15}\right)} \qquad (27)$$

Where

$$\psi = \int_0^{t_f} \frac{T(t)}{300} e^{-138397\left(\frac{1}{T(t)} - \frac{1}{357.65}\right)} dt \qquad (28)$$

$$\phi = Nt = 100t \qquad (29)$$

The unit of the torque is mNmm, T(t) in Kelvin, and t in min. For estimation purposes, Ψ was divided by 300 to stabilize the sensitivity matrix. By having the ability to predict the torque value for waxy corn starch using Eq. (27), the apparent viscosity of a gelatinizing waxy corn starch solution can be predicted using Eq. (25) where the value of k″ is 61220 rad m^{-3} for Brookfield flag impeller (Briggs and Steffe 1996), and Ω is 10.47 rad/s used in this study.

Fig. 5.7 presents the observed apparent viscosity values from experimental mixer viscometer data and also the predicted apparent viscosity values from Eq. (6).

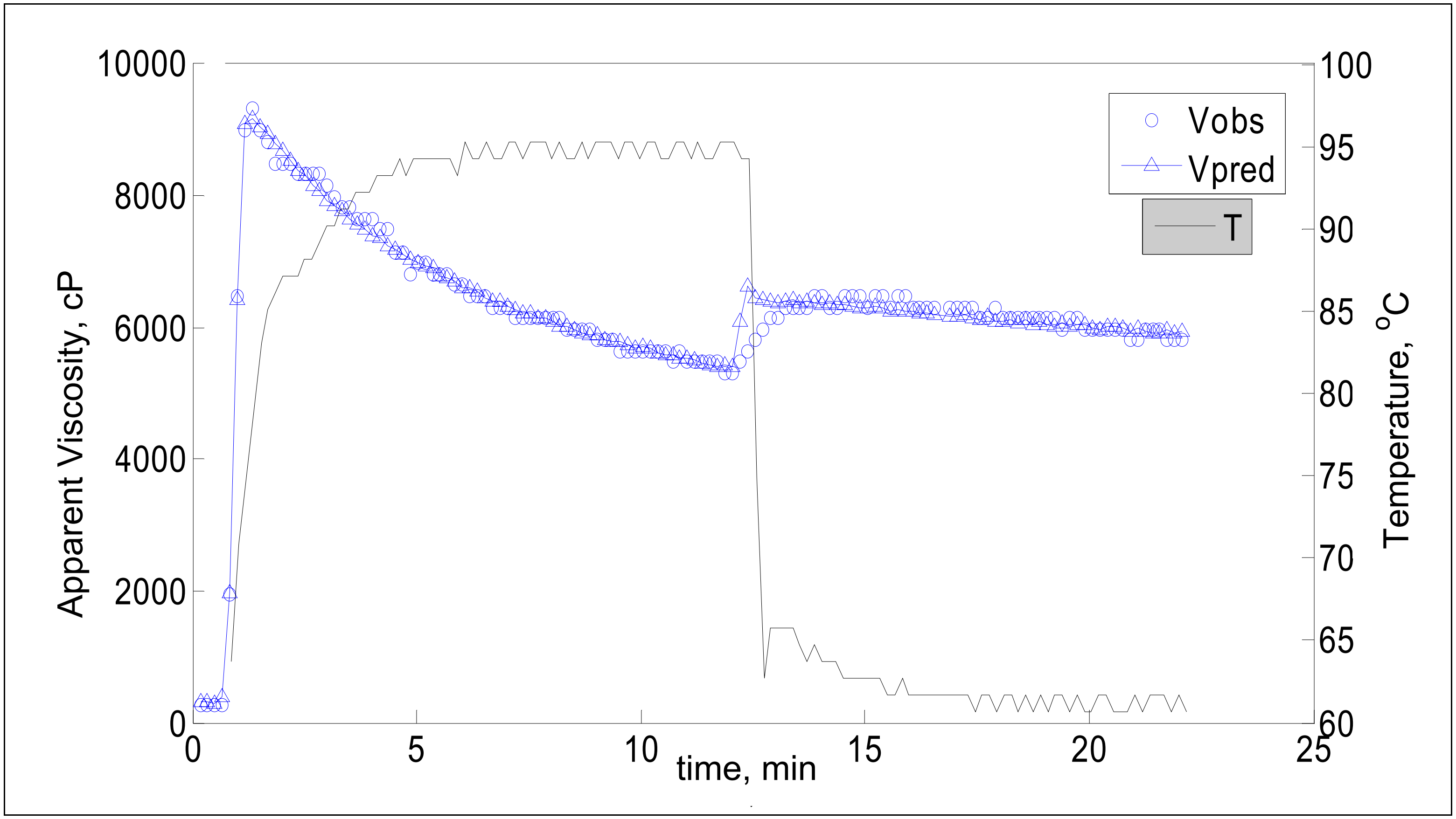

Figure. 5.7: Inverse problem plots of observed apparent viscosity from experimental predicted apparent viscosity from Eq. (5) versus time using data from modified Brookfield viscometer for native waxy corn starch at 6% w/w.

5.3.3 Application of the starch viscosity model on RVA data

The generic torque model for native waxy corn starch was applied to an independent set of data collected from a different instrument (RVA) for the same starch at same concentration. A forward problem to predict the RVA pasting curve was done by using Eq. (27). The only parameter value that needs to be changed is S because a different shear rate is involved in the RVA system. After the initial rapid impeller speed, the standard RVA profile uses an impeller speed of 160 rpm for the rest of the experiment. A new value of S (for 160 rpm) was calculated based on the known value of S (at 100rpm) from the inverse problem results obtained earlier:

$$S_{RVA} = S_{BF} * \left(\frac{N_{RVA}}{N_{BF}} \right)^{n} \tag{30}$$

The n value was obtained from an experiment conducted at different impeller speeds after the waxy corn starch sample was fully gelatinized. Fig. 5.8 shows the plot of apparent viscosity versus shear rate for the gelatinized waxy corn starch sample. The n value of approximately 1.38 was obtained by fitting the line to the non-Newtonian fluid power law model (Steffe 1996). Shear thickening behavior (n>1.0) has also been observed for other corn starch solutions (Dail and Steffe 1990b). The value of S for RVA was calculated as $46.6 \text{x}(1.6)^{1.38}$ = 89.13 mNmm.

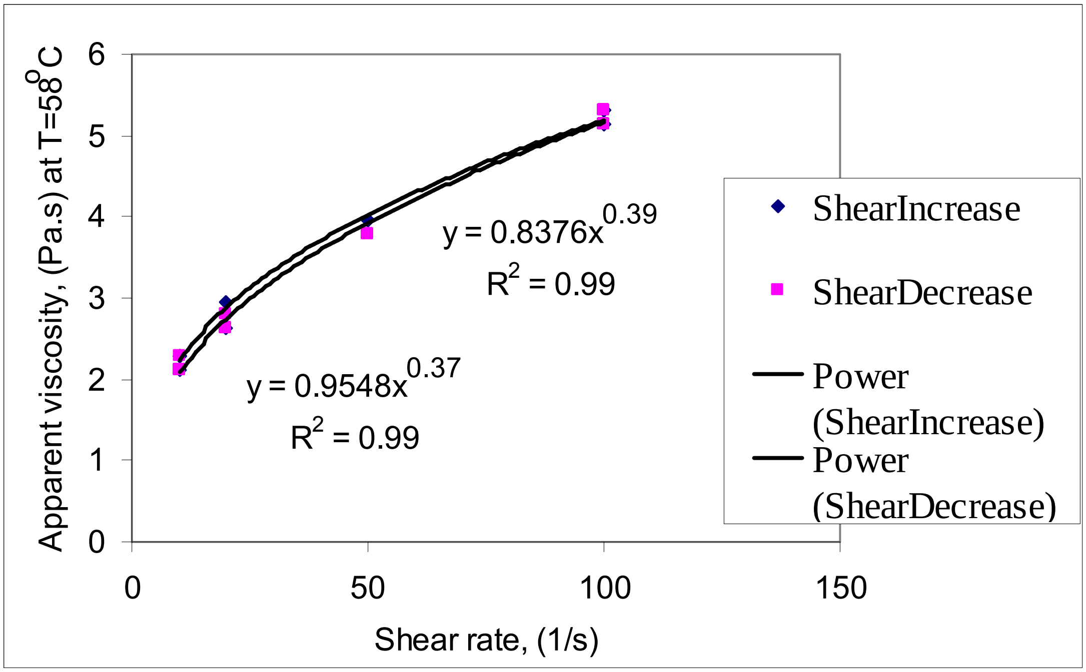

Figure 5.8. Plot of apparent viscosity versus shear rate showing a shear thickening behavior for waxy corn starch.

Incorporating the above results, Eq. (25) was used to predict the apparent viscosity. The value of k" for RVA used was 12570 rad m^{-3} (Lai et al. 2000) and Ω was 16.75 rad/s. Fig. 5.9 shows the RVA observed apparent viscosity values from experimental results, and the predicted values from Eq. (5) with S=89.13. A good prediction was observed. A perfect match was not expected due to the difference in actual sample temperature recorded by RVA, larger sample size (25g RVA versus 13g Brookfield), possible temperature gradient (Hazelton and Walker 1996), and insensitivity of the initial torque measurements for RVA. Variations in the observed viscosity profile (pasting curve) measured by modified Brookfield viscometer (Fig. 5.7) and the RVA (Fig. 5.9) for same waxy corn starch at same concentration are the result of these differences.

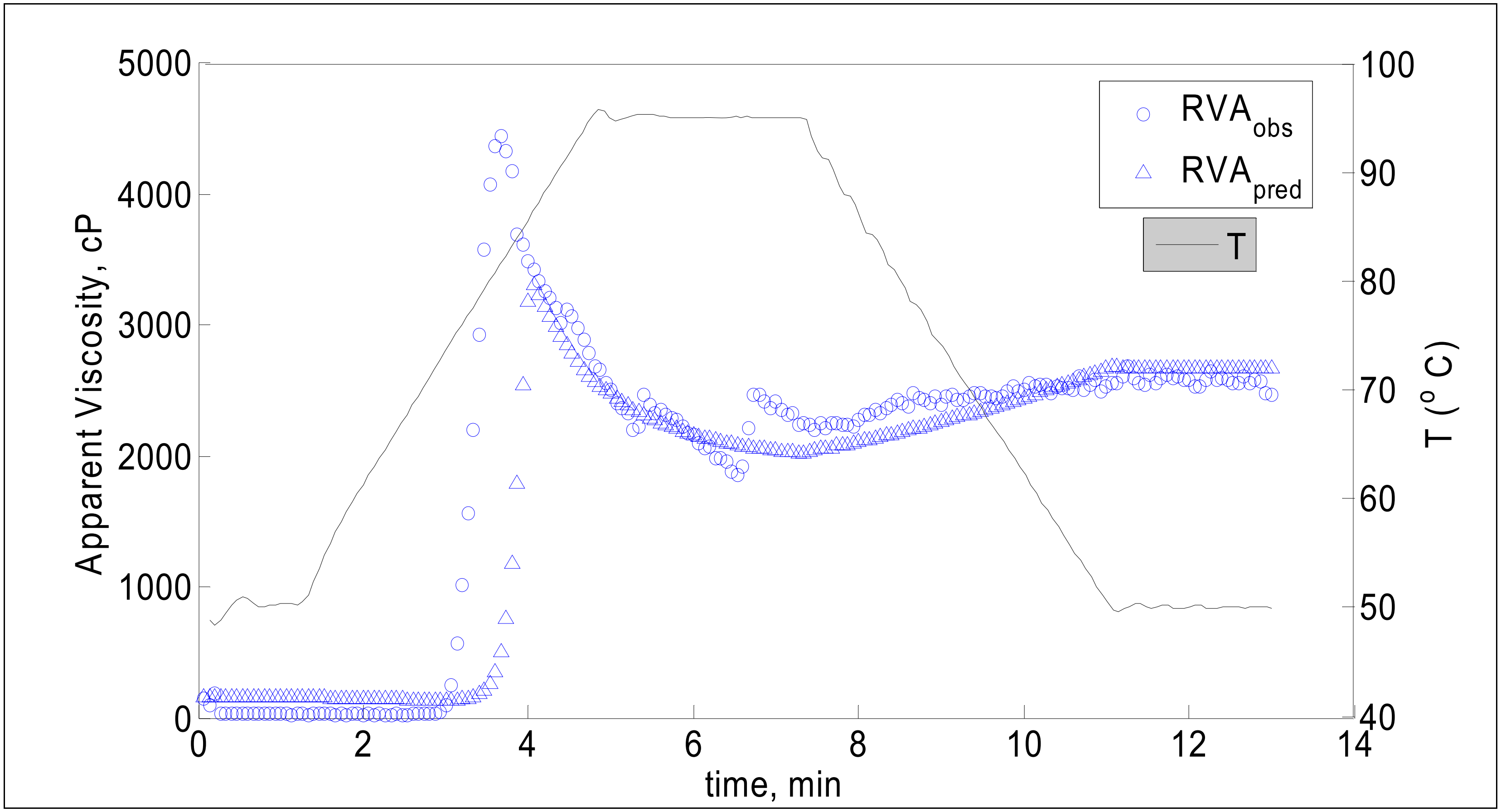

Figure 5.9. Plots of observed apparent viscosity versus time for experimental and predicted apparent viscosity (Eq. 5 with S=89.13) from waxy corn starch model using data from RVA for native waxy corn starch at 6%w/w.

5.3.4 Parameter Estimation for Corn Starch Blends

The estimated parameters using nlinfit for the rest of ten corn starch samples studied are tabulated in Table 5.3. The optimum gelatinization reference temperatures, RMSE, sum of squares of error of parameters are also shown in Table 5.3. The value of the gelatinization rate constant k_g found in this study ranges from 1.5 to 0.087 $(K\ min)^{-1}$. The gelatinization rate constant depends on gelatinization reference temperature (T_{rg}); hence, parameter k_g corrected ($k_{g,2}$) at T_{rg}=91^{o}C was calculated using Eq. (31) for normalizing k_g for comparison purposes. The value of the corrected k_g for all starch blends studied is shown in Table 5.4. Starch amylose content of samples for the assumed (calculated), and experimentally determined using the Con A method, were also tabulate in Table 5.4.

$$k_{g,2} = k_{g,1} * \exp\left[-\frac{E_g}{R}\left(\frac{1}{T_{rg,2}} - \frac{1}{T_{rg,1}}\right)\right] \quad (31)$$

Trends for parameters, and the gelatinization reference temperature, as function of the starch amylose content (assuming the remaining is the amylopectin content) are presented in Fig. 5.10 to Fig. 5.12. Among the parameters present in the starch viscosity model in Eq.(26), the gelatinization rate constant (k_g) was affected the most by the amylose to amylopectin ratios. The gelatinization rate constant was found empirically to increase as a power law function as starch amylose content decreased. As shown in Fig. 5.10. Empirical equations for E_g/R and T_{rg} are given in Fig. 5.11 and 5.12, respectively. The value of gelatinization activation energy E_g for corn starch blends ranges from 121 to 1169 kJ/mol, with a decreasing trend with increasing starch amylose content. Activation energy for waxy rice flour was reported in the range of 504 to 1550 kJ/mol (Lai and others 2002).

Although the empirical equation between gelatinization reference temperature and starch amylose content gave a low R^2, this empirical equation (Fig. 5.12) may help in giving a better prediction for T_{rg} when using the Arrhenius equation for gelatinizing starch solutions. In most cases, one can only use trial and error to guess the reference temperature value in the Arrhenius equation. The importance of reference temperature on the correlation between gelatinization parameters has been shown earlier in Fig. 5. Parameters A^{α}, B, E_v, and S were found to be in the range of 15.7 to 31.2, 0.25 to 0.61,1 to 5kJ/mol, and 31.3 to 50.7 mNmm min^n, respectively. The relative standard errors for the estimated parameters for each corn starch blend are given in Table 5.5. The relative standard errors for parameters k_g, E_g, and A^{α} were ≤10%. While for parameter B and E_v, the relative standard error was ≤13% and ≤19%, respectively.

Table 5.3 Estimated parameters, gelatinization reference temperature, and RMSE from OLS result for each corn starch blends

Parameters	Final Estimates from OLS for System 1		
	Waxy	*WN_10AM*	*Normal*
k_g	3.2±0.2	0.37±0.02	0.35±0.02
E_g (kJ/mol)	1169±95	252±18	964±39
A^{α}	34.5±0.2	29.4±0.5	25.8±2.8
B	0.53±0.01	0.45±0.02	0.65±0.02
E_v (kJ/mol)	7±0.25	5±0.4	0.53±0.17
S	46.6	46.0	64.7
T_{rg}	84.5	86.1	91.6
T_{rt}	95	95	95
RMSE	28.9	32.2	13.9

Table 5.4 Estimated parameters, gelatinization reference temperature, and RMSE from OLS result for each corn starch blends (cont'd)

Parameters	Final Estimates from OLS for System 2		
	WH5_10AM	*WH5_20AM*	*WH5_30AM*
k_g	0.99±0.08	0.13±0.01	0.06±0.006
E_g (kJ/mol)	468±49	121±8	185±12
A^{α}	24.5±0.3	30.3±1.5	27±1.9
B	0.3±0.02	0.61±0.03	0.55±0.025
E_v (kJ/mol)	2±0.35	5±0.54	4±0.37
S	45.8	45.2	44.5
T_{rg}	84.1	86.5	91.0
T_{rt}	95	95	95
RMSE	36.7	27.2	14.8

Table 5.5 Estimated parameters, gelatinization reference temperature, and RMSE from OLS result for each corn starch blends (cont'd)

Parameters	Final Estimates from OLS for System 3			
	WH7_10AM	*WH7_20AM*	*WH7_30AM*	*WH7_40AM*
k_g	1.52±0.1	0.88±0.06	0.29±0.02	0.087±0.008
E_g (kJ/mol)	621±58	308±31.5	150±12.4	174±12
A^{α}	23.3±0.25	31.2±0.52	20.4±0.84	17.2±1.3
B	0.32±0.01	0.25±0.02	0.38±0.04	0.39±0.05
E_v (kJ/mol)	3±0.3	2±0.38	3±0.47	4±0.45
S	45.6	31.3	45.0	44.3
T_{rg}	84.5	85.6	89.0	88.5
T_{rt}	95	95	95	95
RMSE	28.9	32.5	22.4	17.3

Table 5.6 Amylose content of starch blends determined experimentally, assumed (calculated) and corrected kg parameter

Samples	Experimental amylose, (%)	Assumed amylose, (%)	k_g, $(K\ min)^{-1}$ corrected at T_{rg}=91°C
Waxy	3.56	0	3580.310
Normal	13.63	20	0.340
WN_10AM	6.15	10	1.166
WHV_10AM	5.81	10	19.548
WHVII_10AM	9.27	10	63.226
WHV_20AM	13.98	20	0.214
WHVII_20AM	10.46	20	4.097
WHV_30AM	21.28	30	0.061
WHVII_30AM	19	30	0.378
WHVII_40AM	34.85	40	0.130

Table 5.7 Percentage relative standard error for parameters from OLS result for each corn starch blend

Parameters	%Relative Std. Error				
	WN_10AM	Normal	WHV_10AM	WHV_20AM	WHV_30AM
k_g, $(Kmin)^{-1}$	5.4	8.1	8.1	7.7	10.0
E_g ,(kJ/mol)	7.1	10.5	10.5	6.6	6.5
A^{α}	1.7	9.6	1.2	5.0	7.0
B	4.4	6.9	6.7	4.9	4.5
E_v ,(kJ/mol)	8.0	17.0	17.5	10.8	9.3

Table 5.8 Percentage relative standard error for parameters from OLS result for each corn starch blend (cont'd)

Parameters	%Relative Std. Error			
	WHVII_10AM	WHVII_20AM	WHVII_30AM	WHVII_40AM
k_g, $(Kmin)^{-1}$	6.6	6.8	6.9	9.2
E_g ,(kJ/mol)	9.3	10.2	8.3	6.9
A^{α}	1.1	1.7	4.1	7.6
B	3.1	8.0	10.5	12.8
E_v ,(kJ/mol)	10.0	19.0	15.7	11.3

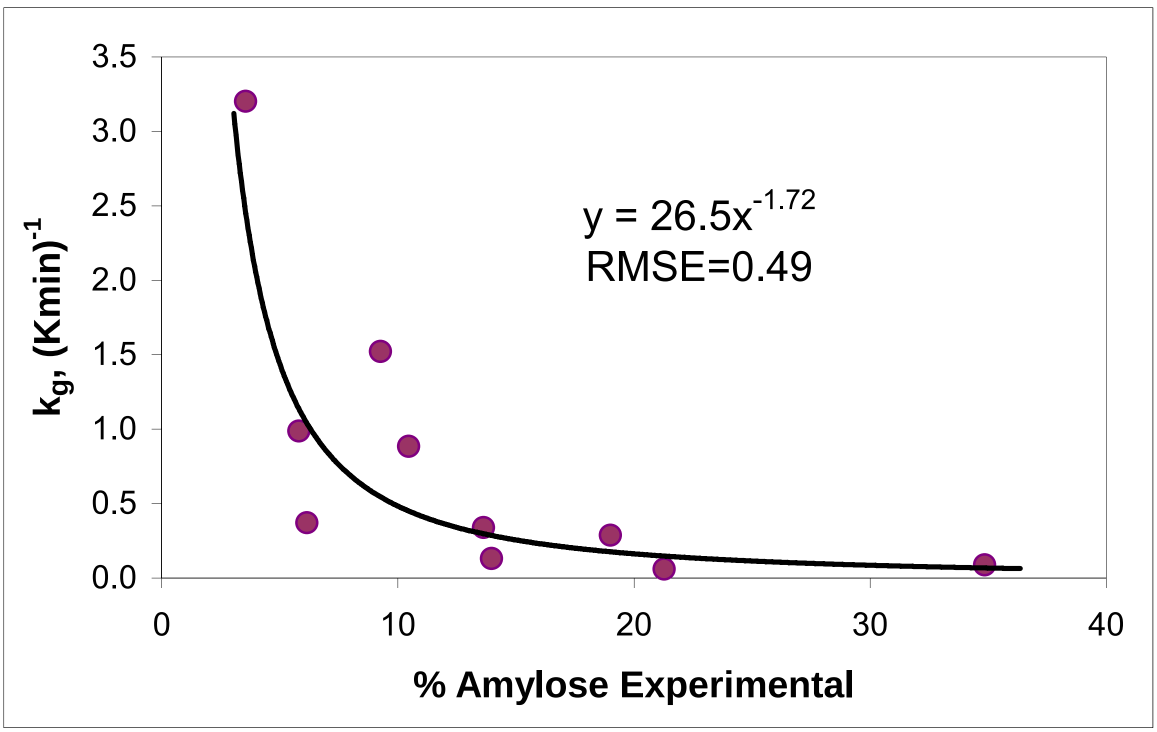

Figure 5.10. Parameter k_g as function of percentage starch amylose content.

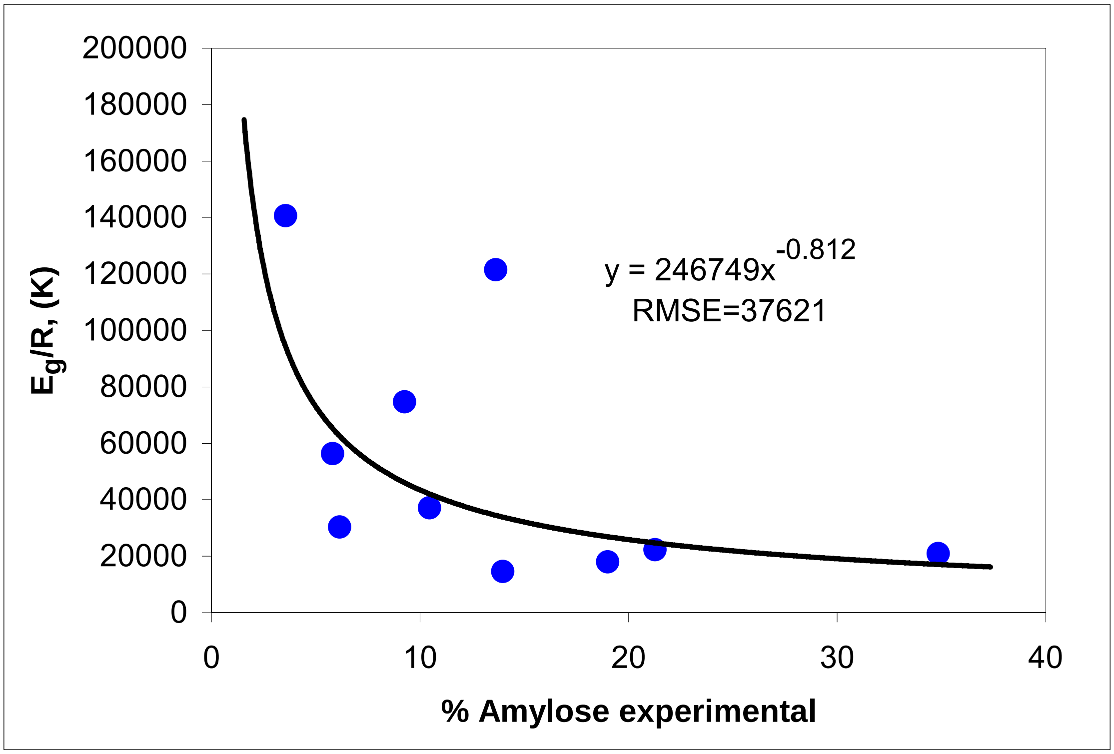

Figure 5.11. Parameter Eg/R as function of percentage starch amylose content.

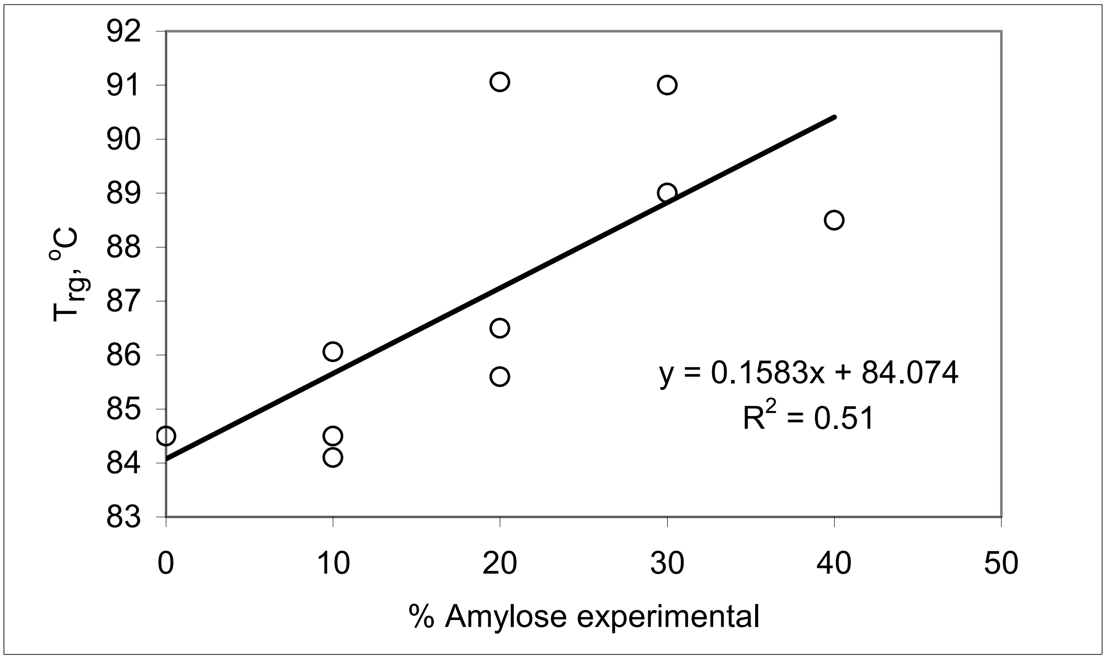

Figure 5.12. Arrhenius gelatinization reference temperature as function of percentage starch amylose content.

5.4 Conclusions

This study proposed a predictive starch viscosity model for waxy corn starch and applied it in two different systems. It is the first to simultaneously estimate the parameters present in a starch viscosity model at different starch amylose to amylopectin ratios. This study also is the first to show that the gelatinization rate constant and activation energy of gelatinization dramatically increases with decreasing amylose present in the starch, especially at lower amylose contents.

5.5 Nomenclature

A^{α}	relative increase in apparent viscosity, dimensionless
AM	amylose
AP	amylopectin
B	relative decrease in apparent viscosity, dimensionless
BF	Brookfield viscometer
CON A	concavalin A
E_v	viscous activation energy, kJ/mol
E_g	gelatinization activation energy, kJ/mol
d	shear-decay rate parameter
k_g	gelatinization rate constant, $(Kmin)^{-1}$
K_r	pseudo consistency coefficient, Nm min^n

M	torque, mNmm
N	speed, rpm
RMSE	root mean square error
RTD	resistance temperature detector
RVA	rapid visco analyzer
S	parameter combines shear rate and concentration, mNmm min^n
SS	sum square of error
t	time, min
t_f	time when the experiment ends, min
T	temperature, K
T_{rg}	gelatinization reference temperature on Arrhenius model, K
T_{rt}	reference temperature on Arrhenius model for temperature term, K
α	dimensionless parameter
ψ	time-temperature history, (Kmin)
ϕ	shear history, rpm min

APPENDICES

Appendix C1

Table C.1 Waxy corn starch data from mixer viscometer

Time(s)	T (^{o}C)	η ,(Pa.s) calculated	Torque (Nm)
10.207	63.704	0.279767	4.78615E-05
20.242	70.832	0.279767	4.78615E-05
30.278	74.905	0.279767	4.78615E-05
40.313	78.978	0.279767	4.78615E-05
50.333	83.051	1.954946	0.000334445
60.368	85.087	6.47793	0.001108221
70.403	86.105	8.990699	0.001538097
80.438	87.124	9.325735	0.001595414
90.458	87.124	8.990699	0.001538097
100.49	87.124	8.823181	0.001509438
110.53	88.142	8.488145	0.001452122
120.56	88.142	8.488145	0.001452122
130.58	89.16	8.488145	0.001452122
140.62	90.178	8.320628	0.001423463
150.65	90.178	8.320628	0.001423463
160.69	91.197	8.320628	0.001423463
170.71	91.197	8.320628	0.001423463
180.75	92.215	8.15311	0.001394805
190.79	92.215	7.985592	0.001366147
200.83	92.215	7.818074	0.001337488
210.86	93.233	7.818074	0.001337488
220.88	93.233	7.650556	0.00130883
230.92	93.233	7.650556	0.00130883
240.96	94.251	7.650556	0.00130883
251	93.233	7.483038	0.001280172
261.04	94.251	7.483038	0.001280172
271.06	94.251	7.148002	0.001222855
281.1	94.251	7.148002	0.001222855
291.13	94.251	6.812966	0.001165538
301.17	94.251	6.980484	0.001194196
311.21	94.251	6.980484	0.001194196
321.23	93.233	6.812966	0.001165538
331.27	95.27	6.812966	0.001165538
341.31	94.251	6.812966	0.001165538
351.35	94.251	6.645448	0.00113688

361.37	95.27	6.645448	0.00113688
371.41	94.251	6.47793	0.001108221
381.45	94.251	6.47793	0.001108221
391.48	95.27	6.47793	0.001108221
401.52	95.27	6.310412	0.001079563
411.54	94.251	6.310412	0.001079563
421.58	95.27	6.310412	0.001079563
431.62	95.27	6.142894	0.001050904
441.66	95.27	6.142894	0.001050904
451.68	94.251	6.142894	0.001050904
461.72	95.27	6.142894	0.001050904
471.76	94.251	6.142894	0.001050904
481.79	94.251	6.142894	0.001050904
491.82	95.27	6.142894	0.001050904
501.85	94.251	5.975377	0.001022246
511.89	95.27	5.975377	0.001022246
521.93	95.27	5.975377	0.001022246
531.97	95.27	5.975377	0.001022246
541.99	94.251	5.807859	0.000993588
552.03	95.27	5.807859	0.000993588
562.07	95.27	5.807859	0.000993588
572.11	94.251	5.640341	0.000964929
582.13	95.27	5.640341	0.000964929
592.17	95.27	5.640341	0.000964929
602.21	94.251	5.640341	0.000964929
612.24	94.251	5.640341	0.000964929
622.28	95.27	5.640341	0.000964929
632.31	95.27	5.640341	0.000964929
642.34	94.251	5.472823	0.000936271
652.38	95.27	5.640341	0.000964929
662.42	94.251	5.472823	0.000936271
672.45	94.251	5.472823	0.000936271
682.48	95.27	5.472823	0.000936271
692.52	95.27	5.472823	0.000936271
702.56	95.27	5.472823	0.000936271
712.58	94.251	5.305305	0.000907613
722.62	94.251	5.305305	0.000907613
732.66	74.905	5.472823	0.000936271
742.7	62.686	5.640341	0.000964929
752.72	65.741	5.807859	0.000993588
762.76	65.741	5.975377	0.001022246

Table C.1 (cont’d)

772.8	65.741	6.142894	0.001050904
782.84	65.741	6.142894	0.001050904
792.88	64.722	6.310412	0.001079563
802.92	63.704	6.310412	0.001079563
812.94	64.722	6.310412	0.001079563
822.98	63.704	6.310412	0.001079563
833.02	63.704	6.47793	0.001108221
843.06	63.704	6.47793	0.001108221
853.1	62.686	6.310412	0.001079563
863.12	62.686	6.310412	0.001079563
873.16	62.686	6.47793	0.001108221
883.2	62.686	6.47793	0.001108221
893.23	62.686	6.47793	0.001108221
903.26	62.686	6.310412	0.001079563
913.3	61.668	6.47793	0.001108221
923.34	61.668	6.47793	0.001108221
933.37	62.686	6.310412	0.001079563
943.4	61.668	6.47793	0.001108221
953.44	61.668	6.47793	0.001108221
963.48	61.668	6.310412	0.001079563
973.51	61.668	6.310412	0.001079563
983.55	61.668	6.310412	0.001079563
993.58	61.668	6.310412	0.001079563
1013.7	61.668	6.310412	0.001079563
1023.7	61.668	6.310412	0.001079563
1033.7	60.65	6.310412	0.001079563
1043.8	61.668	6.310412	0.001079563
1053.8	61.668	6.142894	0.001050904
1063.8	60.65	6.142894	0.001050904
1073.9	61.668	6.310412	0.001079563
1083.9	61.668	6.142894	0.001050904
1093.9	60.65	6.142894	0.001050904
1104	61.668	6.142894	0.001050904
1114	60.65	6.142894	0.001050904
1124	61.668	6.142894	0.001050904
1134.1	60.65	6.142894	0.001050904
1144.1	61.668	6.142894	0.001050904
1154.1	61.668	6.142894	0.001050904
1164.2	60.65	5.975377	0.001022246
1174.2	61.668	6.142894	0.001050904

Table C.1 (cont'd)

1184.3	60.65	6.142894	0.001050904
1194.3	60.65	5.975377	0.001022246
1204.3	61.668	5.975377	0.001022246
1214.4	61.668	5.975377	0.001022246
1224.4	60.65	5.975377	0.001022246
1234.4	60.65	5.975377	0.001022246
1244.5	60.65	5.975377	0.001022246
1254.5	61.668	5.807859	0.000993588
1264.5	60.65	5.807859	0.000993588
1274.6	61.668	5.975377	0.001022246
1284.6	61.668	5.975377	0.001022246
1294.6	61.668	5.975377	0.001022246
1304.7	60.65	5.807859	0.000993588
1314.7	61.668	5.807859	0.000993588
1324.7	60.65	5.807859	0.000993588

Appendix C2

Table C.2 RVA waxy corn starch data

Waxy, rep 1 | Waxy, rep 2

Time(s)	Visc	T (^{o}C)	N(rpm)	Time(s)	Visc(cP)	T(^{o}C)	N(rpm)
4	147	48.85	960	4	135	48.85	960
8	97	48.4	960	8	97	48.3	960
12	184	48.75	160	12	194	48.65	160
16	32	49.5	160	16	51	49.5	160
20	34	50.15	160	20	51	50.3	160
24	35	50.65	160	24	57	50.8	160
28	31	50.9	160	28	52	51	160
32	28	50.75	160	32	51	50.65	160
36	37	50.3	160	36	53	50.35	160
40	30	50	160	40	49	50.2	160
44	32	50	160	44	49	50.2	160
48	30	50.15	160	48	51	50.2	160
52	32	50.2	160	52	51	50.35	160
56	30	50.35	160	56	51	50.25	160
60	30	50.35	160	60	51	50.1	160
64	31	50.3	160	64	46	49.95	160
68	25	50.15	160	68	47	50.15	160
72	28	50.5	160	72	46	50.6	160
76	26	51.2	160	76	45	51.4	160
80	25	52.35	160	80	43	52.55	160
84	28	53.6	160	84	41	53.7	160
88	26	54.75	160	88	42	54.85	160
92	28	55.85	160	92	45	55.95	160
96	29	56.95	160	96	45	56.9	160
100	25	57.95	160	100	42	57.85	160
104	26	58.8	160	104	44	58.75	160
108	22	59.65	160	108	40	59.6	160
112	27	60.5	160	112	44	60.45	160
116	27	61.3	160	116	41	61.3	160
120	24	62.1	160	120	41	62.15	160
124	26	62.9	160	124	38	62.9	160
128	25	63.7	160	128	38	63.75	160
132	28	64.5	160	132	40	64.55	160
136	25	65.3	160	136	36	65.35	160
140	23	66.1	160	140	43	66.1	160
144	27	66.95	160	144	37	66.9	160

Table C.2 (cont'd)

148	25	67.75	160	148	41	67.8	160
152	22	68.55	160	152	40	68.55	160
156	26	69.4	160	156	42	69.4	160
160	27	70.15	160	160	42	70.25	160
164	28	71.1	160	164	39	71.05	160
168	26	71.9	160	168	44	71.85	160
172	34	72.75	160	172	44	72.7	160
176	45	73.6	160	176	51	73.5	160
180	101	74.45	160	180	91	74.4	160
184	252	75.25	160	184	198	75.3	160
188	567	75.95	160	188	461	76	160
192	1010	76.8	160	192	852	76.75	160
196	1558	77.5	160	196	1345	77.55	160
200	2206	78.3	160	200	1937	78.3	160
204	2924	79.15	160	204	2604	79.1	160
208	3572	79.95	160	208	3301	79.9	160
212	4076	80.7	160	212	3829	80.75	160
216	4364	81.5	160	216	4205	81.55	160
220	4445	82.25	160	220	4380	82.3	160
224	4330	83.05	160	224	4365	83.15	160
228	4179	83.9	160	228	4299	83.9	160
232	3698	84.65	160	232	4162	84.7	160
236	3613	85.45	160	236	3952	85.55	160
240	3484	86.35	160	240	3662	86.35	160
244	3423	87.15	160	244	3544	87.2	160
248	3340	88.05	160	248	3482	88.05	160
252	3261	88.85	160	252	3442	88.85	160
256	3206	89.65	160	256	3427	89.6	160
260	3137	90.5	160	260	3333	90.45	160
264	3020	91.25	160	264	3329	91.3	160
268	3115	92.05	160	268	3349	92.05	160
272	3071	92.9	160	272	3375	92.85	160
276	2979	93.7	160	276	3100	93.7	160
280	2885	94.5	160	280	3047	94.5	160
284	2784	95.25	160	284	2977	95.3	160
288	2691	95.85	160	288	2867	95.85	160
292	2655	95.65	160	292	2789	95.8	160
296	2555	95	160	296	2742	95.15	160
300	2501	94.75	160	300	2700	94.9	160
304	2406	94.8	160	304	2604	94.95	160
308	2370	94.95	160	308	2521	95	160
312	2324	95.2	160	312	2499	95.1	160

Table C.2 (cont'd)

316	2205	95.3	160	316	2450	95.2	160
320	2220	95.35	160	320	2379	95.25	160
324	2463	95.25	160	324	2328	95.25	160
328	2391	95.25	160	328	2301	95.25	160
332	2327	95.2	160	332	2655	95.15	160
336	2353	95.1	160	336	2804	95.1	160
340	2319	95.05	160	340	2776	95	160
344	2292	94.95	160	344	2705	95	160
348	2279	95	160	348	2726	95	160
352	2231	95	160	352	2610	95	160
356	2179	95.05	160	356	2539	95	160
360	2165	95.05	160	360	2475	95	160
364	2095	95	160	364	2476	95	160
368	2064	95.05	160	368	2413	95	160
372	2078	95	160	372	2385	95.05	160
376	1981	95	160	376	2330	95.1	160
380	1988	95	160	380	2293	95.1	160
384	1963	95.05	160	384	2312	95.05	160
388	1886	95.1	160	388	2231	95	160
392	1855	95	160	392	2227	95.1	160
396	1924	95.1	160	396	2187	95.05	160
400	2219	95.05	160	400	2203	95.05	160
404	2466	95	160	404	2169	95	160
408	2473	95.05	160	408	2130	95.05	160
412	2417	95	160	412	2084	95	160
416	2369	94.95	160	416	2040	95.05	160
420	2416	94.95	160	420	2062	95.05	160
424	2356	95	160	424	2032	95	160
428	2309	95	160	428	1968	95	160
432	2323	95	160	432	1941	95	160
436	2238	95.05	160	436	1956	95.05	160
440	2254	94.8	160	440	1888	95	160
444	2235	93.35	160	444	1927	93.65	160
448	2194	91.9	160	448	1933	91.85	160
452	2257	91.35	160	452	1939	91	160
456	2213	91.25	160	456	1947	90.9	160
460	2251	90.2	160	460	1973	90.25	160
464	2246	88.75	160	464	2008	88.95	160
468	2241	87.9	160	468	1987	87.9	160
472	2241	87.8	160	472	2023	87.6	160
476	2231	87.05	160	476	2034	86.8	160
480	2280	85.55	160	480	2071	85.6	160

Table C.2 (cont'd)

484	2309	84.45	160	484	2116	84.95	160
488	2311	84.2	160	488	2096	84.45	160
492	2348	83.85	160	492	2103	83.3	160
496	2327	82.7	160	496	2153	82.15	160
500	2372	81.5	160	500	2112	81.55	160
504	2396	81	160	504	2150	81.3	160
508	2430	80.35	160	508	2206	80.3	160
512	2407	79.3	160	512	2214	79.15	160
516	2373	78.2	160	516	2203	78.35	160
520	2478	77.75	160	520	2230	78.05	160
524	2439	77.35	160	524	2223	77.25	160
528	2428	76.3	160	528	2312	76.05	160
532	2406	75.1	160	532	2257	75.05	160
536	2449	74.45	160	536	2298	74.5	160
540	2397	74	160	540	2287	74.05	160
544	2456	73.1	160	544	2348	73.1	160
548	2472	72.15	160	548	2392	72.15	160
552	2434	71.25	160	552	2332	71.35	160
556	2432	70.55	160	556	2328	70.5	160
560	2453	69.85	160	560	2410	69.85	160
564	2487	69.1	160	564	2389	69.1	160
568	2486	68.25	160	568	2379	68.35	160
572	2457	67.45	160	572	2360	67.55	160
576	2461	66.7	160	576	2451	66.75	160
580	2443	65.95	160	580	2422	66.05	160
584	2455	65.2	160	584	2414	65.25	160
588	2499	64.45	160	588	2426	64.4	160
592	2536	63.65	160	592	2449	63.7	160
596	2499	62.9	160	596	2412	62.85	160
600	2503	62.1	160	600	2467	62.1	160
604	2554	61.3	160	604	2464	61.35	160
608	2534	60.45	160	608	2517	60.4	160
612	2546	59.6	160	612	2475	59.7	160
616	2545	58.95	160	616	2364	58.95	160
620	2478	58.2	160	620	2527	58.15	160
624	2529	57.4	160	624	2600	57.35	160
628	2523	56.65	160	628	2552	56.55	160
632	2515	55.8	160	632	2479	55.85	160
636	2509	55	160	636	2474	55.05	160
640	2610	54.35	160	640	2519	54.3	160
644	2504	53.55	160	644	2541	53.5	160
648	2544	52.8	160	648	2472	52.8	160

Table C.2 (cont'd)

652	2577	51.95	160	652	2480	51.95	160
656	2499	51.2	160	656	2474	51.15	160
660	2534	50.45	160	660	2477	50.35	160
664	2557	49.8	160	664	2479	49.85	160
668	2556	49.6	160	668	2517	49.8	160
672	2604	49.85	160	672	2517	49.95	160
676	2681	50.1	160	676	2553	50.2	160
680	2596	50.35	160	680	2573	50.3	160
684	2552	50.3	160	684	2561	50.15	160
688	2542	50	160	688	2498	50	160
692	2620	49.9	160	692	2441	49.95	160
696	2563	50	160	696	2446	50	160
700	2597	50.15	160	700	2559	50.15	160
704	2626	50.2	160	704	2522	50.15	160
708	2590	49.95	160	708	2588	49.95	160
712	2603	49.9	160	712	2573	49.9	160
716	2589	49.95	160	716	2558	50.05	160
720	2583	50	160	720	2513	50.1	160
724	2530	50.15	160	724	2533	50.05	160
728	2528	50.15	160	728	2496	49.9	160
732	2577	49.95	160	732	2510	49.75	160
736	2647	49.9	160	736	2517	49.9	160
740	2586	49.9	160	740	2451	49.95	160
744	2602	50	160	744	2520	50.05	160
748	2578	50.1	160	748	2569	50.2	160
752	2555	50.1	160	752	2618	50	160
756	2560	50	160	756	2497	49.9	160
760	2613	49.95	160	760	2488	49.95	160
764	2552	50	160	764	2509	50.05	160
768	2578	50.05	160	768	2508	50.1	160
772	2568	50.1	160	772	2461	50	160
776	2475	50.1	160	776	2423	49.95	160
780	2472	49.95	160	780	2446	49.95	160

Appendix C3

Example of Matlab syntax

Waxy: Inverse Problem

Nlinfit: Mother file: starch_test_waxy_0AM

```
%%Initial estimate
clear all
global Tr
%  global Tr ind
format long
tfact=60;% unit conversion to get in s,

beta0(1)=tfact*(0.005);%kg at Tr

beta0(2)=5*1e3;%Eg/R

beta0(3)=23.3; %A^alpha
beta0(4)=0.1;
beta0(5)=189;
% beta0(6)=45;

beta0=beta0';

Tr=84.5+273.15;%5parameters from Tr files

% Tr=91.06+273.15;
data=xlsread('waxy.xls');

t=data(:,1)/tfact;%time in min
T=data(:,2)+273.15;
yobs=data(:,4)*1e6;%torque in mN-mm

% index=find(yobs>3*yobs(1));%find y when it starts to gelatinize, to use in SH term
later
% ind=index(1);%the first point Y where starch about to gelatinize

tT=t;
tT(:,2)=T;

%%inverse problem
[beta,resids,J,COVB,mse] = nlinfit(tT, yobs,'st_torque_waxy_0AM', beta0);
rmse=sqrt(Ahmt et al.); %mean square error = SS/(n-p)
```

```
SS=resids'*resids;
%%R is the correlation matrix for the parameters, sigma is the standard error vector
[R,sigma]=corrcov(COVB);
relsterr=sigma./beta;
%confidence intervals for parameters
ci=nlparci(beta,resids,J);

%%forward problem
ypred=st_torque_waxy_0AM(beta,tT);
figure
set(gca, 'fontsize',14,'fontweight','bold');
plot(t*tfact/60,ypred,'--',t*tfact/60,yobs,'or')
legend('ypred','yobs')
xlabel('time (min)','fontsize',14);ylabel('M (mNmm)','fontsize',14)


%break
%%scaled sensitivity coefficients

Xp(:,1)=beta(1)*J(:,1);%Xp mean Xprime which mean scaled sensitivity coeff. J is the
jacobian or known as the sensitivity coefficient
Xp(:,2)=beta(2)*J(:,2);
Xp(:,3)=beta(3)*J(:,3);
Xp(:,4)=beta(4)*J(:,4);
Xp(:,5)=beta(5)*J(:,5);
% Xp(:,6)=beta(6)*J(:,6);

figure
hold on
h(1)=plot(t*tfact/60,Xp(:,1),'ok');
h(2)=plot(t*tfact/60,Xp(:,2),'sb');
h(3)=plot(t*tfact/60,Xp(:,3),'^g');
h(4)=plot(t*tfact/60,Xp(:,4),'pr');
h(5)=plot(t*tfact/60,Xp(:,5),'dm');
% h(6)=plot(t*tfact/60,Xp(:,6),'m');

legend(h,'X''k_g','X''E_g /R','X''A^{\alpha}','X''B','X''E_v /R')%**********

xlabel('time (min)','fontsize',14); ylabel('scaled sens coeffs','fontsize',14)
set(gca, 'fontsize',14,'fontweight','bold');% increases font size of the plot axes

%%residuals histogram
[n1, xout] = hist(resids,10);
 figure
 hold on
 set(gca, 'fontsize',14,'fontweight','bold');
```

```
 bar(xout, n1) % plots the histogram
 xlabel('M_{observed} - M_{predicted}','fontsize',16,'fontweight','bold')
 ylabel('Frequency','fontsize',16,'fontweight','bold')

 %%residuals scatter
 figure
 hold on
 set(gca, 'fontsize',14,'fontweight','bold');
 plot(t*tfact/60, resids, 'square', 'Markerfacecolor', 'k', 'markeredgecolor','k',
'markersize',10)
 plot([0,max(t)*tfact/60],[0,0], 'k')
 ylabel('M_{observed} - M_{predicted}','fontsize',16,'fontweight','bold')
 xlabel('heating time (min)','fontsize',16,'fontweight','bold')
```

Function file: st_torque_waxy_0AM

```
function M = st_torque_waxy_0AM( b,X )% M is the dependent value, b is the
parameter, and the X is the independent variable.
global Tr
% global Tr ind
%%computes psi(t) given time-temperature history
%  t is a nx1 vector of time (Haase et al.)
%X independent variables column 1 is time, column2 T (K)
% T is nx1 vector of temperature (C)
%Tr is a scalar (C)

t=X(:,1);
T=X(:,2);
N=100;%rev/min

intgrnd = (T).*exp(-(b(2))*((1./T)-(1./Tr)));
psi=cumtrapz(t,intgrnd);

%ind is the index of tSH% %tSH is time where shear history begins
% n=length(t);
%  tSH=t;
%
% SH=ones(n,1);
%
% SH(ind:n)= 1-b(4)*(1-exp(-0.0057*(t(ind:n)-tSH)*N));
%
% %Torque Model
% M=(46.6*(1+b(3)*(1-exp(-b(1)*(psi/300))).^0.6235)).*SH.*(exp(b(5)*(1./T-
1/(95+273.15))));
```

```
M=(46.6.*(1+b(3)*(1-exp(-b(1)*(psi/300))).^0.6235)).*(1-b(4)*(1-exp(-
0.0015*N*t))).*(exp(b(5)*((1./T)-(1/(95+273.15)))));
end
```

Sequential file: Sequential_waxy_0AM

```
% clear all
clc

%-------------------------------------
set(0,'defaultaxesfontsize',16);

tol=1e-3;
xvals=tT;

yvals=yobs;

%%Initial estimate

beta=[tfact*(0.005);5*1e3;23.3;0.1;189];
%---------------------------------------------------------------
Y = yvals;
sX = [length(yvals) length(beta)];

sig = .1*ones(sX(1),1);

Ratio1 = 1; Ratio2 = 1; Ratio3= 1; Ratio4= 1; Ratio5 =1;   %need one Ratio per
parameter , %*************

plots=0;
clear betain X1 A delta K BBbP b SeqBeta
b_old =beta ;

figure
hold on
while Ratio1 > tol || Ratio2 > tol || Ratio3 > tol|| Ratio4 > tol || Ratio5 > tol%********
   P = 100^1*eye(sX(2));
   b0 = b_old;
   beta = b0;

     ypred = st_torque_waxy_0AM(beta,tT);%***

   e = yvals-ypred;
```

```
    %----------------------------------------
   d=0.0001;
   for i = 1:length(beta)
      betain = beta;
      betain(i) = beta(i)+beta(i)*d;
%
        yhat{i}=st_torque_waxy_0AM(betain,tT);%***********
%
      X{i} = (yhat{i}-ypred)/(beta(i)*d); %sensitivity coeff cell array
   end
  for k = 1:sX(1)
   if k == 1
      b = b0;
   end
   clear A delta
      X1 = [X{:,1} X{:,2} X{:,3} X{:,4} X{:,5}];%pull out sens coeff from cell array
%*******
      A(:,k) = P*X1(k,:)';
      delta(k) = sig(k)^2+X1(k,:)*A(:,k);
      K(:,k) = A(:,k)/delta(k);
      b = b + K(:,k)*(e(k)-X1(k,:)*(b-b0));
      P = P - K(:,k)*A(:,k)';
      BBbP{k} = [b P];
%
  end


h2(1)=plot(plots,b_old(1),'s','MarkerEdgeColor','k','MarkerFaceColor','r','MarkerSize',5);

%h2(2)=plot(plots,b_old(2)/5e4,'s','MarkerEdgeColor','k','MarkerFaceColor','g','MarkerSize',5);

h2(2)=plot(plots,b_old(2),'s','MarkerEdgeColor','k','MarkerFaceColor','b','MarkerSize',5);

h2(3)=plot(plots,b_old(3),'s','MarkerEdgeColor','k','MarkerFaceColor','c','MarkerSize',5);
%***********

h2(4)=plot(plots,b_old(4),'s','MarkerEdgeColor','k','MarkerFaceColor','c','MarkerSize',5);
%***********

h2(5)=plot(plots,b_old(5),'s','MarkerEdgeColor','k','MarkerFaceColor','c','MarkerSize',5);
%***********
%
h2(6)=plot(plots,b_old(6),'s','MarkerEdgeColor','k','MarkerFaceColor','c','MarkerSize',5);
%***********
```

```
    xlabel('Iteration','FontSize',15,'fontweight','bold');
    ylabel('Sequentially Estimated Parameters','FontSize',15,'fontweight','bold');
    b_new = BBbP{end};
    plots = plots+1;
    Ratioall = abs((b_new(:,1)-b_old)./b_old);
    Ratio1 = Ratioall(1);
    Ratio2 = Ratioall(2);
    Ratio3 = Ratioall(3);
    Ratio4 = Ratioall(4);
    Ratio5 = Ratioall(5);
%     Ratio6 = Ratioall(6);

    b_old = b_new(:,1);

end

%legend(h2,'k_g','E_g /R','A^\alpha', 'B', 'E_v \R')
legend('k_g','E_g /R','A^\alpha', 'B', 'E_v \R')
covmat = P;
corrcoef = covmat(2,1)/(sqrt(covmat(1,1))*sqrt(covmat(2,2)));


Result = BBbP{end};


hold off

for i = 1:length(BBbP)
   BB = BBbP{i};
   SeqBeta(:,i) = BB(:,1);
end



set(gca, 'fontsize',14,'fontweight','bold');
figure
hold on

h3(1) =
plot(xvals(:,1),SeqBeta(1,:),'^','MarkerEdgeColor','b','MarkerFaceColor','r','MarkerSize',1
0);

xlabel('time (min)','FontSize',16,'fontweight','bold');
ylabel('k_g (Kmin)^-1','FontSize',16,'fontweight','bold');

set(gca, 'fontsize',14,'fontweight','bold');
```

```
figure
hold on

h4(1) =
plot(xvals(:,1),SeqBeta(2,:),'^','MarkerEdgeColor','b','MarkerFaceColor','r','MarkerSize',1
0);

xlabel('time (min)','FontSize',16,'fontweight','bold');
ylabel('E_g /R (K)','FontSize',16,'fontweight','bold');

set(gca, 'fontsize',14,'fontweight','bold');
figure
hold on

h5(1) =
plot(xvals(:,1),SeqBeta(3,:),'^','MarkerEdgeColor','b','MarkerFaceColor','r','MarkerSize',1
0);

xlabel('time (min)','FontSize',16,'fontweight','bold');
ylabel('A^\alpha (dimensionless)','FontSize',16,'fontweight','bold');


set(gca, 'fontsize',14,'fontweight','bold');
figure
hold on
h6(1) =
plot(xvals(:,1),SeqBeta(4,:),'^','MarkerEdgeColor','b','MarkerFaceColor','r','MarkerSize',1
0);%*****
xlabel('time (min)','FontSize',16,'fontweight','bold');
ylabel('B (dimensionless)','FontSize',16,'fontweight','bold');

set(gca, 'fontsize',14,'fontweight','bold');
figure
hold on
h7(1) =
plot(xvals(:,1),SeqBeta(5,:),'^','MarkerEdgeColor','b','MarkerFaceColor','r','MarkerSize',1
0);%*****
xlabel('time (min)','FontSize',16,'fontweight','bold');
ylabel('E_v /R (K)','FontSize',16,'fontweight','bold');
```

Appendix C4

Matlab figures: OLS results for corn starch blends

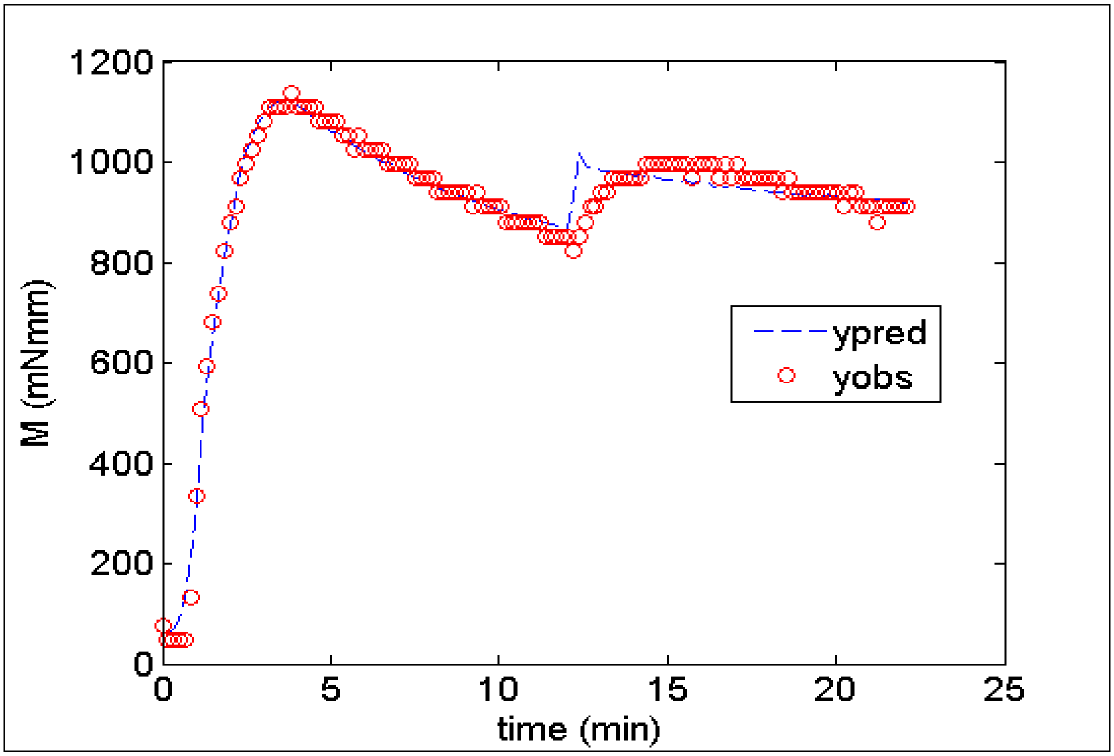

Figure C4.1. Observed and predicted torque for waxy and normal corn starch blends at assumed 10%AM (WN_10AM).

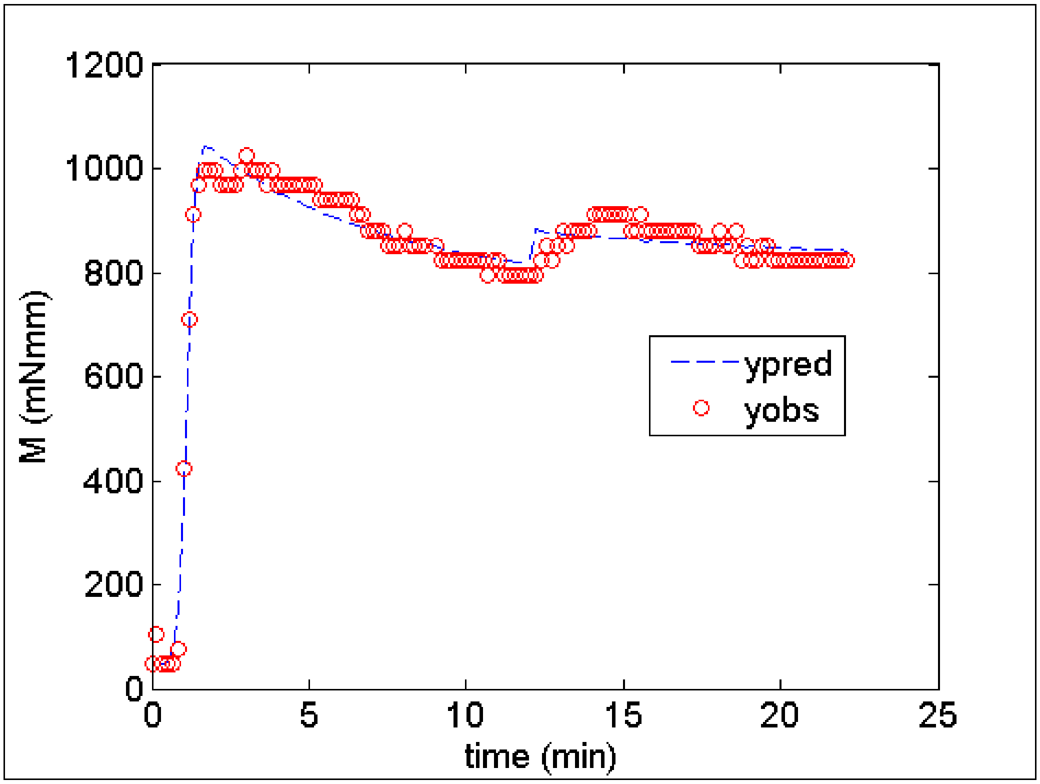

Figure C4.2. Observed and predicted torque for WHVII_10AM

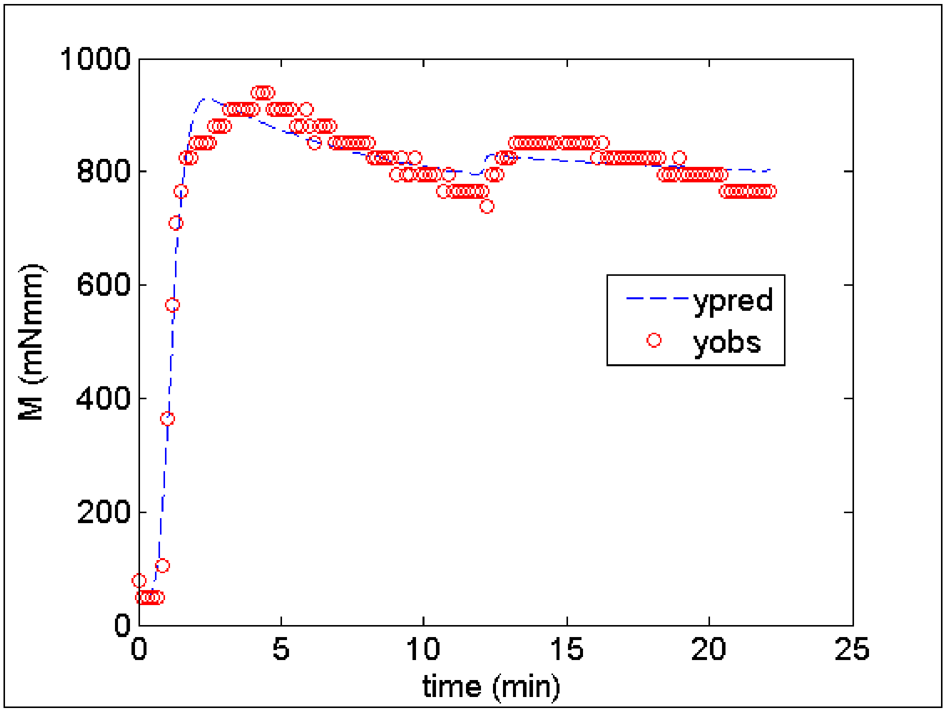

Figure C4.3. Observed and predicted torque for WHVII_20AM

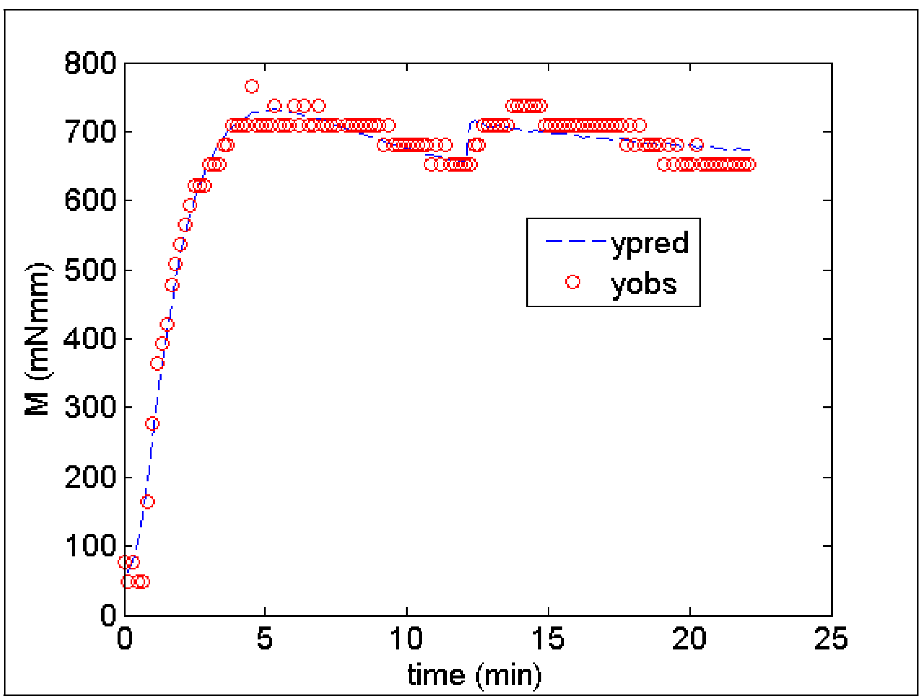

Figure C4.4. Observed and predicted torque for WHVII_30AM

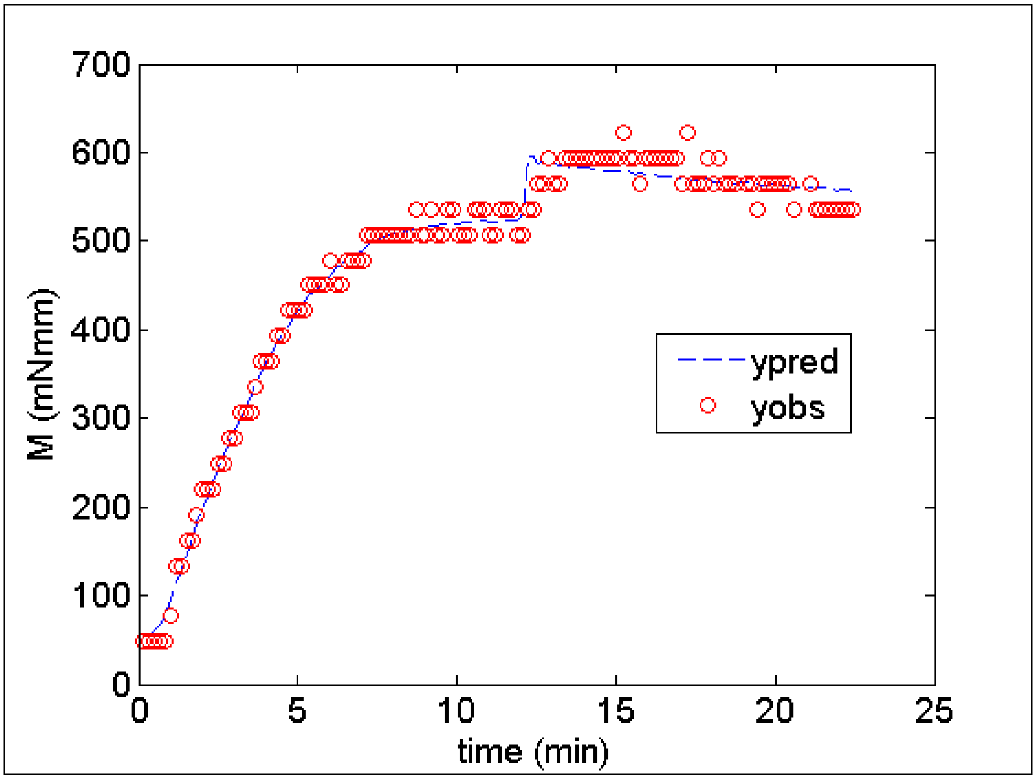

Figure C4.5. Observed and predicted torque for WHVII_30AM

REFERENCES

References

Ahmed J, Ramaswamy HS, Ayad A & Alli I. 2008. Thermal and dynamic rheology of insoluble starch from basmati rice. Food Hydrocolloids 22(2):278-287.

Ahmt T, Wischmann B, Blennow A, Madsen F, Bandsholm O & Thomsen J. 2004. Sensory and rheological properties of transgenically and chemically modified starch ingredients as evaluated in a food product model. Nahrung-Food 48(2):149-155.

Ahromrit A, Ledward DA & Niranjan K. 2006. High pressure induced water uptake characteristics of Thai glutinous rice. Journal of Food Engineering 72(3):225-233.

Alexander RJ. 1995. Potato Starch - New Prospects for an Old Product. Cereal Foods World 40(10):763-764.

Andreev NR. 2002. Chapter 12: Classification of Native Starches and Starch Content Raw Materials. In Book Dietary Starches and Sugars in Man: A Comparison In book Starch and Starch containing origins: Structure, Properties and New Technologies by Yuryev V.P, Cesaro A., and Bergthaller W.J. (2002).165-175.

Andreev NR, Kalistratova EN, Wasserman LA & Yuryev VP. 1999. The influence of heating rate and annealing on the melting thermodynamic parameters of some cereal starches in excess water. Starch-Starke 51(11-12):422-429.

Beck JV & Arnold KJ. 1977. Parameter Estimation in Engineering and Science. John Wiley & Sons, New York.

Briggs JL & Steffe JF. 1996. Mixer viscometer constant (k') for the Brookfield small sample adapter and flag impeller. Journal of Texture Studies 27(6):671-677.

Burhin HG, Rodger ER & Kiener P. 2003. Compound visco-elastic measurements and neural network software modelling - Proactive extrusion control through die swell prediction. Kautschuk Gummi Kunststoffe 56(9):444-449.

Carl Hoseney R. 1998. Principles of Cereal: Science And Technology American Association of Cereal Chemists, Inc. St. Paul, Minnesota, USA Second edition:13-57.

Castellperez ME & Steffe JF. 1990. Evaluating Shear Rates for Power Law Fluids in Mixer Viscometry. Journal of Texture Studies 21(4):439-453.

Castellperez ME, Steffe JF & Moreira RG. 1991. Simple Determination of Power Law Flow Curves Using a Paddle Type Mixer Viscometer. Journal of Texture Studies 22(3):303-316.

Castellperez ME, Steffe JF & Morgan RG. 1988. Adaptation of a Brookfield (Hbtd) Viscometer for Mixer Viscometry Studies. Journal of Texture Studies 18(4):359-365.

Chang YH & Lin JH. 2007. Effects of molecular size and structure of amylopectin on the retrogradation thermal properties of waxy rice and waxy cornstarches. Food Hydrocolloids 21(4):645-653.

Cheetham NWH & Tao LP. 1997. The effects of amylose content on the molecular size of amylose, and on the distribution of amylopectin chain length in maize starches. Carbohydrate Polymers 33(4):251-261.

Cheetham NWH & Tao LP. 1998. Variation in crystalline type with amylose content in maize starch granules: an X-ray powder diffraction study. Carbohydrate Polymers 36(4):277-284.

Chen P, Yu L, Chen L & Li XX. 2006. Morphology and microstructure of maize starches with different amylose/amylopectin content. Starch-Starke 58(12):611-615.

Chung JH, Han JA, Yoo B, Seib PA & Lim ST. 2008. Effects of molecular size and chain profile of waxy cereal amylopectins on paste rheology during retrogradation. Carbohydrate Polymers 71(3):365-371.

Copeland L, Blazek J, Salman H & Tang MCM. 2009. Form and functionality of starch. Food Hydrocolloids 23(6):1527-1534.

Corn Refiners Associations. 2006. Corn Starch. 11th Edition Corn Refiners Association, Pennsylvania Avenue, Washington, D.C.(www.corn.org).

Dail RV & Steffe JF. 1990a. Dilatancy in Starch Solutions under Low Acid Aseptic Processing Conditions. Journal of Food Science 55(6):1764-1765.

Dail RV & Steffe JF. 1990b. Rheological Characterization of Cross-Linked Waxy Maize Starch Solutions under Low Acid Aseptic Processing Conditions Using Tube Viscometry Techniques. Journal of Food Science 55(6):1660-1665.

Dolan KD. 2003. Estimation of kinetic parameters for nonisothermal food processes. Journal of Food Science 68(3):728-741.

Dolan KD & Steffe JF. 1990. MODELING RHEOLOGICAL BEHAVIOR OF GELATINIZING STARCH SOLUTIONS USING MIXER VISCOMETRY DATA. Journal of Texture Studies 21(3):265-294.

Dolan KD, Yang L & Trampel CP. 2007. Nonlinear regression technique to estimate kinetic parameters and confidence intervals in unsteady-state conduction-heated foods. Journal of Food Engineering 80(2):581-593.

Eliasson AC. 1994. Interactions between Starch and Lipids Studied by Dsc. Thermochim Acta 246(2):343-356.

Ford EW & Steffe JF. 1986. Quantifying Thixotropy in Starch-Thickened, Strained Apricots Using Mixer Viscometry Techniques. Journal of Texture Studies 17(1):71-85.

Gibson TS, Solah VA & McCleary BV. 1997. A procedure to measure amylose in cereal starches and flours with concanavalin A. Journal of Cereal Science 25(2):111-119.

Haase NU, Mintus T & Weipert D. 1995. Viscosity Measurements of Potato Starch Paste with the Rapid-Visco-Analyzer. Starch-Starke 47(4):123-126.

Hanashiro I, Abe J & Hizukuri S. 1996. A periodic distribution of the chain length of amylopectin as revealed by high-performance anion-exchange chromatography. Carbohydrate Research 283:151-159.

Hazelton JL & Walker CE. 1996. Temperature of liquid contents in RVA cans during operation. Cereal Chemistry 73(2):284-289.

Hemminger W & Sarge SM. 1994. CALIBRATION AS AN ASPECT OF QUALITY ASSURANCE IN DIFFERENTIAL SCANNING CALORIMETRY (DSC) MEASUREMENTS. Thermochimica Acta 245:181-187.

Jane J, Chen YY, Lee LF, McPherson AE, Wong KS, Radosavljevic M & Kasemsuwan T. 1999. Effects of amylopectin branch chain length and amylose content on the gelatinization and pasting properties of starch. Cereal Chemistry 76(5):629-637.

Jane JL & Chen JF. 1992. Effect of Amylose Molecular-Size and Amylopectin Branch Chain-Length on Paste Properties of Starch. Cereal Chemistry 69(1):60-65.

Jayakody L & Hoover R. 2008. Effect of annealing on the molecular structure and physicochemical properties of starches from different botanical origins - A review. Carbohydrate Polymers 74(3):691-703.

Juhasz R & Salgo A. 2008. Pasting behavior of amylose amylopectin and, their mixtures as determined by RVA curves and first derivatives. Starch-Starke 60(2):70-78.

Kearsley MWaS, P.J. 1989. Chapter 1: The Chemistry of Starches and Sugars Present in Food. In Book Dietary Starches and Sugars in Man: A Comparison Edited by John Dobbing(Springer-Verlag, ILSI Human Nutrition Reviews):1-7.

Kohyama K, Matsuki J, Yasui T & Sasaki T. 2004. A differential thermal analysis of the gelatinization and retrogradation of wheat starches with different amylopectin chain lengths. Carbohydrate Polymers 58(1):71-77.

Kousksou T, Jamil A, El Omari K, Zeraouli Y & Le Guer Y. 2011. Effect of heating rate and sample geometry on the apparent specific heat capacity: DSC applications. Thermochimica Acta 519(1-2):59-64.

Kurakake M, Akiyama Y, Hagiwara H & Komaki T. 2009. Effects of cross-linking and low molecular amylose on pasting characteristics of waxy corn starch. Food Chemistry 116(1):66-70.

Lagarrigue S & Alvarez G. 2001. The rheology of starch dispersions at high temperatures and high shear rates: a review. Journal of Food Engineering 50(4):189-202.

Lai KP, Steffe JF & Ng PKW. 2000. Average shear rates in the rapid visco analyser (RVA) mixing system. Cereal Chemistry 77(6):714-716.

Lai VMF, Halim D & Lii CY. 2002. Chapter 21: Effects of flour compositions and thermal variables on the thermodynamic and kinetic properties during gelatinization of rice flours. In book: Starch and Starch Containing Origins: Structure, Properties, and New Technologies. Edited by Yuryev V.P., Cesaro A., and Bergthaller W.J. . Nova Science Publishers, Inc. New York:297-305.

Lillford PJaM, A. 1997. Structure/Function Relationship of Starches in Food. in Book Starch: Structure and Functionality edited by P.J. Frazier, A.M. Donald and P.Richmond(The Royal Society of Chemistry. Thomas Graham House, Science Park, Milton Road, Cambridge, UK.):1-8.

Lindeboom N, Chang PR & Tyler RT. 2004. Analytical, biochemical and physicochemical aspects of starch granule size, with emphasis on small granule starches: A review. Starch-Starke 56(3-4):89-99.

Liu HS, Yu L, Xie FW & Chen L. 2006. Gelatinization of cornstarch with different amylose/amylopectin content. Carbohydrate Polymers 65(3):357-363.

Liu P, Yu L, Liu HS, Chen L & Li L. 2009. Glass transition temperature of starch studied by a high-speed DSC. Carbohydrate Polymers 77(2):250-253.

Liu XX, Yu L, Xie FW, Li M, Chen L & Li XX. 2010. Kinetics and mechanism of thermal decomposition of cornstarches with different amylose/amylopectin ratios. Starch-Starke 62(3-4):139-146.

Mackey KL, Morgan RG & Steffe JF. 1987. Effects of Shear-Thinning Behavior on Mixer Viscometry Techniques. Journal of Texture Studies 18(3):231-240.

Matveev YI, van Soest JJG, Nieman C, Wasserman LA, Protserov V, Ezernitskaja M & Yuryev VP. 2001. The relationship between thermodynamic and structural properties of low and high amylose maize starches. Carbohydrate Polymers 44(2):151-160.

Megazyme. 2006. Amylose/Amylopectin assay procedure K-AMYL 04/06 : for the measurement of the amylose and amylopectin contents of starch. Megazyme International Ireland Ltd, Bray Business Park, Bray, Co.Wicklow, Ireland.

Mishra DK, Dolan KD & Yang L. 2008. Confidence intervals for modeling anthocyanin retention in grape pomace during nonisothermal heating. Journal of Food Science 73(1):E9-E15.

Mishra DK, Dolan KD & Yang L. 2009. Bootstrap confidence intervals for the kinetic parameters of degradation of Anthocyanins in grape pomace. Journal of Food Process Engineering 34(4):1220-1233.

Mohamed IO. 2009. Simultaneous estimation of thermal conductivity and volumetric heat capacity for solid foods using sequential parameter estimation technique. Food Res Int 42(2):231-236.

Morgan RG. 1979. Modeling the effects of temperature-time history, temperature, shear rate and moisture on viscosity of defatted soy flour dough. Ph.D. dissertation. Agricultural Engineering. Texas A&M University:1-114.

Morgan RG, Steffe JF & Ofoli RY. 1989. A Generalized Rheological Model for Extrusion Modeling of Protein Doughs. J. Food Process Engr. 11:55-78.

Noda T, Takahata Y, Sato T, Suda I, Morishita T, Ishiguro K & Yamakawa O. 1998. Relationships between chain length distribution of amylopectin and gelatinization properties within the same botanical origin for sweet potato and buckwheat. Carbohydrate Polymers 37(2):153-158.

Nuessli J, Handschin S, Conde-Petit B & Escher F. 2000. Rheology and structure of amylopectin potato starch dispersions without and with emulsifier addition. Starch-Starke 52(1):22-27.

Okechukwu PE & Rao MA. 1996. Kinetics of cowpea starch gelatinization based on granule swelling. Starch-Starke 48(2):43-47.

Omura AP & Steffe JF. 2003. Mixer viscometry to characterize fluid foods with large particulates. Journal of Food Process Engineering 26(5):435-445.

Paes SS, Yakimets I & Mitchell JR. 2008. Influence of gelatinization process on functional properties of cassava starch films. Food Hydrocolloids 22(5):788-797.

Park IM, Ibanez AM & Shoemaker CF. 2007. Rice starch molecular size and its relationship with amylose content. Starch-Starke 59(2):69-77.

Ratnayake WS & Jackson DS. 2006. Gelatinization and solubility of corn starch during heating in excess water: New insights. Journal of Agricultural and Food Chemistry 54(10):3712-3716.

Ratnayake WS & Jackson DS. 2007. A new insight into the gelatinization process of native starches. Carbohydrate Polymers 67(4):511-529.

Rolee A & LeMeste M. 1997. Thermomechanical behavior of concentrated starch-water preparations. Cereal Chemistry 74(5):581-588.

Russell PL. 1987. Gelatinization of Starches of Different Amylose Amylopectin Content - a Study by Differential Scanning Calorimetry. Journal of Cereal Science 6(2):133-145.

Sasaki T, Yasui Ta & Matsuki J. 2000. Effect of amylose content on gelatinization, retrogradation, and pasting properties of starches from waxy and nonwaxy wheat and their F1 seeds. Cereal Chemistry 77(1):58-63.

Schwaab M & Pinto JC. 2007. Optimum reference temperature for reparameterization of the Arrhenius equation. Part 1: Problems involving one kinetic constant. Chemical Engineering Science 62(10):2750-2764.

Shalaev EY & Steponkus PL. 2000. Correction of the sample weight in hermetically sealed DSC pans. Thermochimica Acta 345(2):141-143.

Song Y & Jane J. 2000. Characterization of barley starches of waxy, normal, and high amylose varieties. Carbohydrate Polymers 41(4):365-377.

Spigno G & De Faveri DM. 2004. Gelatinization kinetics of rice starch studied by non-isothermal calorimetric technique: influence of extraction method, water concentration and heating rate. Journal of Food Engineering 62(4):337-344.

Stawski D. 2008. New determination method of amylose content in potato starch. Food Chemistry 110(3):777-781.

Steffe JF. 1996. Rheological Methods in Food Process Engineering. Second Edition Freeman Press(East Lansing, MI):2.

Steffe JF, Castellperez ME, Rose KJ & Zabik ME. 1989. Rapid Testing Method for Characterizing the Rheological Behavior of Gelatinizing Corn Starch Slurries. Cereal Chemistry 66(1):65-68.

Steffe JF & Daubert CR. 2006. Bioprocessing Pipelines: Rheology and Analysis. Freeman Press, East Lansing, MI, USA.

Tester RF & Morrison WR. 1990. Swelling and Gelatinization of Cereal Starches .1. Effects of Amylopectin, Amylose, and Lipids. Cereal Chemistry 67(6):551-557.

Thomas DJ & Atwell WA. 1999. Starches. American Association of Cereal Chemists. Eagan Press Handbook Series, St. Paul, Minnesota, USA.

Uzman D & Sahbaz F. 2000. Drying kinetics of hydrated and gelatinized corn starches in the presence of sucrose and sodium chloride. Journal of Food Science 65(1):115-122.

Vasanthan T & Bhatty RS. 1996. Physicochemical properties of small- and large-granule starches of waxy, regular, and high-amylose barleys. Cereal Chemistry 73(2):199-207.

Villwock VK, Eliasson AC, Silverio J & BeMiller JN. 1999. Starch-lipid interactions in common, waxy, ae du, and ae su2 maize starches examined by differential scanning calorimetry. Cereal Chemistry 76(2):292-298.

Walker CE, Ross AS, Wrigley CW & Mcmaster GJ. 1988. Accelerated Starch-Paste Characterization with the Rapid Visco-Analyzer. Cereal Foods World 33(6):491-494.

Wang WC & Sastry SK. 1997. Starch gelatinization in ohmic heating. Journal of Food Engineering 34(3):225-242.

Wu X, Zhao R, Wang D, Bean SR, Seib PA, Tuinstra MR, Campbell M & O'Brien A. 2006. Effects of amylose, corn protein, and corn fiber contents on production of ethanol from starch-rich media. Cereal Chemistry 83(5):569-575.

Xie FW, Yu L, Su B, Liu P, Wang J, Liu HS & Chen L. 2009. Rheological properties of starches with different amylose/amylopectin ratios. Journal of Cereal Science 49(3):371-377.

Xue T, Yu L, Xie FW, Chen L & Li L. 2008. Rheological properties and phase transition of starch under shear stress. Food Hydrocolloids 22(6):973-978.

Yoshimoto Y, Tashiro J, Takenouchi T & Takeda Y. 2000. Molecular structure and some physicochemical properties of high-amylose barley starches. Cereal Chemistry 77(3):279-285.

Yu L & Christie G. 2001. Measurement of starch thermal transitions using differential scanning calorimetry. Carbohydrate Polymers 46(2):179-184.

Yuryev VP, Wasserman LA, Andreev NR & Tolstoguzov VB. 2002. Chapter 2: Structural and Thermodynamic Features of Low-and High Amylose Starches. A Review. In book: Starch and Starch Containing Origins: Structure, Properties, and New

Technologies. Edited by Yuryev V.P., Cesaro A., and Bergthaller W.J. . Nova Science Publishers, Inc. New York:23-55.

Yuryev VPW, Luybov A.; Andreev,Nicolai R. ; and Tolstoguzov,Vladimir B. . 2002. Chapter 2:Structural and Thermodynamic Features of Low- and High Amylose Starches. A Review. in Book Starch and Starch Containing Origins: Structure, Properties and New Technologies:47-48.

Zaidul ISM, Absar N, Kim SJ, Suzuki T, Karim AA, Yamauchi H & Noda T. 2008. DSC study of mixtures of wheat flour and potato, sweet potato, cassava, and yam starches. Journal of Food Engineering 86(1):68-73.

Chapter 6

Overall Conclusions and Recommendation

6.1 Summary and Conclusions

The novel contributions of this study were:

1. It showed that the gelatinization rate constant (k_g) cannot be estimated accurately without determining the optimum gelatinization reference temperature (T_{rg}) by minimizing the correlation between k_g and E_g/R.

2. It showed how to use scaled sensitivity coefficients to determine which parameters in the starch viscosity model are most important.

3. It showed the effect of starch amylose (AM) content on six parameters of the starch viscosity model. Especially, it showed that there were two kinetic parameters, k_g and E_g, that are strongly affected by the starch amylose content described by the following relations:

$$k_g \propto AM^b$$

$$E_g \propto AM^b$$

4. It showed how to estimate up to six parameters simultaneously with most of the estimated parameters having a standard error of less than 10%, and narrow confidence interval bands.

5. It showed how to sequentially estimate the parameters in a starch viscosity model. All the parameters studied approached a constant value before all data were added. For waxy corn starch, the sequentially estimated parameter values

of k_g, E_g/R, A, B, and E_v/R were 3.2 $(Kmin)^{-1}$, $13.8x10^4$K, 34.5, 0.5, and 819 K was obtained after approximately 2.5min, 21min, 2.5min, 10min, and 18min, respectively, over the total experimental time of 22min.

6. It is the first study to report the pasting curve of corn starch at different AM/AP ratios from mixer viscometer data representing absolute (not empirical) rheological testing.
7. It provided thermal properties (using DSC) for corn starch blends at different AM/AP ratios.
8. It showed that the proposed starch viscosity model with estimated parameters from this study also predicts rheological behavior from an alternative measuring system (RVA).

Pasting curves of corn starch blends at different amylose to amylopectin ratios were obtained using a modified Brookfield viscometer. Fundamental rheological data were collected by applying the mixer viscometry approach. The highest peak viscosity, the holding strength and the set back viscosity points of pasting curves were observed for waxy corn starch (containing the lowest amylose content) with values of 9325cP, 5472cP, and 5807cP, respectively. For normal corn starch, the peak viscosity, the holding strength and the set back viscosities were 3965cP, 3462cP, 3630cP, respectively. For high amylose corn starches, there was not much increase in apparent viscosity throughout the testing period, and a flat value of 268cP was achieved for all points of the pasting curve. The overall trend shows that all points on the pasting curves decreased exponentially as the amylose content of the corn starch blends increased.

Thermal property values were obtained from DSC data for corn starch blends at different amylose to amylopectin ratios. Results showed higher enthalpy values for low amylose content corn starches. A broad endotherm peak was observed for higher amylose contents, and the conclusion temperatures (Paes and others) were also high, up to 116.5^{o}C for high amylose content starches.

Parameters in the starch viscosity model for corn starch at different amylose to amylopectin ratios were successfully estimated simultaneously, and sequentially, using advanced parameter estimation techniques. The activation energy of gelatinization E_g for waxy and normal corn starches were 1169±95 kJ/mol and 964±39 kJ/mol, respectively. The gelatinization rate constant k_g for waxy and normal corn starches was 3580 $(Kmin)^{-1}$ and 0.35 $(Kmin)^{-1}$ at a reference temperature of T_{rg}=91^{o}C.

6.2 Recommendations for Future Research

The following topics are recommended for future research:

i) Investigate the applicability of the starch viscosity model on the pasting curves of starches from other botanical sources with known amylose contents.

ii) Conduct a comprehensive study on the effect of interaction among starch components (amylose, amylopectin, lipids, and proteins) and; starch molecular structure (granule size, amylopectin branch chain length, and starch crystallinity) on starch viscosity.

iii) Test the suggested starch viscosity model at different impeller speeds, heating rates, and sample concentrations in other viscosity measuring systems.